UNIVERSITY OF WARWICK

SCHOOL OF ENGINEERING SCIENCE

CUMULATIVE DAMAGE FATIGUE IN NOTCHED MILD STEEL SPECIMENS

BY

D. J. ASHBY B. Sc.

A THESIS SUBMITTED FOR CONSIDERATION FOR THE DEGREE OF DOCTOR OF PHILOSOPHY

ABSTRACT

The work presented is specifically concerned with improving cumulative fatigue damage life predictions in the region of long lives where most of the stress levels experienced by a specimen or structure are below the constant amplitude fatigue limit. Further, an attempt has been made to improve these predictions in such a manner as to be feasable in the design process, i.e. mathematical simplicity and minimum data requirements to enable predictions of improved accurancy to be made. Several existing cumulative damage prediction rules are examined with reference to their accuracy, areas of application and suitability for the design process.

Results are presented for constant amplitude tests on four different specimen configurations and various forms of block loading tests with finally a triangular modulation of applied load on a single specimen configuration in rotating bending. The cumulative damage experimental results are used to investigate the resultant effect of loads below the original constant amplitude fatigue limit. The observed behavioural patterns have been rationalized to form the basis of a cumulative damage rule. The main feature of the rule is the division of the fatigue life into two stages termed Stage A and Stage B which are defined as follows:-

Stage A Initiation and Micro-crack propagation.

Stage B Macro-crack propagation.

A linear summation is performed on each stage simulating observed patterns of behaviour, using a modified S-N curve derived from the standard constant amplitude S-N curve. The length of each stage is determined by the length of that same stage in a constant amplitude test at the highest damaging stress level in the spectrum. The division of the life between Stage A and Stage B has been shown to be a unique

quantity dependant on specimen geometry and an empirical relationship has been derived relating the K_T value of the notch to the slope of a life in Stage A versus Total life to failure plot. As a consequence of different behaviour in Stages A and B different cummulative damage behaviour is predicted for differing notch severities.

Certain aspects of size effects are examined and discussed and the general areas of application of the cumulative damage rule are outlined. Finally, the proposed rule is tested against other cumulative damage rules and experimental results presented in the cumulative damage literature.

Suggestions are presented for further research work to further investigate and extend the areas of applicability of the proposed method.

CONTENTS

other test data existing in the literature.

Chapter 8 — Discussion, conclusions and suggestions for further research.

References

Appendix I — A brief account of the work of R. M. Puckridge.

Appendix II — Stress analysis programs.

Appendix III — Detailed calculations using the proposed cumulative damage rule.

Acknowledgement

Note — In each chapter the pages, figures and tables are numbered consecutively from 1 onwards, and prefixed by the chapter number, e.g. 6.3 is the third page in chapter 6, Fig. 6.3 is Fig. 3 in chapter 6, etc. Figures and tables are presented at the end of each chapter in the order to which they are refered in the text.

CHAPTER 1

INTRODUCTION

The literature and basic knowledge on the many aspects of fatigue damage has expanded at a rapid rate in recent years. Improved testing facilities have led to data on more complex stress spectra, the influence of the continuum mechanics approach overlapping from the fracture mechanics field has deeply influenced the concepts of crack propagation laws, and recently advances have been made in the signal analysis and specification. These factors together with the knowledge of the basic fatigue mechanism should lead to improvements in the field of cumulative fatigue damage.

An area of cumulative fatigue damage which has received little attention is the improvement of design rules particularly in the case of notched specimens which spend most of their life below the constant amplitude fatigue limit. An extreme problem which occurs in this range is typified by the design of gas cooling systems in a nuclear power station, where the designer faces welded details excited to resonance at frequencies of approximately 1, 2, and 3 Kc/s with a design life of 25 years i.e. a number of cycles in the region of 10^{12}. The vast majority of the stress cycles will be below the constant amplitude fatigue limit and the design engineer possesses no information on accurate life assessment in such cases.

The weakness of nearly all cumulative damage rules is their incomplete treatment of stresses below the constant amplitude fatigue limit and the effect of their interaction with stresses above the constant amplitude fatigue limit. Past attempts to incorporate these factors have led to an expanding complexity in cumulative damage rules and in some cases a requirement for special testing before life estimates can be made, but

these very features prevent such a rule becoming accepted as a design procedure because of the limited benefit of a more cumbersome rule together perhaps with additional testing to achieve marginally better life predictions. To quote Hardrath (1964), "The eventual development of a fatigue design procedure should be pursued vigorously, but with the thought in mind that it must treat a complex array of parameters. Too narrow an outlook can lead to the development of too many more procedures that cannot solve the designer's problem".

The centre of the problem is thus to take a situation affected by many complex factors and include those which prove to be quantitatively significant in a simple design rule. It is unimportant whether these factors are included precisely in the cumulative damage rule the only matter of importance is that the rule predicts, to a much greater degree of accuracy than those available at present, the life of the specimen or detail.

The objective of the work was to examine cumulative damage behaviour in specimens subjected to stress histories which contained a high proportio of stresses below the constant amplitude fatigue limit. Then to attempt to rationalize this behaviour and to formulate from it a simple cumulative damage rule which possesses as wide a range of application as possible.

In this thesis a range of cumulative damage tests are presented and a new method of approaching cumulative damage behaviour is proposed. A simple cumulative damage rule is formulated, the areas of its application outlined and it is compared with other results presented in the literature which fall in these areas.

CHAPTER 2

The overall objective of the proposed programs was stated in Chapter 1 i.e. an attack on the problem of cumulative damage life predictions in the area of notched specimens which are subjected to a high proportion of stresses below the constant amplitude fatigue limit. There are several different philosophies of approach within this overall framework and they lie at or between the two extreme cases. The first is to work on a special batch of material which has been produced under rigorously controlled conditions, a single geometry only would be considered, specimens not machined to the highest standard would be rejected, all specimens would be stress relieved in vacuo after machining and prior to testing, strictest control would be exercised over all testing and the observed patterns of behaviour would be simulated exactly in the cumulative damage rule. The net result would probably be a prediction technique which worked very well for all the above conditions but which was of a very dubious nature when applied to other test conditions. The other extreme is to obtain a series of production components suitable for testing and to base the test program around these. The obvious disadvantages are the requirement for specially designed testing rigs and the large degree of scatter inherent in components both due to variations in material properties and the state of the finished surface. The test program is a study of the peculiarities of a particular component geometry and the prospect of obtaining a degree of generality from such testing is remote. Obviously there are a large number of combinations of factors from these two extreme approaches which constitute intermediate philosophies. The philosophy adopted for the program of work presented in this thesis lies between these two extremes, trying to include as many factors as possible whilst excluding those which would give prohibitive scatter, alternatively impose severe limitations

on the generality or applicability of the results presented. The philosophy is presented in greater detail when experimental material and specimen design are considered in Chapter 3. The most important factor when considering cumulative damage life predictions is to avoid being directed into too narrow a field, detail information must be assimilated from various fields but rationalised to form part of an overall pattern of behaviour.

The object of a good cumulative damage design rule is to provide sufficiently accurate data at the design stage to obviate the necessity for long and expensive fatigue testing and redesign in the development process. If this accuracy can be obtained from a minimum of simple test data then an important saving has been made, but if the predicition technique relies heavily on specific complex test data then nothing has been gained and the technique is of no real practical interest. Thus the data required for a design oriented cumulative damage life prediction should be as simple as possible within the limitations of the required accuracy. These overall concepts should be used when examining cumulative damage rules in addition to assessing their ability to predict certain test data.

The field of cumulative fatigue damage theories has been dominated for a long time by the Palmgren-Miner hypothesis. This hypothesis although demonstrably inaccurate in a wide variety of circumstances, has maintained an important role due to the simplicity of its concepts and the ease with which it allows computations from the standard S-N curve to be made. It is therefore necessary to examine this hypothesis, its foundations, limitations and areas of applicability before moving on to examine other cumulative damage rules.

PALMGREN-MINER HYPOTHESIS (1945)

This cumulative damage rule is expressed mathematically as $\sum \frac{n_i}{N_i} = 1$ where n_i is the number of cycles at the i^{th} stress level and N_i

is the number of cycles to failure at that level in a constant amplitude test. Miner based his derivation of the rule on the assumption that:- "the total amount of work that can be absorbed produces failure assuming that no work-hardening occurs". The factors implicit in this theory are as follows:-

1) That the accumulation of damage per cycle at any given stress level is constant i.e. it is a linear rule.

2) Damage accumulates in the same manner at all levels i.e. it is not stress dependant.

3) The increment of damage due to a particular cycle is not affected by the previous stress history i.e. there is no interaction.

These three factors linearity, stress dependance and interaction effects can be used to examine and evaluate other cumulative damage rules.

The areas of applicability of the Palmgren-Miner hypothesis may be set out and governed approximately by the rules below:-

1) All stress levels used in the computation would individually give "N" values between 10^4 and 10^6 cycles.

2) Life errors in the region of 200% are acceptable.

3) The loading spectrum actually applied is reasonably mixed.

Important exceptions to the general rules above are:-

a) Service histories having infrequent applications of very high stress.

b) Loading spectra with large numbers of low stress cycles.

Other cumulative damage rules can now be classified generally as improvements to the Palmgren-Miner hypothesis or as deviations in certain aspects as follows:-

1) Improved accuracy in dealing with simple stress histories, still based on an S-N curve obtained experimentally. Specific areas are:-

(a) Better predictions in the finite life region.

(b) Allowance for stresses below the fatigue limit.

(c) Allowance for isolated high stresses.

2) Improved accuracy obtained by making more extensive and complex tests to replace the simple S-N curve.

3) Reduction in the quantity of initial complex data required, sometimes by using hypothetical S-N curves.

4) Extension of computing methods so that complex stress spectra can be handled either:-

(a) Using Miners law in its basic form with a Goodman diagram.

(b) Using some alternative hypothesis.

In the period until the early sixties most effort had been concentrated on 1a. however, since that time the availability and development of machines capable of performing complex tests together with an influx of ideas from the fracture mechanics field, has led to a wider variety of possible solutions existing in the literature.

Cumulative-damage rules other than the Palmgren-Miner Hypothesis.

The basic fatigue mechanism is today well understood but this has not led to any significant improvement in the approach to cumulative damage fatigue rules. A great number of the hypotheses put forward in the period from 1950 to 1963 were based on some qualitative assessment of the basic fatigue mechanism and its representation in a cumulative damage rule. The particular factor or factors selected for attention as significant points by each author can soon be nullified in the ensuring mathematical derivation, thus the final product purports to be something which it is not A good example of this style of theory is that put forward by Corten and Dolan (1956) at the International Conference on fatigue in 1956. It is worth examining this theory in detail both to see the very complex nature of a cumulative damage theory which takes into account most of the required factors and also how this very complexity enforces certain

assumptions which reduce the rule to a slightly modified version of Miners Law. The assumptions on which Corten and Dolan based their theory are as follows:-

1) A nucleation period may be required to initiate permanent fatigue damage.

2) The number of damage nuclei that form throughout the member increases as the stress increases.

3) Damage at a given stress amplitude propagates at rates that increase with the number of cycles.

4) The rate of propagation of damage per cycle increases as the stress increases.

5) The total damage that constitutes failure in a given member is constant for all stress histories.

These assumptions form the basis of a non-linear, stress dependant interaction theory. The first factor to be excluded is the initiation period which is postulated as being negligible. The general damage equation is given by Corten and Dolan as:-

$$D = m\ r\ N^{a}$$

where D = Damage

m = No. of sub-micro scopic damage voids.

r = Crack propagation constant

N = No. of cycles

a = A constant.

The total damage to failure, D_f, at constant amplitude is given by the following equations

$$D_f = m_1\ r_1\ N_1^{a_1} = m_2\ r_2\ N_2^{a_2} .$$

Corten and Dolan then went on to consider a block loading program as shown in Fig. 2.1. A sketch of the damage curves is shown in Fig.2.2. but as

$m_1 > m_2$ the damage curve for the low stress level becomes effectively represented by

$$D = m_1 r_2 N_2^{a_2}$$

and this interaction curve is shown also.

As the stress level is changed progress is switched from one curve to the other as shown by the solid lines in Fig. 2.2.

Now $$\frac{dD}{dN} = a_1 m_1 r_1 N_1^{a_1-1}$$

Using this equation the damage increment ΔD shown in Fig. 2.2. can be expressed as follows:-

$$\Delta D = a_1 m_1 r_1 N_e^{(a_1-1)} . \Delta N_1$$

$$\Delta D = a_2 m_1 r_2 N_f^{(a_2-1)} . \Delta N_2$$

Also by equating the damage at level "e" it can be derived that

$$\Delta N_1 = A R^{\frac{1}{a_1}} (N_f)^{A-1} . \Delta N_2 \qquad - \quad (1)$$

where $A = \frac{a_2}{a_1}$ and $R = \frac{r_2}{r_1}$

Damage may now be summed along one curve, giving according to Corten & Dolan

$$D = \sum_1^g \Delta D = m_1 r_1 \left[N_g \alpha + A R^{\frac{1}{a_1}} (1-\alpha) n \left\{ n^{A-1} + (2n)^{A-1} + (3n)^{A-1} + \cdots\cdots (gn)^{A-1} \right]^{a_1} \right.$$

Where N_g is the total number of cycles to failure and g is the number of blocks to failure.

Where n, $2n$, $3n$, etc represent appropriate values of N_f in equation (1). Evaluation of this series by integration gives

$$D = m_1 r_1 \left[N_g \alpha + R^{\frac{1}{a_1}} (1 - \alpha) N_g^{A} \right]^{a_1}$$

also from this equation:-

$$N_1 = N_g \alpha + R^{\frac{1}{a_1}} (1 - \alpha) N_g^{A} .$$

Corten and Dolan then state a_1 and a_2 are approximately equal. i.e. our

equation for damage is no longer stress dependant.

$$N_g = \frac{N_1}{\alpha + R^{\frac{1}{a}} (1 - \alpha)} \qquad - \quad (2)$$

If we examine the values of N_f placed in equation (1) in order to evaluate and sum the series a further contraction of the original hypothesis is noted. It is possible to obtain a similar expression to equation (1) with ΔN_2 in terms of ΔN_1 for the relevant section of the plot i.e. the true value for c-f not the αn assumed by the limits used in the series and if this true value is substituted in the summation then a long and complex series results after only a few steps. In order to be able to sum the series conveniently Corten and Dolan have introduced these assumed values of N_f. However this is equivalent to introducing linearity into the summation. This point can be conveniently illustrated in another fashion.

If we revert to equation (2) Corten and Dolan claim to have established a unique value of $R^{\frac{1}{a}}$ from experimental results and suggest that R is proportional to the ratio of s_1 and s_2. They investigated the relationship $R^{\frac{1}{a}} = (s_2/s_1)^d$ and using experimentally determined values of $R^{\frac{1}{a}}$ they verified this relationship on a log log plot.

Substituting $R^{\frac{1}{a}} = (s_2/s_1)^d$ in equation (2)

we get

$$N_g = \frac{N_1 \; s_1^{\,d}}{\alpha s_1^{\,d} + s_2^{\,d} (1 - \alpha)} \qquad - \quad (3)$$

Now consider an S-N curve which plotted on a log log basis can be assumed to be a straight line as shown in Fig. 2.3. Let the stress levels in a two level block test be S_1 and S_2 respectively. If we now rotate the S-N curve about the point (S_1, N_1) we attain some modified slope say $\frac{1}{p}$.

Performing a Miner summation for the two level block test on the modified S-N curve we get:-

$$1 = \frac{\alpha N_g}{N_1} + \frac{(1-\alpha) N_g}{N_2}$$

from this we obtain

$$N_g = \frac{N_1 N_2}{\alpha N_2 + (1-\alpha) N_1} \qquad - (4)$$

from S-N curve $\frac{N_1}{N_2} = \left(\frac{s_2}{s_1}\right)^P$

$$N_2 = N_1 \times \left(\frac{s_1}{s_2}\right)^P$$ Substituting this equation

in equation (4) we obtain

$$N_g = \frac{N_1 \times s_1^P}{\alpha s_1^P + (1-\alpha) s_2^P} \qquad - (5)$$

Compare equation (3) and equation (5) .

Thus what started as a non-linear, stress dependant, interaction theory after assumptions made in the derivation finished as a linear, stress independant, interaction theory.

It is interesting to examine the following equation

$$N_1 = N_g \alpha + R^{\frac{1}{a_1}} (1-\alpha) N_g^A$$

The unknown quantities are a_1, a_2, r_1 and r_2 and the enormity of the task of establishing these values is immediately obvious, further, evaluating these would involve a formal definition of damage and no current method is perfectly satisfactory in this respect.

Corten and Dolan performed a large amount of experimental work to justify their theory and this was performed on high strength aluminium

alloys. Excellent agreement was obtained with the theory which is not altogether surprising when the experimental results are examined.

Their theory is in fact Miners Law with another factor based on experimental results to give best fit to data. Miners Law as already postulated works well when most of the stress levels are above the fatigue limit. As, all their applied stresses were relatively high, blocks of high stress formed a large proportion of total life, and fairly large blocks were used, we would expect Miners Law to be reasonably accurate in this case and hence Corten and Dolan to be slightly closer because they have used one more fit to data parameter. This in fact appears to be so with Miner being less than 20% in error in the majority of cases.

The work of Corten and Dolan typifies many attempts at the formulation of a cumulative damage rule. The complications and laboriousness of trying to consider a number of important factors precludes the formulation of a simple rule, but simplicity is required if the rule is to become an effective tool in the bands of the design engineer in the early stage of the design process.

The Corten and Dolan theory has been examined by other authors, notably Kaechele (1963) in his excellent review and Marsh (1964) in his experimental work. Marsh finally concludes that the unique value for $R^{\frac{1}{a}}$ is doubtful, particularly for plain specimens.

Two further rules of this overall type are worthy of individual attention and these are the theories of Freudenthal-Heller and Grover. Freudenthal and Heller (1959) proposed a theory which was based on interaction effects occurring below a certain fairly high stress level.

These interaction effects are such as to give the modified S-N curve the following form:-

$$N_i = \frac{K}{S_i^x}$$ this being a straight line on a logarithmic plot. K is a constant determined by the condition that the modified S-N curve passes through the point of the original S-N curve corresponding to the stress level below which interaction effects are present. Freudenthal and Heller tried and succeeded in relating the exponent x to characteristics of the applied stress spectrum in simple 4 to 6 level block tests on plain fully reversed bending specimens. This represents the first attempt to take account of the general properties of the applied stress spectrum in a cumulative damage rule. Although successful on simple block programs and plain specimens, Freudenthal and Heller comment that quite different results have been observed in notched specimens. The rule is therefore extremely limited and a plain specimen is not typical of many engineering components it does however start to emphasize the importance of the applied stress spectrum.

The theory propounded by Grover (1960) suggests that the fatigue life should be divided into two stages, basically an initiation period and then propagation of damage to failure. So some fraction of the life say x is spent in initiating damage and the remaining fraction (1 - x) in propagating the damage to failure. These fractions are postulated as being different for different stress levels i.e. the theory is stress dependant but, the fraction remains unaffected by the application of other load levels so no interaction effects have been considered. In cumulative damage calculations Miners law is applied to both stages which gives the following equations:-

Stage 1 Initiation $$\frac{n_i}{x_i N_i} = 1$$

Stage 2 Propagation to Failure $\frac{n_i}{(1 - x_i)N_i} = 1$

The problem is then to determine the values of x_i at varying stress levels as they will almost certainly vary also with the notch geometry under consideration. Also before these results can be obtained a meaningful concept of the fraction x has to be defined either in empirical physical terms of theoretically. This theory provides an infinite number of solutions depending on the values assigned to the fraction x, similarly the Freudenthal-Heller concept could be used to generate an infinite number of S-N curves from the slope and intercept parameters so that all data could be fitted. The major step however is to be able to define these parameters for a wide range of stress spectra and specimen geometries and this has not been achieved.

Kaechele (1963) also examines the theories of Valluri, Shanley and the Shanley 2-X Method, as well as the theories already examined, in an excellent review paper. On reviewing all the above methods part of his conclusions are:- "In conclusion, no radical 'breakthroughs' appear in the area of cumulative fatigue damage evaluation in aircraft structures, either in physical understanding or in theoretical techniques."

Since this period the attempts at formulating cumulative damage rules have dwindled and a greater effort has been made to quantify certain aspects of cumulative damage behaviour. Certain aspects are worthy of mention, the first is the attempt of Marsh (1964) to allow for stresses below the original constant amplitude fatigue limit. Marsh took the Corten and Dolan hypothesis using the slope parameter of the S-N curve as a method of obtaining best fit to data. The tests were on sharply notched rotating bending specimens with a triangular modulation of the applied load, and the fit of the Corten and Dolan hypothesis was not at all encouraging.

Marsh re-examined his data and concluded that the best overall fit to data was to be obtained by considering stresses down to 0.8 σ_f (σ_f = constant amplitude fatigue limit) as damaging in the summation performed on the modified S-N curve. This modified form of the Corten and Dolan hypothesis certainly improved the prediction techniques for this particular set of test data and was a great deal safer than the Palmgren-Miner hypothesis, however the improvements were not maintained when it was extended to other stress spectra in later work and the large majority of the total program was performed on sharply notched specimens with a K_T value of 13.6. These later results are fully discussed in later chapters of this thesis, but the main feature of this work is that both interaction effects and stresses below the original constant amplitude fatigue limit are allowed for, albeit on a best fit to data basis using a linear summation technique.

Kirkby and Edwards (1966) provided another approach to the problem of cumulative damage prediction by the utilization of random load testing. They give a method of synthesising a complex stress spectrum into a number of Rayleigh distributions each with a different R.M.S. stress level σ . If an r.m.s. stress versus cycles curve is available a Miner type summation can be made on this curve. Obviously some of the interaction effects etc are included in the random loading S-N curve but it should be noted that the method depends on random-loading test results. Thus if different geometries behave significantly differently one is committed to extensive random loading tests in order to be able to predict with greater accuracy the results of more complex spectra, and for basic design purposes this is a severe limitation.

The situation may thus be summarised as follows:- A wide variety of cumulative damage life prediction techniques are available, none of which

have been demonstrated to have an area of application extending beyond the data from which they were formulated. In many cases the application of the rule depends on the availability of special test data or conversely they depend on concepts which cannot at present be given a firm basis in practical engineering terms.

Throughout the previous discussion some emphasis has been placed on the geometry of the specimen and in particular the notch geometry or its severity. The differences in behaviour displayed by specimens of different geometry, even in constant amplitude tests, would suggest that the cumulative damage performance of these differing geometries would be different. The existence of non-propagating cracks in sharply notched specimens has been firmly established. Frost (1961) has attempted to clarify the interpretation of sharply notched fatigue data in terms of a critical alternating stress required to propagate a crack, including the depth of the notch in the value assigned to crack depth. Although some workers maintain that these results may be explained by residual stress effects, the fact remains that non-propagating cracks exist and they are evident only in sharply notched specimens. The large differences in scatter between notched and plain specimen results also indicates differences in behaviour and there is most probably a gradual change in behaviour patterns through the range from plain to very sharply notched specimens. These arguments are supported by the results and comments of Freudenthal and Heller, mentioned earlier in this Chapter.

A great deal of effort has been expended by many authors in the development of crack propagation laws. These studies mainly concern the propagation of cracks in sheet specimens. An excellent overall analysis and review of these methods is given by Paris and Erdogan (1963). The crack propagation law proposed by Paris based on the crack tip stress intensity

factor has been shown to give good agreement to data supplied by other authors. The method has been extended to cover complex loading both by Paris (1964) and also Forman, Kearney and Engle (1967). These results are limited in the case of Paris by no allowance for ordering effects and in the case of Forman et al by the very limited nature of the stress spectrum which the program is capable of dealing with i.e. simple block programs. These results are obviously of great value and importance in predicting growth rates of large cracks and enabling inspection intervals etc. to be correctly determined. However, in the cumulative damage predictions they neglect the important and major portion of the life of mildly notched specimens in the long life region when the crack will be initiating or very small and propagating at very low rates.

The necessity of considering all phases of the life, initiation, micro-crack propagation and macro-crack propagation reverts attention to more conventional testing techniques in order to determine the damaging effect of low and high loads. Naumann (1962) has shown that high loads in blocks of 10 cycles or under, in statistically significant terms may be considered as non-damaging or slightly beneficial but that in blocks greater than 10 then the damaging effect of these loads must be allowed. In the same test program Naumann investigated the presence and absence of low load levels below the constant amplitude fatigue limit and although not showing a high damaging effect Naumann suggested that the role of these low stress cycles was to relax residual stresses. Freudenthal (A) in the discussion following the presentation of this paper emphasized the great difference between applying low stress cycles in sequence with one another or well mixed with higher stress levels. Then there is Marsh's suggestion that stresses down to $0.8\,\sigma_f'$ should be considered as damaging although the value of this result in engineering terms must be

limited when related to the K_T of 13.6 which was used for most tests. Information of this nature can be found throughout the literature for example the work of Manson et al.(1965) in developing S-N curves for varying amounts of pre-stressing on 4 materials. Although the propagation potential of low stress cycles late in the life are allowed for no allowance is made for actual interaction effects.

To summarize it would appear that no real advance in a "simple" cumulative damage design rule has been made since Miners Law. The damaging effects of low loads are clearly recognized but adequate quantification of these effects and more important the effect of their interaction with higher loads is not available. Geometrically differing specimens will behave differently but again this has not been quantified in terms of cumulative damage rules. The nature of this difference will probably relate closely to the differences in initiation periods for damage in the varying geometries. This suggests that possibly a rule of the type proposed by Grover, in two stages initiation and propagation but with varying interaction and propagation effects allowed for in the two stages, would prove a more successful approach to cumulative damage predictions than any previously quantified. The experimental objectives were thus quite clear;-

(1) To examine and attempt to quantify the effects of low loads at varying stages in the cumulative damage life of a specimen.

(2) To develop a method of classifying and observing the damaged state of the specimen and to use this to rationalize any information gained in (1).

(3) The information gained in (1) and (2) should be formulated into as simple a cumulative damage rule as possible and this should be extended over as wide a range of data as possible.

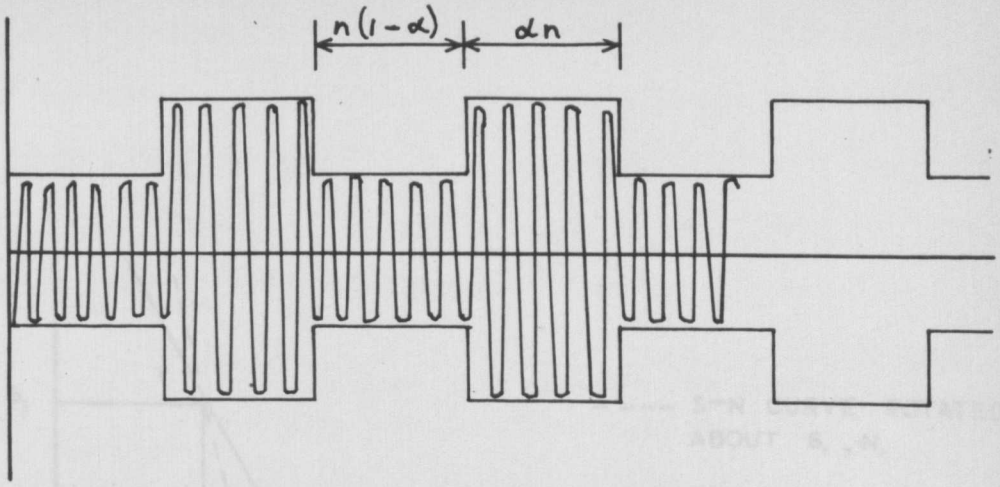

BLOCK STRESS SYSTEM.

FIG. 2.1.

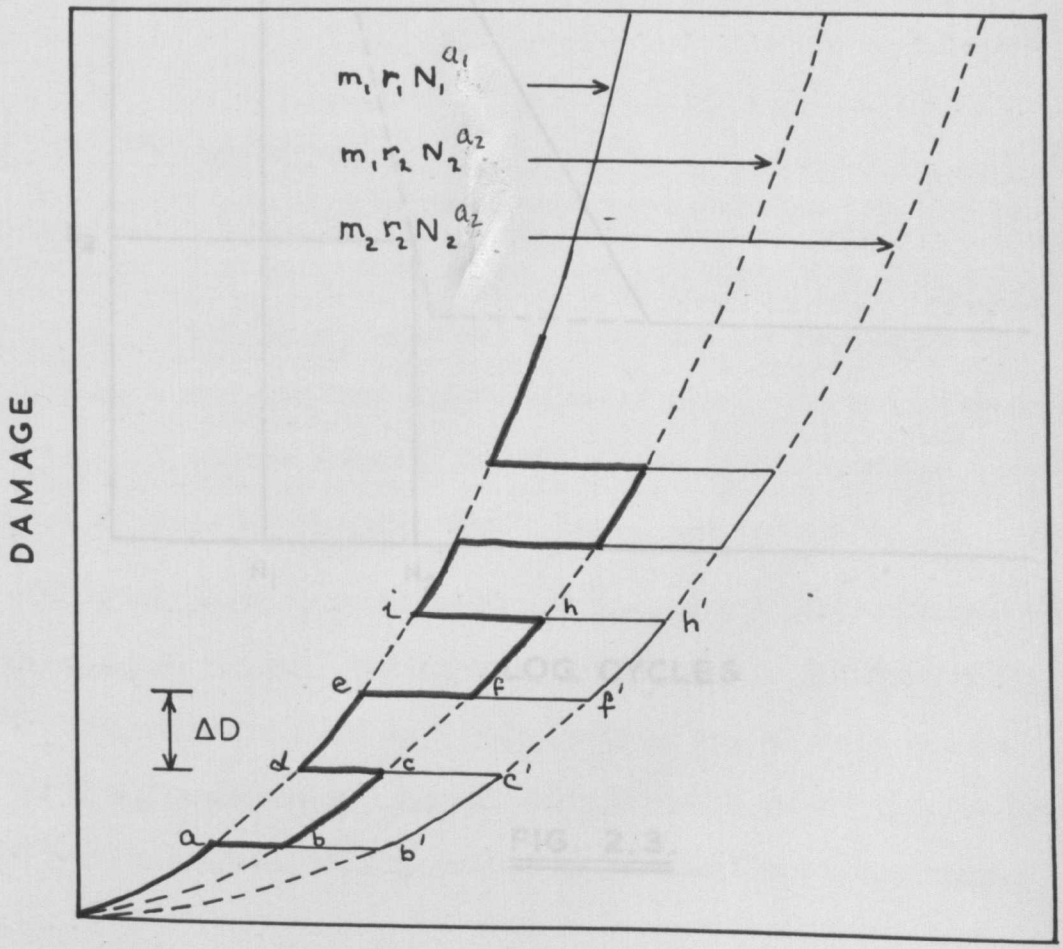

FIG. 2.2.

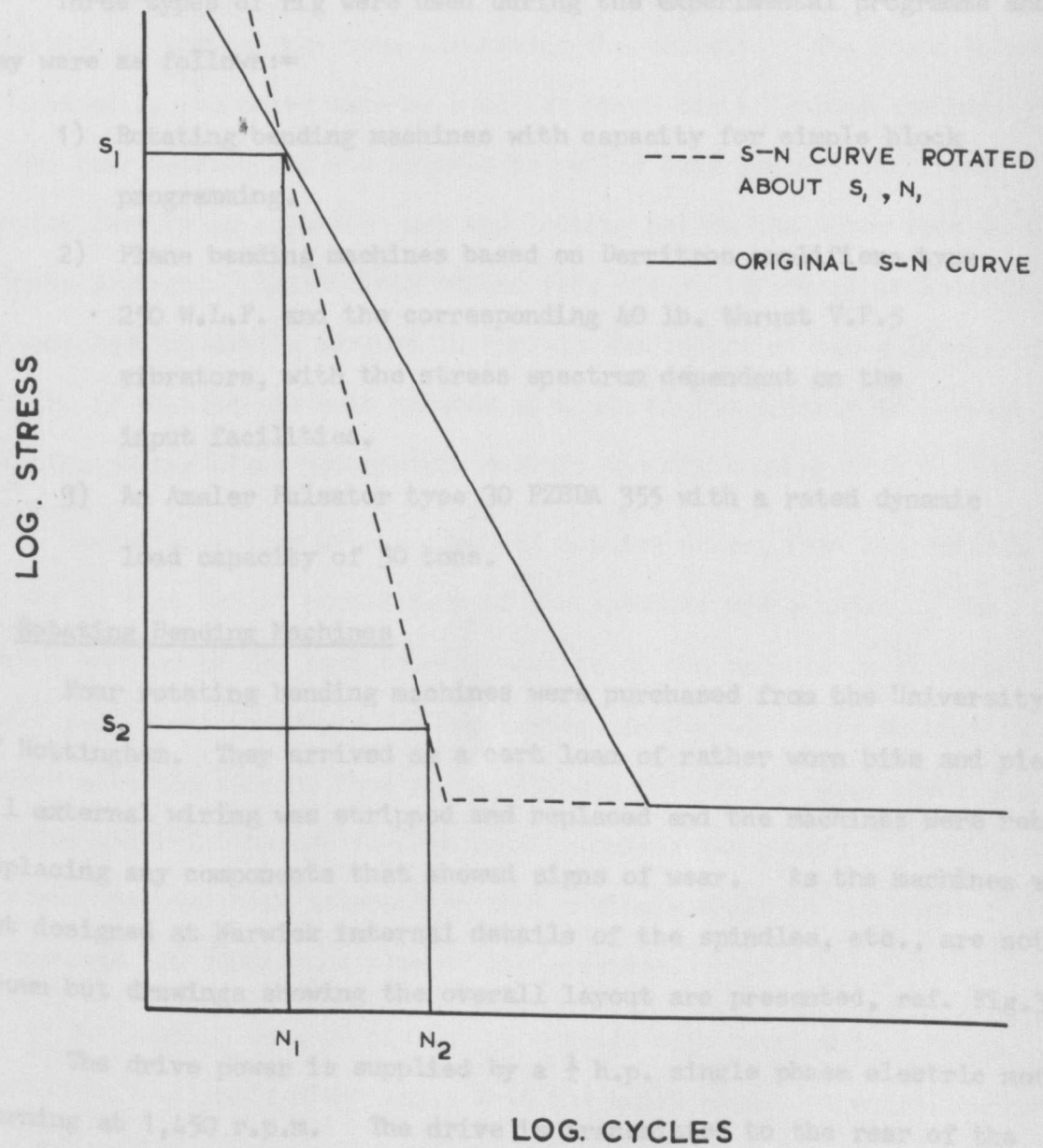
S1
S2
N1
N2
LOG. STRESS
LOG. CYCLES
---- S-N CURVE ROTATED ABOUT S1, N1
—— ORIGINAL S-N CURVE

FIG. 2.3.

CHAPTER 3

DESCRIPTION OF APPARATUS USED

Three types of rig were used during the experimental programme and they were as follows:=

1) Rotating bending machines with capacity for simple block programming.
2) Plane bending machines based on Derritron amplifiers type 250 W.L.F. and the corresponding 40 lb. thrust V.P.5 vibrators, with the stress spectrum dependant on the input facilities.
3) An Amsler Pulsator type 30 PZBDA 355 with a rated dynamic load capacity of 30 tons.

1) Rotating Bending Machines

Four rotating bending machines were purchased from the University of Nottingham. They arrived as a cart load of rather worn bits and pieces. All external wiring was stripped and replaced and the machines were rebuilt, replacing any components that showed signs of wear. As the machines were not designed at Warwick internal details of the spindles, etc., are not shown but drawings showing the overall layout are presented, ref. Fig.3.1.

The drive power is supplied by a $\frac{1}{4}$ h.p. single phase electric motor turning at 1,450 r.p.m. The drive is transmitted to the rear of the spindle by a standard flexible V belt, with no reduction in gearing. The spindle itself consists of a centre shaft threaded at the forward end to locate in the specimen holding collett with a drilled flange located

at the rear end by a tapered pin to enable extra leverage to be obtained for tightening the specimen in the collett. The load bearing outer section of the spindle runs in two single row ball bearings front and aft located in an outer casing. The front section is tapered to accept a special Hardinge $\frac{5}{8}$" collett and its outer section is drilled for insertion of locking key when tightening the collett. The whole spindle is located in the outer case by a collar which seats against the back face of the rear bearing and the spindle is pulled back against the front bearing face by an adjusting nut and locking nut on the outer face of the spindle section. Immediately behind this the pulley wheel is located by a taper locking device screwed in through the centre of the pulley. The collett is slotted and this locates on a pin in the spindle to prevent rotation taking place between the collett and its housing.

Counting is done by a mechanical counter driven from the spindle itself so that actual revolutions of the specimen are counted. The centre portion of the load bearing section of the spindle is threaded and a gear wheel is mounted in the casing immediately above so that it meshes with the thread, thus as the spindle rotates the gear wheel shaft rotates and this through further gearing drives the counter. The threads and gearing have been selected so that a single digit on the counter represents 100 complete cycles of the specimen.

The loading beam is pivoted on a knife edge located in a sharp slot with a slightly wider angle than the knife edge. A weight hanger and a load connecting rod to the specimen are both suspended from knife edges positioned on either side of the fulcrum and giving a 5:1 ratio for load on specimen to load on weight hanger. One machine has a 10:1 ratio but Nottingham had problems due to the short lever arm causing excessive bouncing and so this machine was not used for any of the tests requiring

accurate quantitive results.

The load is transferred to the specimen via a small ball race which is a tight fit onto the specimen and is held against the shoulder by a spring circlip. The ball race is mounted in an outer cover and the loading arm is attached to this via a double horizontal leaf spring and pin joints into the cover. The leaf spring arrangement damps out oscillations between the specimen and the loading beam through the loading arm and thus ensures a steady load is applied to the specimen.

The most interesting sections of the machines is the facility for block programing or ultimately a triangular modulation of the load envelope. The load is varied by traversing a jockey weight along the loading beam, i.e. altering its position relative to the fulcrum. The jockey weight is pulled along the beam by a small D. C. electric servo-motor which can be reversed in direction by changing the polarity of the input voltage, and obviously the jockey remains in a fixed position when the power supply to the motor is interrupted. Thus the position of the jockey weight may be controlled by manipulating the supply to the drive motor. This is done by activating a series of micro-switches and use of a relay control system. In order to avoid having the weight of the micro-switches and their attachments at points on the loading beam and also the problems of tripping micro-switches with a large and awkward jockey weight a dummy beam carrying the micro-switches and a dummy jockey weight were used. The system was wired so that the dummy jockey weight followed the movement of the jockey weight on the loading beam. Four micro-switches were positioned on the dummy beam giving four positions or load levels at which the motor could be interrupted and a block of load applied at that level in any one test.

The length of the blocks was determined on a cycle count basis as follows:- The counter as stated previously was mechanical and part of the top cover was cut away to expose the gear wheels during the various stages of the counter. A shaft was positioned above the counter with a gear wheel which could be mounted to mesh with any of the counter wheels. This shaft is then rotated periodically by a few degrees and the length between the small rotations is uniquely related to the number of stress cycles experienced by the specimen and determined both by the number of teeth on the mesh wheel and the particular wheel on the counter with which it was engaged. Attached to the end of the shaft was a small cam which operated a pair of contacts which were connected to a traversing motor supply. When the cam closes the contacts the supply to the traversing motor is supplied on another circuit and, as the jockey weight leaves the micro-switch the relative relay closes again and so the supply is completed through the relay circuit. Once the supply is interrupted by a microswitch the weight remains stationary until the contacts are operated by the cam, thus the block lengths are determined by the cam profile. The end micro-switches operate on special relays which reverse the supply to the traversing motor, thus causing the weight to commence traversing back along the beam.

Electro-Magnetic Rigs

The maximum thrust vibrators that were available within the financial limitations were 40 lb. f. together with 250 V.A. amplifiers. The amplifiers were A.C. responsive only so that variations in mean stress at constant amplitude are not possible, however all other types of output are possible with the relevant input facilities.

The small forces available eliminated the prospect of doing axial tests and therefore the testing would be restricted to bending tests of some sort. As circular section specimens were already in use on the

rotating bending machines it was decided to keep to a circular cross section. The use of a lever arm to give pure bending with no shear forces on a specimen was considered but the design features required to eliminate excessive side loading on the vibrator table introduce the penalty of greatly increasing the external table weight and significantly reducing the system performance.

This left three main alternatives for a rig configuration.

1) A four point bending rig.

2) Central load application bending rig.

3) Cantilever bending rig.

If rig performance is assessed at given frequency then the critical features are as follows:-

a) Deflection of the driving system.

b) Force available from the drive system.

c) Stress levels available at the test section of the specimen.

d) The size, shape, and mass of specimen.

If simple comparisons are made on the basis of deflection and force close to the upper limits of the system then a cantilever bending system allows larger diameter specimens to be tested which are shorter in overall length or conversely specimens with the same diameter can be reduced in overall length and the deflection required from the system much reduced. Therefore the dynamic response of the system will be better for the cantilever. Also specimens of shorter overall length although not saving on material costs do significantly reduce the quantity of machining to be performed.

A further argument against multipoint bending rigs is that unless excessive penalties are to be incurred in specimen size and hence system performance the specimen must effectively be on simple supports at the

ends. This is relatively easy to achieve when the tests are conducted with a pulsating load, i.e., on one side of the zero and fluctuating about some mean value but when alternating loads are considered then the supports required to accommodate translation and rotation whilst being able to supply reaction in two directions are of a very complex and sophisticated nature. The small loads involved would necessitate extremely accurate machining and construction.

On the basis of the above arguments it was decided to construct suitable cantilever rigs.

The small forces involved mean that adequate stiffness is provided quite easily. The prototype rig was constructed from hollow rectangular steel section with clamping plates and bush mounting members in solid. It was all welded construction and finally welded on to a one inch thick base mounting plate which carried the vibrator. The use of all welded construction introduced certain alignment problems due to the distortion of the welded structure. The final design is shown in Fig. 3.2.

The specimen is mounted between two plates which contain a 90 degree V slot in which the specimen is located. The dimensions of the slot are such that when the shank of the specimen is inserted into the slot the plates are separated and can be bolted up clamping the specimen firmly between the two plates. The bottom plate is welded in between two hollow rectangular section columns and extends to a further pair of columns behind, it therefore acts both as a clamping plate and as a structural connection between the two pairs of columns. The top clamping plate is removable and clamping is achieved by the three rows of $\frac{1}{2}$" bolts. At the drive end of the specimen two columns carry a solid cross member which is drilled to locate a linear ball bushing originally used to control drive shaft location.

The three pairs of columns are welded on to two long narrow base plates and the cross members at the clamping end are cross braced to the structure at the drive end by two further hollow rectangular sections thus providing a very rigid sub-structure.

The two baseplates were pulled down on to the mounting plate by six countersunk cap head bolts, the mounting plate being drilled and tapped to accept these. The vibrator and drive system could then be aligned using a specimen. Locations were established for the vibrator mountings and the ball bushing controlling drive alignment. The sub-structure could then be removed for final machining. The base plate was then mounted on a concrete block which had been cast with rag bolts in position. The base plate was pulled down onto these bolts and a layer of grout. The blocks were manufactured so that when free standing on rubber vibration pads the relevant portions of the rig were at a convenient working height.

The first drive system used is shown in Fig. 3.3. The specimen end was held by four 4 B. A. screws with brass locknuts as shown. The table of the vibrator is equipped with nine 2 B. A. tapped holes and helicoils. The baseplate of the drive system is attached using 8 of these points. Vertical adjustment of the drive head is achieved by having the lower section of the drive shaft threaded L. H. at the bottom and R. H. at the top. Any lateral movement can be taken out by slots in the baseplate although with good alignment this should not be necessary. Above the clamping block with four holding screws the drive shaft is continued and runs up through a linear ball bushing. This provides some relief of the side loading on the ram. This drive system provides no real method of accommodating translation and rotation at the ends of the specimen, except after fretting between the specimen and the clamping screws. The structure is very stiff and movements in the longitudinal direction due to deflection are very small (0.0003") therefore the total end float is small and could be taken

out even by give in threaded portions. The rotation at the drive end of the specimen is significant. Test runs showed that the clamping screws quickly fretted a slight groove at the point of contact with the specimen. In long running specimens a certain amount of chatter from the drive clamping screws was evident, it did stabilize after about three hours of run time and not get significantly worse on any particular specimen. Strain gauged specimens were used to check the waveform for gross distortion but there was none apparent. The system therefore appeared to function in a satisfactory manner. One major fault became evident when longer trial runs were performed,,the clamping screws themselves were subject to fatigue and several failed just inside the housing, this led to the lock nut on that particular screw becoming slack and then the general slackness quickly led to the other lock nut and screws starting to unwind. Although it would have been possible to increase the size of the screws a slightly longer clamping block was required and this introduces further table weight penalties. A Rose uniball joint was tried with the drive system as shown in Fig. 3.4. In order to accommodate the greater length of the drive system a packing plate was inserted underneath each foot of the sub-frame. The rotation has been accommodated in the ball joint, the translation as stated previously is very small and is taken up in the inherent flexibility of the drive system. As the alignment control of the drive shaft has been eliminated when under load the drive shaft will be canted at a very small angle and this will lead to side loads on the ram but even at maximum output these will be less than 0.5 lbs. The same mounting plate attaching the drive system to the vibrator table is used together with right and left hand threads at respective ends of the drive shaft.

The specimens were turned down at the ends to fit the ball joint and several trial runs using strain gauged specimens were performed. The

ball joints started to show signs of wear and commenced chattering at around 30 hours of hard fatigue testing or about 6×10^6 cycles. It would be expected that on long runs with lower drive forces that the life would be considerably greater than this. Although the ball joints started chattering at 30 hours they ran on for long periods seemingly without getting a great deal worse and the wave form as displayed by the strain gauge records showed no significant distortion but none-the-less it was decided to replace ball joints at the end of any test during which they showed signs of deterioration.

As the results presented in this thesis performed in the electro-magnetic rigs do not depend on a knowledge of the stress levels involved only a brief description of the calibration procedure will be given.

Overall specimen performance was investigated by the use of strain gauges situated on either side of the notch. Due to the close proximity of the notch also the curvature and taper of the specimen it is not practicable to perform an analysis of the expected gauge output at varying stress conditions and therefore calibration is an empirical comparison of the dynamic gauge output with output in the statically loaded condition.

A sketch showing the position of the active strain gauges on the specimen is given in Fig. 3. 5. The gauges were bonded to the specimen surface using a 10:1 mixture by weight of Araldite MY 753 and Hardener HY 951.

The initial calibration and investigation of waveform produced by the rig was performed using an ultra violet recorder type S.E. 2800 recording strain gauge signals. A galvanometer was required which had high sensitivity and a flat frequency response up to at least 50 c/s. The galvanometer chosen was the B 100 which had the following properties:-

Natural frequency	100 c/s
Flat frequency response	60 c/s
Nominal Galvo resistance	80 Ω
Damping resistance	250 Ω
Max. safe current	10 m.A. r.m.s.
Galvanometer sensitivity	0.0025 mA/cm
	0.180 mV/cm.

The damping resistance of the galvanometer must be matched by the source resistance i.e. the resistance of the Wheatstone bridge strain gauge circuit. Any lack of balance between source and damping resistance must be eliminated by the use of series or parallel resistors and the consequent loss of sensitivity. It is therefore important that a gauge resistance is chosen which gives the best possible balance between the source and damping resistances. It had been decided to use gauges manufactured by Tokyo Sokki and the most appropriate gauge, taking into consideration gauge dimensions and resistance matching requirements, was the P.L. 10 S which has a resistance of 300Ω. This gave a source resistance of 300Ω from the bridge and a parallel matching resistor of 1.5K was required across the input to the galvanometer.

The Wheatstone bridge was completed by three dummy gauges bonded to a 0.3 inch thick mild steel plate to obtain some correction for overall temperature fluctuations. Each of the two active gauges had their own complete Wheatstone bridge so that accurate balancing of the bridge output could be obtained at zero load before connecting the output to the galvanometers. All terminals possible were enclosed as were the dummy bridge circuits and interconnecting cables used were sheathed with all sheathing being interconnected and finally earthed to the rig to eliminate noise problems. A 15 Volts d.c. supply to the bridge was provided by a

Farnell power pack and the supply was earthed to the mains. A simple sketch showing the basic circuit together with the calculation of the basic system sensitivity are given in Fig. 3.6.

The rigs are situated in a test cell and considerable fluctuation in the gauge output was noted due to strong fluctuating air currents from spurious large holes in the ceiling. Some fast rotating bending machines were producing a fine mist of oil which, spread by the air currents was steadily coating everything in the test cell with a film of oil. It was therefore necessary to eliminate the air currents and this stabilized conditions in the cell as far as short term temperature deviations were concerned.

The system was run open circuit with no feedback control and it was found to give a frequency response that was within 10% of being flat in a frequency range from 20 c/s to 50 c/s. Response to increased input voltage was linear within this range at a fixed frequency and gauge outputs in constant amplitude tests could be reproduced within a $\pm$ 2% band using a Servomex signal generator. A typical plot of voltage input to the amplifier versus strain gauge output is shown in Fig.3.7 for 3 frequencies. Further variation of course arises from the setting of the specimen in the machine and special setting procedures were followed to ensure repeatability. The specimen was set in the clamping blocks using a gauge produced to seat in the groove, run along the specimen surface and seat against the clamping block face when the correct distance between notch and clamping face had been obtained. Before the drive shaft is attached to the specimen two dial gauges are positioned at right angles and in contact with the specimen as close to the tip as possible. The drive shaft is connected ensuring that the specimen and hence vibrator table are not moved during the process.

A detailed appraisal of the random loading performance of the rigs is not presented as it is hoped that the performance will be assessed in the

future using on-line facilities to the G.E.C. 90/2 computer, and special signal analysis programs developed by Dr.Sherratt at the University which have more fatigue sensitive specification parameters.

Amsler Pulsator Type 30 PZBDA

This is a standard Amsler pulsator with a rated dynamic capacity of 30 tons. As implied by the name the ram is single acting and fatigue tests can only be carried out about a mean load. There are facilities on the Amsler for carrying out tensile, compressive or bending tests. The axial tensile and also the bending facilities were used for the tests described in Chapter 7.

The machine cylinder is carried at the top of the 4 main structural columns along with a heavy structural cross member which provides end load reaction in both compression and bending tests. The loading head is attached to the ram by two long threaded hanging columns which almost extend down to the bottom cross member which also contains the lower wedge chambers for axial tests. The loading head can be moved up and down the threaded columns driven by a small electric motor, and as it contains the upper wedge chambers for axial tensile tests also the top face is used with various attachments for either compression tests or the load application point in bending tests, a working space is provided which can accommodate long axial specimens.

The minimum stress is produced by a 3 piston pump and oil flow to the machine passes through a minimum load maintainer. The fluctuating load is superimposed on this static load and is produced by two pulsator cylinders. At zero load these have a phase displacement of 180° and so oil is pushed from 1 cylinder to the other with no output to the ram. When the phase displacement is altered by rotating one cylinder a pulsating output of oil is produced to the ram with maximum output when there is no

phase displacement between the two cylinders. Both the above supplies can be regulated and the maximum and minimum load on the specimen are shown on two pressure gauges. The gauges have trips which can be set once the running conditions have been attained so that the machine cuts out when significant increases or decreases in pressure occur. Standard safety precautions are taken throughout the machine construction.

The machine has two speeds of operation either 375 or 750 c.p.m. In dynamic tests it is necessary to correct the applied load for inertia effects due to the moving parts of the machine and the specimen itself. Amsler provide standard calculations and the necessary correction charts for individual machines for both speeds, and different specimen configurations.

SPECIMEN DESIGNS

The object of this work was to examine cumulative fatigue damage behaviour and to try and improve in a narrow field the approach to the design problem. The case for notched specimens has already been stated and it was further decided that a stress concentration $K_T = 2$ on net cross sectional area was in a region of major interest. Subsequently this has been upheld by a British Railways research divisions decision to base a long term cumulative damage research program on K_T values of approximately 2.

A major decision is the type of material to be used in the test program. There are strong arguments to be made in favour of using one special batch of material with uniform properties. The overall scatter of test results is reduced, the testing required is less due both to reduced scatter and the smaller number of S-N curves and other basic data requirements and, comparison of test results is easier when the possible influence of material properties in certain modes of behaviour is eliminated. Despite these strong recommendations for using a single special batch of material it was decided to purchase material in batches from a local steel stockist within the specification of B. S. 15 which is very widely used constructional steel.

The specification of B. S. 15 is very wide carbon content being specified as between 0.15 - 0.30% carbon and this variation in carbon content causes fairly large variations in material strength properties as will be shown later. In fact various batches of steel received swing almost the full extent of the specification. This wide variation in material behaviour is an embarrassment sometimes when trying to formulate test programs and analyse the results of these programs, however it does have one great advantage. The presentation and analysis of fatigue results

and the formulation of theories often suffers from a lack of generality of application, the results being strictly tied to a certain specimen configuration with a single material. Dealing with a widely varying material even within one specification and a range of specimen configurations forces an acute consciousness of the design problem and also rivets attention on general patterns of behaviour rather than a distorted pattern associated solely with one set of conditions.

All specimens except the large bending specimens were stress relieved at 700°C for 1 hour before machining operations commenced. No heat treatment was performed after completion of machining operations due both to the lack of facilities for stress relieving in vacuo and also the fact that most practical components contain some residual stresses due to machining.

Rotating Bending Specimens

The overall length and diameter of the specimens was determined by the existing machines. The only details to be decided were the position of the notch, its design and the required tolerances.

In order to avoid any concentrations due to the holding collett at the test section, the notch was placed one specimen diameter away from the holding collett. A KT value of 2.0 on stress on the nett cross-sectional area was required and this was achieved using a notch of 0.044 inches radius with a depth of 0.047 inches. This gives a KT value of 2.0 according to the tables of Peterson. Overall specimen diameter is 0.625 inches thus giving a throat diameter of 0.531 inches at the test section.

The above notch was the best balance between maximum size of test section and being able to generate the required stress levels.

A drawing of the specimen together with the notch detail are shown in Fig. 3.8. The tolerances were defined by the mechanics of the rotating bending machines and the desired accuracy in the stress levels. The sections of the specimen which are held in the collett and on which the end bearing are mounted respectively must be machined to within + 0.0005 inches. Also the two surfaces must be concentric, in order to prevent any bouncing of the loading arm when running speeds of 1500 r.p.m. are attained. A good turned finish is satisfactory for all of the specimen surfaces except that of the notch. The dimensions of the spigott on the loading end of the specimen are determined by the bearing size and the type of spring circlip used to retain the bearing. Details are shown in Fig. 3.8.

The notch was cut by form tools which were bought out. During the course of preparation of 3 batches of specimens both high speed steel and carbide tipped steel tools were used. The form of all tools was checked on a Nikon profile projector at a magnification of 50:1 both for irregularities in the cutting surface and also for radius. The position of the notch was specified relative to the spigott to maintain the loading lever arm and this was tied to a tolerance of $\pm$ 0.0005 inches giving a variation in stress level of less than 0.5%. The throat diameter of the notch was specified to a tolerance of $\pm$ 0.001 inches thus eliminating the need for individual load corrections on each specimen. The notch was cut with a low feed rate and lubrication to keep residual machining stresses to a minimum. The form tools were used to cut the notch on 18 specimens before they were re-sharpened and reformed. To avoid undue wastage or variation in the specimens the first specimens machined after a new notch tool had been set up were checked before the machining of the rest of the specimens allotted to that tool was allowed to proceed. Any grooves which showed bad machining pits at the root were rejected and the grooves in remaining specimens were lightly polished using three grades of emery

paper finishing with 00 cloth.

On the completion of all machining and polishing operations every specimen was checked on critical dimensions. The following checks were performed:-

1) The diameter of the spigott and the section to be held in the collett were measured.

2) The throat diameter of the notch was measured.

3) The distance from the spigott end face to notch centre line was measured.

4) The notch profile was inspected, using the Nikon profile projector on 50:1 magnification, for radius and general regularity of profile. Deviations of more than 0.0005 inches from desired profile were not accepted, except at the outer edges where the polishing operations gave a rounding of the edge.

5) The notch surface was examined and if any machining pits still remained and it was close to the limiting tolerances on groove dimensions the specimen was rejected.

Specimens with any dimension outside the specified tolerances was considered as a reject. Although not used as specimens during test programs they were utilized to obtain some idea of testing stress levels required for various purposes. They therefore served as useful guides in the formulation of the main test programs.

Due to the checks instituted during the machining of the notch and early trials performed to get the best machined surface possible direct from turning at the root of the notch, the actual rejection rate of specimens was very low.

Once the specimens were inspected and passed they were listed and then smeared with a coating of oil and stored in layers between oil soaked rags until required in the test programs.

Small Plane Bending Specimens

The electro-magnetic plane bending rigs were designed about a 40 lb f thrust vibrator.

A specimen with a test section of not less than 0.250 inches was desirable and also at the time that the design was conceived a specimen that could also run as a plane specimen was required. The solution decided upon was a lightly tapered cantilever specimen with a heavy reinforcing radius leading up to the clamping shank of the specimen. On static load considerations this moved the maximum stress out from the root by approximately 1.5 inches on a cantilever arm of 6 inches. Maximum stress was again approximately 40% in excess of root stress neglecting reinforcing and clamping stress concentrations. Approximate calculations were performed to investigate any redistribution of stresses due to inertia loading at a frequency of 40 c/s but the effect was minimal. A check on the calculated stress distribution was made using strain gauged specimens and agreement to within 5% of the calculated and measured distribution was obtained. No specimens have so far been run in the plain condition in a test program, all the results reported being for notched specimens.

The notch on the specimens was positioned in the region of maximum stress on a plane specimen and placed 1.5 inches away from the root of the cantilever. Although a greater test section could have been obtained by moving the notch closer to root, sufficient room was left to mount a strain gauge between the notch and the root of the cantilever. To minimize tooling costs the same notch radius as for the rotating bending specimens was used, the tools being reformed and sharpened before use.

Petersen was used for design of the notch which was made semi-circular to give a maximum KT value of 1.67, this is a figure neglecting the taper on the specimen and the variation in bending movement across the section.

A drawing of the specimen and the notch detail are shown in Fig.3.9. The use of the 0.044 inch radius and a semi-circular notch gave a throat diameter of 0.250 inches at the notch.

The specimens were machined from a batch of steel to B.S. 15 specification purchased from the local stockist. The steel was stress relieved in bar form before being machined. Due to pressure on the University workshops the specimens were manufactured out except for the machining of the notch. A mistake was made in the drawing released to the manufacturers, the drawing was done on centre lines but the concentricity between the two ends of the specimen was not given a specific tolerance, therefore the manufacturers assumed the normal open limit of 0.010 inches. This of course gives a slight twist in the specimens if the concentricity deviates from zero. Random checks showed that most specimens were out by between 0.006 inches and 0.009 inches on concentricity. Check calculations were performed to investigate this lack of concentricity and it was found that the variation in stress levels was less than 1% which was considered as tolerable.

The lack of concentricity proved to be a considerable problem in the machining of the notch and the standard specified on the drawing could not be achieved. The specimens were inspected on each of the specified dimensions but on the notch considerable latitude was allowed on the actual notch depth although the notch throat diameter was measured in each case so that loading corrections could be applied to individual specimens. Rigid control of the radius at the root of the notch was maintained as with the rotating bending specimens, and the variations in notch depth of up to 0.004 inches do not cause significant variations in the value of the stress concentration factor.

The same polishing and inspection operations were performed on each specimen as had been performed on the rotating bending specimens.

The specimens were again stored smeared with a coating of oil while awaiting testing.

Axial Specimens for the Amsler Pulsator

Mild steel is reported in the literature notably by Frost (1962) as being insensitive to mean load. Therefore when designing a specimen no great reduction in the total stress range is possible, but if the mean load is pitched too high then gross yielding takes place, and if the mean load is too low then the required alternating stress may take the machine load below the recommended limit of the manufacturers. This precludes the testing of small notched specimens where the required machine loading is very low. As tools had already been purchased for radius 0.044 inches and 0.100 inches an attempt was made to base the notch design on grooves with either of the above radii. The final specimen design is shown in Fig. 3.10. The specimen diameter was 1.300 inches where it was gripped in the jaws and this was reduced to 1.200 inches over the 4 inch centre section with a tolerance of $\pm$ 0.0005 inches. The notch was positioned at the centre of the above section and was a 0.100 inch radius circumferential groove with a depth of 0.100 inches. This gave a throat diameter on the notch of 1.000 inches, and a K_T value of 2.17.

The specimens were machined from 1½ inch diameter mild steel bar to B. S. 15 which had been stress relieved. The usual precautions were taken in machining the notch.

The notches received the same polishing treatment as all previous specimens and when this was completed each specimen was inspected. The machining of the notches was not to very high standard and the $\pm$ 0.001 inches tolerance on root diameter was not held. Therefore an individual load correction was applied to each specimen when testing commenced.

All specimens were again smeared in oil whilst awaiting testing.

Large Plane Bending Specimens

Some testing on the axial specimens had been completed when the specimens were designed. Therefore the range and mean of surface stress to be provided was a great deal clearer.

The object was to obtain close to the largest size of test section in the Amsler, therefore the span was of great importance. The limiting factor on span proved not to be the size of the Amsler but the maximum length that could be machined in the University workshop. Diameter was no problem but no greater length than 42 inches would be accepted on lathes for machining, with allowances for the end loading plate width and a small overlap this effectively reduces the span to 36 inches. The location of the notch was next considered, it is essential that it be displaced from the loading point.

Trial calculations were performed with the notch of $K_T = 2.0$ on net cross sectional area located 6 inches away from the point of load application, these showed that the maximum net test section size was approximately 4.3 inches and the selection finally made was for a 0.258 inch radius groove with a depth of 0.323 inches, giving a total specimen diameter of 4.946 inches. During the initial machining stages it was found that the 5 inch diameter bar would not clean up at this dimension and the outer diameter was therefore reduced to 4.823 inches. The notch dimensions were maintained and the final K_T value of the notch from Petersen was 2.21 on net cross sectional area. A drawing of the specimen showing final dimensions is shown in Fig. 3.11.

The batch consisted of 12 specimens and two form tools of 0.258 inch radius were purchased for the machining of the 24 grooves. Due to the much greater depth of the groove one tool was used for roughing out

and the other tool for finishing operations. The tools themselves were checked for profile on the Nikon but with such large specimens it was impossible to mount them in the Nikon for checking. Replicas of the grooves were considered, but as no trouble had been experienced with profile on all previous specimens these were accepted with no formal profile check. Throat diameter and overall diameters were checked, and the machining had been excellent, 10 out of 12 specimens being to nominal dimensions on throat diameter.

During final machining processes on the notch the specimen was marked in order to facilitate an accurate longitudinal setting in the Amsler.

LAYOUT OF ROTATING BENDING MACHINE

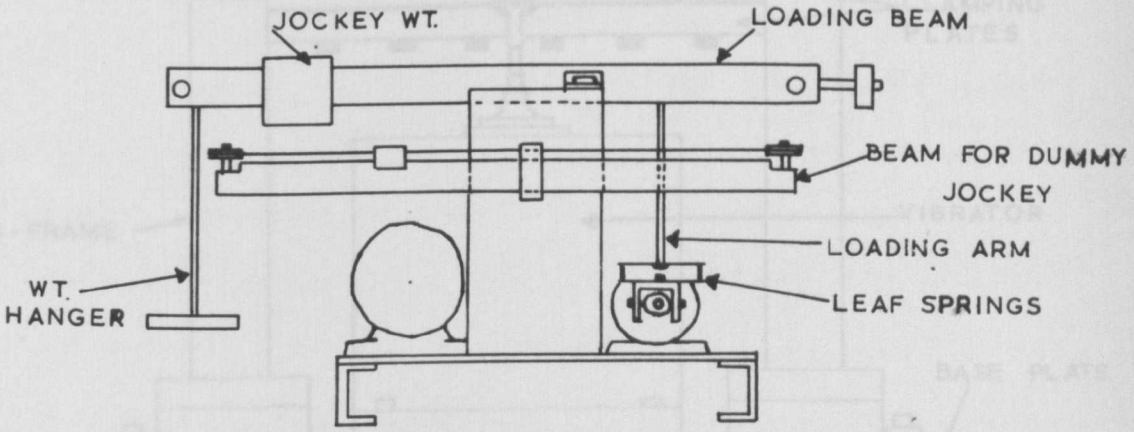

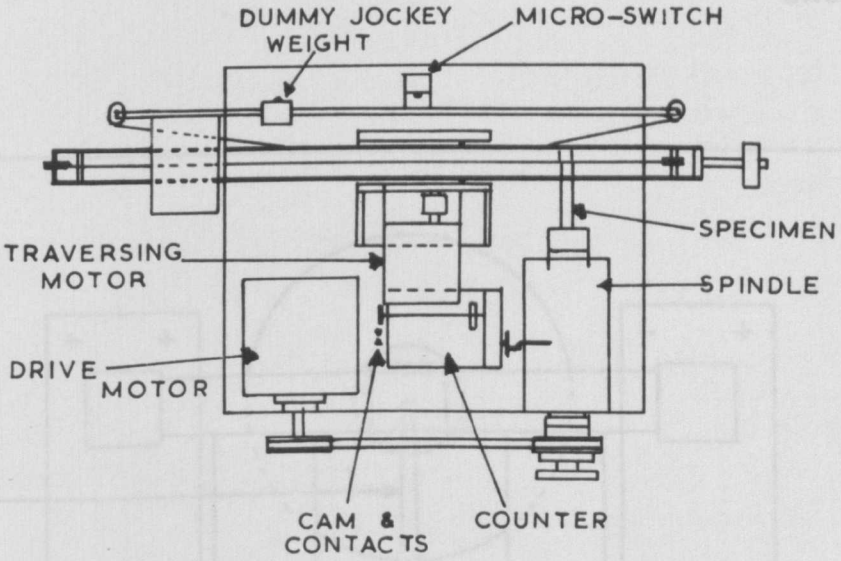

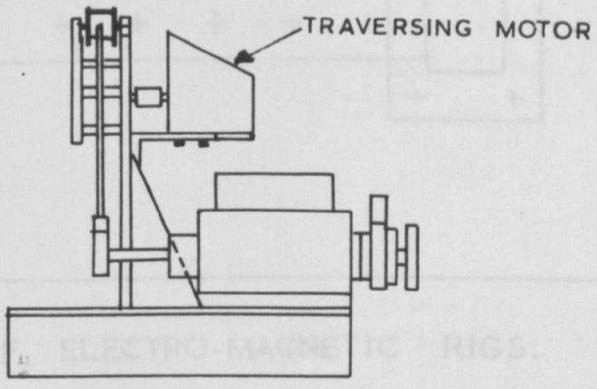

FIG. 3.1.

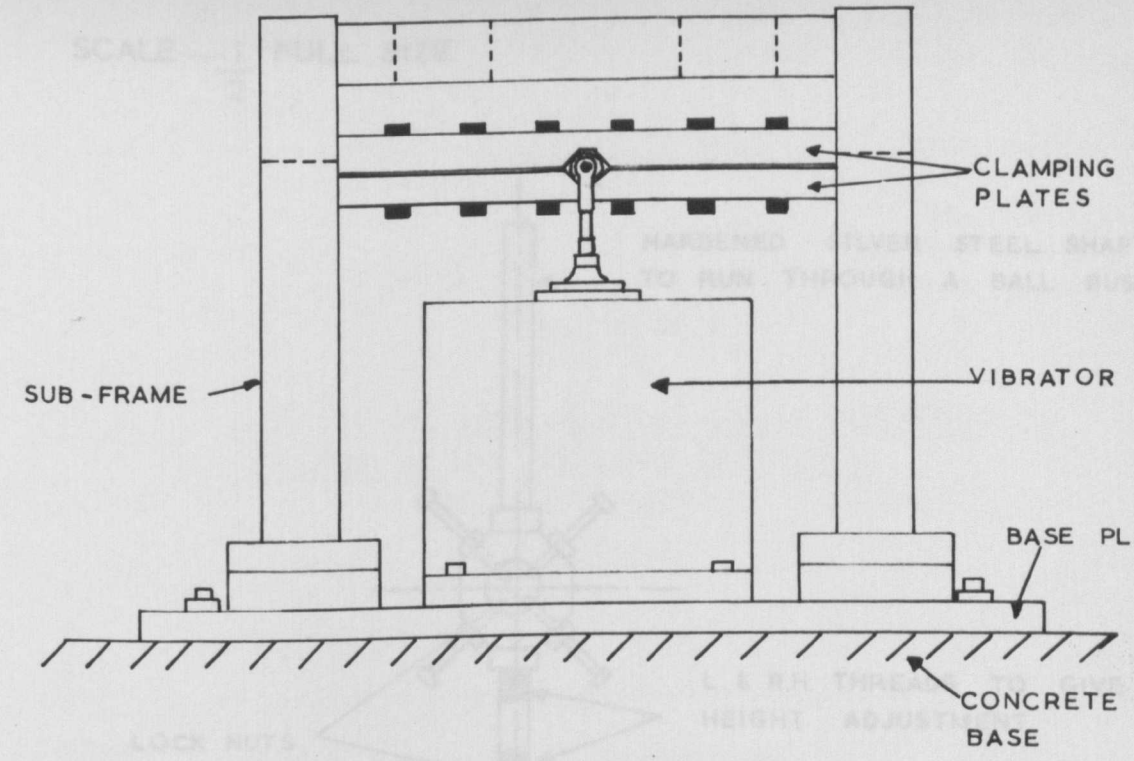

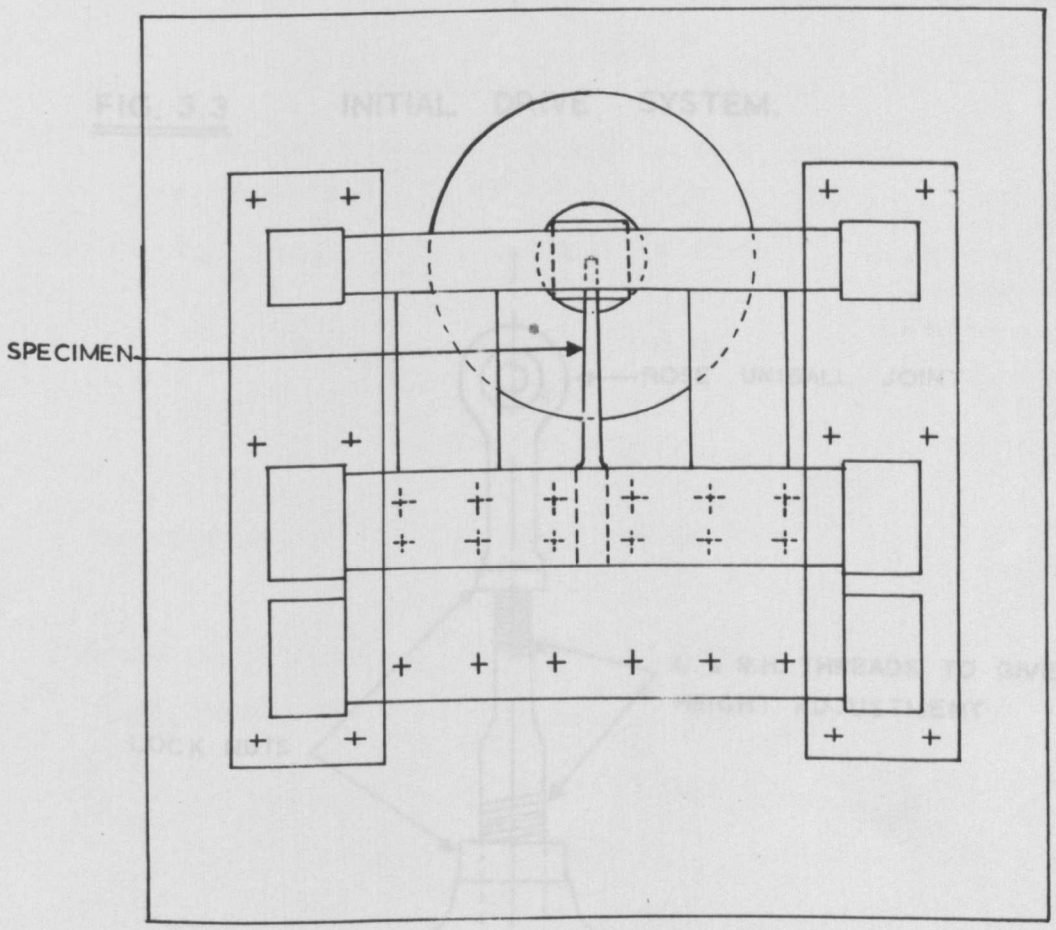

LAY-OUT OF ELECTRO-MAGNETIC RIGS.

FIG. 3.2

SCALE — $\frac{1}{2}$ FULL SIZE

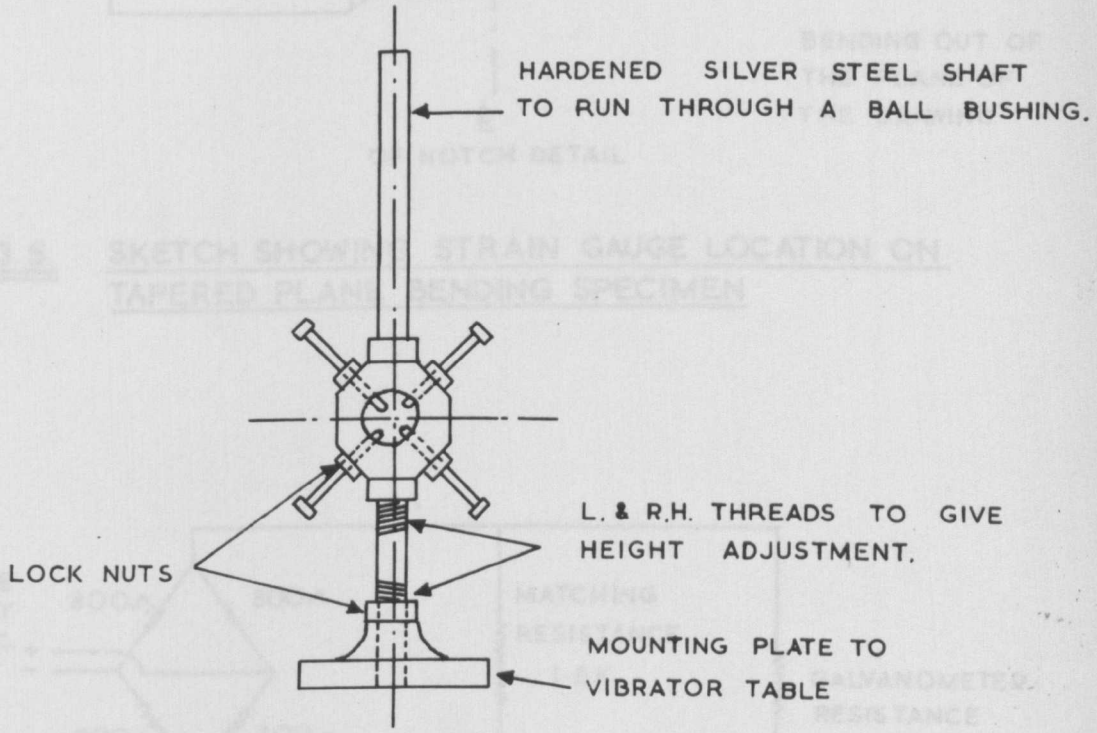

FIG. 3.3 INITIAL DRIVE SYSTEM.

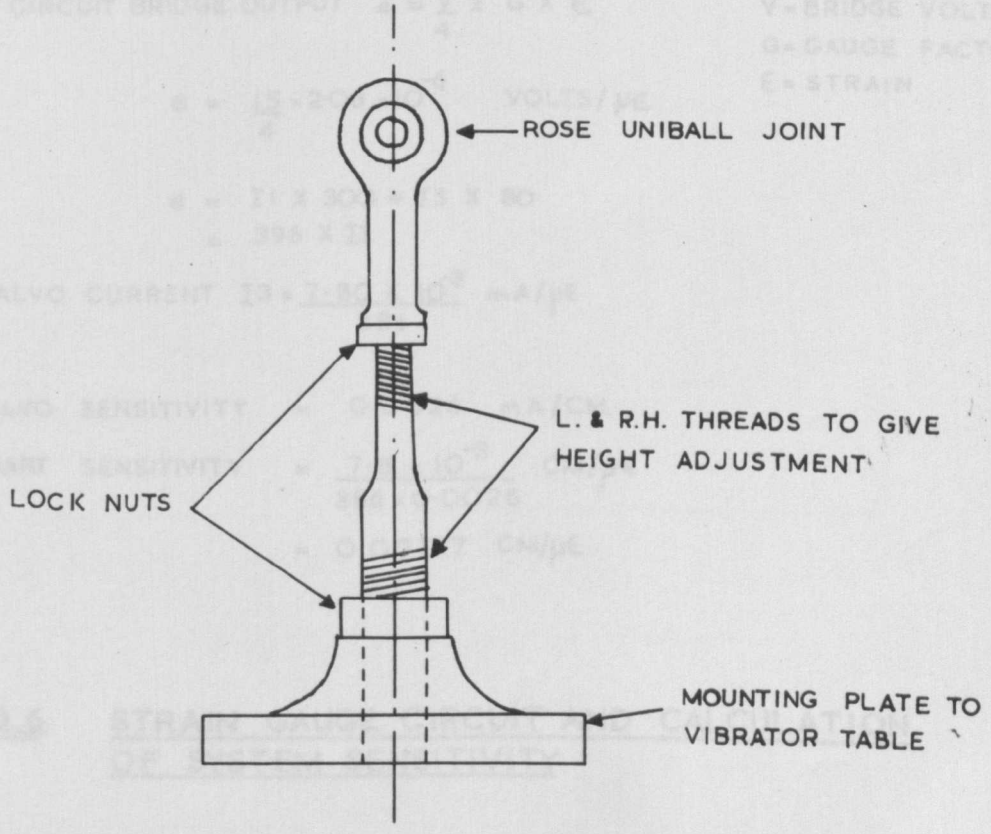

FIG. 3.4 FINAL DRIVE SYSTEM.

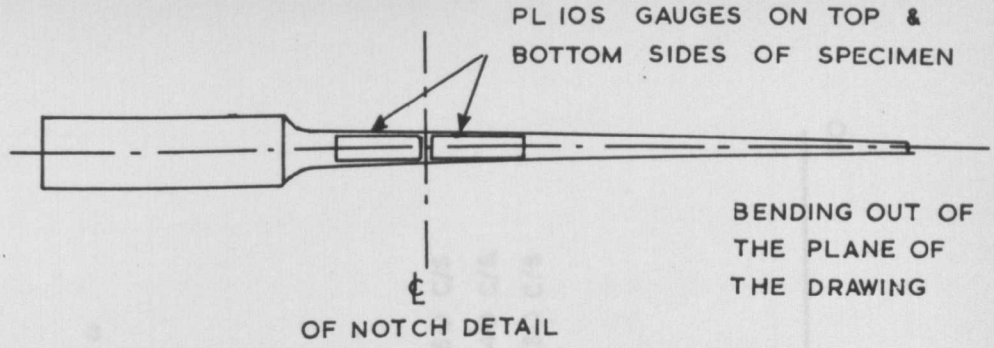

FIG. 3.5. SKETCH SHOWING STRAIN GAUGE LOCATION ON TAPERED PLANE BENDING SPECIMEN

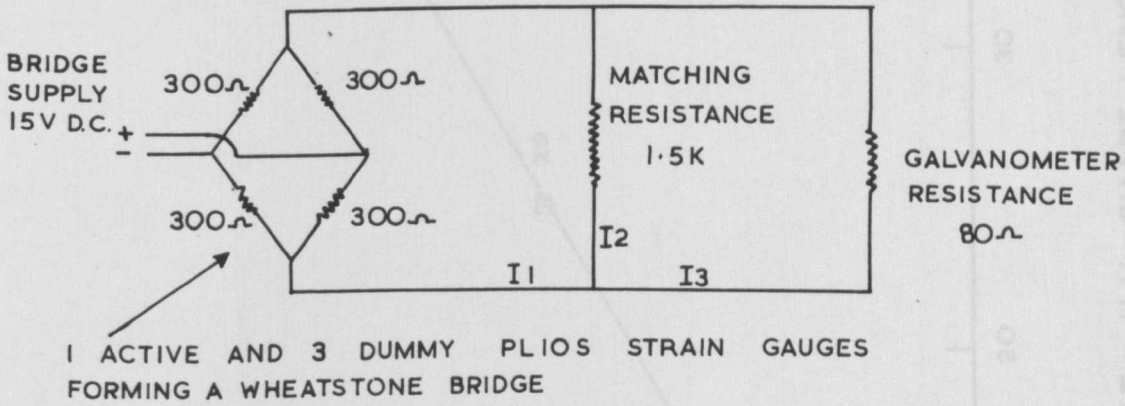

OPEN CIRCUIT BRIDGE OUTPUT $e = \frac{V}{4} \times G \times \epsilon$

V = BRIDGE VOLTS
G = GAUGE FACTOR
ϵ = STRAIN

$$e = \frac{15}{4} \times 2{\cdot}08 \times 10^{-6} \quad \text{VOLTS}/\mu\epsilon$$

$$e = I1 \times 300 + I3 \times 80$$
$$= 396 \times I3$$

GALVO CURRENT $I3 = \frac{7{\cdot}80 \times 10^{-3}}{386}$ mA/$\mu\epsilon$

GALVO SENSITIVITY = 0·0026 mA/CM.

CHART SENSITIVITY $= \frac{7{\cdot}8 \times 10^{-3}}{386 \times 0{\cdot}0026}$ CM/$\mu\epsilon$

$= 0{\cdot}00777$ CM/$\mu\epsilon$

FIG. 3.6. STRAIN GAUGE CIRCUIT AND CALCULATION OF SYSTEM SENSITIVITY

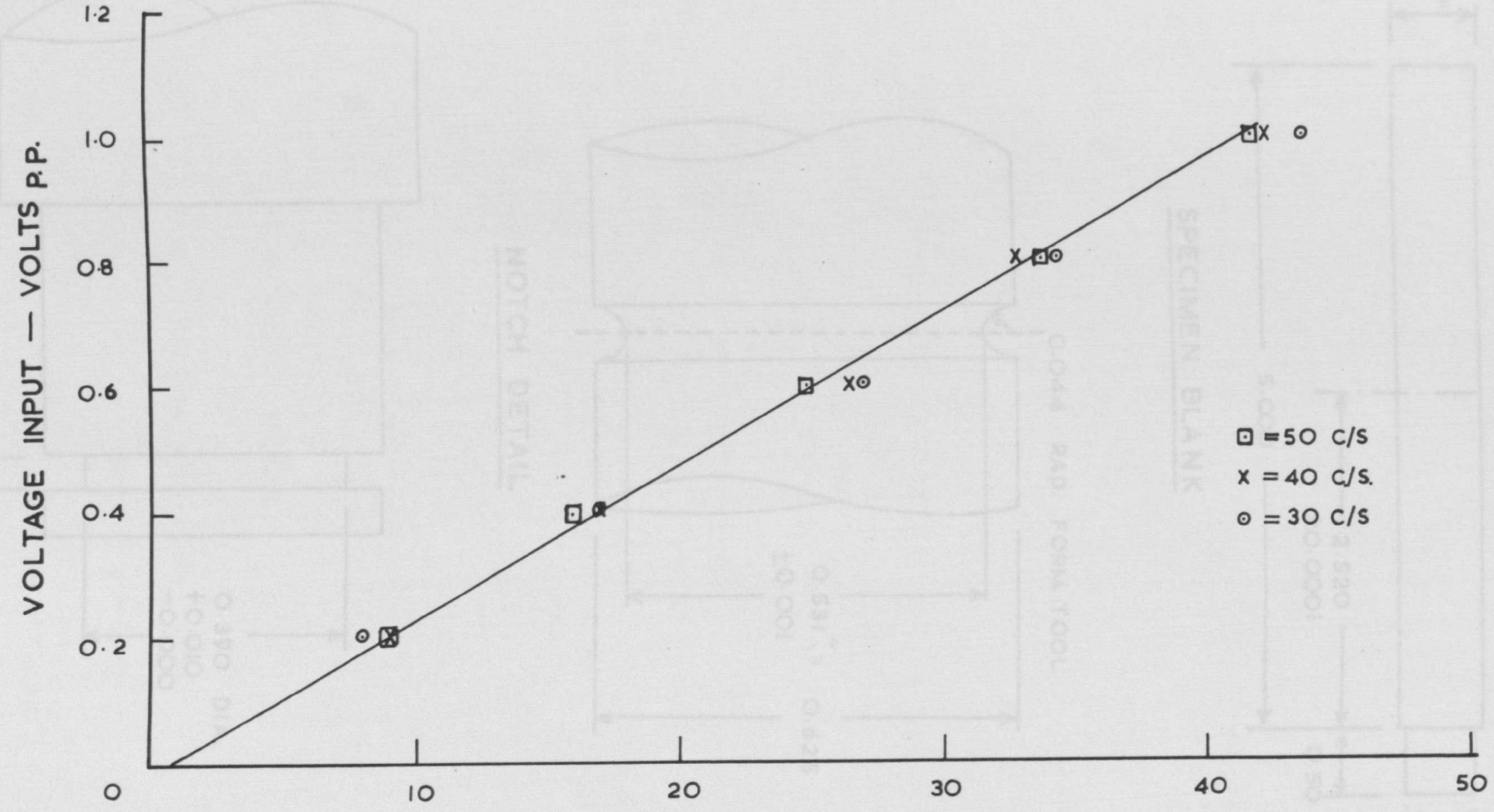
VOLTAGE INPUT — VOLTS P.P.
1·2
1·0
0·8
0·6
0·4
0·2
0
10
20
30
40
50
⊡ =50 C/S
X =40 C/S.
⊙ =30 C/S
SYSTEM RESPONSE — U.V. CHART LENGTH M.M.

FIG. 3.7.

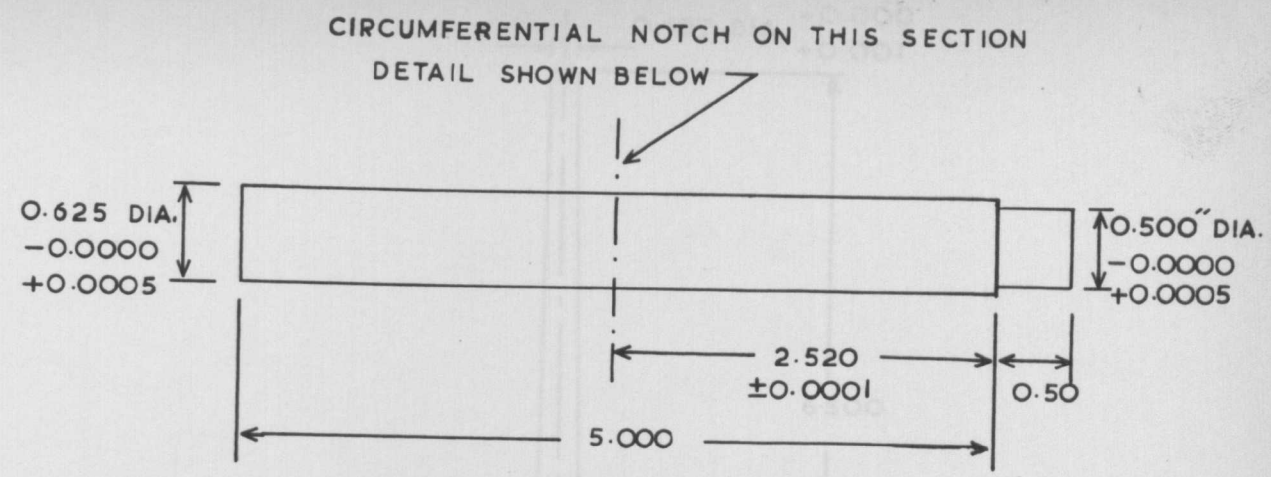

SPECIMEN BLANK

TYPE I

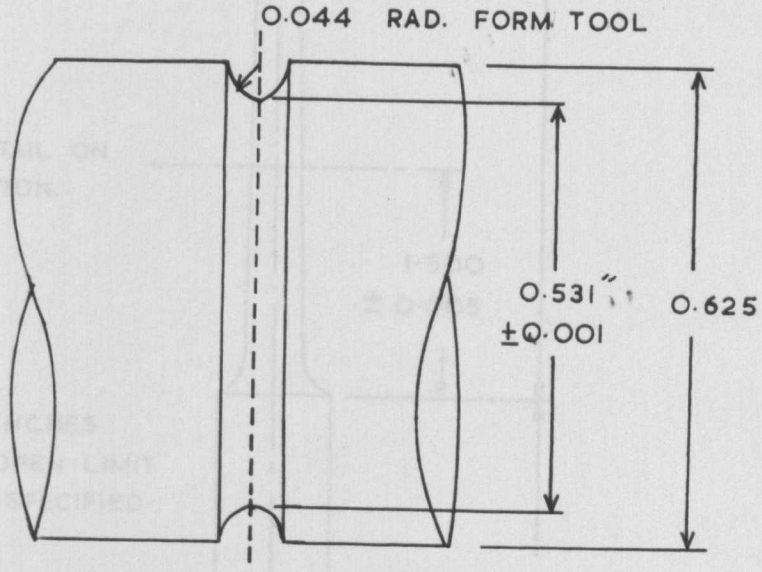

NOTCH DETAIL

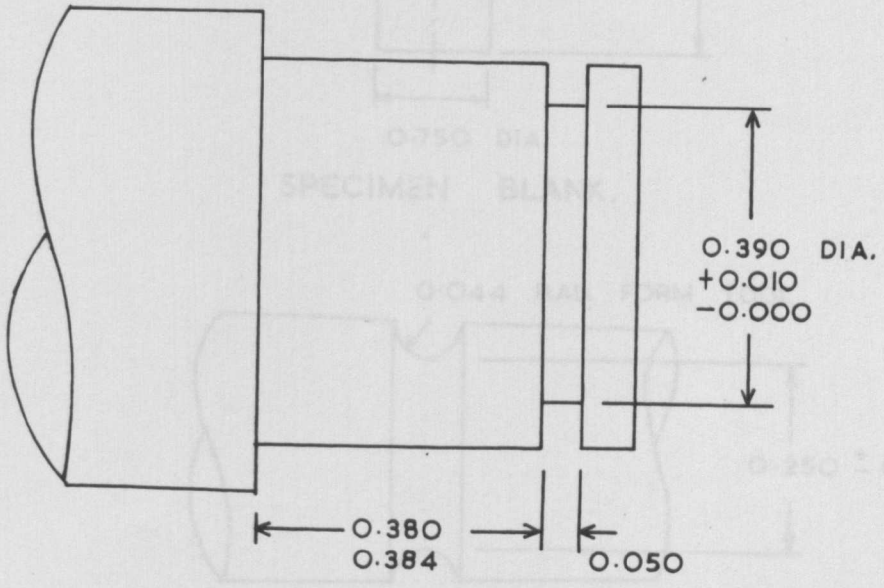

SPIGOT DETAIL

DIMENSIONS :— INCHES

FIG. 3.8.

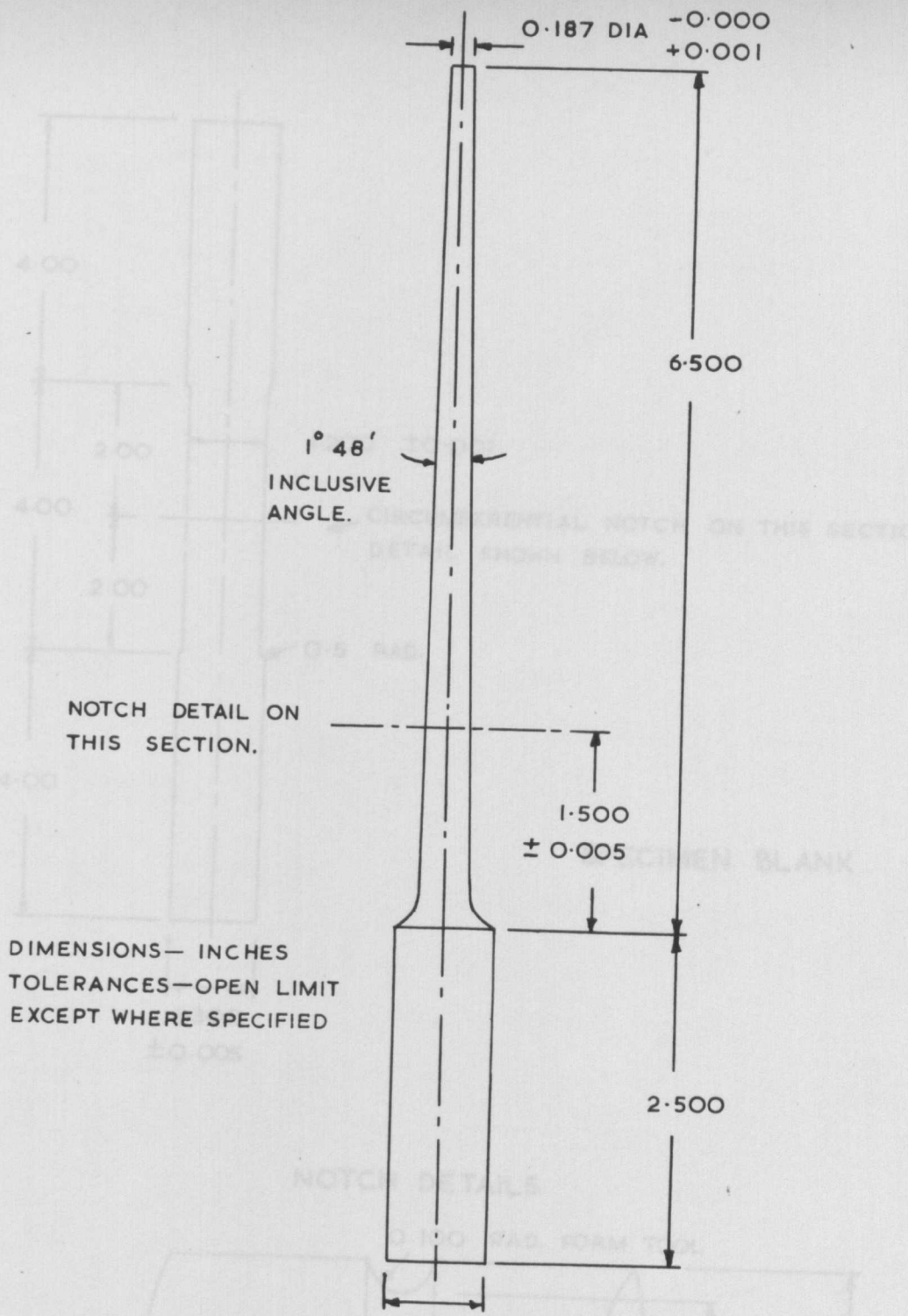

SPECIMEN BLANK.

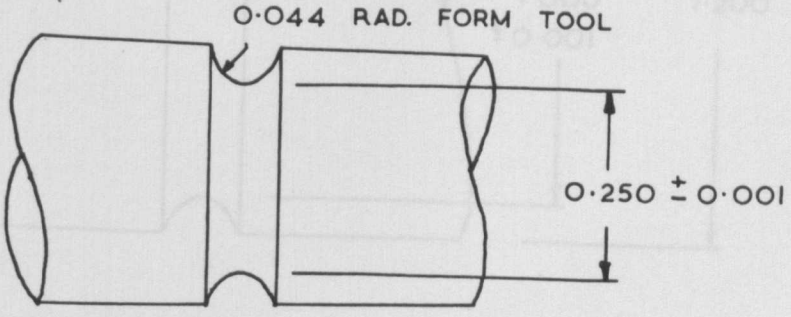

NOTCH DETAIL.

FIG. 3.9.

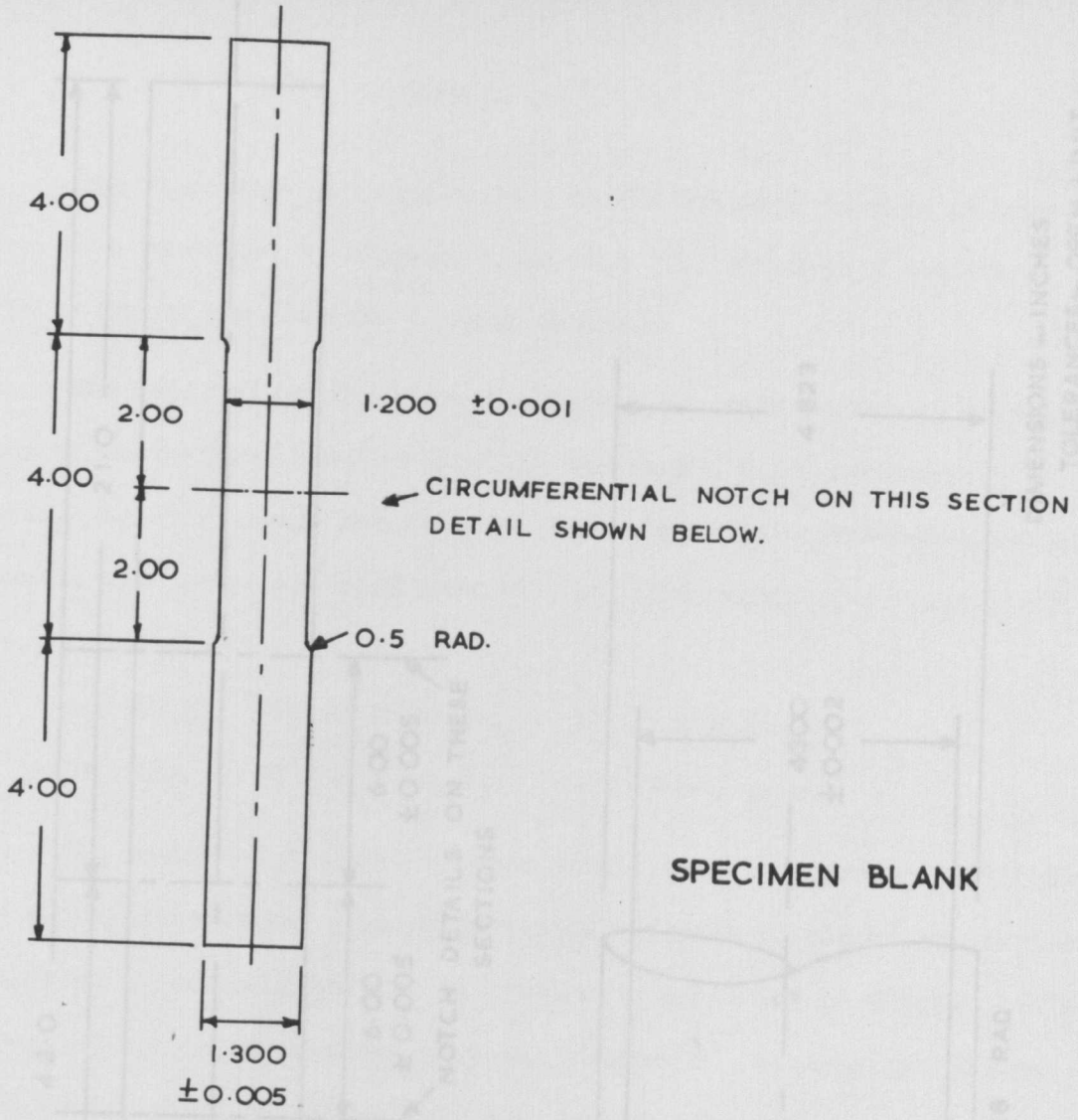

SPECIMEN BLANK

NOTCH DETAILS

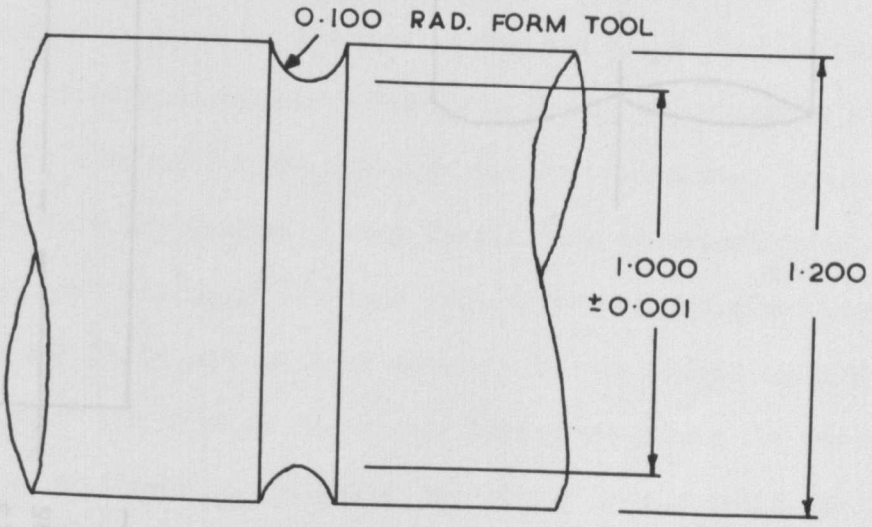

DIMENSIONS — INCHES
TOLERANCES — OPEN LIMIT EXCEPT WHERE SPECIFIED

FIG. 3.10.

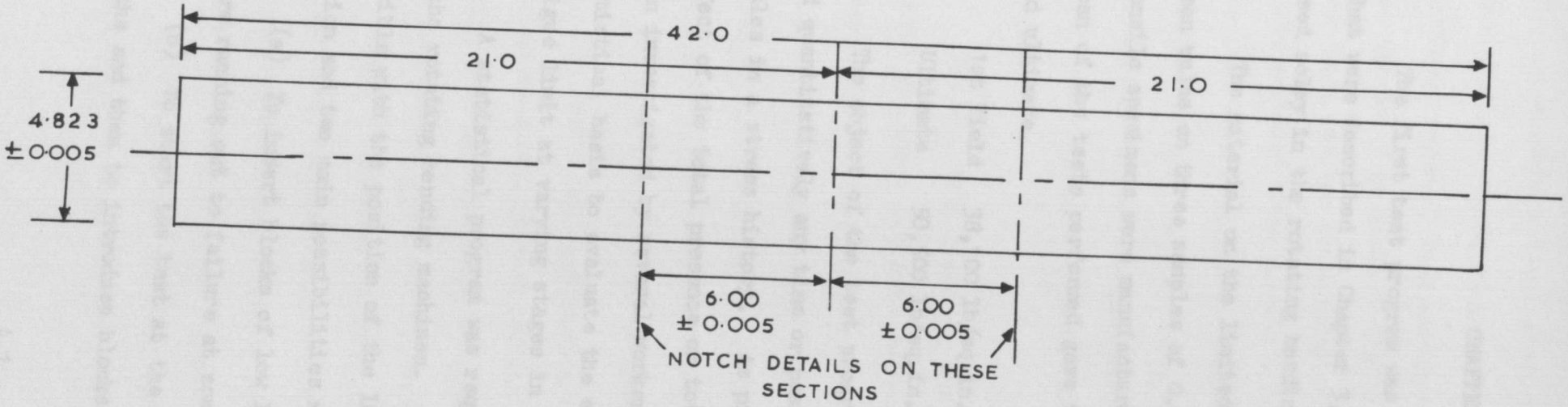

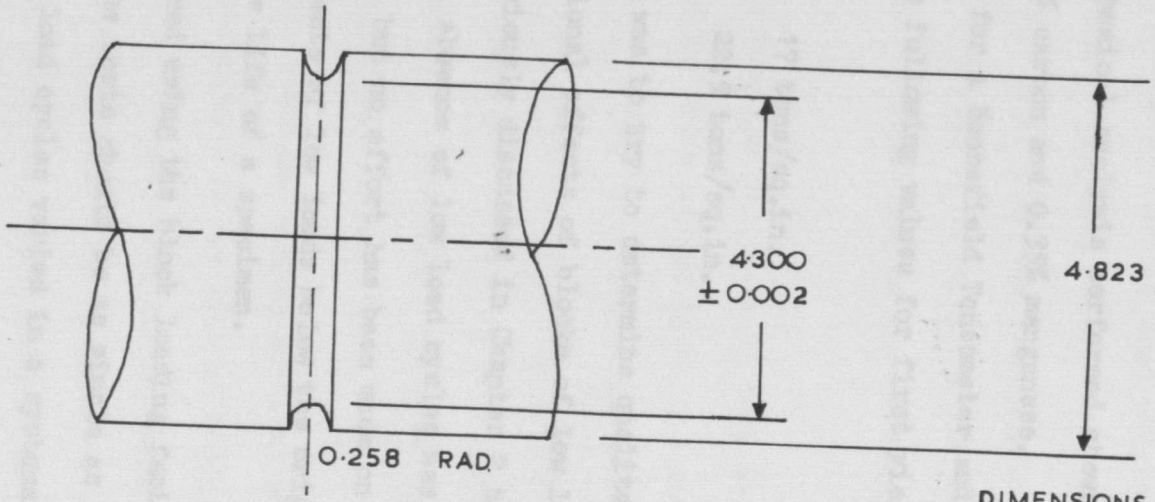

DIMENSIONS — INCHES
TOLERANCES — OPEN LIMIT —
EXCEPT WHERE STATED.

FIG. 3.11

CHAPTER 4

The first test program was run on the rotating bending machines that were described in Chapter 3, as were also the type I specimens used soley in the rotating bending machines.

The material on the limited chemical analysis performed showed a mean value on three samples of 0.15% carbon and 0.35% manganese. Tensile specimens were manufactured for a Hounsfield Tensometer and the mean of the tests performed gave the following values for first yield and ultimate.

1st Yield	38,100 lb/sq.in.	17 tons/sq.in.
Ultimate	50,500 lb/sq.in.	22.5 tons/sq.in.

The object of the test program was to try to determine qualitatively and quantitatively any time or positional effects of blocks of low load cycles in a stress history. As previously discussed in Chapter 2 the effect of the total presence or total absence of low load cycles has been investigated by several workers, but no effort has been made on a statistical basis to evaluate the effects of low loads below the original fatigue limit at varying stages in the life of a specimen.

A statistical program was required using the block loading facilities of the rotating bending machines. The tests should be as simple as possible with the position of the low load cycles varied in a systematic fashion and two main possibilities were feasible on an experimental basis:-

(a) To insert blocks of low load cycles for various given periods before running out to failure at some constant higher stress amplitude.

(b) To start the test at the higher stress amplitude for varying lengths and then to introduce blocks of low stress levels until failure.

A simple two level block program was used with the testing split into two main sections, hereafter called Section X and Section Y, with different types of load envelope for each section. The load envelope for Section X is shown in Fig. 4.1 and consists of a program of high and low load, the low loads being present from the start of the test and being excluded after a certain predetermined number of load programs, M. The test then continues to failure at the high load level. The load envelope for Section Y is shown in Fig. 4.2. The low load levels are excluded for a predetermined number of cycles N_R after which the same two level load program as used in Section X was introduced and continued until failure.

The high load level σ_h was the same for all tests in both Sections X and Y and three different values of the lower stress level σ_1 were investigated. Four different values of M and N_R were used in Sections X and Y respectively so that each section consisted of a 4 x 3 block giving 12 test conditions. Four specimens were tested at each condition giving a total of 48 specimens per section. The values assigned to σ_1 were all below the original constant amplitude fatigue limit.

The design and construction of the rotating bending machines and also the specimen, imposed certain restrictions on the type of block loading program which could be obtained. The counting system was such that programs of length 2,000, 20,000, 200,000 could be obtained before repetition. A program length of 2,000 cycles was too short for the slow speed of the traversing motors and programs of 200,000 cycles and greater presented some difficult problems in the cam operation. The minimum traversing time was approximately 1 minute, thus on a machine doing 1,500 r.p.m. the length of cam available for the operation of closing and re-opening the contacts was less than 3 degrees. The slack

in the drive mechanism could easily account for this amount of movement and it was felt that reliable operation would not be secured, so a program length of 20,000 cycles was used. The block lengths selected were 8,000 cycles at high load and 12,000 cycles at low load, and obviously these figures differ slightly by the length of traversing time for individual machines.

The range of stress available on the rotating bending machines is limited by the weight of the jockey and the length of traverse along the jockey beam allied to the particular specimen design. A total possible range of 4.60 tons/sq.in. nominal stress on net cross-sectional area was available for the Type I specimens.

In order to select the relevant test stress levels a preliminary S-N curve was run at constant amplitude. The stress level giving a mean life of approximately 1 million cycles was selected as the high stress level, and then 5 specimens were run on each machine both to obtain a reliable mean life at this level, and a statistical calibration of the machines. The results of these tests are shown in Table 4-1 along with the abbreviated statistical calculations which show that there is no significant difference in the mean lives produced by the three machines. The S-N curve was then completed and is shown plotted in Fig. 4.3. The three values of σ_1 to be investigated were selected as 7.84, 7.19, 6.53 tons/sq.in. nominal, respectively. The values selected for M in Section X were 27, 54, 81 and 108 programs and for N_R in Section Y were 100,000, 300,000, 500,000 and 700,000 cycles.

The tests were distributed between the three machines in a regular pattern, but the selection of specimens for a particular test was by a random draw. The specimens, which had all been stored smeared with oil, were cleaned with carbon tetrachloride immediately before a test commenced.

Setting of the specimen in the collett accurately was a problem and so a small setting tool was made which fitted on the specimen surface, locating in the groove at one end and seating against the collett face when the correct distance was set.

The machines had originally been designed with an oil drip feed which lubricated both the counter drive and the main bearings of the spindle. Under test conditions oil seeped out past the bearings and collett along the specimen producing a thin coating of oil over much of the specimen including the notch. Packing the bearings and the casing around the counter drive with grease and eliminating the oil feed cured this problem and also the machines ran cooler.

Section X of the test program was run first and the results are presented in Table 4-2. The value of the Miner summation while the jockey weight was traversing to the new position was calculated using the method given by Marsh(R64) for evaluation of Miner summation with a sawtooth modulation of applied load.

The data was tested for fit to the normal distribution and it was found that the best fit was obtained with the log-normal distribution. The plot to test the fit is shown in Fig. 4.4. The results were analysed using standard statistical techniques, the deviation in variances was checked using the "F" test and found to be significant so that several test conditions were censored. The remainder of the results were examined for significant differences in mean values using a series of one factor analyses. No statistically significant variations in mean values was detected and thus it is futile to attempt any further analysis of this section of the program.

A time lapse of several weeks occurred between running Section X and Section Y of the program due to holidays and moving the testing equipment. When testing was re-commenced considerably longer lives were being obtained and so further constant amplitude tests were conducted at the σ_h stress level of 9.80 tons/sq.in. The mean life at this level was found to have increased from 1,052,000 cycles to 1,755,000 cycles. Some of this was undoubtedly due to the change in humidity between when Section X was run during the winter and its level during the early summer when Section Y was run. Lui and Corten(1960) have reported a 20% rise in life due to the decrease in humidity during the summer. Another possible explanation is a difference in residual stresses due to machining between the two batches of specimens. They were machined as separate batches and a different operative and a slightly different technique were used on the second batch. Subsequently specimens were pushed through the shop for machining in batches of 200 - 250 specimens. As corrections to the Miner summation for the traversing line are generally small the S-N curve was assumed to have the same slope with a knee at the same cycles limit i.e. at a slightly higher stress level. It is expected that errors induced by this assumption are less than 1%.

The results of the program together with the Miner summation values are shown in Table 4-3. The results were again tested for fit to the normal distribution, the log conversion giving the best fit to data. The same style of statistical analysis was performed on these test results, i.e. comparison of variances using the "F" test and one factor analysis to determine significant differences in means. Although the test data was more consistent in this section the quantitative analysis was almost equally disappointing with insufficient statistically viable data to

establish any definite trends. The only notable feature was that the lower stress levels appeared to be more damaging than those immediately below the fatigue limit.

However this section of the program provided a large number of specimen fractured surfaces with block program markings on them. Measurement of the markings was performed on the Nikon projector. The fractured surface could be projected onto a screen containing a graticule at magnifications of 10:1, 20:1 or 50:1. The illuminating power at 50:1 magnification was insufficient to allow program markings to be distinguished and although they could be seen at 20:1 the very much sharper image at the lowest magnification of 10:1 was used for obtaining measurements. The specimen is mounted on a table which is manipulated by two micrometers each reading to 0.0001". Readings were only taken on radial lines which were perpendicular to the program markings i.e. on sections where the program markings are parallel to the specimen surface. This section was lined up on the vertical graticule of the screen and thus the specimen could be traversed relative to the horizontal graticule along the section of interest using a single micrometer on the table. Photographs of typical fracture surfaces are shown in Fig. 4.5 and Fig. 4.6. As the exact borders of the propagation at the low stress level is indistinct it was decided to chart the progress for each block of cycles consisting of 12,000 cycles at σ_l and 8,000 cycles at σ_h. Measurements were performed on all specimens which exhibited more than five sets of markings. In general the first 0.080 inches to 0.120 inches of the specimen do not exhibit any program markings as they are either too small to be distinguishable or have been eradicated by the fractured surfaces rubbing together. In exceptional cases markings were observed at a crack depth of 0.036 inches and over twenty sets of block marking were visible.

Semi-logarithmic plots of $\log_{10} L$ versus the number of cycles proved to be non-linear but plots were also made following Frost's (1958) suggestion of $\log_e L/L_o$ versus cycles where L is the length of the crack including the depth of the notch and L_o is the original crack depth i.e. in notched specimens the depth of the notch: The plots were in general linear and typical examples are shown in Fig. 4.7 and Fig. 4.8. When plotting such a parameter as $\log_e L/L_o$ most of the scatter in the actual rate of propagation is passed over and therefore another semi-logarithmic plot was examined in which the log of the increment in crack length during one block was plotted against the crack length excluding the depth of the notch. A few of these plots are shown in Figs. 4.9 and Fig. 4.10. An interesting feature of these plots is the way in which the curve smooths out at crack lengths in the order of 0.11 to 0.13 inches. Thus the actual crack growth rate per block appears to be very irregular below this crack length although the normal crack propagation plots indicate a very steady and predictable overall rate of growth.

The slopes of the $\log_e L/L_o$ versus cycles plots for the specimens examined appeared to bear no general relationship either to the life of the specimen or the particular stress conditions involved and so the available data was extrapolated back to a crack depth of 0.005 inches. In some cases a change in slope of the $\log_e L/L_o$ versus cycles plot was observed close to the limit at which markings were visible. An example is shown in Fig. 4.11 where the plot for Spec. No. 1.2.13. is shown. It is possible that this increase in the crack propagation rate is merely that the very finely spaced program markings have not been observed correctly but this possibility is largely eliminated by Spec. No. 1.2.13. which exhibits the same break in crack propagation rate. Estimates based on the final rate of propagation lead to an estimate of high cycles sustained with a

crack > 0.005 inches long as 456,000 cycles. The actual number sustained during total life was 501,600 cycles and this leads to a figure of 45,600 cycles of high stress for initiation and development of a crack 0.005 inches long. Allowing a nominal initiation period of say 20,000 cycles the final crack propagation rate is only 2½ times faster for a crack of 0.080 inches as compared to a crack of under 0.005 inches. It is likely therefore that the final rate observed in this case is a slow crack propagation phase as the crack grows quickly in other sections of the specimen re-orienting the crack front. The portion of the life spent from growing a crack from 0.005 inches to failure was calculated for each of the specimens examined from the $\log_e 4l_o$ data plotted on a log scale versus cycles to eliminate the knees in some of the curves based on the assumption that the same crack propagation behaviour existed during this period. Table 4-4 shows all the data produced from the test program tabulated in terms of life up to a crack of 0.005 inches length, life after this length to failure, total life and also the percentage of the life spent with a crack present greater than 0.005 inches in depth. The total variation in formation of cracks up to 0.005 inches is 5,800,000 cycles whereas beyond this stage the variation is only 2,040,000 cycles. Fig. 4.12 shows the percentage of life with a crack greater than 0.005 inches plotted against the life to failure. A large amount of scatter is present probably due to extrapolating results but there appears to be a definite trend for the proportion of the life with a crack > 0.005 inches to decrease with increasing life.

The crack propagation behaviour observed was shown to extend back to crack depths of 0.036 inches and the results have been extrapolated back to crack depths of 0.005 inches. These results have indicated a

a decreasing importance of the crack propagation phase with increasing life and also that most of the scatter takes place, certainly within the period when the crack is less than 0.035 inches, and probably when the crack is of much smaller depth. Although the programs have provided no statistically viable quantitative information they have shown in agreement with other workers that the propagation of larger cracks is a predictable stage in the life but also that the major region of interest for long lives is when the cracks are much smaller. Obviously information is required on the damaged or cracked state of the specimen when the cracks are less than 0.040 inches and it seems likely that cracks of 0.010 inches and less will be of critical interest.

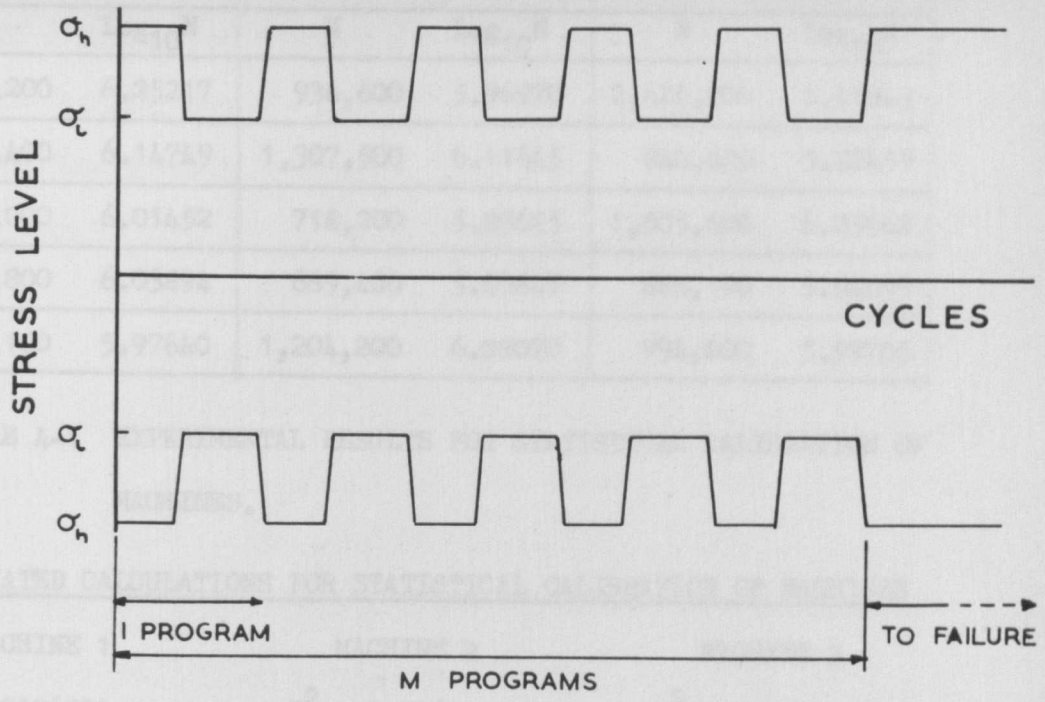

FIG 4.1 BLOCK PROGRAM FOR SECTION X.

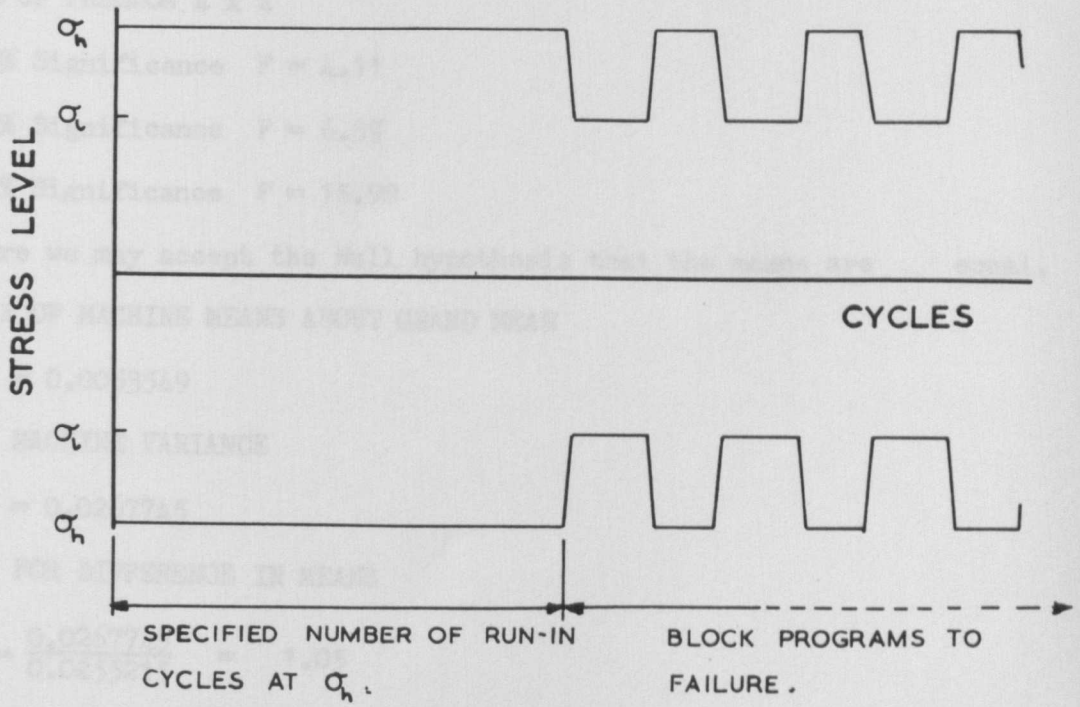

FIG 4.2 BLOCK PROGRAM FOR SECTION Y.

MACHINE 1		MACHINE 2		MACHINE 3	
N	$Log_{10}N$	N	$Log_{10}N$	N	$Log_{10}N$
1,787,200	6.25217	936,600	5.96970	2,626,800	6.41943
1,404,400	6.14749	1,307,500	6.11645	840,600	5.92459
1,034,000	6.01452	718,200	5.85625	1,805,600	6.25662
1,093,800	6.03894	689,400	5.83847	885,100	5.94699
947,100	5.97640	1,204,200	6.08070	994,600	5.99765

TABLE 4-1 EXPERIMENTAL RESULTS FOR STATISTICAL CALIBRATION OF MACHINES.

ABBREVIATED CALCULATIONS FOR STATISTICAL CALIBRATION OF MACHINES

MACHINE 1	MACHINE 2	MACHINE 3
$S^2 = 0.0126824.$	$S^2 = 0.0161800$	$S^2 = 0.0477030$

F TEST FOR SIGNIFICANT DIFFERENCE INVARIANCES

$$\frac{\text{LARGEST VARIANCE}}{\text{SMALLEST VARIANCE}} = \frac{0.0477030}{0.0126824} = 3.76$$

DEGRESS OF FREEDOM 4 x 4

10% Significance F = 4.11

5% Significance F = 6.39

1% Significance F = 15.98

Therefore we may accept the Null hypothesis that the means are equal.

VARIANCE OF MACHINE MEANS ABOUT GRAND MEAN

$S^2 = 0.0053549$

BETWEEN MACHINE VARIANCE

$S^2 = 0.0267745$

F. TEST FOR DIFFERENCE IN MEANS

$$F = \frac{0.0267745}{0.0255215} = 1.05$$

DEGREES OF FREEDOM 2 x 12

BETWEEN MACHINES = 3 - 1 = 2

WITHIN MACHINES = (5 - 1) x 3 = 12

10% Significance F = 2.81

5% Significance F = 3.89

1% Significance F = 6.93

Therefore we may accept the Null hypothesis that the means are equal.

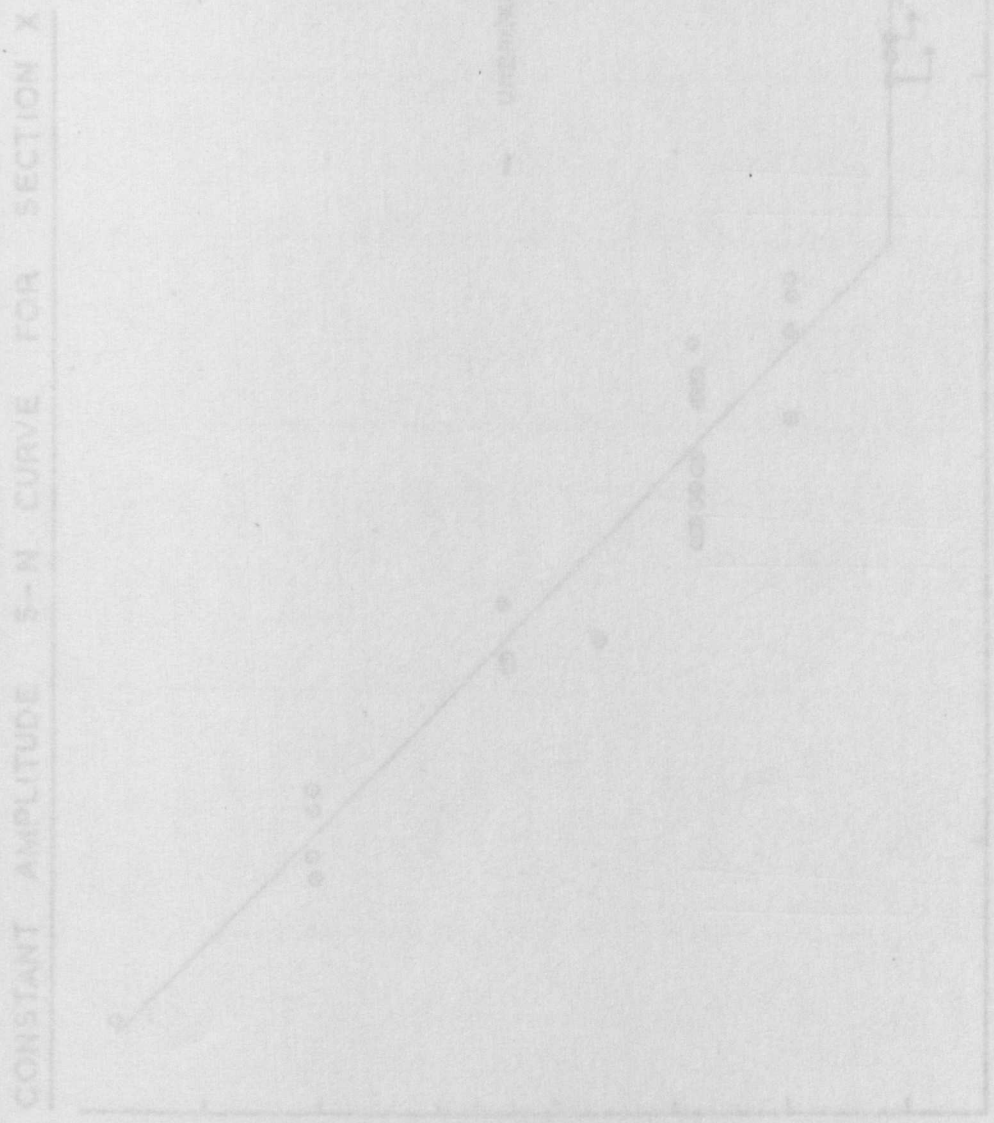

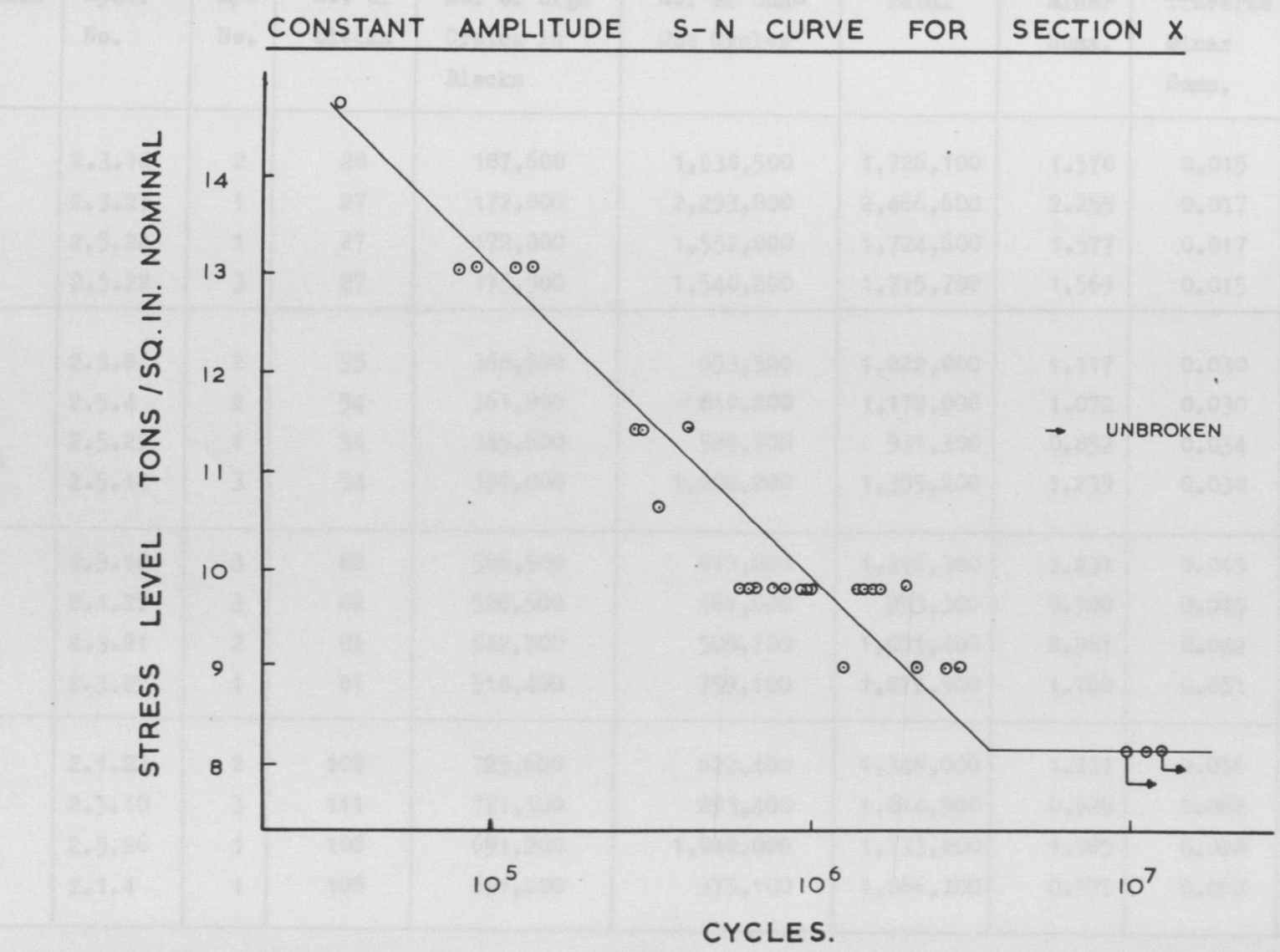
CONSTANT AMPLITUDE S-N CURVE FOR SECTION X
STRESS LEVEL TONS/SQ.IN. NOMINAL
14
13
12
11
10
9
8
UNBROKEN
10^5
10^6
10^7
CYCLES.

FIG 4.3

TABLE 4-2 Page 1

Condition	Spec. No.	M/C No.	No. of Blocks	No. of High Cycles in Blocks	No. of Run-Out Cycles	Total	Miner Summ.	Traverse Miner Summ.	Total Miner Summ.
A 7.84	2.3.18	2	28	187,600	1,538,500	1,726,100	1.578	0.015	1.593
	2.3.27	1	27	172,800	2,293,800	2,466,600	2.255	0.017	2.272
	2.5.24	1	27	172,800	1,552,800	1,724,600	1.577	0.017	1.594
	2.5.22	3	27	175,500	1,540,200	1,715,700	1.569	0.015	1.584
B 7.84	2.5.8	2	55	368,500	853,500	1,222,000	1.117	0.030	1.147
	2.5.4	2	54	361,800	810,200	1,172,000	1.072	0.030	1.102
	2.5.29	1	54	345,600	585,700	931,300	0.852	0.034	0.886
	2.5.14	3	54	351,000	1,004,200	1,355,200	1.239	0.030	1.269
C 7.84	2.3.10	3	82	526,500	819,800	1,346,300	1.231	0.045	1.276
	2.1.29	3	82	526,500	466,800	993,300	0.908	0.045	0.953
	2.3.21	2	81	542,700	508,700	1,051,400	0.961	0.042	1.003
	2.3.22	1	81	518,400	759,100	1,277,500	1.168	0.051	1.219
D 7.84	2.1.22	2	108	723,600	622,400	1,346,000	1.231	0.056	1.287
	2.5.10	3	111	721,500	293,400	1,014,900	0.928	0.062	0.990
	2.5.26	1	108	691,200	1,042,000	1,733,200	1.585	0.068	1.653
	2.1.4	1	108	691,200	375,100	1,066,300	0.975	0.068	1.043

TABLE 4-2 Page 2

Condition	Spec. No.	M/C No.	No. of Blocks	No. of High Cycles in Blocks	No. of Run-Out Cycles	Total	Miner Summ.	Traverse Miner Summ.	Total Miner Summ.
A 7.19	2.1.3	3	27	162,000	885,200	1,047,200	0.957	0.015	0.972
	2.5.25	2	27	164,700	1,766,900	1,931,600	1.766	0.014	1.780
	2.5.1	2	27	164,700	1,534,800	1,699,500	1.554	0.014	1.568
	2.1.19	1	27	153,900	1,391,200	1,545,100	1.413	0.017	1.430
B 7.19	2.5.23	3	54	324,000	1,355,700	1,679,700	1.536	0.030	1.566
	2.1.6	3	54	324,000	1,717,200	2,041,200	1.866	0.030	1.896
	2.3.20	2	54	329,400	1,374,700	1,704,100	1.558	0.028	1.586
	2.3.19	1	55	313,500	270,000	583,500	0.534	0.035	0.569
C 7.19	2.3.25	3	81	486,000	1,144,300	1,630,300	1.491	0.045	1.536
	2.1.14	2	81	494,100	3,248,700	3,742,800	3.422	0.042	3.464
	2.5.18	1	68	387,600	0	387,600	0.354	0.043	0.397
	2.5.16	1	81	461,700	1,364,100	1,825,800	1.669	0.051	1.720
D 7.19	2.5.11	3	115	690,000	1,367,300	2,057,300	1.881	0.064	1.945
	2.3.7	2	108	658,800	4,997,700	5,656,500	5.172	0.056	5.228
	2.5.28	2	108	658,800	723,800	1,382,600	1.264	0.056	1.320
	2.3.4	1	108	615,600	2,636,900	3,252,500	2.974	0.068	3.042

Condition	Spec. No.	M/C No.	No. of Blocks	No. of High Cycles in Blocks	No. of Run-Out Cycles	Total	Miner Summ.	Traverse Miner Summ.	Total Miner Summ.
A 6.53	2.5.7	1	27	139,050	2,911,600	3,050,650	2.789	0.017	2 .806
	2.5.13	2	27	151,200	1,341,800	1,493,000	1.365	0.014	1.379
	2.5.5.	3	27	151,200	2,539,400	2,690,600	2.460	0.015	2 .475
	2.5.20	3	27	151,200	1,564,800	1,716,000	1.569	0.015	1.584
B 6.53	2.3.6	1	54	278,100	1,147,200	1,425,300	1.303	0.034	1.337
	1.2.17	1	54	278,100	1,469,400	1,747,500	1.598	0.034	1.632
	2.3.29	2	54	302,400	1,339,900	1,642,300	1.502	0.028	1.530
	2.3.12	3	54	302,400	1,210,900	1,513,300	1.383	0.030	1.413
C 6.53	2.5.3	1	81	417,150	1,129,500	1,546,650	1.414	0.051	1.465
	1.2.6	2	81	453,600	750,100	1,203,700	1.101	0.042	1.143
	1.1.22	2	81	453,600	1,316,900	1,770,500	1.619	0.042	1.661
	2.3.24	3	81	453,600	1,971,200	2,424,800	2.217	0.045	2.262
D 6.53	2.1.20	1	108	556,200	1,968,800	2,525,000	2.309	0.068	2.377
	2.5.9	2	80	448,000	0	448,000	0.410	0.043	0.453
	2.5.12	3	108	604,800	1,109,300	1,714,100	1.567	0.060	1.627
	2.3.15	3	108	604,800	1,210,400	1,815,200	1.660	0.060	1.720

TABLE 4-2 Page 3

TEST OF FIT OF EXPERIMENTAL DATA IN SECTION X TO LOG NORMAL DISTRIBUTION.

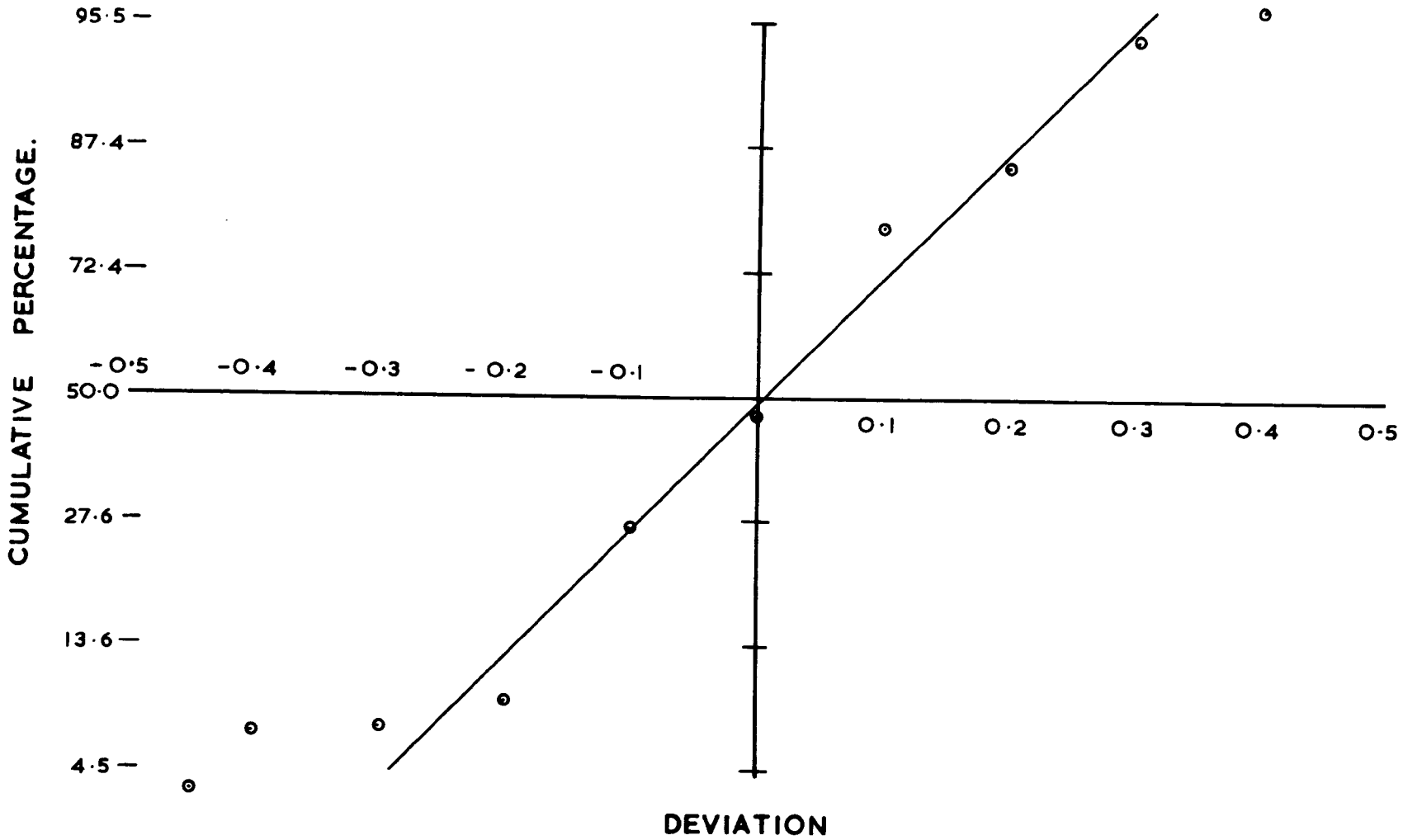

FIG 4.4

TABLE 4-3 Page 1

Condition	Spec. No.	M/C No.	No. of Blocks	No. of High Cycles in Blocks	No. of Run-In Cycles	Total	Miner Summ.	Traverse Miner Summ.	Total Miner Summ.
E 7.84	1.4.25	1	168	1,125,600	100,000	1,225,600	0.694	0.090	0.784
	1.4.11	1	158	1,058,600	100,000	1,150,600	0.656	0.084	0.740
	1.1.11	2	158	1,058,600	100,000	1,158,600	0.656	0.084	0.740
	1.4.21	3	226	1,469,000	100,000	1,569,000	0.889	0.126	1.015
F 7.84	1.2.24	1	90	603,000	300,000	903,000	0.511	0.048	0.559
	1.1.17	2	129	864,300	300,000	1,164,300	0.659	0.069	0.728
	1.2.7	2	96	643,200	300,000	943,200	0.534	0.051	0.585
	1.2.19	3	168	1,092,000	300,000	1,392,000	0.788	0.094	0.882
G 7.84	1.4.2	1	92	616,400	500,000	1,116,400	0.632	0.049	0.681
	1.2.8	2	88	589,600	500,000	1,089,600	0.617	0.047	0.664
	1.1.9	3	121	786,500	500,000	1,286,500	0.729	0.068	0.797
	1.4.29	3	140	910,000	500,000	1,410,000	0.799	0.078	0.877
H 7.84	1.2.28	1	168	1,125,600	700,000	1,825,600	1.039	0.090	1.129
	1.4.16	2	145	1,306,500	700,000	2,006,500	1.137	0.104	1.241
	1.2.11	2	113	757,100	700,000	1,457,100	0.825	0.060	0.885
	1.2.15	3	73	474,500	700,000	1,174,500	0.665	0.041	0.706

TABLE 4-3 Page 2

Condition	Spec. No.	M/C No.	No. of Blocks	No. of High Cycles in Blocks	No. of Run-In Cycles	Total	Miner Summ.	Traverse Miner Summ.	Total Miner Summ.
E 7.19	1.2.16	1	280	1,708,000	100,000	1,808,000	1.024	0.150	1.174
	1.1.21	2	174	1,061,400	100,000	1,161,400	0.658	0.093	0.751
	1.1.24	3	170	1,020,000	100,000	1,120,000	0.634	0.095	0.729
	1.1.23	3	155	930,000	100,000	1,030,000	0.583	0.086	0.669
F 7.19	1.2.14	1	271	1,653,100	300,000	1,953,100	1.106	0.145	1.251
	1.1.19	1	184	1,122,400	300,000	1,422,400	0.806	0.098	0.904
	1.2.9	2	256	1,561,600	300,000	1,861,000	1.054	0.137	1.191
	1.1.5	3	93	558,000	300,000	858,000	0.486	0.052	0.538
G 7.19	1.2.20	1	169	1,030,900	500,000	1,530,900	0.867	0.090	0.957
	1.4.15	2	187	1,140,700	500,000	1,640,700	0.929	0.100	1.029
	1.1.6	2	217	1,323,700	500,000	1,823,700	1.033	0.116	1.149
	1.1.18	3	378	2,268,000	500,000	2,768,000	1.568	0.211	1.779
H 7.19	1.1.10	1	303	1,848,300	700,000	2,548,300	1.443	0.162	1.605
	1.4.26	1	86	524,600	700,000	1,224,600	0.694	0.046	0.740
	1.1.14	2	226	1,378,600	700,000	2,078,600	1.177	0.121	1.298
	1.1.2	3	355	2,130,000	700,000	2,830,000	1.603	0.198	1.801

Condition	Spec. No.	M/C No.	No. of Blocks	No. of High Cycles in Blocks	No. of Run-In Cycles	Total	Miner Summ.	Traverse Miner Summ.	Total Miner Summ.
E 6.53	1.2.2.	1	110	616,000	100,000	716,000	0.406	0.059	0.465
	1.1.20	2	341	1,909,600	100,000	2,009,600	1.138	0.182	1.320
	1.1.8	2	152	851,200	100,000	951,200	0.539	0.081	0.620
	1.4.20	3	260	1,456,000	100,000	1,556,000	0.881	0.145	1.026
F 6.53	1.2.25	1	149	834,400	300,000	1,134,400	0.643	0.080	0.723
	1.2.13	2	36	201,600	300,000	501,600	0.284	0.019	0.303
	1.2.18	3	201	1,125,600	300,000	1,425,600	0.807	0.112	0.919
	1.4.14	3	280	1,568,000	300,000	1,868,000	1.058	0.156	1.214
G 6.53	1.4.5	1	93	520,800	500,000	1,020,800	0.578	0.050	0.628
	1.1.7	1	202	1,131,200	500,000	1,631,200	0.924	0.108	1.032
	1.2.5	2	137	767,200	500,000	1,267,200	0.718	0.073	0.791
	1.4.22	3	334	1,870,400	500,000	2,370,400	1.343	0.186	1.529
H 6.53	1.2.4	1	61	341,600	700,000	1,041,600	0.590	0.033	0.623
	1.4.6	2	115	644,000	700,000	1,344,000	0.761	0.061	0.822
	1.1.1	3	163	912,800	700,000	1,612,800	0.914	0.091	1.005
	1.2.3	3	112	627,200	700,000	1,327,200	0.752	0.062	0.814

TABLE 4-3 Page 3

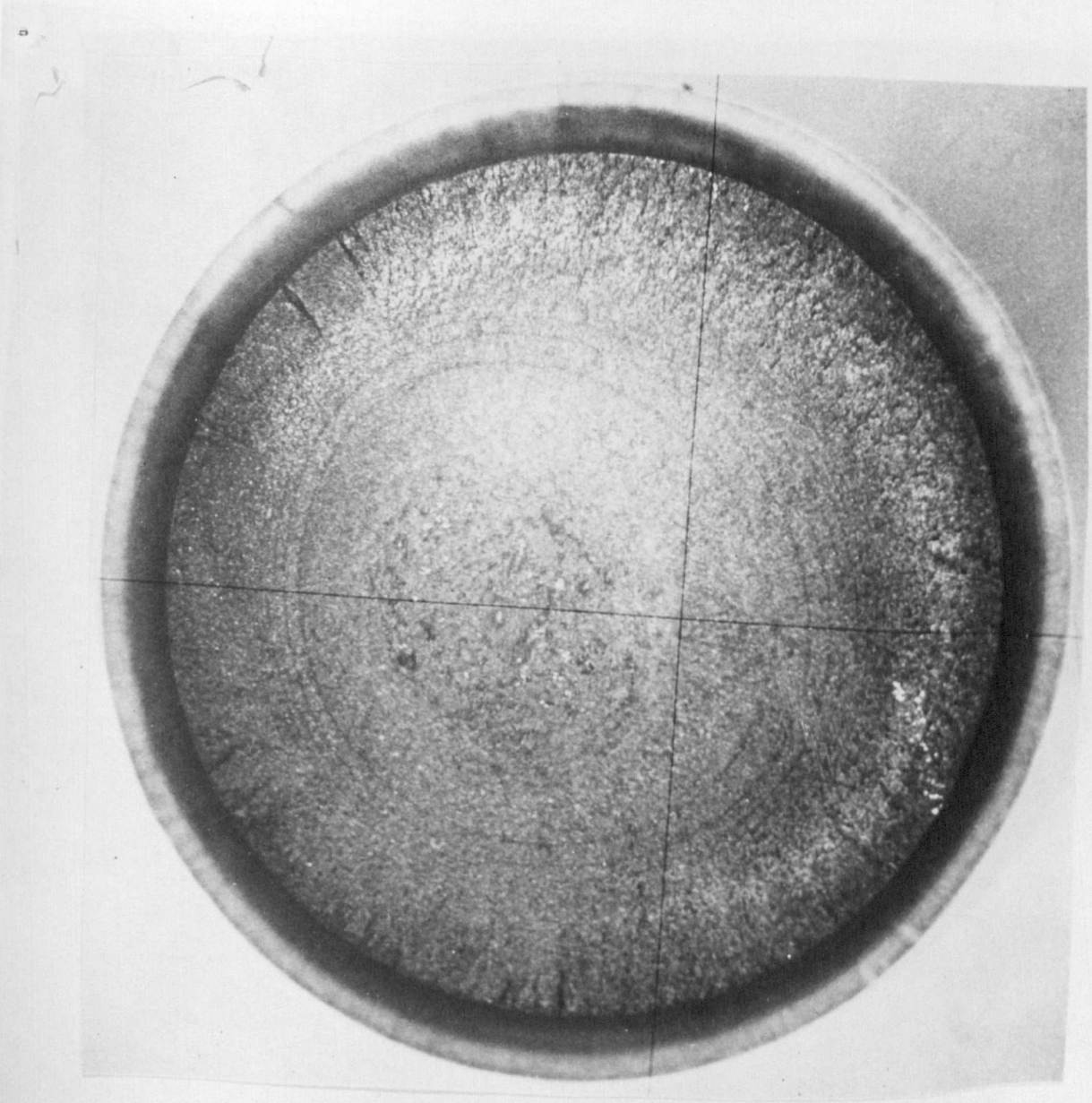

PHOTOGRAPH OF FRACTURED SURFACE AS PROJECTED BY THE NIKON.

FIG. 4. 5.

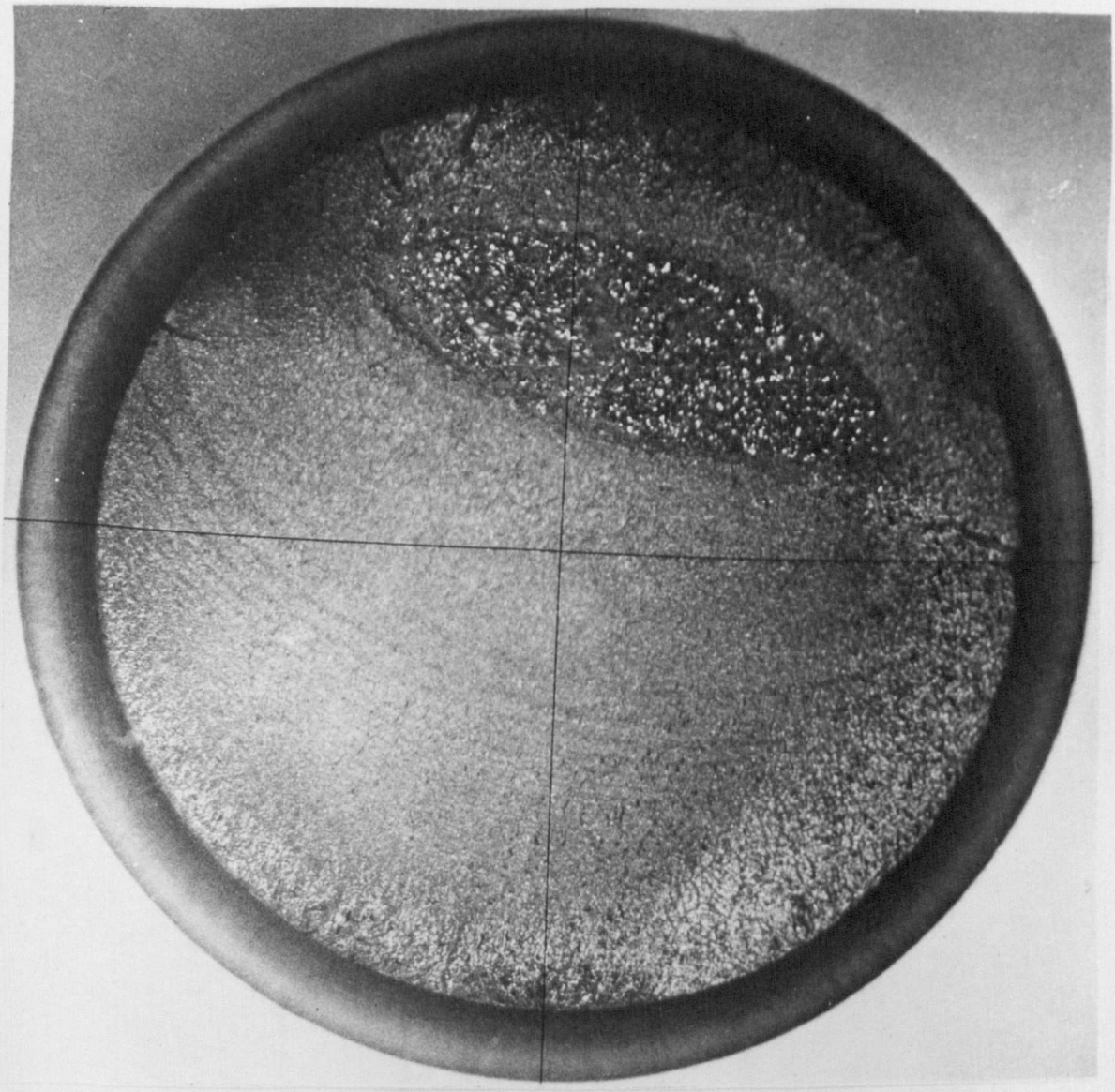

PHOTOGRAPH OF FRACTURED SURFACE AS PROJECTED BY THE NIKON.

FIG. 4.6.

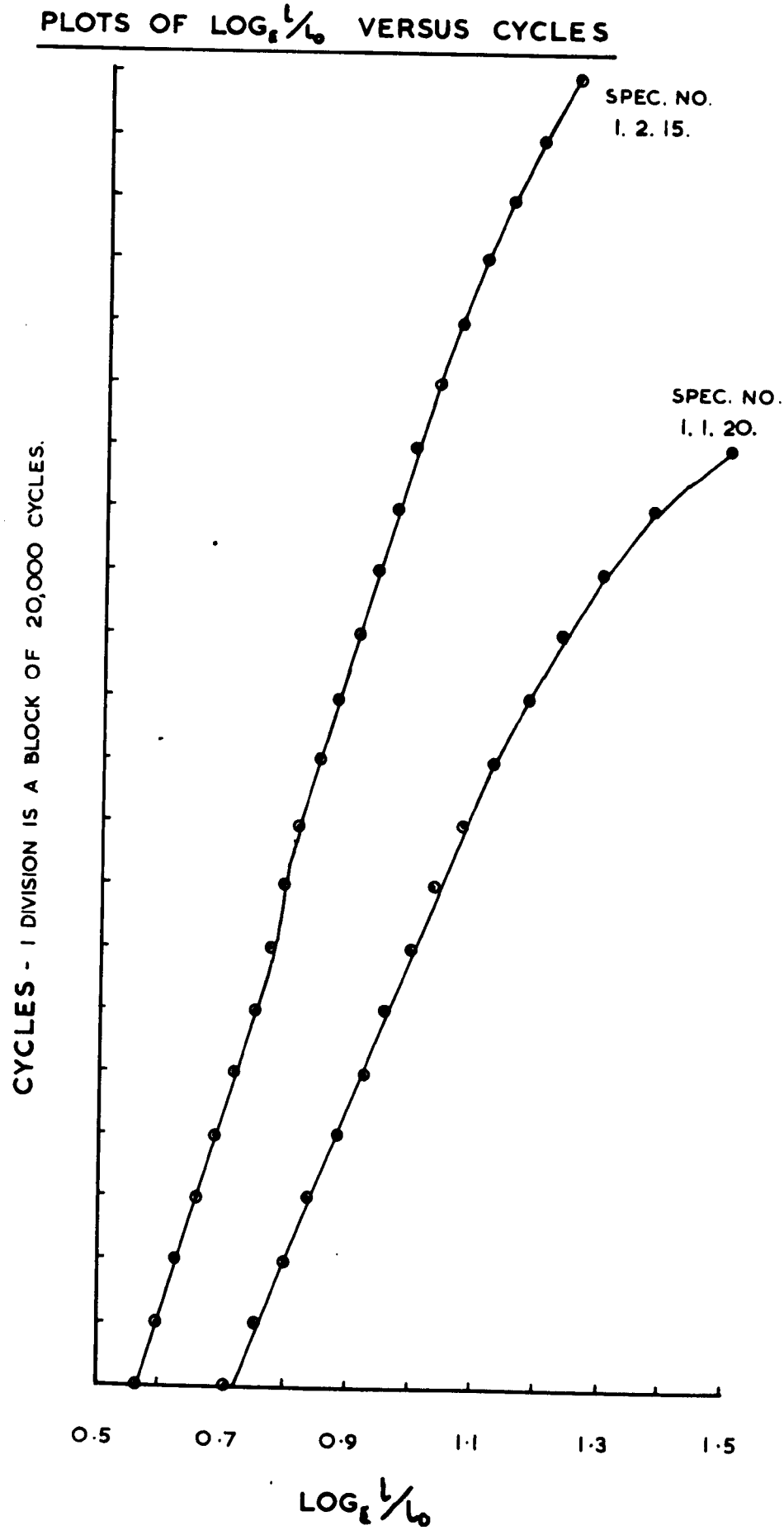
PLOTS OF LOG$_e$ l/l_0 VERSUS CYCLES
SPEC. NO.
1. 2. 15.
SPEC. NO.
1. 1. 20.
CYCLES - 1 DIVISION IS A BLOCK OF 20,000 CYCLES.
0·5
0·7
0·9
1·1
1·3
1·5
LOG$_e$ l/l_0

FIG. 4.7

PLOTS OF $\log_e L/L_o$ VERSUS CYCLES

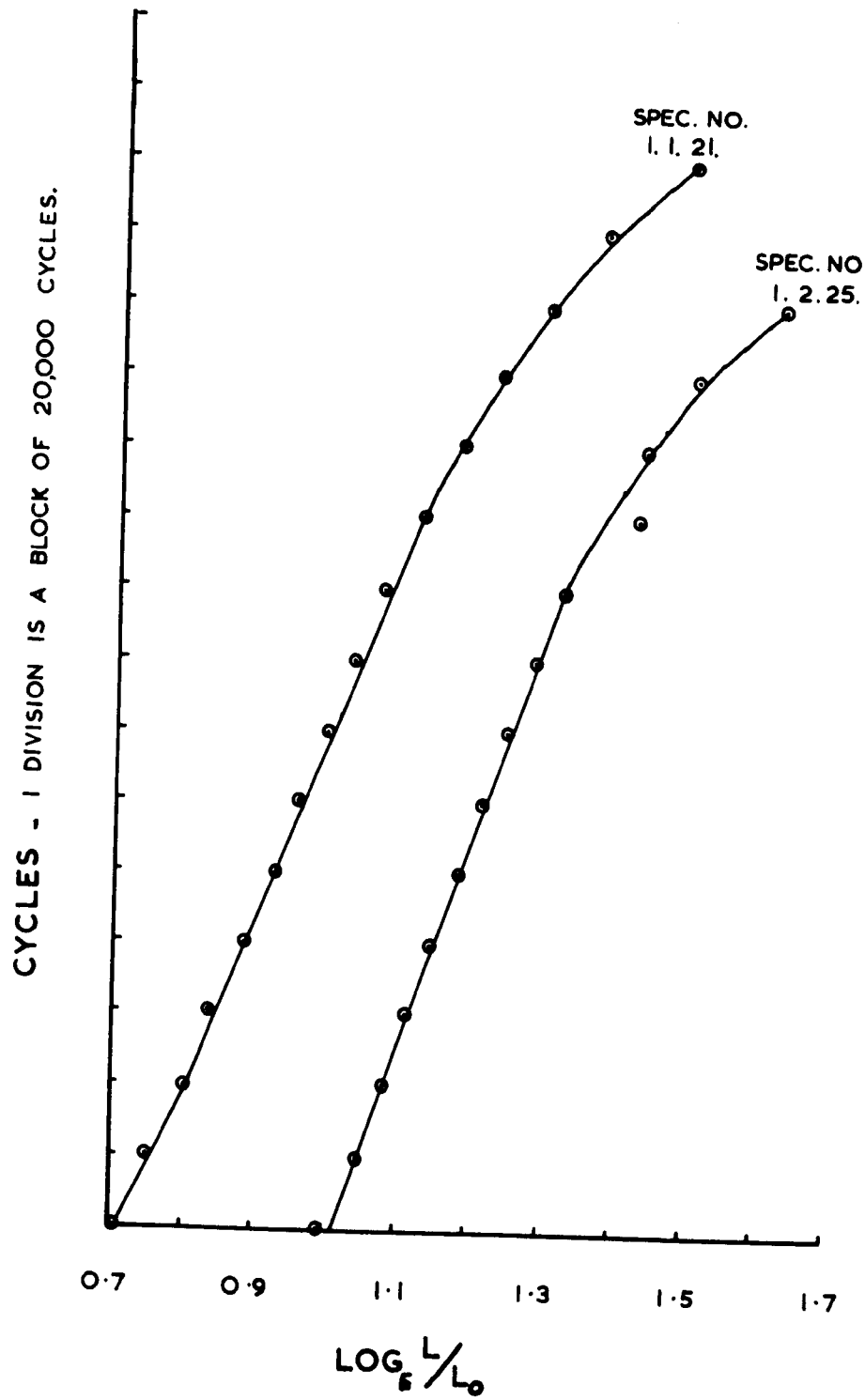

FIG. 4.8

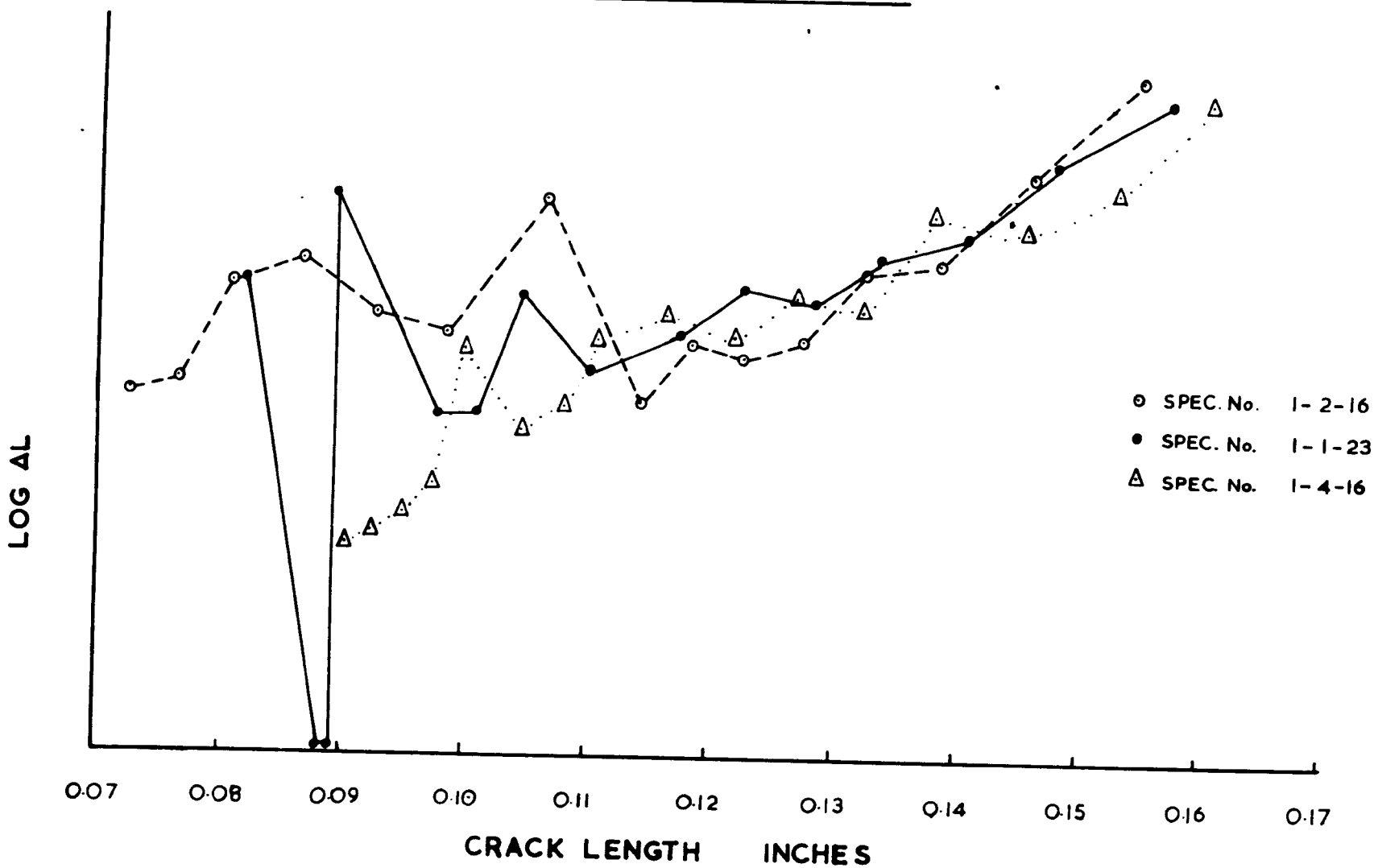
PLOT OF LOG ΔL V CRACK LENGTH
LOG ΔL
0·07
0·08
0·09
0·10
0·11
0·12
0·13
0·14
0·15
0·16
0·17
CRACK LENGTH INCHES
SPEC. No. 1-2-16
SPEC. No. 1-1-23
SPEC. No. 1-4-16

FIG. 4.9

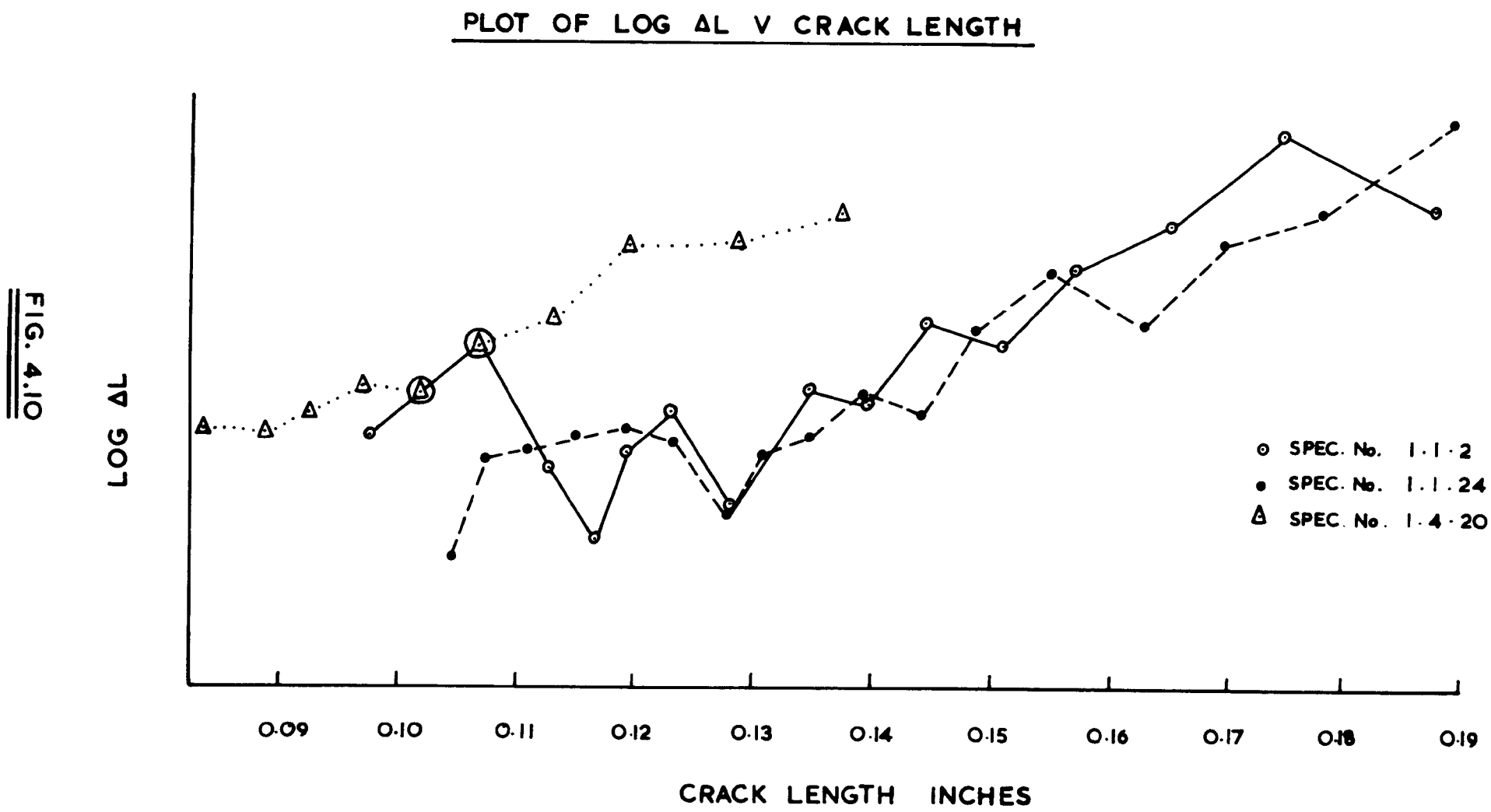
PLOT OF LOG ΔL V CRACK LENGTH
LOG ΔL
SPEC. No. 1·1·2
SPEC. No. 1·1·24
SPEC. No. 1·4·20
0·09
0·10
0·11
0·12
0·13
0·14
0·15
0·16
0·17
0·18
0·19
CRACK LENGTH INCHES

FIG. 4.10

PLOT OF $LOG_E \, L/L_o$ V CYCLES FOR SPEC. No. 1.2.13

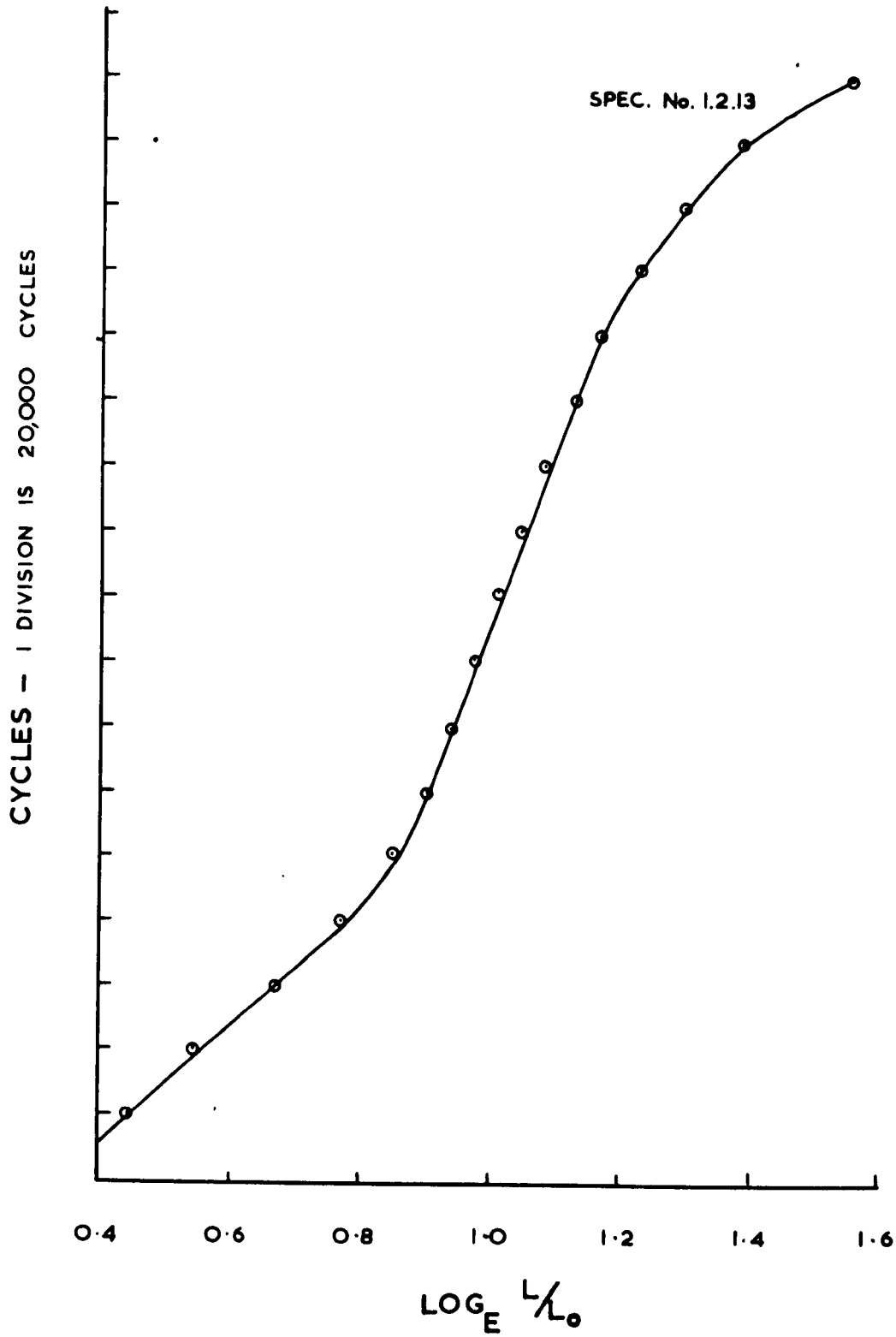

FIG 4.11

Specimen No.	Life up to Crack of 0.005"	Life between 0.005" Crack and Failure	Total Life	% Life between 0.005" & Failure
1.2.8	1,401,000	859,000	2,260,000	38%
1.4.2.	1,251,000	1,089,000	2,340,000	47%
1.1.9	1,650,000	1,270,000	2,920,000	44%
1.2.5	2,064,000	1,176,000	3,240,000	36%
1.2.4	340,000	1,580,000	1,920,000	82%
1.2.3	1,220,000	1,720,000	2,940,000	59%
1.4.22	5,020,000	2,160,000	7,180,000	30%
1.4.6	1,120,000	1,880,000	3,000,000	63%
1.4.11	2,392,000	868,000	3,260,000	27%
1.4.16	2,725,000	1,875,000	4,600,000	41%
1.4.21	3,380,000	1,240,000	4,620,000	27%
1.1.17	1,280,000	1,600,000	2,880,000	56%
1.2.11	2,250,000	710,000	2,960,000	24%
1.4.29	1,300,000	2,000,000	3,300,000	61%
1.2.28	3,151,000	917,000	4,068,000	22%
1.2.14	2,970,000	2,750,000	5,720,000	51%
1.1.5	480,000	1,680,000	2,160,000	78%
1.2.9	4,330,000	1,090,000	5,420,000	20%
1.1.19	1,790,000	2,190,000	3,980,000	55%
1.1.11	1,380,000	1,880,000	3,260,000	58%
1.2.24	190,000	1,910,000	2,100,000	91%
1.2.15	910,000	1,250,000	2,160,000	58%
1.2.7	830,000	1,390,000	2,220,000	63%
1.1.21	2,480,000	1,100,000	3,480,000	32%
1.2.16	3,810,000	1,890,000	5,700,000	33%
1.1.23	1,385,000	1,815,000	3,200,000	57%
1.1.24	1,080,000	2,420,000	3,500,000	69%
1.4.15	2,400,000	1,840,000	4,240,000	43%
1.2.20	2,470,000	1,410,000	3,880,000	36%
1.1.18	5,990,000	2,070,000	8,060,000	26%
1.1.10	4,940,000	1,820,000	6,760,000	27%
1.1.8	1,690,000	1,550,000	3,140,000	49%
1.1.2	5,290,000	2,510,000	7,800,000	32%

TABLE 4-4

Specimen No.	Life up to Crack of 0.005"	Life between 0.005" Crack and Failure	Total Life	% Life between 0.005" & Failure
1.1.20	5,920,000	1,000,000	6,920,000	14%
1.4.20	2,970,000	2,330,000	5,300,000	44%
1.2.2	880,000	1,420,000	2,300,000	62%
1.2.25	1,910,000	1,370,000	3,280,000	42%
1.1.7	2,390,000	2,150,000	4,540,000	47%
1.2.18	2,170,000	2,150,000	4,320,000	50%
Total Variation	5,800,000	2,040,000	6,140,000	

TABLE 4-4 (page 2)

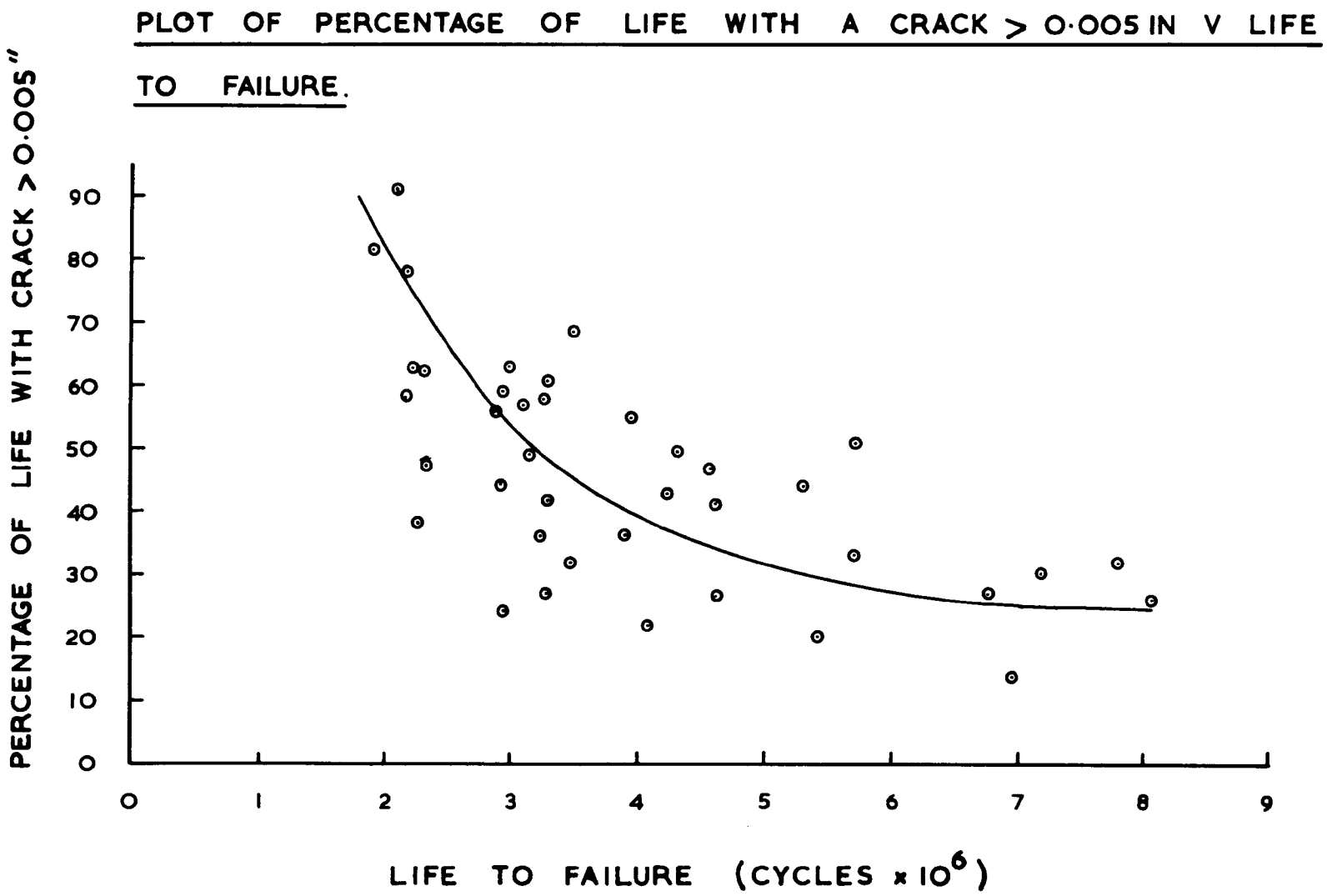
PLOT OF PERCENTAGE OF LIFE WITH A CRACK > 0·005 IN V LIFE TO FAILURE.
PERCENTAGE OF LIFE WITH CRACK > 0·005"
0
10
20
30
40
50
60
70
80
90
0
1
2
3
4
5
6
7
8
9
LIFE TO FAILURE (CYCLES × 10^6)

FIG 4.12

CHAPTER 5

Although the first test program was unsuccessful quantitatively, the examination of the block program markings had indicated that the major region of interest was probably when the cracks were under 0.020 inches long.

In order to derive the maximum information from tests it was necessary to be able to determine the fatigued, or cracked state of the specimen quantitatively. The obvious facilities required were reliable detection of small cracks under 0.010 inches in length and reasonably reliable quantitative information between 0.010 inches and 0.040 inches. If maximum advantage was to be taken of the testing method developed then testing would have to take place with the specimen still in the machine, with the minimum possible disturbance of the test and the operation should be capable of rapid execution.

Penetrant dyes and magnetic methods give no quantitative information on crack depth, this leaves ultrasonics and eddy current crack detection as the main contenders.

(1) Ultrasonic Methods

The use of a common transmit-receive probe to send pulses up the longitudinal axis of the specimen would lead to many spurious echoes from the notch face and as the orientation of the crack front is not unique, separation of echoes from the notch and a small crack would prove almost impossible.

(1967)

Brook and Parry had performed some work at Bristol on small axial fatigue specimens in a Vibrophore. They measured the changes in resonant frequency of the specimen in the machine and also the ouput of the amplifier, thus they were able to deduce the changes in dynamic modulus

and damping of the material in the specimen. They found that plots of E/E_o versus cycles (E = dynamic modulus, E_o = original dynamic modulus) were in fact straight lines for a significant portion of the life and further that the slope of the E/E_o versus N plot could be correlated to the actual life of the specimen. A plot was produced of $d(E/E_o)/dN$ versus cycles to failure and this was a unique curve for all the conditions investigated i.e. the slope of the E/E_o versus N plot gives a value for the life to failure regardless of the stress level at which the test is performed. This work was performed at constant amplitude with some very limited block programs. The advantages are great if it were established that the rate of change of dynamic modulus was proportional to life under random loading conditions also. After about 20% of the life it would be possible to predict the life. This 80% reduction in the total testing time would allow another four types of loading history to be examined in the same testing time. It should be noted however, that Brook and Parry's work is restricted to small plain specimens.

The propagation of ultrasonic shear waves through a material is dependant on the dynamic modulus, therefore a change in the dynamic modulus should be reflected by a change in the velocity of transmission of ultrasonic shear waves. It was therefore decided to attempt to reprodduce, with ultrasonics, some of these measurements and to try and correlate the total change in modulus at any time to the fatigued state of the specimen. The small size of the specimen combined with the relatively small changes in dynamic modulus mean that changes in transmission velocity are of the order of nano-seconds, and obviously it is desirable to have the wave traversing the greatest possible length of fatigued material. The latter is achieved by passing the shear wave

around the surface circumference of the notch, and this requires that the specimen be immersed and shear waves impinged on the surface at a critical angle. This method would be very difficult to use in situ on varying types of machinery and also time consuming. On these grounds this method was rejected and the method adopted was to pass shear waves across the throat diameter of the notch to be picked up by a separate receive probe positioned diametrically opposite. This eliminates any spurious reflection difficulties and one only has to time the first pulse received. As good contact is required to permit transmission of the shear waves, a high contact pressure has to be used. Two probes were manufactured together with a clamping brace. An ultrasonic rig was available and this was used for preliminary measurements on the rotating bending specimens turned down to give a plain specimen of 0.500 inches diameter at the test section. A similar curve qualitatively to that of Brook and Parry was obtained with six specimens. The results showed some promise but the contact pressures were so high that residual compressive stresses were introduced where the probe was clamped to the surface of the test section and these influenced the overall pattern of crack propagation. The clamping of a probe in the root of the notch was simple in itself, but obtaining the necessary degree of contact proved impossible in a limited investigation. The surface of the notch is a compound of curves and attempts at machining a probe to fit this shape well were unsuccessful. Other arrangements were far more complex and would require long development periods, therefore it was decided to try the eddy current crack detection methods.

A Forster defectomer Type No. D.158 was available together with the standard probe and calibration block. As the standard probe was too large to reach the bottom of the groove, Forster's were approached and they manufactured a prototype probe which could be used at the root of

the notch of the rotating bending specimens. One of the difficulties is the sensitivity of the apparatus to edge effects which affect the instrument response to a crack of given length. The notch acts as a very severe edge effect and also complicates adjustment of the lift-off compensation. These factors make the use of the standard calibration block impossible for a notched specimen. Thus the only practical solution is to decide on a standard method of using the defectometer and to calibrate the output with crack length by running specimens until a certain reading is obtained and then sectioning the specimen, polishing and observing the crack under a microscope. This calibration is unique to the particular specimen configuration and to the settings used on the instrument.

After some experimentation with the calibration block it was decided not to adjust the lift-off compensation so that there was zero shift in reading when the probe was lifted from the material in the region of edge effects as this decreased the response to a crack considerably. This means that probe contact with the specimen must be maintained when measurements were taken. The maximum sensitivity was used together with a compromise lift-off compensation adjustment. The zero set, which is a potentiometer backing off the detection circuit output to the meter, was used initially as a means of obtaining a greater total range of readings.

The intital experimental work was to run specimens at three different nominal stress levels, 13.04, 11.42 and 9.79 tons/sq.in. all above the constant amplitude fatigue limit. Each specimen was followed with the Forster at a single arbitrary point marked on the surface, the readings being noted and the change from the original reading at that point is denoted as the Forster reading. Response was dependant on both probe pressure and load on the speeimen when the reading was taken. Care was taken therefore to ensure a uniform probe pressure was applied and readings were taken with the specimen unloaded. The speeimens were run until certain predetermined values of Forster reading were obtained and then the specimen was stopped, sectioned, and polished at that point and examined

under a Vickers M.55 microscope. Crack lengths were then measured using the micrometer stage on the microscope.

A plot of Forster reading versus crack length is shown in Fig. 5.1. This plot also shows some results from the block program tests described later in this chapter. It was found that scatter in the test results was prohibitive above crack lengths of 0.050 inches and these are not included in the plot.

The scatter in the portion of the curve with the cracks less than 0.010 inches is due to two main reasons:-

1) The profile of small cracks is such that their length varies considerably with small increments in distance around the circumference of the specimen. Thus considerable errors are possible due to the section examined under the microscope being slightly displaced from the point at which measurements were actually taken. In later tests the measuring techniques were modified to eliminate this problem, the circumference of the specimen being scanned for maximum Forster reading and then when the specimen was sectioned a series of small slices were taken across the region of maximum reading in order to locate the maximum crack length. Using both maximum readings reduced the scatter in the results as will be seen later.

2) Temperature effects due to the running temperature of the machine in which the test was performed. A section is devoted to a full discussion of these effects later in this chapter.

The Forster readings at a single point showed a rapid initial rise, then a period of stationary or very slow increase followed by a rapid and steady increase. This type of response is shown in a generalised form in Fig. 5.2 where the life has been split into three main stages, labelled A, 1A and B as shown, as indicated by the Forster response. The

calibration data had shown that cracking was present at the start of Stage B at any single point on the surface of the specimen, thus Stage B could certainly be regarded as a macro-crack propagation phase. The significance of Stages A and 1A was not so apparent. Examination of the data available showed that the magnitude of the initial rise was apparently dependent on the machine in which the specimen was run and with no detectable trend due to the stress level at which the specimen was tested, further discussion of this topic is deferred until later in this chapter.

It is obvious that readings at a single point do not give an overall indication of the fatigued state of the specimen, therefore further tests were performed at 11.42 tons/sq.in. in which readings were taken at four points equally spaced around the circumference of the specimen. The cumulative total of the four readings was then plotted against cycles. These plots are shown in Fig. 5.3. Examination of these plots brings out several interesting points.

1) If we accept the cumulative Forster reading as an indication of the damaged state of the specimen, then the rate of accumulation of damage during Stage B is remarkably uniform for the specimens exhibiting marked variations in total life.

2) The highest readings at one of the four points when compared with the calibration curve showed that a crack was certainly present when the overall rise is apparent in the cumulative Forster reading.

3) A break-down of the results is shown in Table 5-1. It can be seen that over 70% of the scatter in the results is accounted for in Stages A and 1A, further that the proportion of the life spent in Stage B decreases as the overall life increases.

Fig. 5.4 shows a plot of Forster reading versus cycles for a single point at a stress level of 13.04 tons/sq.in. It can be seen that Stages

A and 1A are very short with most of the life being spent in Stage B. Fig. 5.5 shows a similar plot at 9.79 tons/sq.in., this is one of the specimens sectioned in the calibration data and the life to failure is estimated from a combination of test data. The length of Stages A and 1A has increased both in overall length and in proportion to the time spent in Stage B. All the preceding data is shown in Fig. 5.6 with the life to failure plotted against the percentage of life spent in Stage B. As the beginning of Stage B indicates the presence of a crack between 0.003 inches and 0.008 inches, the graph in Fig. 5.6 effectively represents the proportion of life with a crack greater than 0.008 inches related to total life.

This plot agrees qualitatively with results of Schijve on aluminium alloys.

At this stage the Forster had satisfied most of the requirements. Testing could be completed in situ, the method was fast with minimum damage to the surface of the specimen, and finally valuable information was obtainable in the region of major interest when cracks were very small. It was therefore decided to continue with the Forster and make this the main source of crack detection and depth information.

The investigation of the Forster's response, its significance and use in cumulative damage was split into three sections at this stage.

i) Temperature effects both due to rises in machine and specimen temperature and also changes in ambient temperature.

ii) The significance of Stages A and 1A with particular regard to the cracked state of the specimen. This is allied to a great extent to section (i).

iii) An investigation of the effect of low loads below the original fatigue limit using the Forster as an indication of the damaged or cracked

state of the specimen when these loads were applied, thus enabling their effect at different stages in the fatigue life of a specimen to be assessed.

As it was desirable to maintain the instrument settings section (iii) was completed first then followed by section (i). Section (ii) was considered to be a suitable topic for a third year undergraduate Honours project and so the experimental work in this section was performed by R. M. Puckridge and will be described briefly. The sections are described in the order in which the work was performed.

SECTION iii INVESTIGATION OF SOME ASPECTS OF CUMULATIVE DAMAGE

Maximum ambiguity and scatter existed in stages 1 and 1A and therefore this section of the second program was concentrated on the investigation of the macro-crack propagation stage. A crack was started at the high stress level 11.42 tons/sq.in. and then the specimen was subjected to various block loading conditions and the progress of the crack followed using the Forster. The main points investigated were interaction effects and the effect of block length and mixing on cumulative damage.

Initially specimens were run at 11.42 tons/sq.in. until the beginning of Stage B had been reached, the stress level was then reduced to one of the following values:- 9.79, 8.16, 7.34 tons/sq.in. The results of these tests are shown in table 5-2 and some typical plots for these stress levels are shown in Figs. 5.7, 5.8, and 5.9. Two specimens were run at a stress level of 6.52 tons/sq.in. and these remained unbroken at 2.49×10^6 and 10.99×10^6 cycles respectively. A plot of cumulative Forster reading versus cycles is shown in Fig. 5.10 for specimen No. 2.2.23. which survived 10.99×10^6 cycles. Both of these unbroken specimens were sectioned and examined for cracks, the specimen above showed a maximum

crack length of 0.038 inches and specimen 2.4.30. which was unbroken at 2.49×10^6 showed a maximum crack length of 0.019 inches.

This information from Table 5-2 is shown plotted as an S-N curve for macro-crack propagation in Fig. 5.11.

Unfortunately during the previous group of tests the Forster was meddled with during the night thus upsetting the set conditions of the instrument. The instrument was reset as closely as possible to the original condition and subsequently sectioned specimens gave good agreement when the results were plotted on the original calibration curve as shown in Fig. 5.1.

The life of a specimen has already been divided into two main stages:- crack initiation together with macro-crack propagation. As already stated in Chapter 2, it is very unlikely that the same conditions govern these two stages in cumulative fatigue damage. An S-N curve for macro-crack propagation stage was now available and thus it is possible to investigate the validity of the Miner-type summation during this region. As expected this S-N curve also showed a fatigue limit but this value of course reduces with increasing crack length. Two possible S-N curves were considered for use with a Miner summation as follows:-

i) The S-N curve with a fatigue limit as shown in Fig. 5.11.

ii) The S-N curve shown in Fig. 5.11 but with no fatigue limit i.e. the damage line continuing as a straight line plot. The results of both of these alternatives together with the results of the test, which are described in the following paragraphs, are shown in Table 5-3.

The specimens were again run at 11.42 tons/sq.in. until the beginning of Stage B and then various types of loading were introduced.

The first two tests consisted of alternate blocks of 9.79 and 8.16 tons/sq.in. of 40,000 cycle length and then run out to failure at 8.16 and 9.79 tons/sq.in. respectively. A typical plot of cumulative Forster

reading versus cycles is shown in Fig. 5.12. The next test started with alternate 40,000 cycle blocks of 9.79 and 6.52 tons/sq.in. to approximately 700,000 cycles. This section of the life of the specimen, no. 2.4.26. is shown in Fig. 5.14. Then the specimen was run at 6.52 tons/sq.in. for 1.5 million cycles. The Forster indicated that the crack was no longer propagating and so further block programs of 9.79 and 6.52 tons/sq.in. were introduced. After three blocks of 9.79 tons/sq.in. the specimen was run to failure at 6.52 tons/sq.in. If we compare the Miner summations for alternative (i) S-N curve and alternative (ii) it is obvious that alternative (ii) provides the most accurate life prediction, alternative (i) being optimistic by a factor of 2.

The specimen No. 2.4.24. was run first with 10,000 cycle blocks of 9.79 and 6.52 tons/sq.in. and then the load levels were changed to 9.79 and 8.16 tons/sq.in. The plot of cumulative Forster readings versus cycles is shown in Fig. 5.14. These observations confirm the observations of the first test program where the 9.79 - 6.52 loading combination, which must be considered as less damaging, actually propagates the crack at a faster rate. After the block programs, the specimen was run to failure at 8.16 tons/sq.in. The Miner summations are shown in Table 5-3.

Specimen No. 2.2.19. was subjected to a 3 level block program, 10,000 cycles at each level of 9.79, 8.16 and 6.52 tons/sq.in. respectively. A low to high sequence was used, followed by a high-low sequence as shown in Fig. 5.15. The specimen was then run to failure at 6.52 tons/sq.in. The Miner summation for alternative (i) is optimistic by a factor of 3 and even that for alternative (ii) by 0.5. Thus the tests on specimens 2.4.26. and 2.2.19. have shown that cycles below the fatigue limit on macro-crack propagation stage must be considered as damaging when applied in well mixed blocks or in large blocks when a much larger crack is present.

Specimen 2.4.29. was used to investigate change in block length and also the presence of large blocks of low load at smaller crack lengths. The initial portion of the plot of cumulative Forster reading versus cycles is shown in Fig. 5.16. The test started with 40,000 cycle lengths of 9.79 and 6.52 tons/sq.in., the block lengths were then changed to 10,000 cycles with the same load levels. The effect of changing block length is demonstrated effectively here indicating the stronger interaction effects as the spectrum becomes better mixed. Then with a cumulative Forster reading of 65 as compared with 80 - 90 in the previous tests, the specimen was run at 6.52 tons/sq.in. for 5.8 million cycles. The Forster readings showed that the crack had stabilized and so further block loading of 8.16 and 6.52 tons/sq.in. was introduced until the crack started to grow again. The specimen was then run for a further 13.5 million cycles at 6.52 tons/sq.in. without failure occuring. The specimen was sectioned and the crack observed and this will be discussed later in detail.

Specimen No. 2.4.9. was used initially to investigate further the difference between 10,000 cycle lengths of 9.79 and 8.16 as compared to 9.79 and 6.52 tons/sq.in. and this section of the plot is shown in Fig. 5.17. Then with the cumulative Forster reading at 53 the specimen was run for 8.0 million cycles at 6.52 tons/sq.in. and again the Forster indicated no significant advance in the damaged state. Further block loading of 9.79 and 8.16 and 9.79 and 6.52 was introduced and the plots for this section of the life are shown in Fig. 5.18. The specimen was then subjected to a further 1.0 million cycles at 6.52 tons/sq.in., the stress level was reduced still further to 4.89 tons/sq.in. and this was applied for 5.9 million cycles. The damaged state was stable during this period and so further block loading of 8.16 and 6.52 was introduced but after the initial rise due to temperature change the specimen proved to be settled into a steady state in which the rate of accumulation of damage

was much slower than normally expected for this loading. A further 10 million cycles of 4.89 tons/sq.in. were then applied and with no increase in Forster reading being shown during this period the specimen was sectioned and crack length measured. Crack lengths of up to 0.085" were observed. Again there is a large difference between the Miner summations obtained from alternative (i) and alternative (ii).

SUMMARY OF INFORMATION GAINED ON STAGE B

The slopes of the Forster versus cycles plot are shown in Table 5-4 but it should be remembered that these are not corrected for temperature effects, however the qualitative information contained in these reults is valid. It can be seen that with one stress level well below the original fatigue limit i.e. the 9.79 - 6.52 tons/sq.in. the rate of crack growth accelerates with decreasing block size. The 9.79 - 8.16 tons/sq.in. case where the low stress level is only just below the original constant amplitude fatigue limit shows a reversal of this trend, in agreement with the results of program 1.

Examination of the results of taking Miner summations on two alternative S-N curves for macro-crack propagation shows that if some care is taken to select the correct crack length at which to insert large blocks of stress of amplitude $0.8\sigma_f$ almost any result can be produced. Certain patterns of behaviour do emerge however and these can be summarised as follows:-

1) Large blocks of stress cycles at $0.8\sigma_f$ must be considered damaging if they occur sufficiently late in the life of a specimen.

2) Large blocks of stress cycles $0.8\sigma_f$, if considered as damaging during the early stages of macro-crack propagation will lead to unduly pessimistic predictions of the life available.

3) The rate of crack growth or damage is dependant on the mixing of the stress spectrum, with the rate of damage in general increasing as the spectrum becomes better mixed.

Thus ideally any cumulative damage rule should contain the following features:-

a) A summation on an S-N curve for which the fatigue limit steadily falls as damage is accumulated.

b) A modification to the S-N curve or to the summation procedure which allows different degrees of mixing of the stress spectrum to be considered.

The last specimens of the batch were used to gain some preliminary information on Stage A and 1A. Specimen 2.4.8. was subjected to 40,000 cycle blocks of 11.42 and 8.16 tons/sq.in., the plot being shown in Fig. 5.19. Specimen 2.2.12. was subjected to the same stress amplitudes but in block lengths of 10,000 cycles as shown in Fig. 5.20.

Similarly Fig. 5.21 shows the results from two specimens subjected to alternate 40,000 cycle blocks of 11.42 and 6.52 tons/sq.in., and Fig. 5.22 shows the same loading conditions but 10,000 cycle blocks applied to a further specimen.

Comparison of the average number of cycles at 11.42 tons/sq.in. required to reach Stage B with the results of the constant amplitude tests showed no significant differences i.e. blocks of stress cycles below the original constant amplitude fatigue limit did not appear to affect the fatigue life during Stage A when applied in blocks.

Two further tests were conducted and these were intended to clear up two points.

i) When the Forster indicated the start of Stage B in block loading tests was there a crack present of the same order of magnitude as in constant amplitude tests?

ii) Did very large blocks of low stress actually propagate the existing cracks present at the start of Stage B?

Specimen No. 2.4.25. was run with alternate blocks of 11.42 and 6.52 tons/sq.in. The plot of cumulative Forster reading versus cycles is shown in Fig. 5.23. When the Forster indicated that a point on the specimen had reached Stage B the specimen was sectioned and examined for cracks. A maximum crack length of 0.008 inches was observed confirming earlier observations.

Specimen No. 2.4.14. was run at 11.42 tons/sq.in. until the beginning of Stage B. The stress level was then reduced to 6.52 tons/sq.in. and the specimen was subjected to 37 million cycles at this level before being sectioned and examined for cracking. The Forster had indicated a small increment in crack growth during this period. The reason for this indication of growth was apparent when the specimen was examined. Photographs of cracking are shown in Figs. 5.24 and 5.25. Both photographs exhibit crack growth in a direction parallel to the sectioned surface i.e. propagation along the longitudinal axis of the specimen. Fig. 5.25 shows the initial trans-granular movement of the crack at the high stress level, subsequent growth of the crack is mainly restricted to grain boundaries and very little depth penetration is achieved. The photographs also show numerous examples of sub-surface damage confined to the grain boundaries.

It had been noted earlier that macro-cracks at stresses above the fatigue limit developed prominent forks but examples of longitudinal propagation had not been evident. The specimens which had been subject to block loading from the start of their life as described previously were re-examined, specifically to look for any signs of longitudinal propagation. The specimens subjected to blocks of cycles at 6.52 tons/sq.in. showed examples of longitudinal propagation and it was also noted that the crack

started fairly straight and trans-grannular but then became more irregular and exhibited longitudinal propagation. Measurements were taken of crack length to the first signs of longitudinal propagation and the four sections examined at the above loading gave values between 0.009 and 0.016 inches. Specimens subjected to loading just below the fatigue limit showed almost no longitudinal propagation.

Section ii INVESTIGATION OF STAGES 1A and A

The object of the test program undertaken by Puckridge was to ascertain the cracked state of the specimen during the long period when Forster readings remained constant or rose steadily.

Specimens from the first two batches of material which were shown statistically to give equivalent results had almost run out. It was therefore necessary to use specimens from the third batch of material. This batch proved to have a significantly higher carbon content and hence yield stress and fatigue limit. This factor in itself was unimportant but with the higher carbon content the pearlite content was very much higher. The detection of cracks in pearlite grains is very difficult using ordinary optical microscopic observations and this hampered the progress of the test program.

In the sectioning of specimens undertaken previously in the calibration tests, due to the relatively long cracks slight rounding of the notch edge during polishing could be tolerated. However, with this investigation, high magnifications were used and therefore this rounding could not be tolerated both due to the small depth of focus and the fact that this first 0.001" was of critical interest. The specimen preparation therefore had to be improved and the final technique used was as follows:-

When the position of the section had been decided this portion of the specimen was sawn out after being marked up, and then the surface to be observed was rubbed down until reasonably flat. The specimen was then mounted in electrically conducting resin. This block was then taken, mounted in a special holding attachment, and ground using cuts of 0.002" reducing to 0.0005" as the final surface was approached. The specimen was then mechanically polished to remove the grinding surface, great care being taken to ensure that the whole surface remained flat. After a satisfactory finish had been obtained from mechanical polishing the specimen was then polished and etched in an electro-polishing machine.

This technique proved adequate for observations at up to 2000 times magnification using a Vickers M55 microscope.

As sectioned specimens cannot be re-run it is impossible to know relatively at which stage the specimen has been sectioned. Specimens were sectioned after various lengths of quasi-stationary Forster readings at the point exhibiting the greatest Forster response. Evidence of micro-cracking during early parts of this pause period was established. The possibility that cracking of depth greater than 0.003" developed very rapidly and then growth slowed by forking or critical stress field conditions was definitely eliminated.

Therefore, although the results of these tests were not quite as successful as hoped for, due to the difficulties of establishing the presence of micro-cracks in a pearlite structure, they did indicate that the stages A and 1A could be classified together as consisting micro-crack initiation and micro-crack propagation.

This work mainly performed by Puckridge is presented in greater detail in Appendix I.

INVESTIGATION OF TEMPERATURE EFFECTS

The sharp initial rise in Forster reading was possibly explained by the following factors:-

1) Attainment of the machine working temperature and the consequent rise in temperature of the specimen.

2) Specimen temperature rise due to plastic work being done at the root of the notch.

3) Response either to work hardening or the relaxation of residual stresses due to machining.

4) Fast initial micro-cracking.

5) Fluctuations in the out-put of the Forster measuring circuit with temperature.

As, has been stated previously, the cumulative damage investigations in this program were executed prior to looking at temperature effects in order to preserve the particular settings on the Forster. It was observed during the long running tests in the cumulative damage section that, if a specimen was left running overnight at a low stress level then the readings taken in the early part of the following day showed a significant decrease in Forster reading, but that during the day the readings rose again to their former level. This pattern followed the overall fluctuation of temperature within the laboratory, so that variation in reading with ambient temperature seemed to be significant when no correction for the basic output of the measuring circuit was considered.

The calibration tests performed using the Forster were described earlier in this chapter. During the course of these tests some 6 specimens were left in the machine after the desired Forster reading had been obtained and further Forster readings were taken after approximately one hour when the machines had cooled down close to the ambient temperature. Decreases in Forster response of the same order of magnitude as the initial rapid

rise were observed. It was also noted during the calibration tests that the magnitude of the initial rise in Forster response was dependant mainly on the machine in which the specimen was run rather than the stress level. Thus the main sources of fluctuation in readings appeared to be due to variation in the ambient temperature of the laboratory and the temperature rise due to the particular machine running temperature.

The output of the measuring circuit to the gauge on the Forster is available at a socket on the rear of the instrument. To improve accuracy during the investigation of temperature effects this output facility was used connected to a Weyfringe digital voltmeter with 100 micro-volts sensitivity.

The tests were conducted in a constant temperature room using the calibration block as supplied by Forster's. The calibration block was used in preference to actual specimens because of the great difficulty in obtaining repeatable results when in the region of severe edge effects in notched specimens, where a small variation in probe position can cause large variations in the instrument response. The calibration block is simply a piece of steel measuring 0·3" thick and across the width of the block three thin slots simulating cracks of 0.1, 0.5 and 1.0 m.m. depth have been inserted. It is desirable to eliminate edge effects and variations in crack depth across the width of the calibration block. Therefore a line was marked on the block as close to the centre line as possible and all readings were taken along this line noting maximum response as the probe passed over each crack. One point was also marked on the calibration block away from the slots to be used as a reference for response to uncracked material at any temperature.

Several conditions of ambient temperature were investigated and for each test the digital voltmeter and the Forster were left switched on in

the constant temperature room along with the calibration block for 24 hours prior to readings being taken to allow conditions to stabilize. The test performed at each temperature condition was as follows:-

The output of the circuit with no probe contact was noted together with the output given by the uncracked reference point on the calibration block. Then five runs were made along the line marked on the calibration block, crossing each of the three cracks with the probe in contact with the surface of the calibration block. Maximum response to the cracks during the traverse was noted and care was taken to try and ensure uniform probe contact pressures and probe angle.

The ambient temperatures investigated were in the range $46^{\circ}F$ - $77^{\circ}F$ and readings were taken at 6 values in this range. These results are presented in Table 5-5 where the mean values are given. The response on the uncracked portion of the off block readings follow the same pattern and these are omitted. The deviation from the basic circuit output is shown in the second part of the table. It can be seen that apart from the case at $56^{\circ}F$ the results are within a 5% band. This suggests that the result at $56^{\circ}F$ was subject to some gross experimental error. As the readings were not repeated this cannot be verified. These results show that ambient temperature effects on the instrumentation and specimen can be corrected for by noting the basic circuit output and making the appropriate adjustments.

It has already been stated that most of the sharp initial rise appeared to be due to machine running temperature and this was verified qualitatively and to a small extent quantitatively by tests in which the temperature of the calibration block was raised above the constant temperature of the room and the measurements described previously were performed. The same pattern of results emerged but an accurate and

exhaustive series of tests were not completed for the following reasons. The work of Puckridge discussed earlier in this chapter showed that the sharp initial rise could not be connected with the rapid formation of cracks between 0.002 - 0.005 inches in depth. All the experimental evidence indicated that this was mainly a temperature effect,the major contribution of which originated from the machine running temperature. Therefore this phase did not appear to be significant in the development of fatigue damage. This led to reducing the three stages in the life of a specimen as discussed previously to two stages as follows:-

Stage A - Crack initiation and micro-crack propagation.

Stage B - Macro-crack propagation.

If further division of Stage A was required it would involve a long program based on the specimens used with results required for each machine. Lengthy microscopic examination of specimens would necessitate several months of work on this aspect. As the effects observed during this stage apparently were not significant in cumulative damage observations it was decided to work on the basis of the division of fatigue life into the two stages as described above.

Having established this pattern of behaviour, the limited cumulative damage investigations described earlier in the chapter pointed to a different pattern of behaviour in Stage A and Stage B. Obviously the next step was to assess in a statistical test program the sensitivity of the specimen, during stages A and B respectively, to stresses below the constant amplitude fatigue limit.

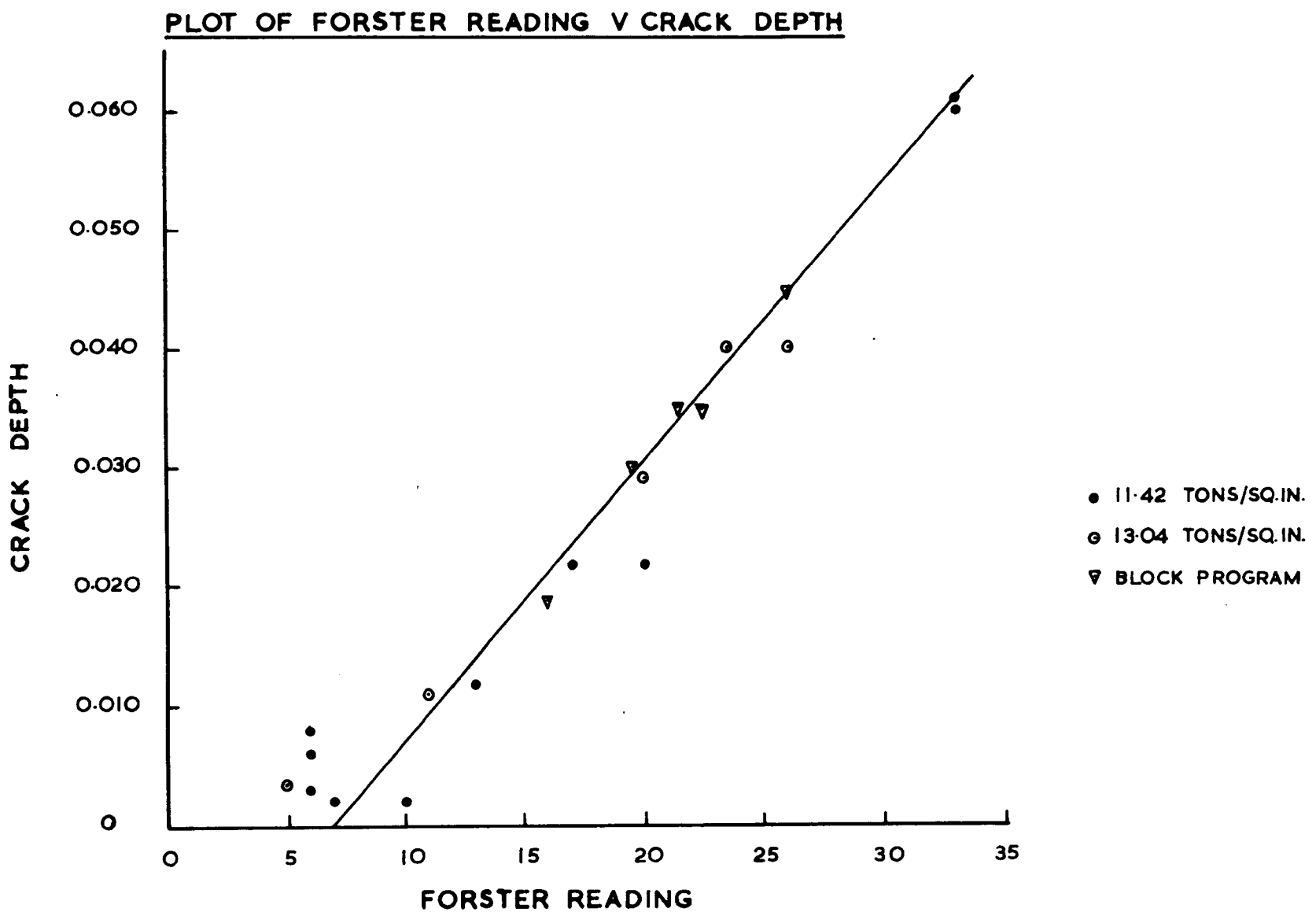
PLOT OF FORSTER READING V CRACK DEPTH
CRACK DEPTH
0.060
0.050
0.040
0.030
0.020
0.010
0
0
5
10
15
20
25
30
35
FORSTER READING
11·42 TONS/SQ.IN.
13·04 TONS/SQ.IN.
BLOCK PROGRAM

FIG. 5.1.

FIG. 5.2

GENERALISED FORSTER READING V CYCLES PLOT SHOWING DIVISION OF LIFE INTO STAGES

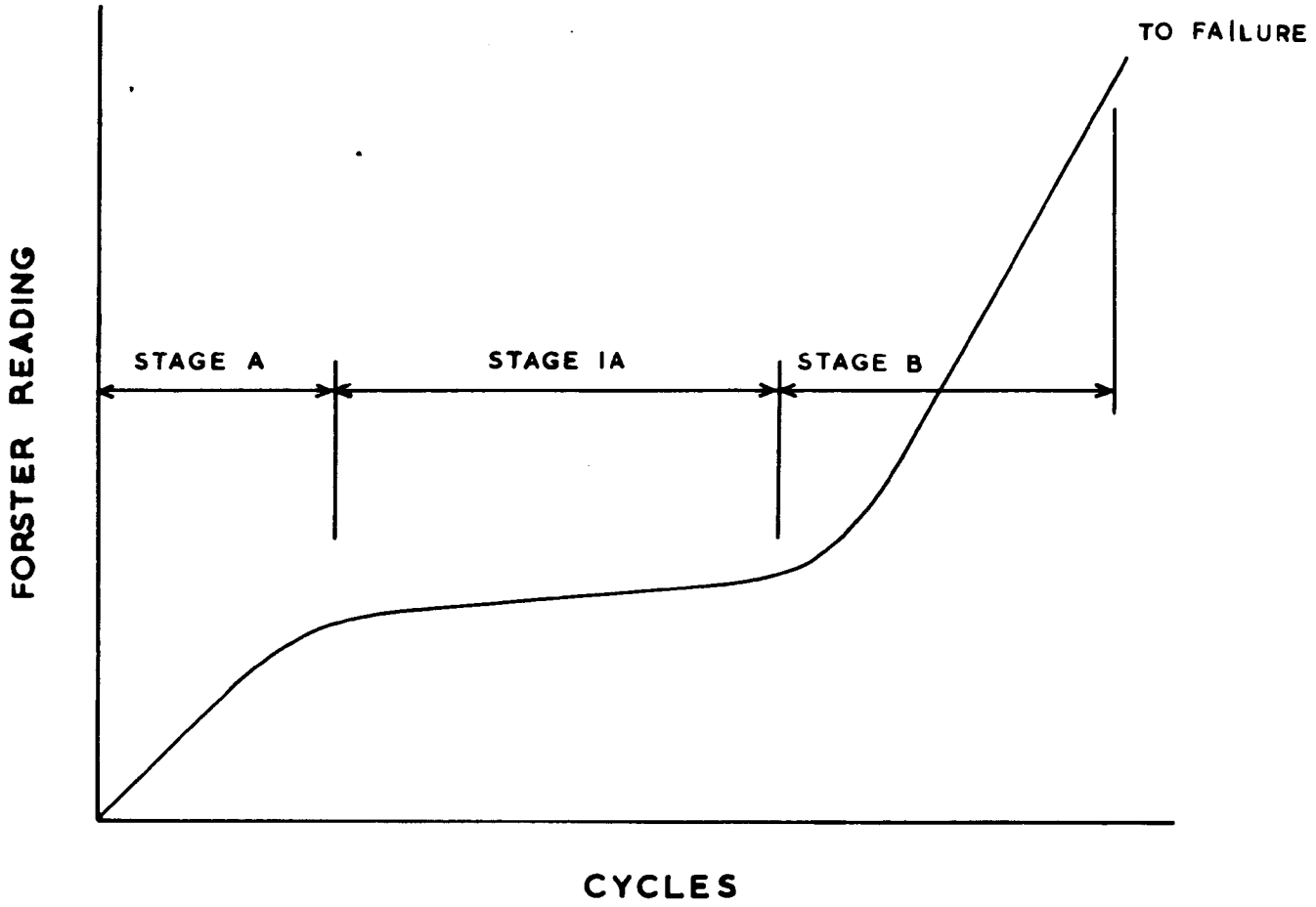

FIG. 5.3

PLOTS OF CUMULATIVE FORSTER READINGS V CYCLES AT STRESS LEVELS 11.42 TONS/SQ. IN.

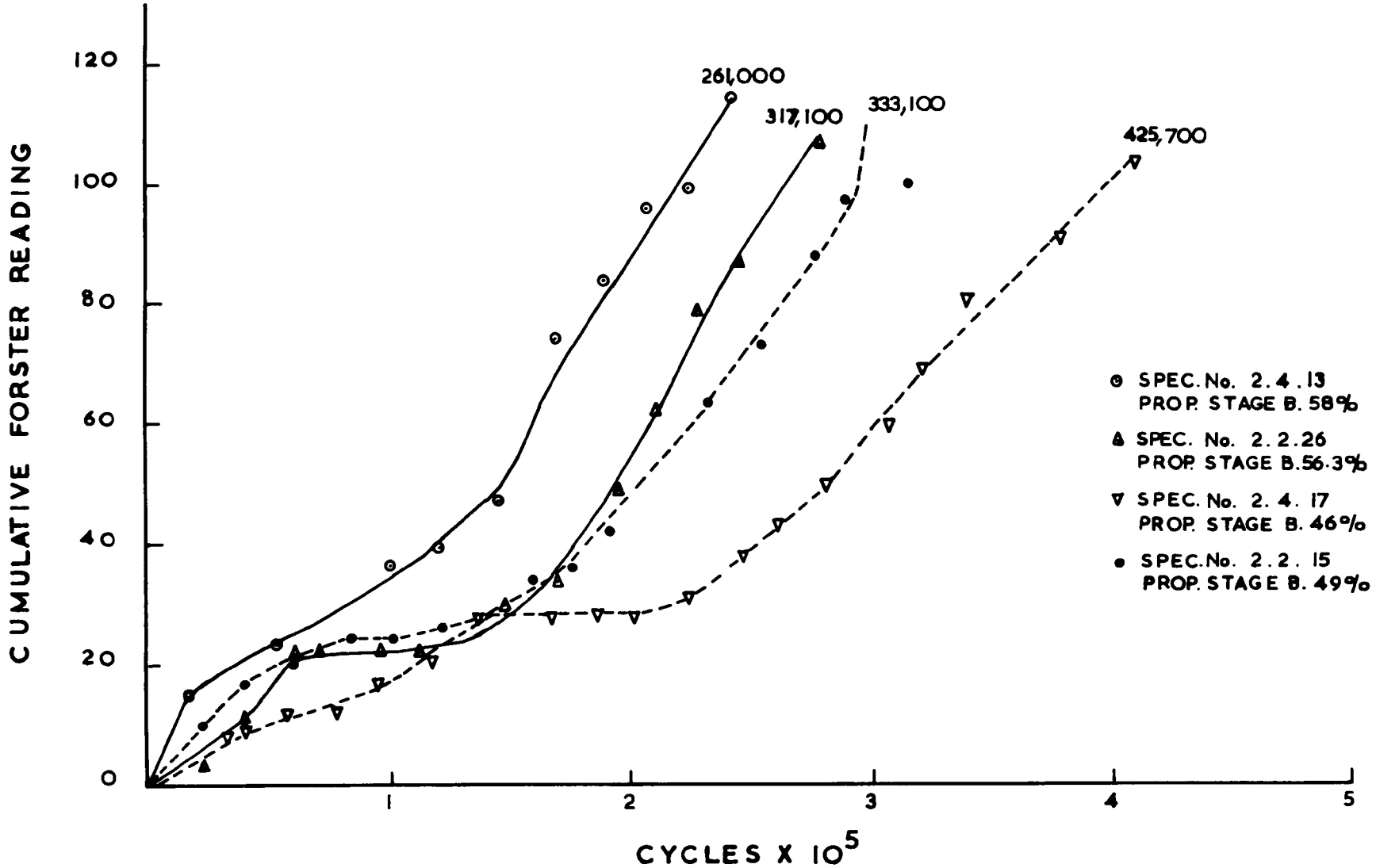

Spec. No.	Total Life	Life in Stages A & 1A	Life in Stage B	Prop. of Life in B
2.4.13	261,000	110,000	151,000	58%
2.2.26	317,100	139,000	178,100	56.3%
2.2.15	333,100	170,000	163,100	49%
2.4.17	425,700	230,000	195,700	46%
		Scatter	Scatter	
		120,000	44,700	

Stress Level 11.42 Tons/Sq.In.

TABLE 5-1

PLOT OF FORSTER READING V CYCLES AT STRESS LEVEL OF 13·04 TONS / SQ.IN.

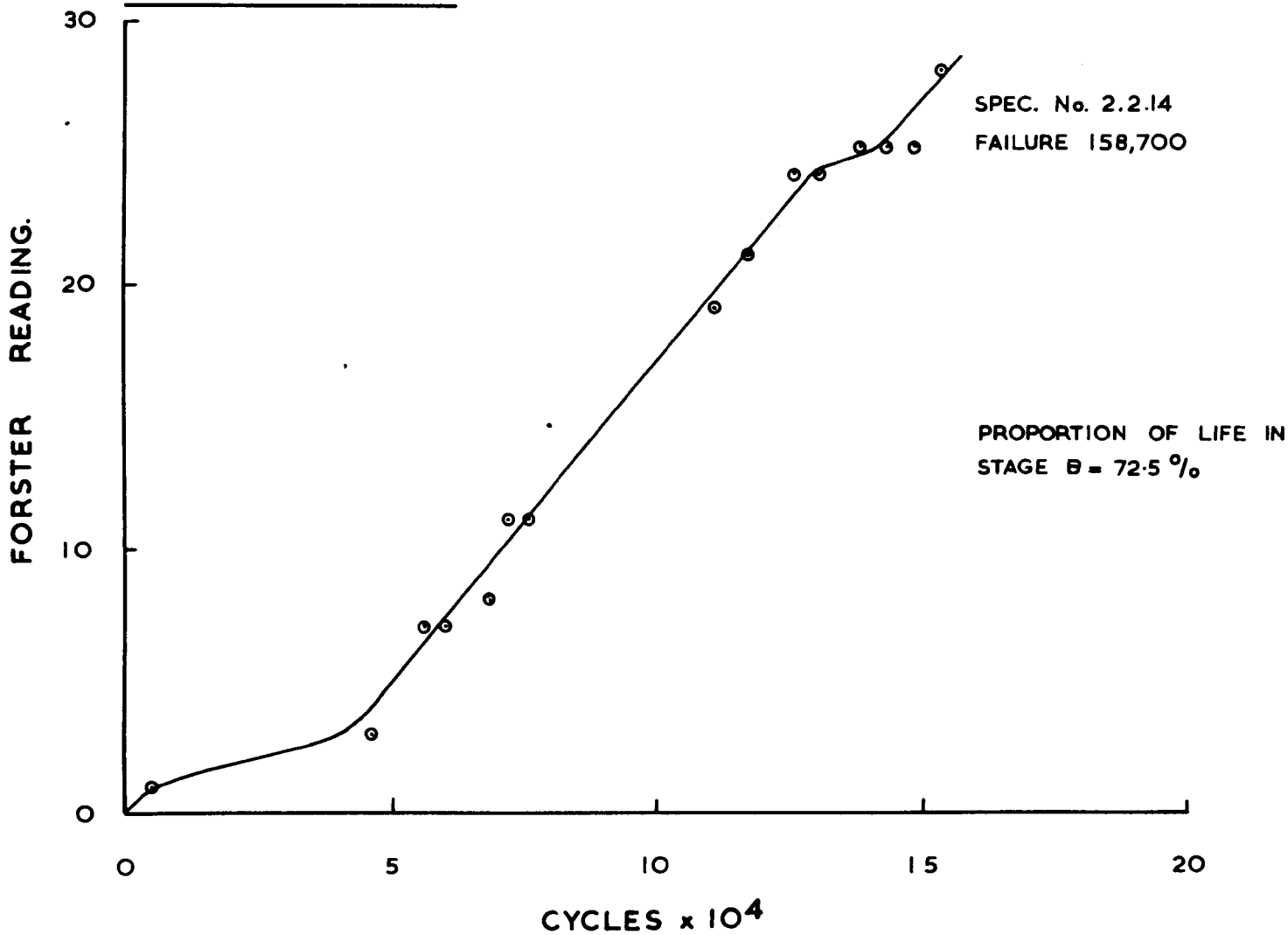

FIG. 5.4

FIG. 5.5

PLOT OF FORSTER READING V CYCLES AT STRESS LEVEL OF 9·79 TONS / SQ.IN.

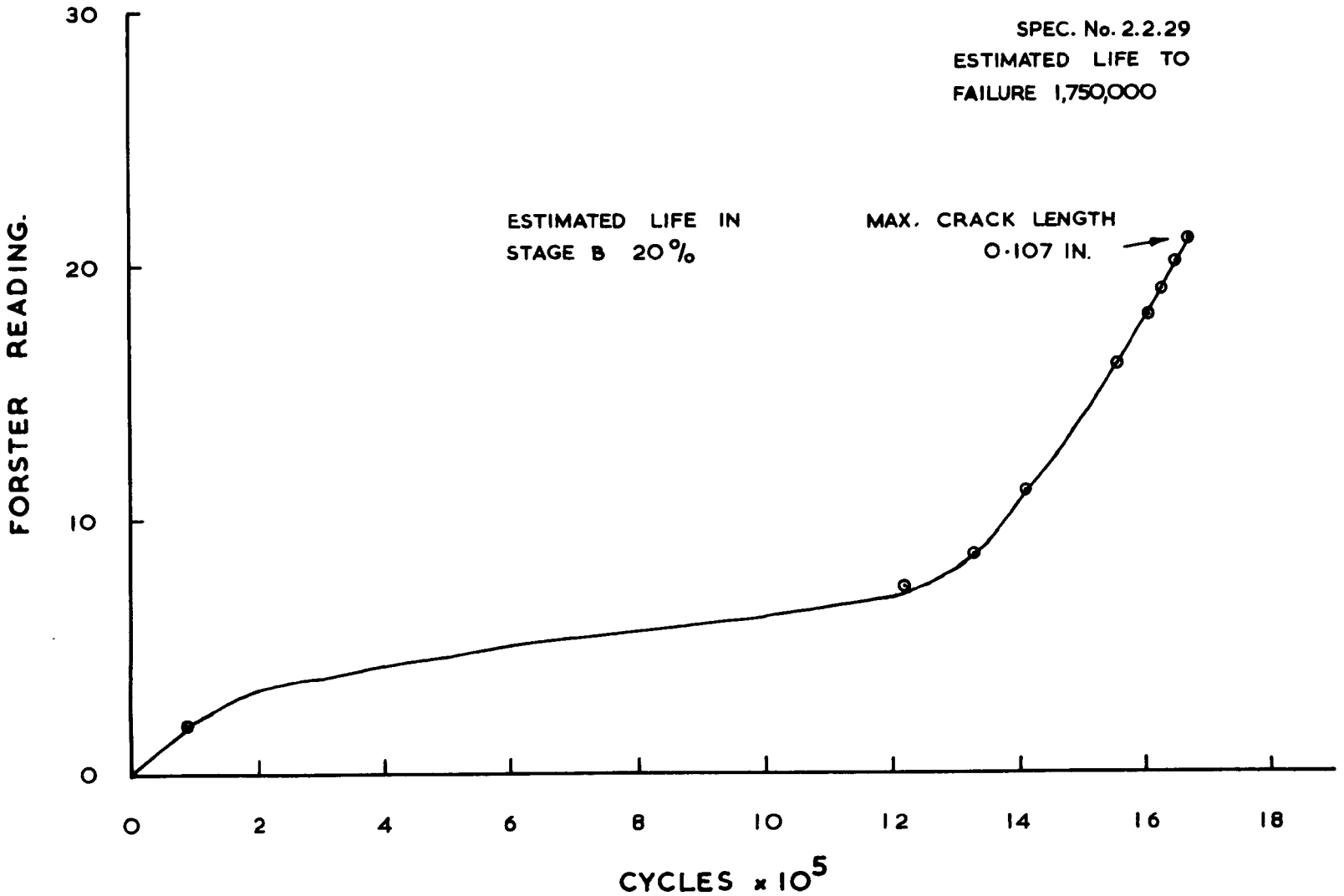

TONS/SQ.IN	CYCLES	% AGE
STRESS LEVEL	LIFE TO FAILURE	PROPORTION IN STAGE B
13·04	158,700	72·5
11·42	261,000	58·0
11·42	317,100	56·3
11·42	333,100	49·0
11·42	425,700	46·0
9·79	1,750,000•	20·0 •

• FIGURES ESTIMATED FROM A COMBINATION OF TEST DATA.

PLOT OF LIFE TO FAILURE V PROPORTION OF LIFE IN STAGE B

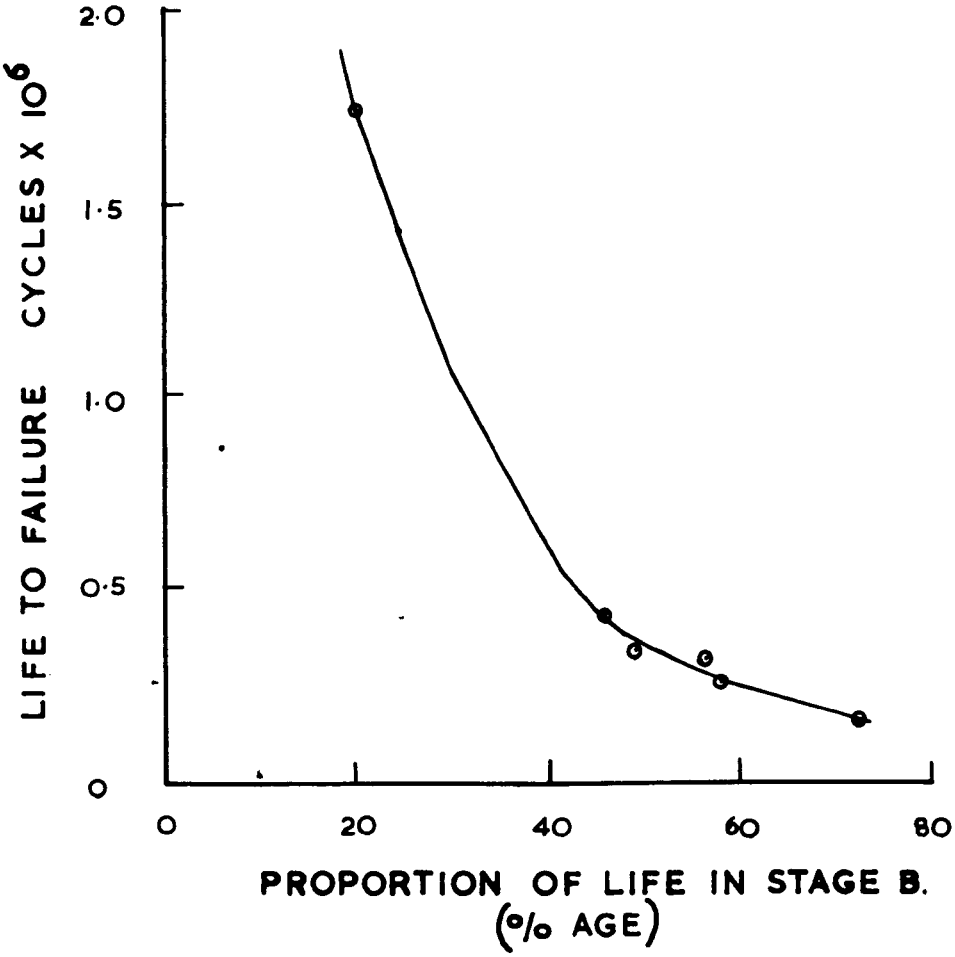

FIG. 5.6

Specimen No.	Stress Condition	Cycles in Stage A	Cycles in Stage B	Life to Failure	Log_{10}
2.4.17	11.42 constant	230,000	185,700	425,700	5.2916
2.2.15	11.42 constant	150,000	183,100	333,100	5.2627
2.2.26	11.42 constant	140,000	177,000	317,000	5.2480
2.4.13	11.42 constant	100,000	161,000	261,000	5.2068
2.4.6	11.42 constant 9.79	150,000	486,200	636,200	5.6868
2.2.16	11.42 constant 9.79	195,000	615,300	810,300	5.7891
2.2.22	11.42 constant 9.79	207,800	435,300	643,100	5.6388
2.2.9	11.42 constant 9.79	121,300	538,800	660,100	5.7314
2.4.22	11.42 constant 9.79	500,100	696,900	1,197,000	5.8432
2.2.17	11.42 constant 8.16	190,900	1,586,800	1,777,700	6.2007
2.2.18	11.42 constant 8.16	186,400	1,330,000	1,516,400	6.1239
2.4.28	11.42 constant 8.16	163,400	1,202,800	1,366,200	6.0802
2.2.7	11.42 constant 8.16	205,200	1,192,800	1,398,000	6.0766

TABLE 5-2

Specimen No.	Stress Condition	Cycles in Stage A	Cycles in Stage B	Life to Failure	Log_{10}
2.2.6	11.42 constant 7.34	178,200	3,520,600	3,698,800	6.5466
2.2.3	11.42 constant 7.34	257,100	1,832,700	2,072,700	6.2632
2.4.30	11.42 constant 6.52	180,000		2,493,100 Unbroken	6.3967
2.2.23	11.42 constant 6.52	171,600		10,990,000 Unbroken	7.0411

TABLE 5-2 (page 2)

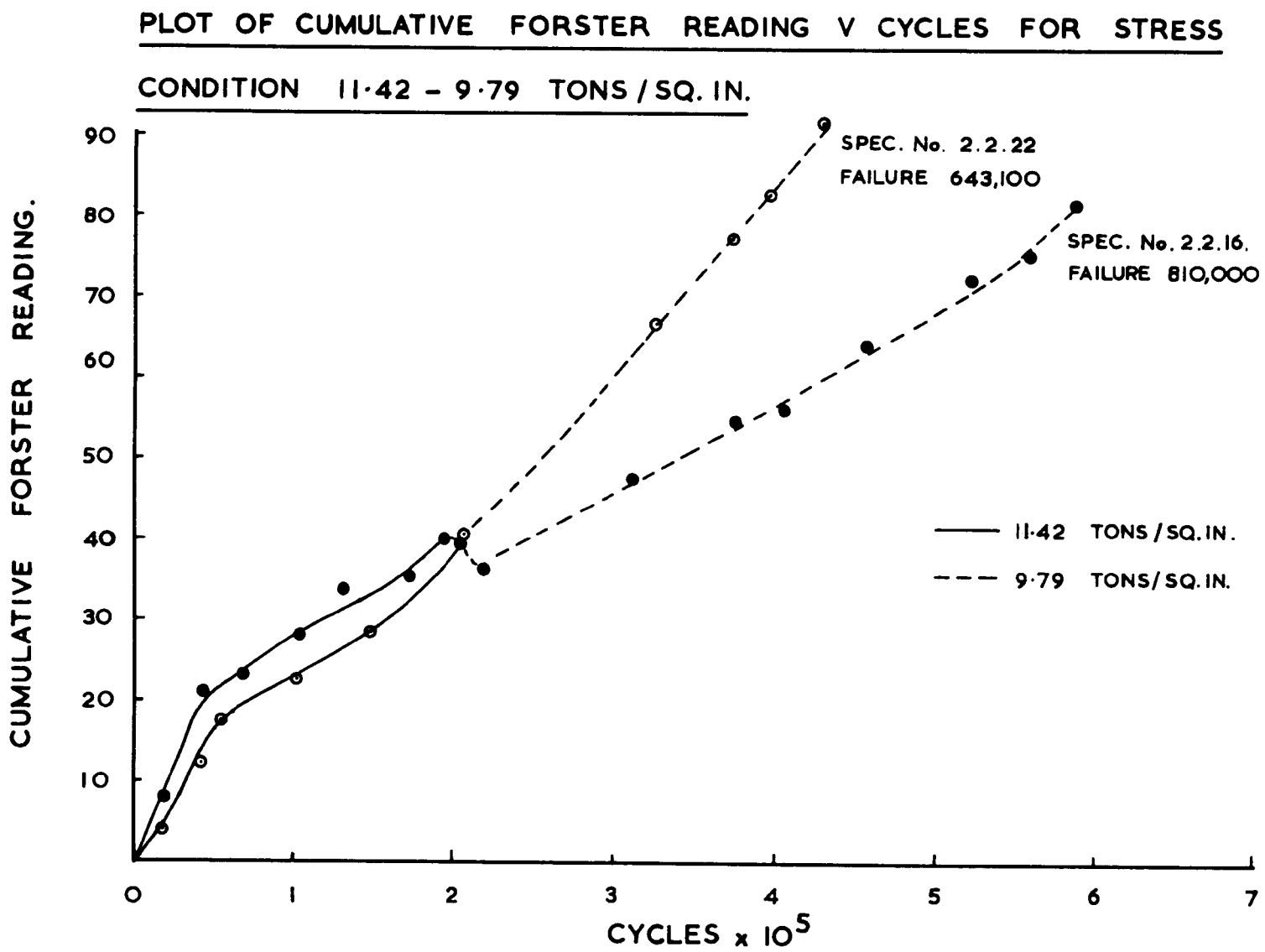
PLOT OF CUMULATIVE FORSTER READING V CYCLES FOR STRESS
CONDITION 11·42 – 9·79 TONS / SQ. IN.
CUMULATIVE FORSTER READING.
90
80
70
60
50
40
30
20
10
0
1
2
3
4
5
6
7
CYCLES x 10^5
SPEC. No. 2.2.22
FAILURE 643,100
SPEC. No. 2.2.16.
FAILURE 810,000
11·42 TONS / SQ. IN.
9·79 TONS / SQ. IN.

FIG. 5.7

FIG. 5.8

PLOT OF CUMULATIVE FORSTER READING V CYCLES FOR STRESS CONDITION

11·42 – 8·16 TONS / SQ. IN.

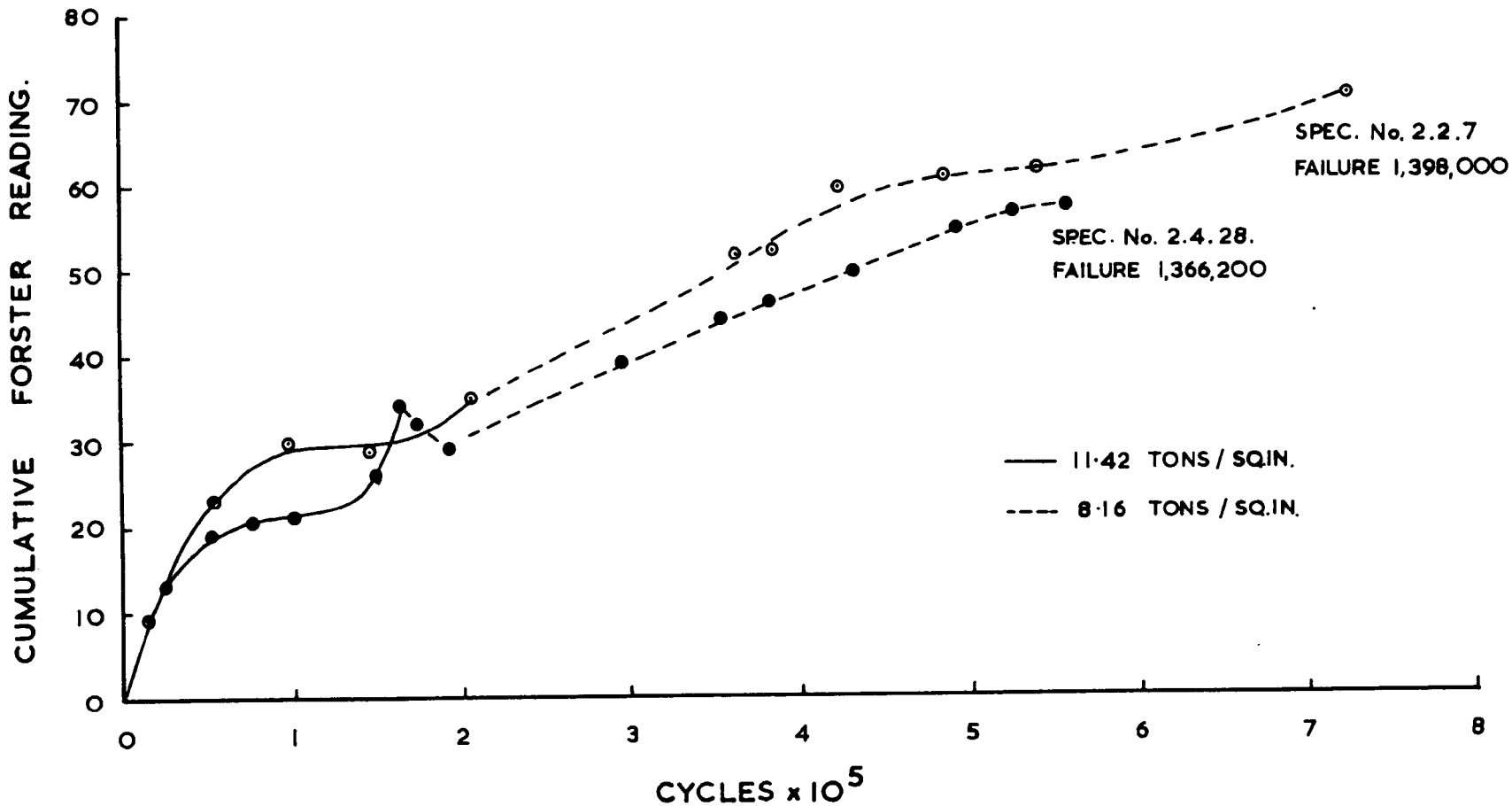

FIG 5.9

PLOT OF CUMULATIVE FORSTER READING V CYCLES FOR STRESS CONDITION 11·42 – 7·34 TONS / SQ. IN.

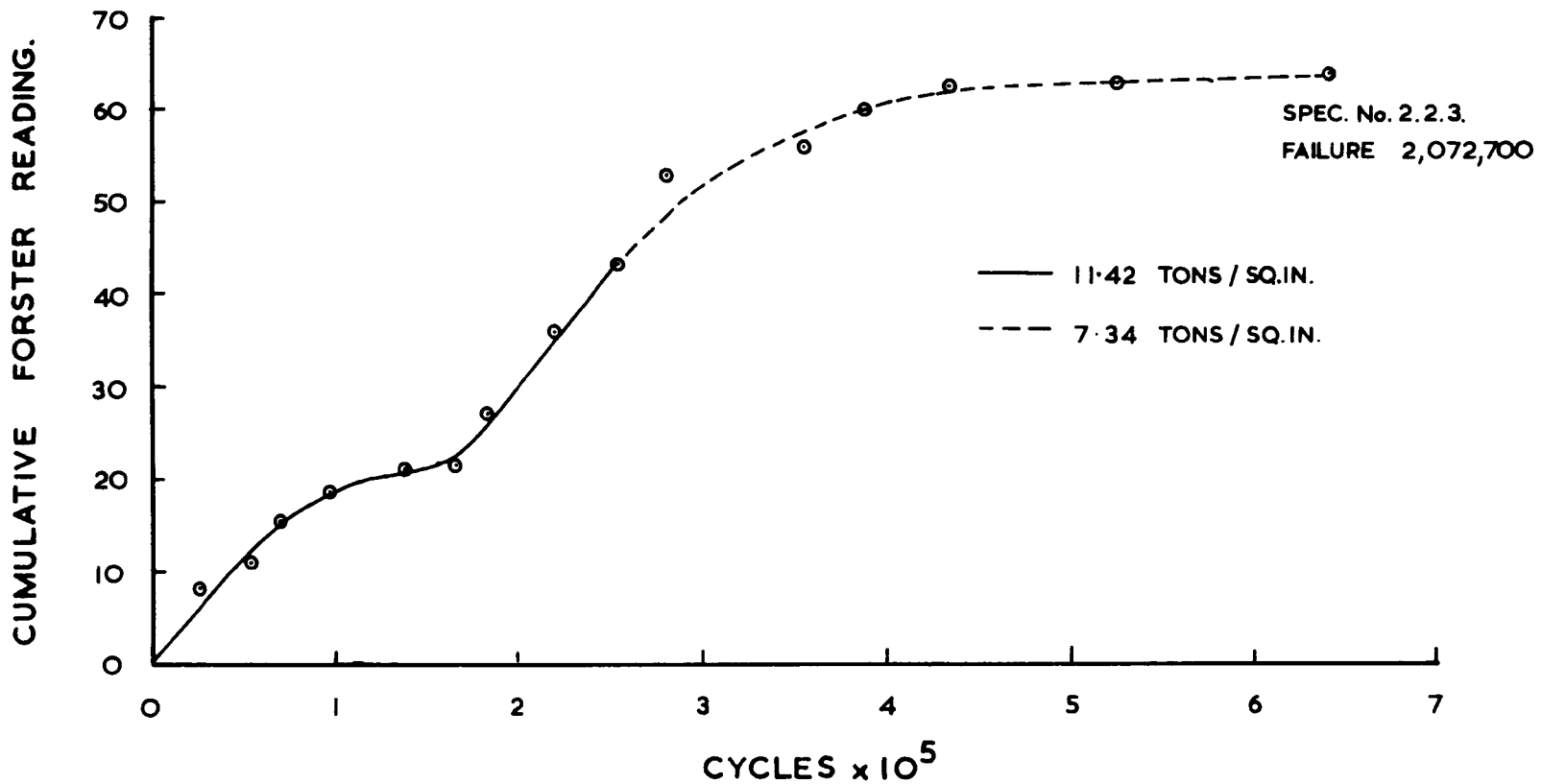

PLOT OF CUMULATIVE FORSTER READING V CYCLES FOR STRESS CONDITION 11·42 6·52 TONS / SQ. IN.

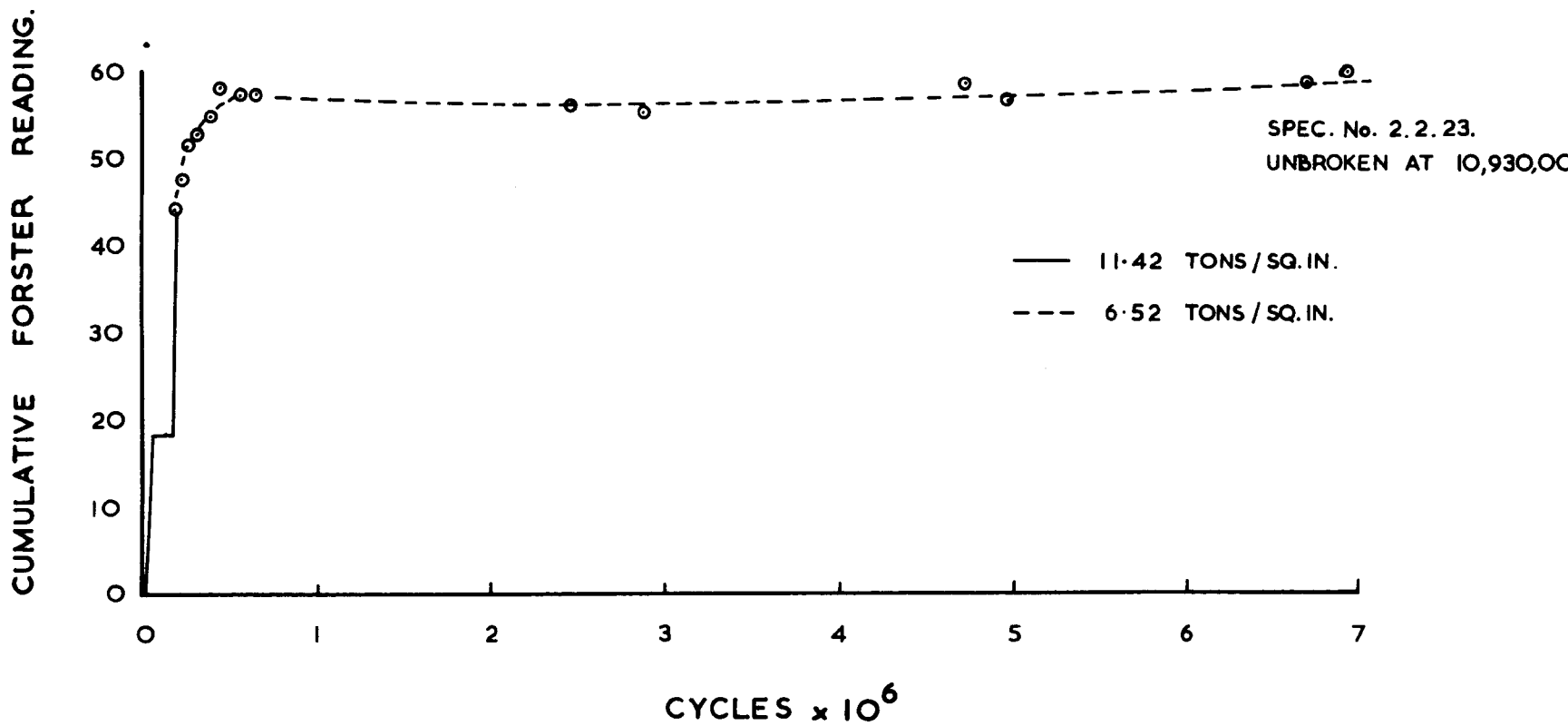

FIG. 5.10

S-N CURVE FOR MACRO CRACK PROPAGATION

(LIFE IN STAGE B)

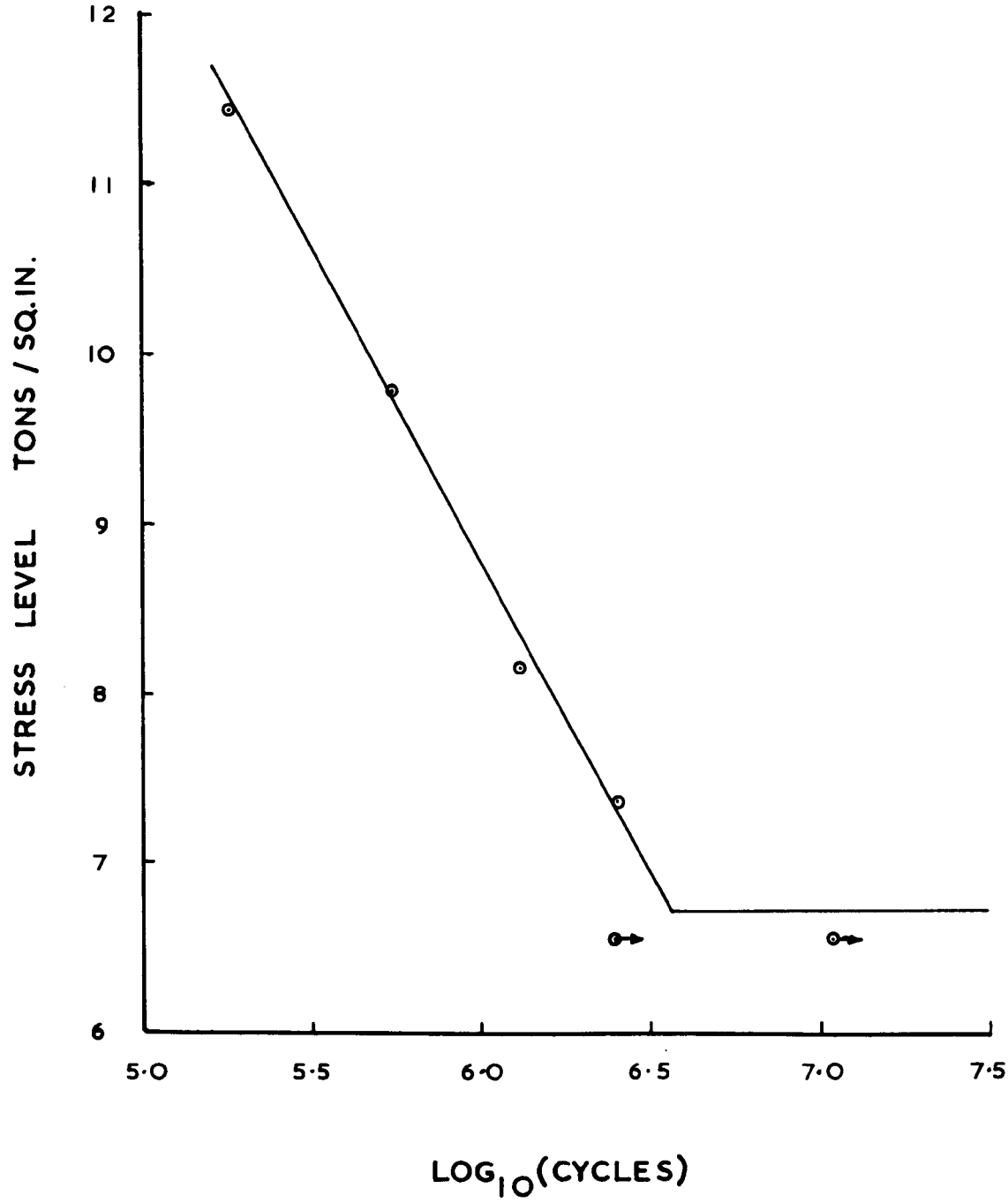

FIG 5.11

TABLE 5-3

Spec. No.	Cycles and B Summ. at 9.79 Tons/ Sq. In.	Cycles and B Summ. at 8.16 Tons/ Sq. In.	Cycles and B Summ. at 7.34 Tons/ Sq. In.	Cycles and B Summ. at 6.52 Tons/ Sq. In.	Total B Summ.	Description of Test.
2.2.11	143,400	935,500				40,000 Blocks of 9.79 &8.16
Alt(i)	0.26	0.82	-	-	1.08	& then 8.16 to Failure.
Alt(ii)	0.26	0.82			1.08	
2.2.4	358,000	91,000	-	-		40,000 Blocks of 9.79 & 8.16
Alt(i)	0.66	0.08			0.74	& then 9.79 to Failure
Alt(ii)	0.66	0.08	-	-	0.74	
2.4.26	310,000		-	2,169,500		40,000 Blocks of 9.79 & 6.52
Alt(i)	0.57	-	-	0	0.57	to approximately 700,000 -
Alt(ii)	0.57	-	-	0.50	1.07	1.5×10^6 at 6.52 Tons/sq.in.-
						Blocks of 9.79 & 6.52- 6.52 to failure.
2.4.24	144,600	592,400	-	69,600		10,000 Blocks of 9.79 & 8.16 - 10,000
Alt(i)	0.26	0.52		0	0.78	Blocks of 9.79 & 6.52 - 8.16 to Failure.
Alt(ii)	0.26	0.52		0.02	0.80	
2.4.9	141,600	112,100		9,848,000		In addition 15,297,000 at 4.19 Tons/sq.in
Alt(i)	0.26	0.10		-	0.36	$\sum \frac{n}{N} = 1.33$
Alt(ii)	0.26	0.10		2.24	3.93	
2.2.19	120,000	120,000		1,436,100		10,000 Cycles Blocks of 9.79,6.52,8.16 -
Alt(i)	0.22	0.11		-	0.33	10,000 Cycle Blocks of 9.79,8.16,6.52 -
Alt (ii)	0.22	0.11		0.33	0.66	6.52 to Failure.

Spec. No.	Cycles and B Summ. at 9.79 Tons/ Sq. In.	Cycles and B Summ. at 8.16 Tons/ Sq. In.	Cycles and B Summ. at 7.34 Tons/ Sq. In.	Cycles and B Summ. at 6.52 Tons/ Sq. In.	Total B Summ.	Description of Test
2.4.29	200,000	60,000		19,550,000		
Alt(i)	0.37	0.05			0.42	
Alt(ii)	0.37	0.05		4.70	5.12	

TABLE 5-3

PLOT OF CUMULATIVE FORSTER READING V CYCLES FOR A BLOCK PROGRAM LOADING

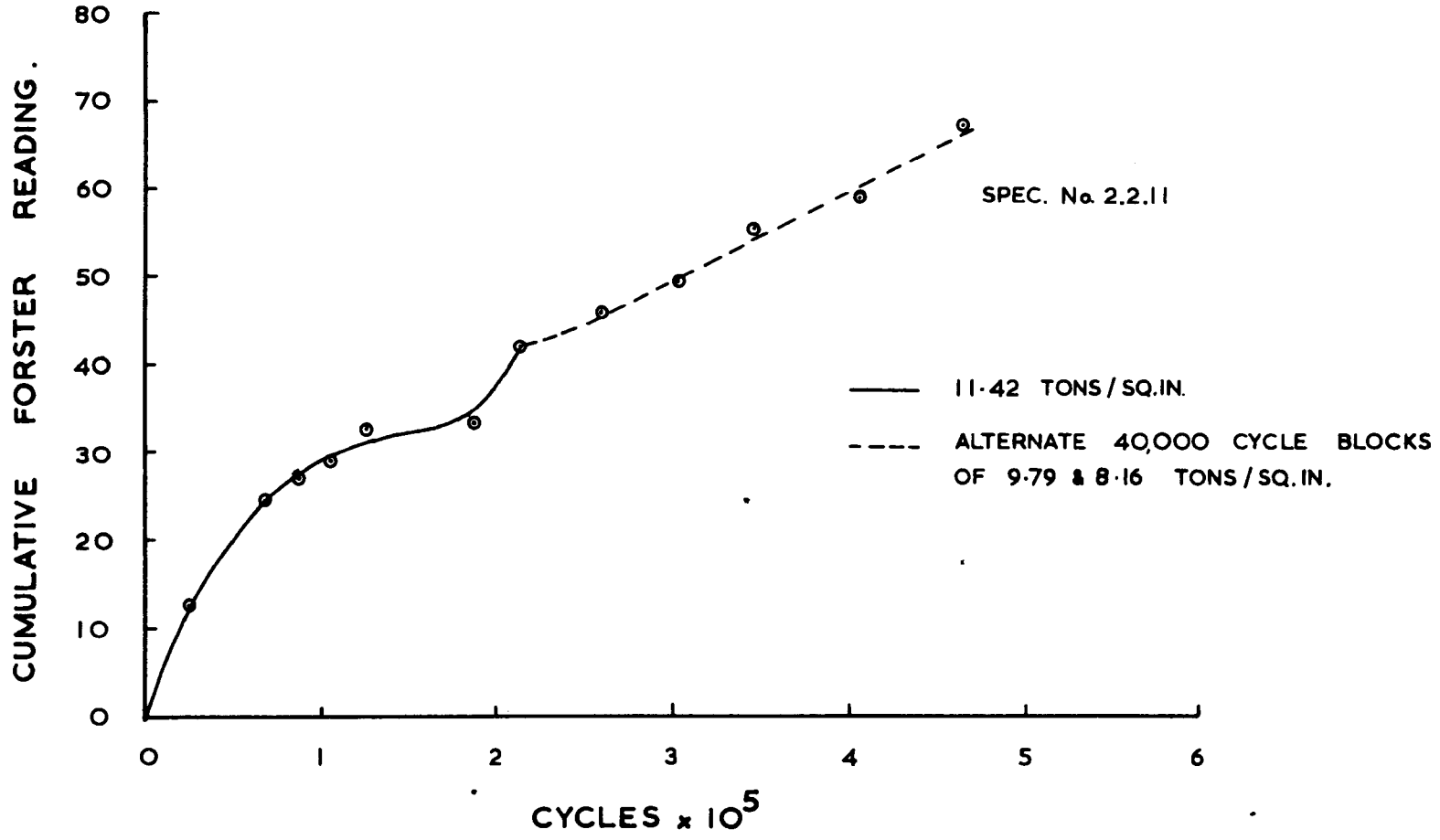

FIG 5.12.

PLOT OF CUMULATIVE FORSTER READING V CYCLES FOR VARIOUS BLOCK LOADING PROGRAMS.

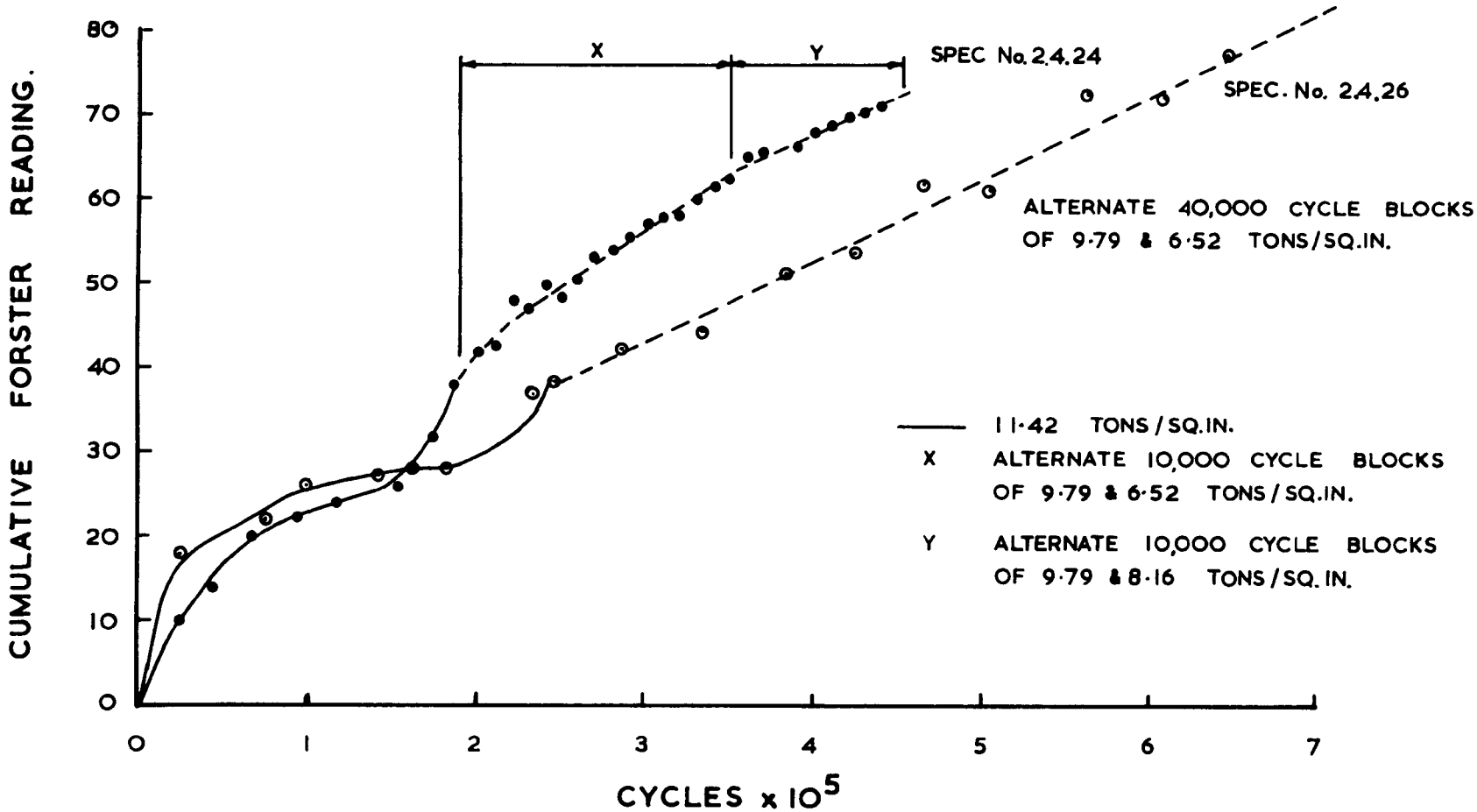

FIG 5.14

FIG 5.15.

PLOT OF CUMULATIVE FORSTER READING V CYCLES SHOWING EFFECT OF LOAD SEQUENCE.

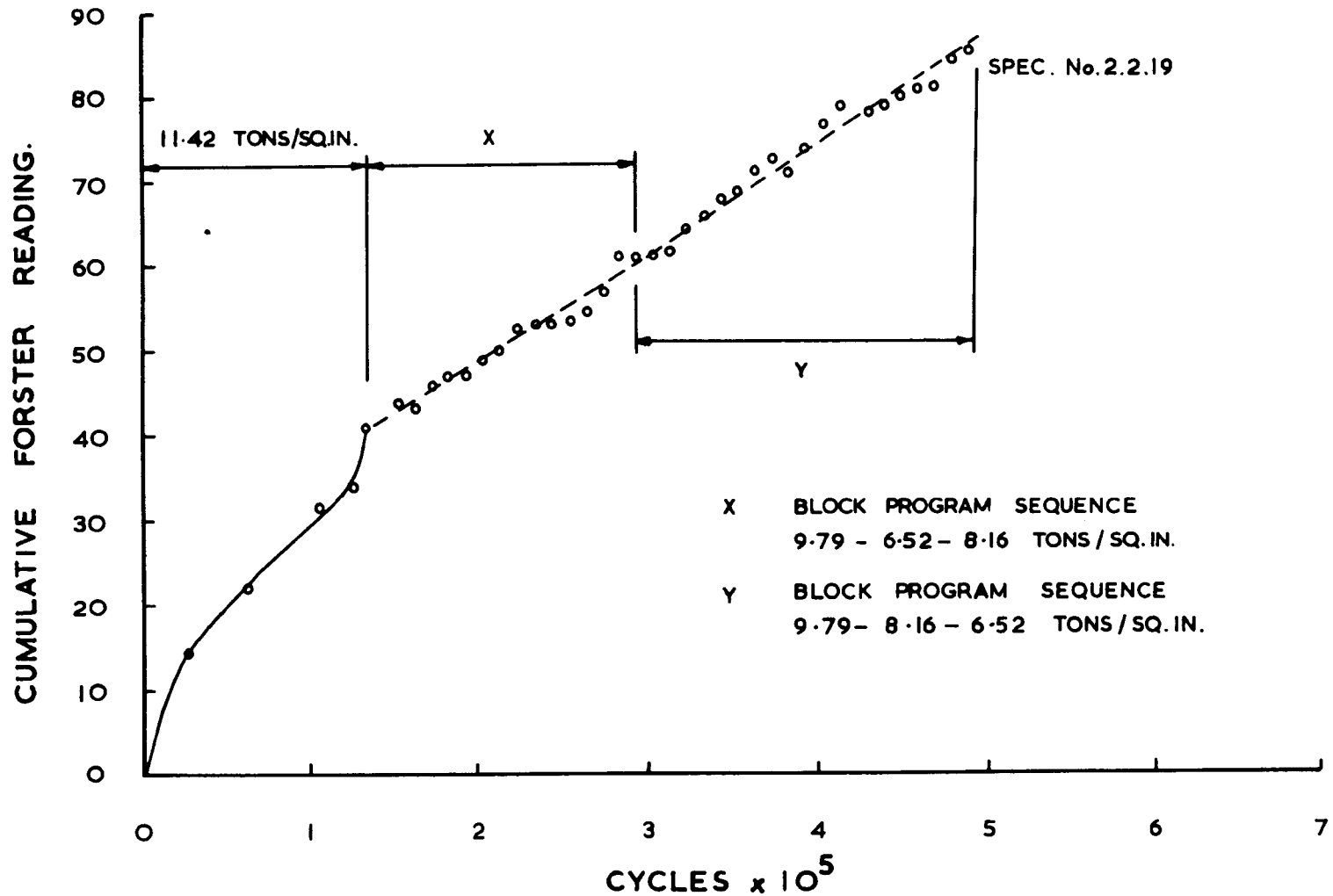

PLOT OF CUMULATIVE FORSTER READING V CYCLES SHOWING EFFECT OF CHANGE IN BLOCK LENGTH.

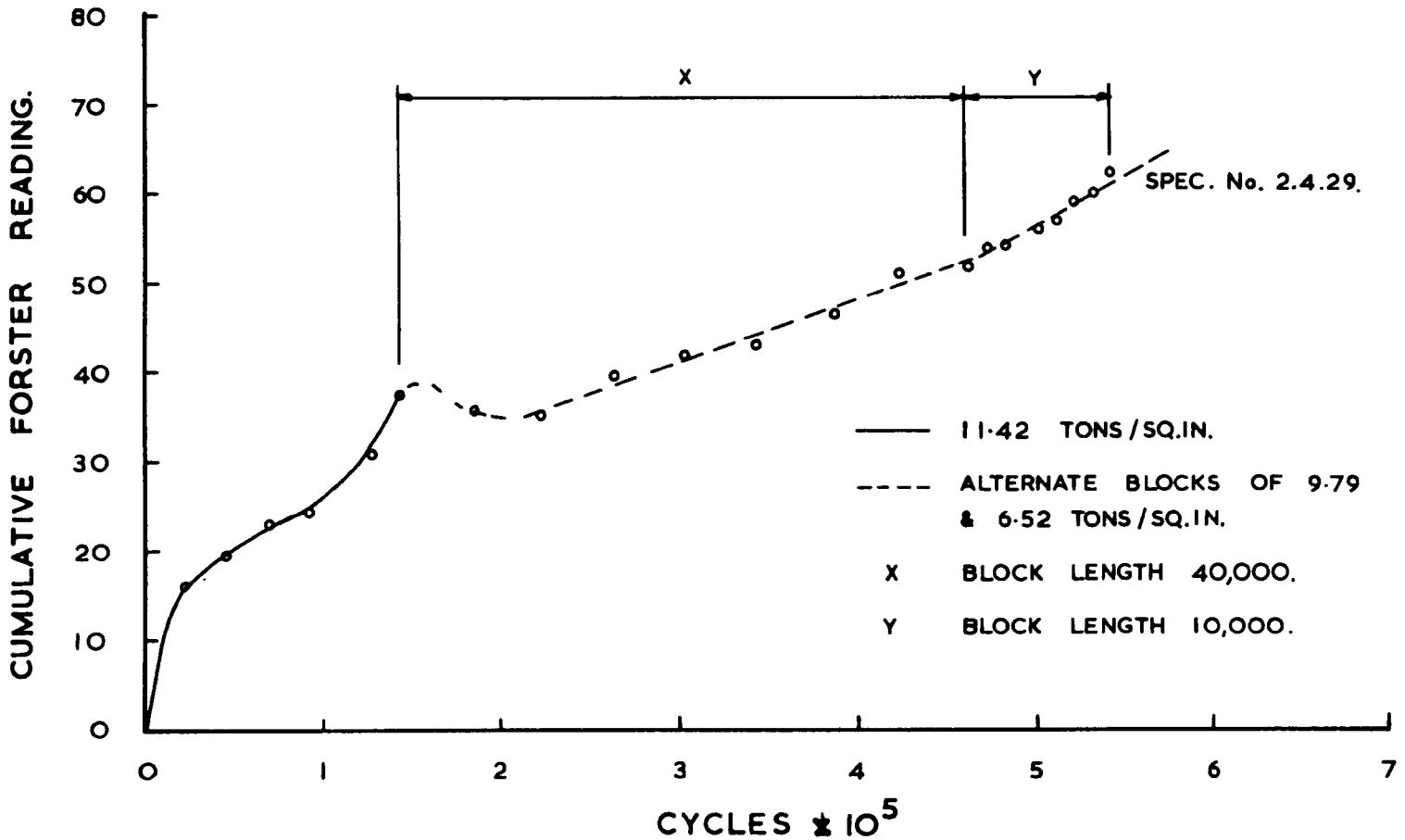

FIG 5.16

FIG 5.17

PLOT OF CUMULATIVE FORSTER READING V CYCLES FOR BLOCK LOADING PROGRAMS.

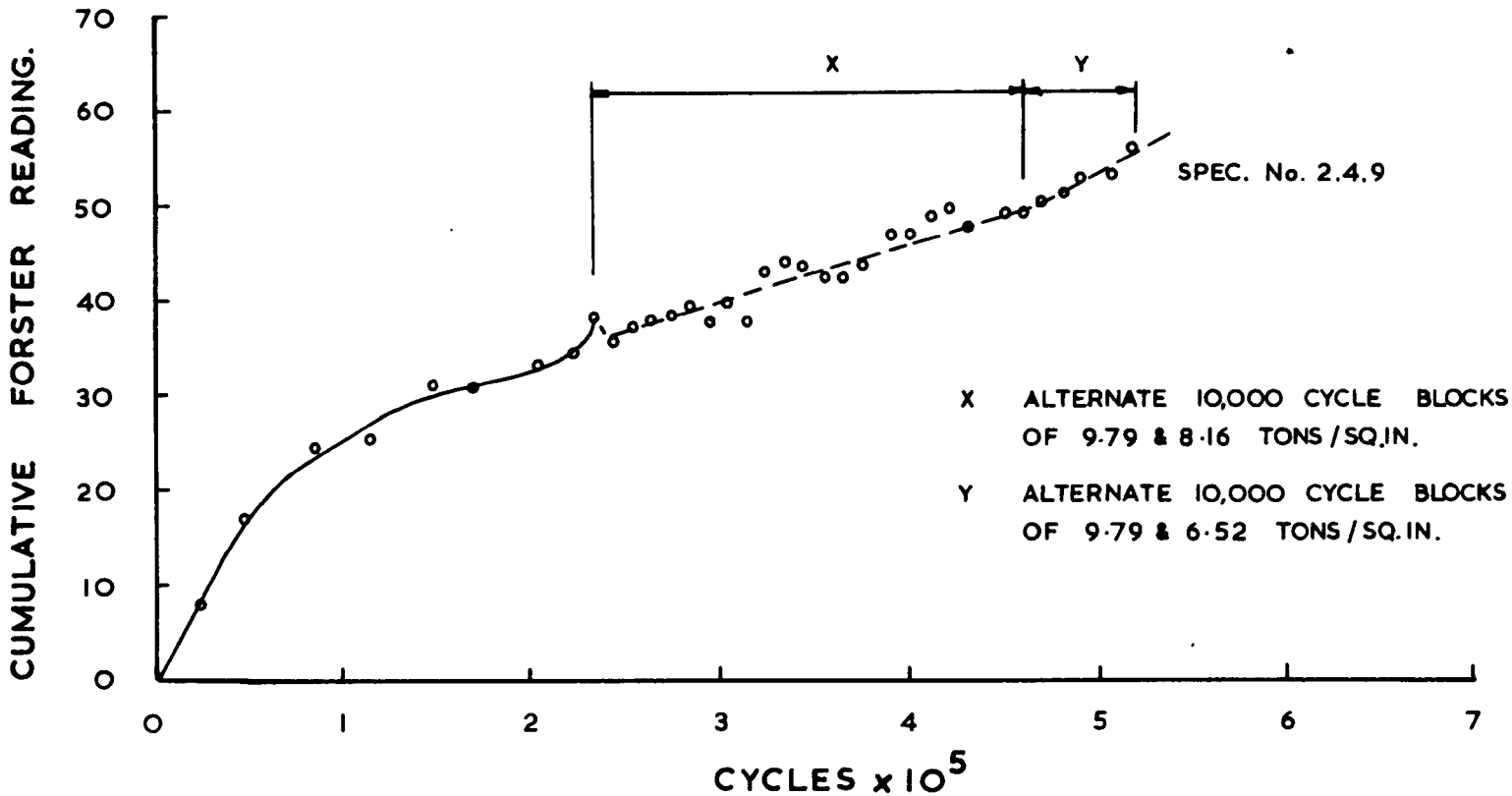

FIG 5.18

PLOT OF CUMULATIVE FORSTER READING V CYCLES FOR BLOCK LOADING PROGRAMS.

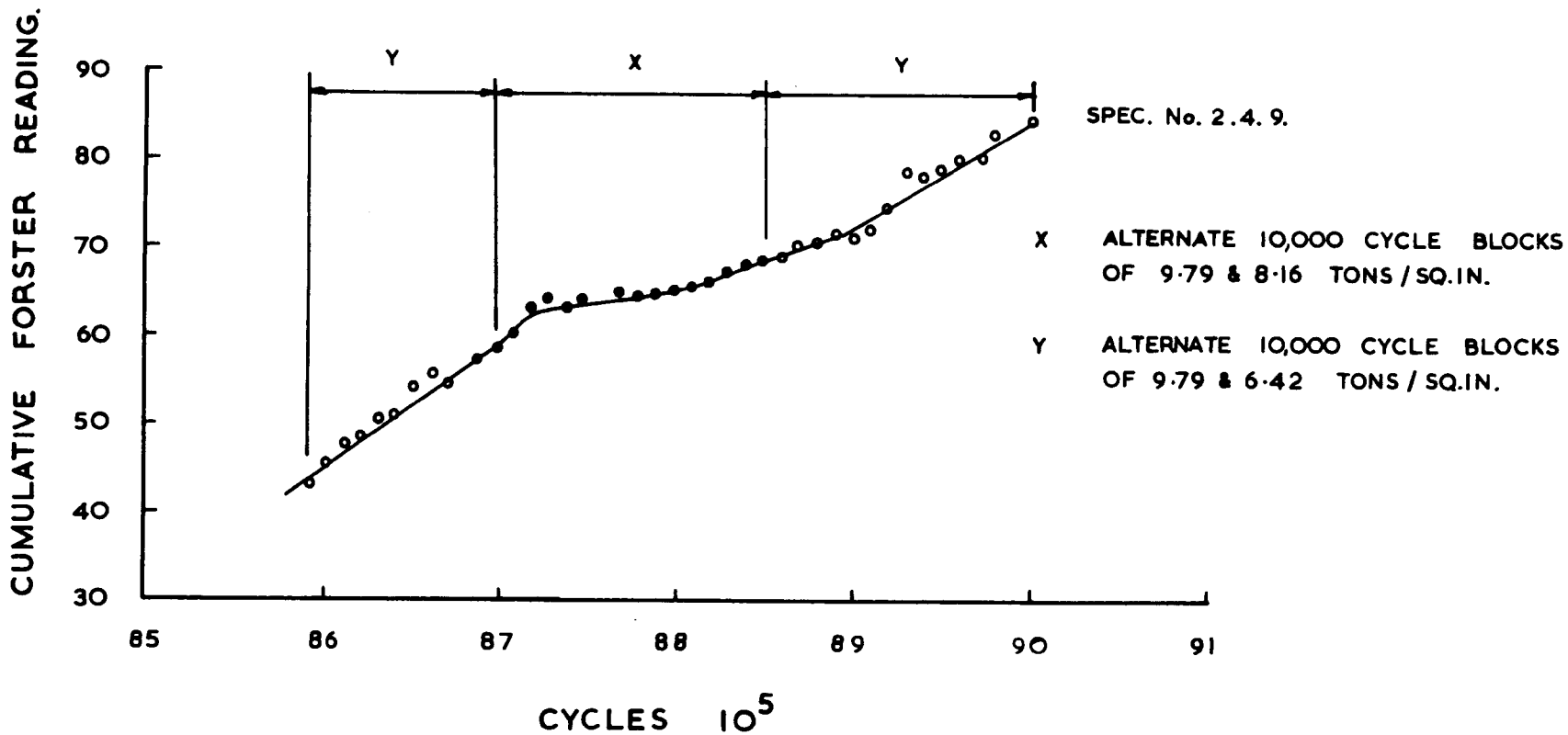

Block Stress Levels	40,000 Cycles Blocks	10,000 Cycle Blocks
9.79	0.50	0.66
6.52	0.36	0.54
		0.57
		0.70
		0.62
Mean	0.43	0.62
9.79	0.83	0.44
8.16	0.50	0.30
		0.37
Mean	0.67	0.37

TABLE 5-4

FIG. 5.19

PLOT OF CUMULATIVE FORSTER READING V CYCLES FOR BLOCK LOADING OF 11·42 & 8·16 TONS/SQ.IN.

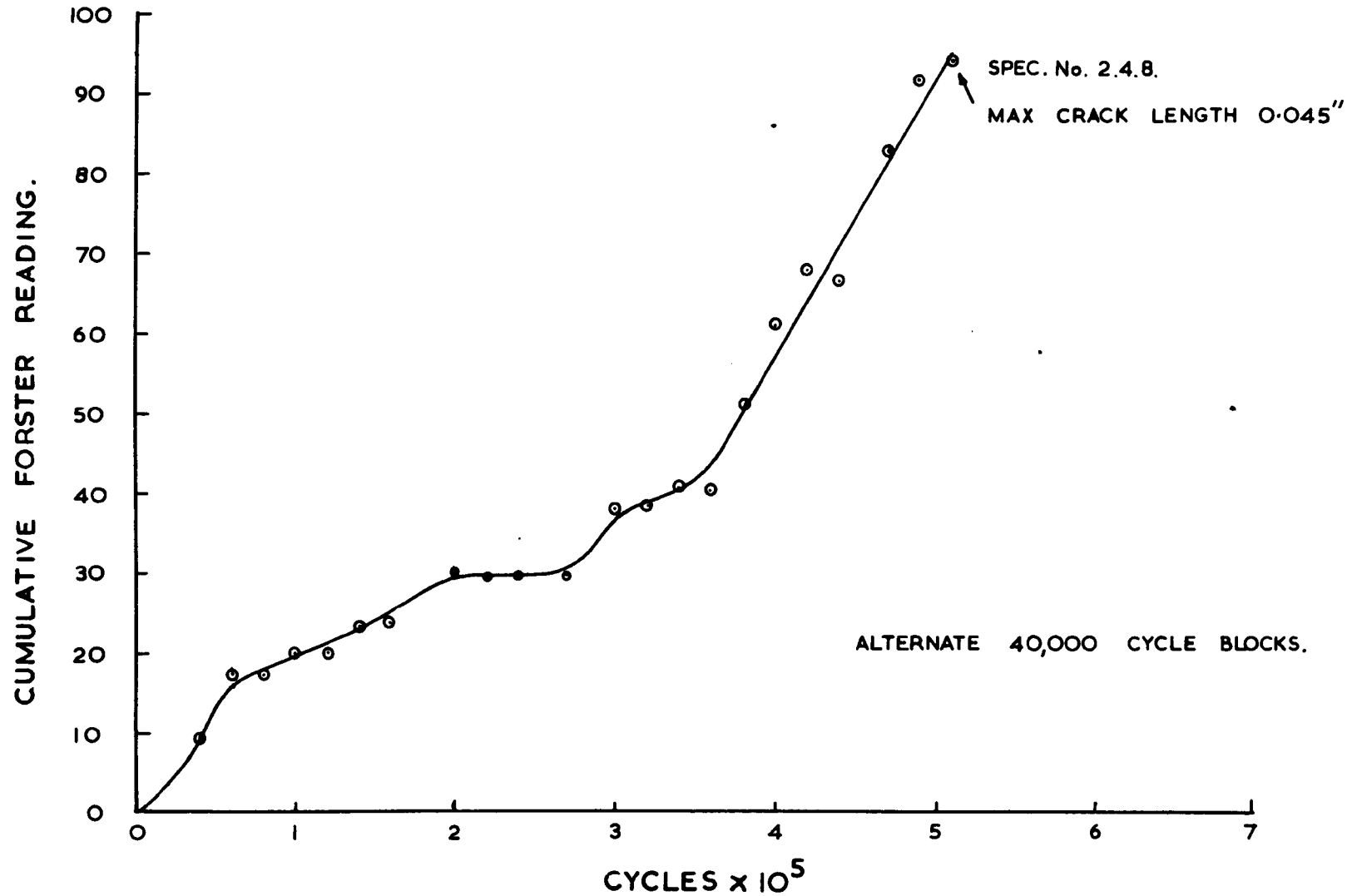

PLOT OF CUMULATIVE FORSTER READING V CYCLES FOR BLOCK LOADING 8·16 & 11·42 TONS / SQ. IN.

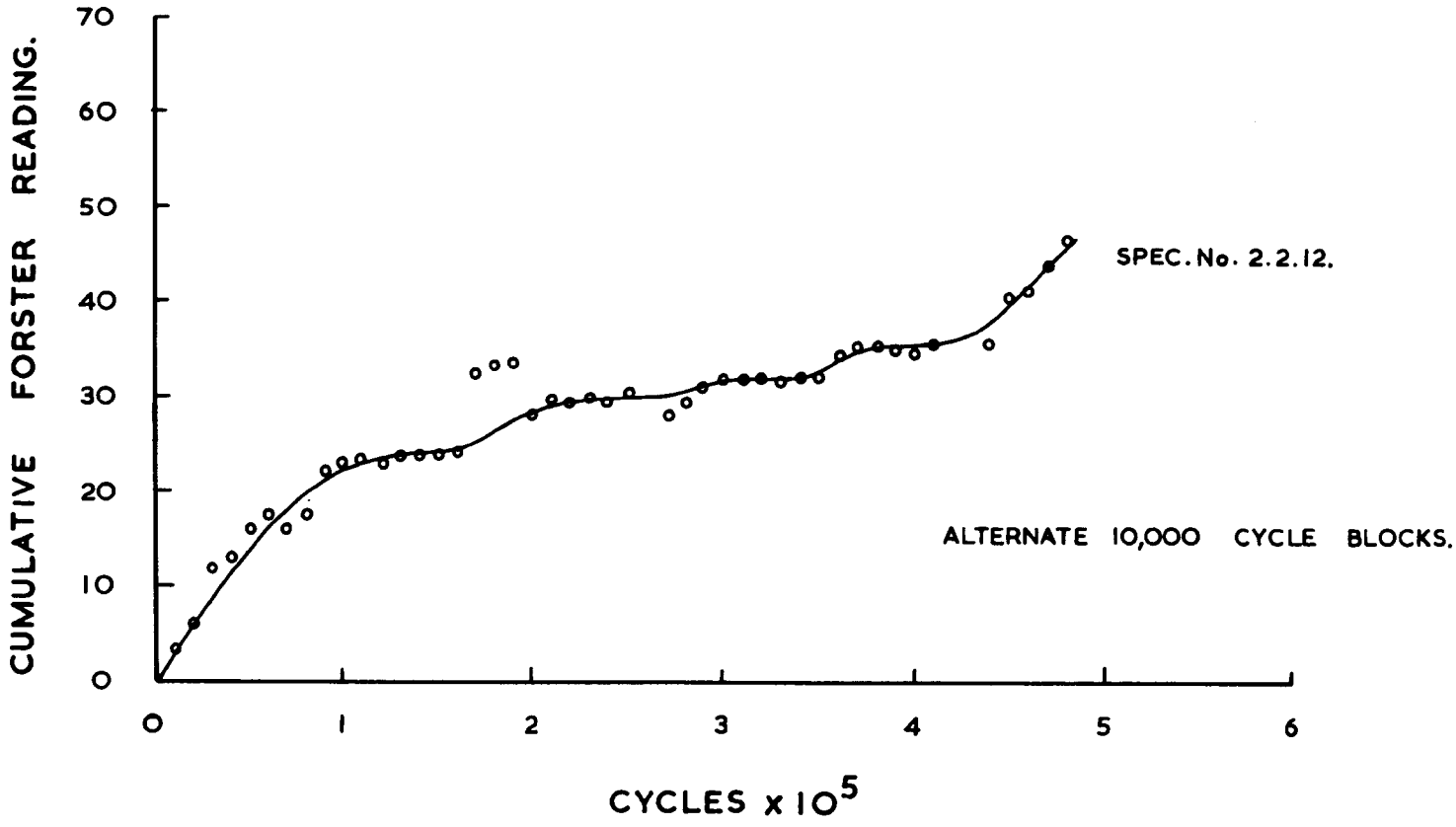

FIG. 5.20

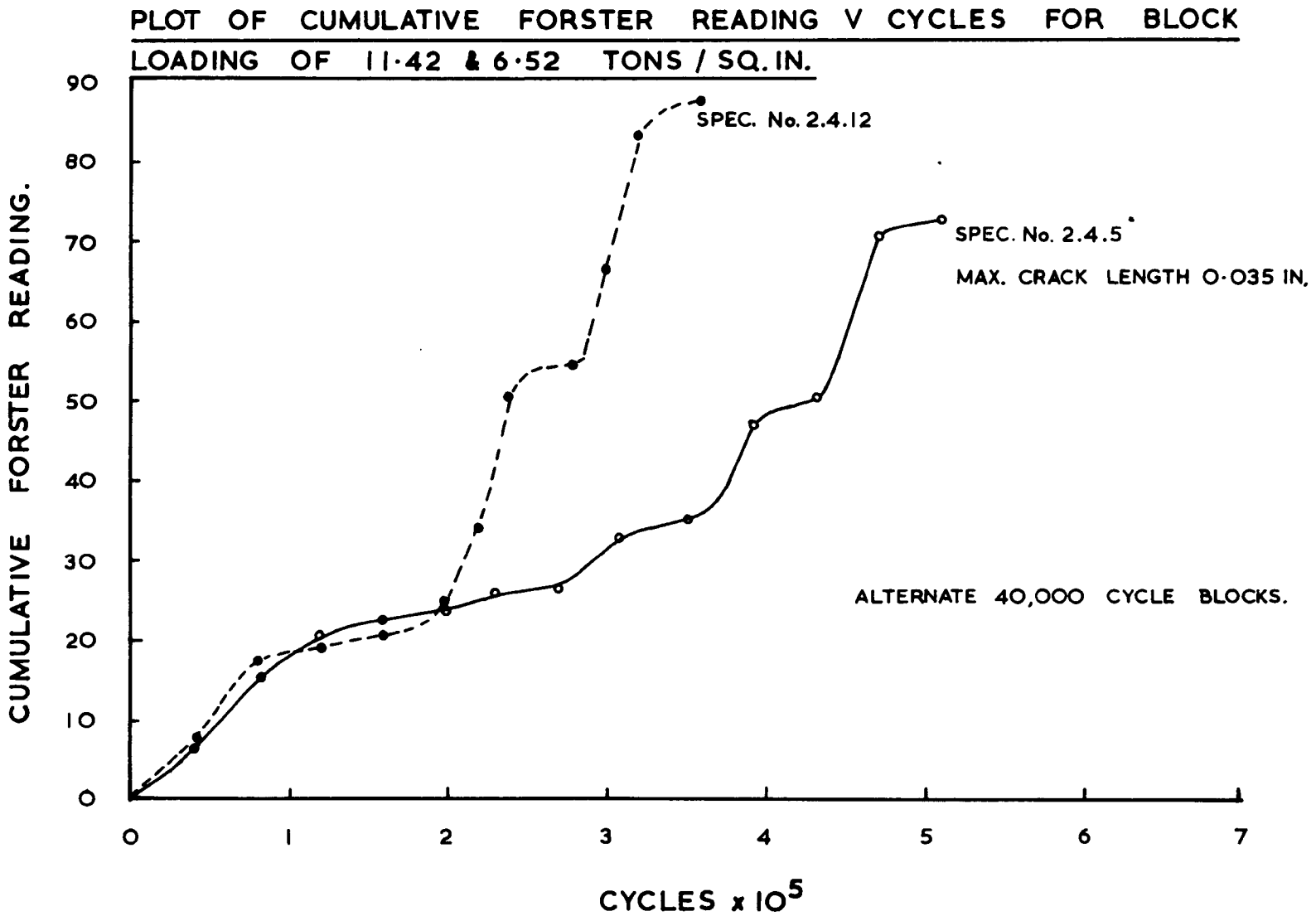
PLOT OF CUMULATIVE FORSTER READING V CYCLES FOR BLOCK LOADING OF 11·42 & 6·52 TONS / SQ. IN.
SPEC. No. 2.4.12
SPEC. No. 2.4.5
MAX. CRACK LENGTH 0·035 IN.
ALTERNATE 40,000 CYCLE BLOCKS.
CUMULATIVE FORSTER READING.
CYCLES x 10^5
0
10
20
30
40
50
60
70
80
90
0
1
2
3
4
5
6
7

FIG. 5.21

PLOT OF CUMULATIVE FORSTER READING V CYCLES FOR BLOCK LOADING OF 11·42 & 6·52 TONS / SQ. IN.

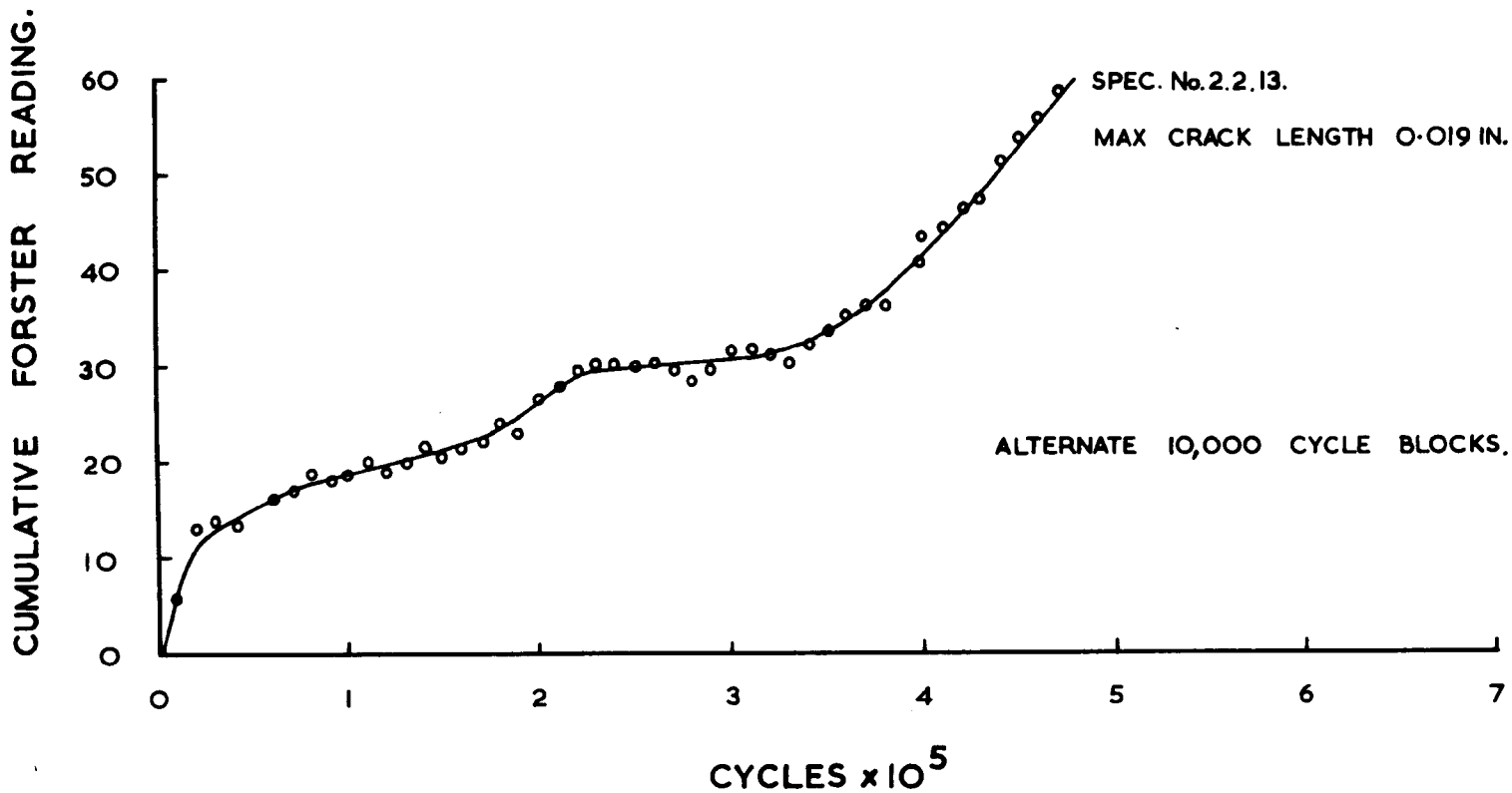

FIG 5.22

PLOT OF CUMULATIVE FORSTER READING V CYCLES FOR BLOCK LOADING OF 11·42 & 6·52 TONS / SQ. IN.

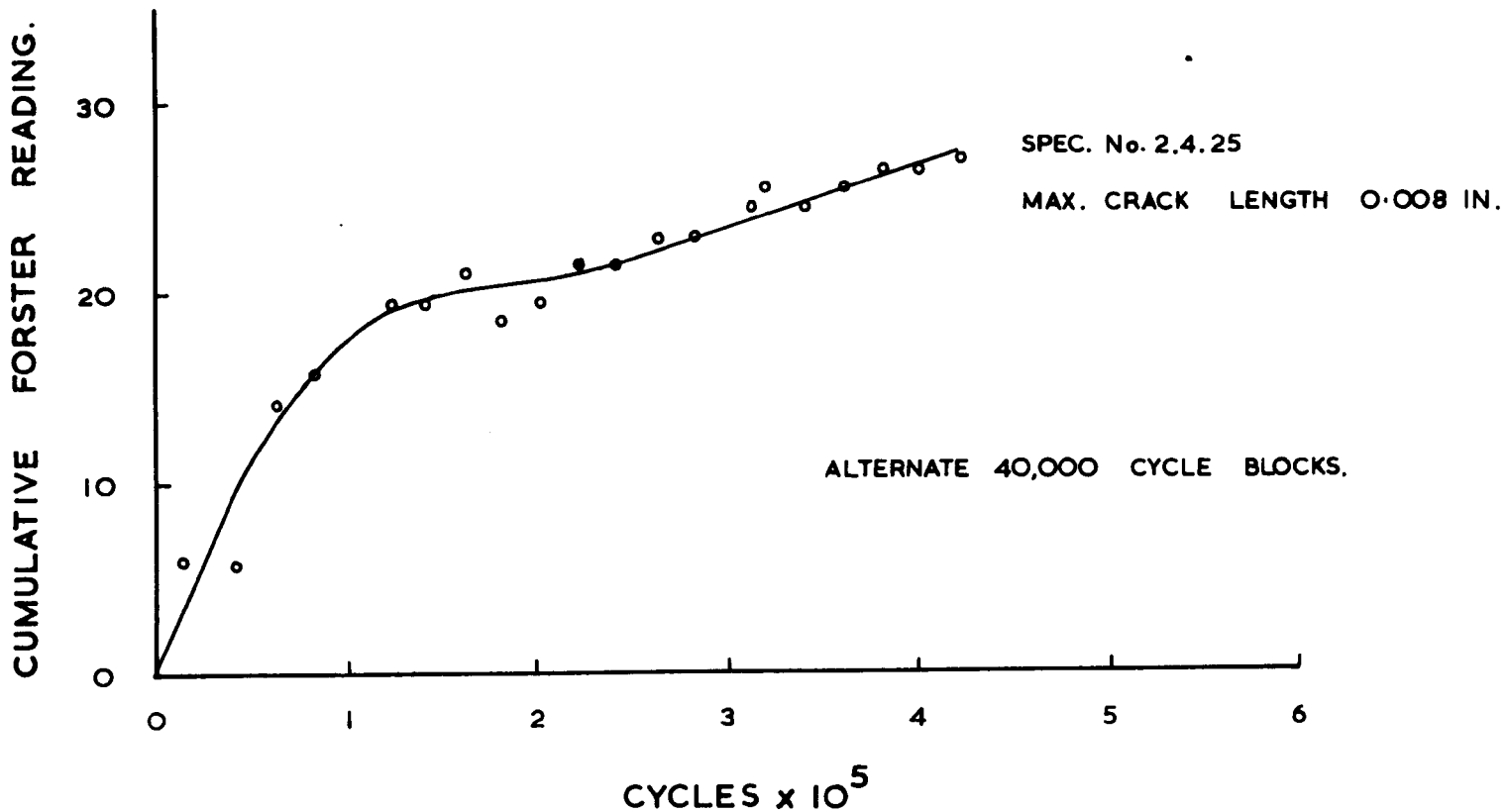

FIG 5.23

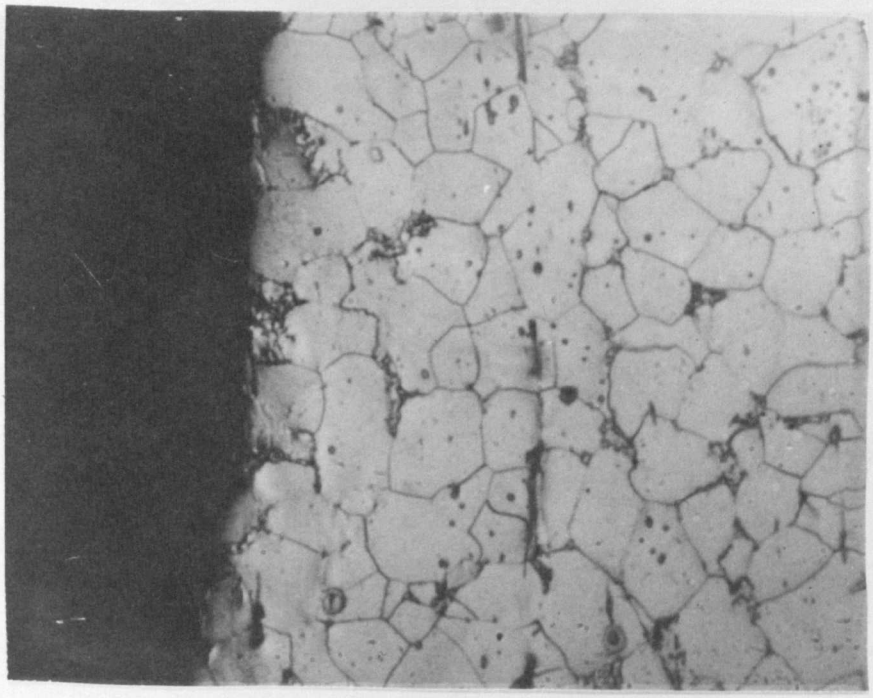

MAG. X 340

FIG. 5.24

SPECIMEN 2. 4. 14.

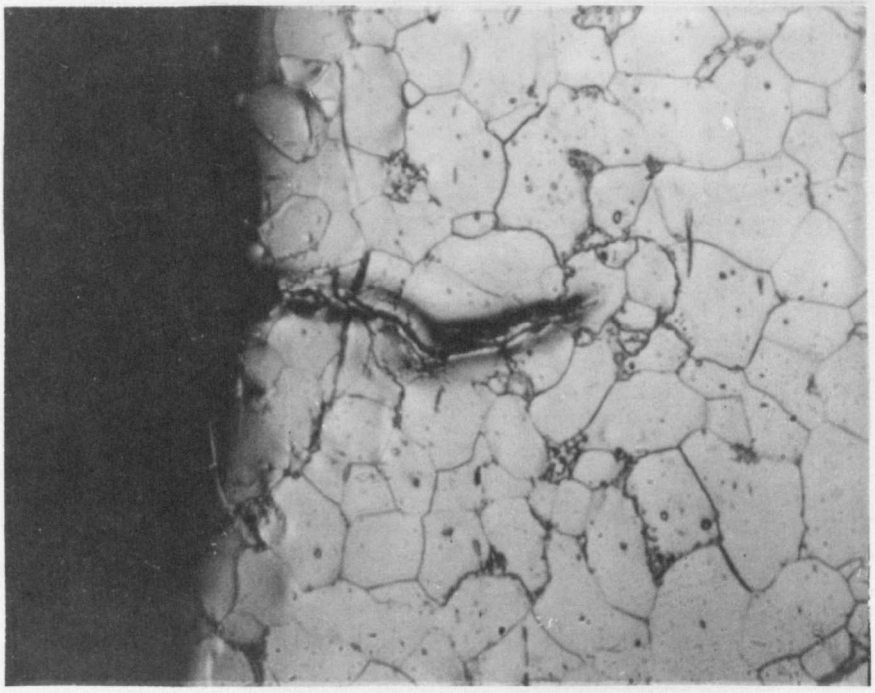

MAG. X 340

FIG. 5. 25.

Temperature	Crack Length			
	1.0	0.5	0.2	Off Block
46^0 F	2926	3227	3327	3775
56^0 F	2938	3240	3356	3740
65^0 F	2823	3137	3270	3690
70^0 F	2782	3101	3223	3663
75^0 F	2759	3073	3186	3610
77^0 F	2705	3009	3117	3575

Temperature	Deviation from off Block Reading			
	1.0	0.5	0.2	
46^0 F	849	548	458	
56^0 F	812	500	384	
65^0 F	867	553	420	
70^0 F	882	562	440	
75^0 F	851	537	424	
77^0 F	870	566	458	

Forster Output Volts x 10^4

TABLE 5-5

CHAPTER 6

The second test program showed that using the Forster defectometer, the life of a specimen could be reliably divided into two main stages.

Stage A. Micro-crack initiation and micro-crack propagation.

Stage B. Macro-crack propagation.

The third test program was aimed at separating the effect of loads below the original constant amplitude fatigue limit during Stage A and Stage B. Program 1 had shown that, statistically, simple block programs were ineffectual and the limited cumulative damage investigations completed in Program 2 had shown clearly that interaction effects were perhaps the most important factor when considering cumulative damage, and therefore the most complex loading program possible on the rotating bending machines was used in Program 3.

The loading envelope used was a triangular modulation as shown in Fig. 6.1. This was obtained by using the end two micro-switches on the dummy beam with the cam driven contacts permanently closed so that the jockey weight traversed continuously between the two micro-switch positions. Another cut-out was attached to the loading beam to break the supply to the traversing motor when the specimen failed.

The batch of material used for Program 3 had a significantly higher carbon content than that used for Programs 1 and 2.

The mean carbon and manganese contents for 3 samples were:-

Carbon Content = 0.33%

Manganese Content = 0.72%

Mean tensile strength properties from tests using a Hounsfield tensometer were:-

1st yield	45,300 lb/sq.in.	20.2 tons/sq.in.
Ultimate	76,500 lb/sq.in.	34.1 tons/sq.in.

Constant amplitude tests were run to determine the S-N curve which is shown in Fig. 6.2. and also to allow selections to be made of the required stress levels. It was desirable that the test program should have a sound statistical basis and thus provide quantitative as well as qualitative information. This meant that several tests had to be performed at each condition, thus in a large program many hours would be spent taking crack detection readings. In order to avoid considerable wastage of time and specimens it was decided to arrange the stress levels to achieve a total life in the region of 10^6 cycles, thus allowing all the crack detection information on any one test to be gathered in under 10 hours.

The modulated load envelope is shown in Fig. 6.1. The value of σ_h was kept constant in all tests but four different values of σ_l, all below the constant amplitude fatigue limit, were investigated. Thus the pattern of loading above the original fatigue limit remained constant, enabling the effect of lower stress levels and an increasing number of stresses below σ_f to be investigated. As previously discussed the range of stress available on the rotating bending machines was limited and the following conditions within the above limitations were investigated.

σ_h	σ_l
12.24 tons/sq.in.	9.79 tons/sq.in.
12.24 tons/sq.in.	8.98 tons/sq.in.
12.24 tons/sq.in.	8.16 tons/sq.in.
12.24 tons/sq.in.	7.75 tons/sq.in.

After these tests had been performed the trend of the results was extremely interesting and a very simple modification was performed on the machines to enable a greater range of stress to be obtained. An

additional five pound weight was attached to the jockey which allowed three smaller values of σ_1 to be investigated. The traversing motor on machine 2 ceased to function almost immediately under the increased load and the spare motor when fitted followed suit. However, the traversing on machines 1 and 3 continued to be satisfactory and so the extension of the program was run on these two machines alone. Soon after starting to run the tests in the extension it became obvious that the results being produced by machines 1 and 3 were significantly different from each other. There were at this stage two possible causes.

1) Another research student was now using the other rotating bending machine located on the same table as machine 3. This could possibly have affected the results from machine 3.

2) It was noted that when machine 1 was shut-down, in order to take crack detection readings, the loading beam oscillated badly on the knife-edge thus probably producing overloads.

Cause (1) was quickly eliminated by re-arrangement of the laboratory and moving the fourth machine to a new location. It had been noted that the major difference in the results was the length of Stage A, Stage B being about the same for both machines. As three specimens had been run at the first extension condition in machine 1, a further three tests were run at the same condition and no crack detection measurements were taken i.e. the machine was not shut-down during the test.

These latter results showed a considerable decrease in average total life and came into line with the results from machine 3. This was confirmed in subsequent tests by providing support to the beam during shut-down. As the machines were required for use on an M.Sc. course the tests were not repeated with crack detection work, but as reliable information was already available on the length of Stage B from both machines, the mean life for Stage B was used to generate estimated data

from the tests with no crack detection measurements.

The increase in weight of the jockey meant that the rate of change of load had increased. In order to ascertain whether the results produced by the modified machines were significantly different, five specimens were run at the condition σ_h = 12.24 tons/sq.in., σ_l = 8.16 tons/sq.in. No crack detection measurements were taken and only the total lives to failure were compared but the statistical analysis indicated that there was no significant variation in the mean life produced by the modified and unmodified machines. It seems reasonable therefore to assume that no difference will occur in the relative lengths of Stage A and Stage B.

The mounting and preparation of specimens for tests was as described previously in Chapter 4. All specimens were taped on either side of the notch and four reference points marked at approximately 90° intervals around the circumference. Forster readings were taken at each of these points at intervals of approximately 40,000 cycles but regions either side of the highest readings were scanned to ensure picking up the first running crack. Typical plots of the cumulative total of the four readings versus cycles are shown in Figs. 6.3. and 6.4. The point "R" marked on each plot indicates the start of macro-crack propagation at some point on the circumference of the specimen.

The results of the whole program are shown in Tables 6-1 and 6-2. A calibration curve for the Forster on this particular material was obtained by running specimens to certain readings then sectioning, polishing and measuring crack length. The results and plot are shown in Table 6-3 and Fig. 6.5. respectively.

ANALYSIS OF RESULTS

The analysis was again based on a Miner summation for convenience

and easy comparison. The evaluation of a Miner summation for a triangular modulation of applied load given by Marsh was utilized again in analysing these results. The Miner summation to failure M was evaluated for each specimen, and also the portion of this life spent in Stages A and B respectively known as M_A and M_B. These values are also shown in Tables 6-1 and 6-2. The values of M_F population were checked against a normal and log normal distribution, the log normal gave the best fit and the plot is shown in Fig.6.6. The analysis was thus based on the normal distribution with a log. conversion to normality.

The first stage in the analysis was to examine the variances of M_F, M_A and M_B at each test condition. The "F" test was performed and it was found that significant differences in the variance did exist. However, the most convenient form in which to present the results quantitatively is to accept the mean values of M_F, M_A, M_B at one test condition as being valid, and to calculate significant differences between these means and the mean values for other test conditions. The test condition with the highest mean value of M_F was accepted as being valid and significant variations calculated from this mean.

The student "t" test was to be used to test the hypothesis that $\mu_1 - \mu_2 = d$ where μ_1 and μ_2 are the population means and d the suggested difference between the means. This test includes the assumptions that the samples are independent and that the population standard deviations are equal. In order to satisfy this last condition the "F" test was used to compare the variances of the other test conditions referred to the selected test condition. Three sets of test results from 18 failed to establish no significant difference in variance at 5% significance. These sets of data are excluded from the final analysis.

The "t" test was then used on the remaining data to determine the differences in means in a single tail test at 10% significance.

The results of this analysis are shown in Table 6-4. Fig. 6.7. shows the values of Miner summation in Stages A and B plotted against the value of the lower load level. Fig. 6.8. shows the Miner summation for life to failure together with the proportions spent in Stages A and B plotted against the value of the lower load level.

These results validate the original hypothesis that different behaviour would be encountered in Stages A and B. It can be seen that in Stage A as the lower load level decreases i.e. as the proportion of the stress levels below the fatigue limit increases, the Miner life drops sharply at first and then appears to level out.

The results indicate that stresses down to $0.7\sigma_f$ may be considered as damaging during the crack initiation and micro-crack propagation stage. The plot for Miner summations versus lower load level during macro-crack propagation is a straight line. This suggests that lower stress levels are equally damaging as higher stress levels but this is certainly not true when based on crack propagation data at constant amplitude. Therefore the only plausible explanation of this phenomena is severe interaction effects. Naumann (1962) has suggested that the role of stress levels below the fatigue limit is to relax the residual compressive stresses in the plastic zone at the crack tip. It is interesting to examine this in relation to the observed crack behaviour during macro-crack propagation. It has been observed in Chapter 5 Section iii that a characteristic of the presence of stresses well below the fatigue limit is the numerous examples of longitudinal propagation. These are cracks which have propagated into the region of high stresses and hence high residual stress areas around a crack tip. The formation of even a small crack in this direction must relax and redistribute the crack tip stress

field in the immediate area of the crack tip. This would probably lead to higher concentrations of stress immediately in front of the main crack propagation line leading to faster initial propagation when high stress levels are re-applied. It was also noted in Chapter 5 section iii that specimens which had been subjected to stress levels just below the constant amplitude fatigue limit showed very limited signs of longitudinal propagation. It is possible that this difference in behaviour of the crack explains the two contrasting propagation rates obtained when these stress levels are mixed with others well above the fatigue limit, and the faster crack propagation rates obtained when very low stress levels are well mixed with stresses above the fatigue limit can be compared to the slower crack propagation rates when stress levels just below the fatigue limit in the same circumstances exhibit much weaker tendencies to produce longitudinal propagation.

CUMULATIVE DAMAGE ASPECTS

The analysis of the results has already been described and if we refer back to the Miner summations given in Table 6-2 it can be seen that the magnitude of error in using this summation is as much as a factor of 5 in some cases. Even higher margins of error have been quoted in the literature for example Kawamoto (1965) et al and Marsh (1964) give factors of 10 in certain cases. To deal with such large errors a gross correction to Miners Law is required. The plot of Miner summation in Stage B against lower load level shown in Fig. 6-7 is a straight line. As the pattern of applied loads above the fatigue limit is the same in all cases, if we assume a summation on a linear basis this means that the lower stress levels must be equally as damaging as those slightly higher. As already stated this is certainly not true in terms of crack propagation rates at constant amplitude. If therefore a rule is proposed with crack length and propagation as the defined measures of damage then non linear

accumulation and interaction effects must be considered and dealt with in the rule. It thus becomes convenient not to define a concept of damage in strict terms but if say the summation of cycle ratios can be kept to unity for a wide variety of conditions then however unsatisfactory this may be in a scientific sense it realizes the solution to the design problem:

This test program has demonstrated effectively the existence of two stages and that the cumulative damage behaviour in these respective stages is different. Returning to the plot of Miner Summation in Stage B against lower load level, if this stage is considered as a separate section of a cumulative damage rule and we wish to achieve a cycle ratio summation to unity in this section, the implications of the straight line plot makes it obvious that the S-N curve for Stage B must be a line parallel to the stress axis with a cut-off not as yet determined. Similarly if the coaxing exhibited in Stage A is ignored and the plot of Miner Summation in Stage A against lower load level approximated to a straight line the S-N curve again becomes a line parallel to the stress axis but with a cut-off or fatigue or damage limit at $0.7\sigma_f$. This technique applied to the test results gives the best fit to data as shown in Table 6-5. The ordinate of the S-N curves are determined simply from the highest stress level experienced in the spectrum as a triangular modulation is a severe applied stress spectrum.

OTHER ASPECTS RAISED BY THE TEST RESULTS

The test results validated the original argument that response to low loads would differ in each stage of the life. If the response to the low loads observed in these tests is the same for other conditions, then the next important question is what determines the relative length

of Stage A and Stage B. Stage A is concerned with cracks of very short length and their formation. As large blocks of stress levels below the fatigue limit do not appear to be damaging during this stage (ref. Chapter 5), then this suggests that Stage A is dominated by the stress field due to the notch rather than that due to the crack. Once a crack is formed then theoretically the stress concentration is infinite and the crack should propagate, however the existence of non-propagating cracks in sharply notched specimens is now well documented in the literature especially by Frost. The work of Frost and Phillipps (1956) is particularly interesting with respect to crack propagation dominated by the stress field due to the notch. They subjected sharply notched mild steel rotating bending specimens to various stresses below the fatigue limit. The depth of non-propagating crack developed was dependant on the applied nominal stress. Frost and Phillipps used Neubers solution for a deep hyperbolic notch to establish the stresses in the specimen and they found that the crack propagated to the depth at which the material was subjected to stresses at or above the plain fatigue limit of the material. This type of observed behaviour presents very strong evidence in support of the argument that not only initiation of a small defect but also the continued propagation of this defect to a certain depth is dependant on the stress field due to the notch.

The non-propagating crack may be considered as a function of the gross elastic stress field associated with that particular specimen configuration and in particular as a function of the gross stress gradient. The stress concentration of a very sharp notch dies away very rapidly from the root of the notch, therefore a small crack is propagating into a rapidly deteriorating gross elastic stress field. If the applied stress and stress concentration are of the correct values then the stress field due to the notch fails to propagate the crack until it is sufficiently

long itself to provide the gross elastic stress field required for continued propagation. This type of behaviour explains why notched fatigue specimens do not exhibit the full strength reduction indicated by their stress concentrations. Although capable of initiating damage the progress through what we may term micro-crack propagation, is a function of the stress gradient, thus as the micro-crack propagates into a rapidly deteriorating gross stress field the propagation rate drops until macro-crack propagation is attained i.e. when the stress field due to the crack itself is dominant. The sharper the notch then the higher is the stress gradient and the rate of micro-crack propagation falls rapidly. This prolongs the micro-crack propagation phase and leads to an increase in life which is probably related to the gross stress gradient.

The work of Irwin, Paris(1963) et al on cracked high strength aluminium alloy plate specimens has shown that parameters connected with the gross elastic stress field surrounding the crack are of relevance in describing crack propagation rates. Paris and Erdogan (1963) have further correlated a wide variety of crack propagation data using Irwin's concept of the stress intensity factor K to formulate a crack propagation law of the general form $\frac{da}{dN} = G\{K\}$. The majority of work in this field has been performed on high strength aluminium alloys which exhibit strong work-hardening characteristics. The efficacy of such methods in low strength materials with a high degree of plastic deformation and poor work hardening characteristics has yet to be established. However in the field of fracture mechanics low strength materials are dealt with by introducing empirical corrections for plasticity effects within the broad concept of stress intensity factors. Thus although the methods of Paris et al may not be directly applicable to crack propagation in such a material as mild steel it can be argued that, since the intensity and distribution of the elastic stress field determines the size and shape

of the plastic zone, the properties of the elastic stress field can still be considered as dominant features of the behaviour and propagation of macro-cracks.

Thus the fatigue life of a specimen may divide into two distinct phases, one dominated by the stress fields due to the notch and the other dominated by the stress fields associated with the crack itself. These are in fact the Stage A and Stage B established by the pattern of Forster response and crack length measurements.

It has been argued that some well defined law connected with the elastic stress fields governs the macro-crack propagation phase. Similarly the stress fields due to the notch govern initiation and micro-crack propagation and it is likely that eventually a well ordered law based on properties of the notch stress field to cover this behaviour will emerge. Therefore the two phases are dependant on properties which are in turn dependant on the geometry, overall size and cracked state of a specimen. Thus it is expected that there is some relationship between the two stages and the total life to failure for a particular specimen configuration.

Fig. 6.9. shows a plot of life in Stage A versus total life to failure for a number of constant amplitude tests on which crack detection measurements were taken. If the previous arguments are correct and the main factors determining the form of this relation are overall size, geometry and cracked state of the specimen then a change in the material properties of the specimen should not affect this relationship for a particular specimen configuration provided that they are subjected to the same preparation and style of test. Fig. 6.10 shows a further plot of life in Stage A v. Total life to failure, the solid line is that from Fig. 6.9 and the points on the graph are constant amplitude test results from the second test program where the material had a much lower carbon

content and approximately a 20% variation in the fatigue limit. The close agreement between the two sets of results validates the original arguments. A further test is possible and this is that if the division of the life into these two stages is correct and the behaviour in cumulative damage is different in Stage A and Stage B then similar specimens subjected to the same style of cumulative damage test should also exhibit a relationship between life in Stage A and Total life modified by the particular cumulative damage behaviour. Fig. 6.11. shows the results of the triangular modulation tests on a life in Stage A v. Total life plot and the line from the plot of constant amplitude results is also shown. The effect of other important factors such as residual machining stresses is discussed in some detail later in this chapter.

The most important feature of this plot is the independance of the necessity to specify the stress level of a particular test. Therefore having established this relationship for a particular specimen configuration it may be possible to predict S-N curves for specimens with wide variations in material properties using the strength properties to establish stress level conditions.

The importance of relating the properties of the plot of life in Stage A v. Total life to failure to the S-N curve is a function of the cumulative damage rule proposed earlier in this chapter. The main feature of this rule was the division into life in Stage A and Stage B at the top damaging stress level. Obviously if the properties of the plot could be tied to a specimen configuration i.e. notch severity overall size etc. then the only testing required would be a single S-N curve at constant amplitude with no ancillary crack-detection measurements for a given material. Once this S-N curve was obtained a whole family of S-N curves and life in Stage A v. Total life plots could be derived for different specimen configurations in the same material. A certain amount of progress in extending this type

of behaviour can be made by again considering the case of the sharply notched specimen which produces non-propagating cracks below the fatigue limit. It is widely accepted that the sharply notched develops a small crack rapidly even at stress levels close to the fatigue limit. It has been argued that the factor which decides whether this defect propagates until failure occurs is the stress field due to the notch. Once the crack attains a certain length the stress field due to the crack becomes dominant and failure of the specimen is assured. The initiation and development of this defect to a critical size has been termed initiation and micro-crack propagation and correlates to the Stage A observed in the experimental program. A sharply notched specimen at a stress level just above the fatigue limit will develop the defect rapidly, most of the life will then be spent in propagating this defect to the critical size but just below the fatigue limit the defect will fail to develop to the critical size i.e. the increase in life has been due to an increase in the length of Stage A and the slope of the life in Stage A v. Total life to failure plot will approach 45 degrees. Similar arguments could be presented for mildly notched specimens but the difference in this case is that the original defect fails to develop. It is therefore postulated that the slope of the plot will approach 45 degrees for a sharply notched specimen and that the effect of actual defect initiation in mildly notched and plain fatigue specimens will be accounted for in the intercept value on the total life axis.

EFFECT OF RESIDUAL MACHINING STRESSES

The specimens used in all these tests were stress relieved before machining but received no heat treatment between or after all machining operations. This means that there are almost certainly some residual compressive machining stresses around the root of the notch, even though

during machining the feed rate was kept slow and lubrication used on the cutting of the notch. It was possible therefore that the existence of Stage A was due wholly to residual machining stresses and was in no way related to the overall specimen geometry. During the first years of the department facilities did not exist within the department to enable stress relieving in vacuum to be completed. Subsequently a facility was available for very limited use and as only 1 specimen could be heat treated at a time the quantity of specimens which can be treated is very limited. Due to leaks in the vacuum system only 3 satisfactory treatments were achieved before the reporting of this work. These specimens were used for a very limited investigation at a single constant stress amplitude. It is intended when further satisfactorily treated specimens are obtained both to extend the constant amplitude results over a greater range of total life and to perform a limited investigation of the results under the triangular modulation of the applied stress range.

The three specimens were tested at a stress level of 11.42 tons/sq.in. nominal. A plot of cumulative Forster reading v. cycles for the longest running specimen is shown in Fig. 6.12. Table 6-6 shows the results tabulated as life in Stage A and B and total life. It can be seen from this table that as before the majority of the scatter occurs in Stage A. The untreated specimens from the S-N curve give a mean life of 1,148,000 cycles as compared to 535,000 cycles from the stress relieved specimens. This is composed of a 62% reduction in the length of Stage A and a 38% reduction in Stage B. The reason for the reduction in the length of Stage B is as follows:- the start of Stage B is defined as when one point on the specimen attains macro-crack propagation. The crack thus still has to propagate around the circumference of the groove and the greater ease with which this is done in the stress relieved condition should lead to a

reduction in the length of Stage B.

The results of the stress relieved specimens are shown in a Stage A v. life to failure plot in Fig. 6.13. where the solid line shown is the result for the untreated specimens. The fact that they lie so close to the line for untreated specimens is due to the reduction in the length of Stage B as previously discussed, this being a peculiarity of the specimen configuration and the definition of Stage B. It is to be expected that with a different specimen configuration, for example an edge notched plate specimen, the plot of life in Stage A v. cycles to failure would be rotated due to the effect of residual stresses. Stage A being affected but with no significant effect observable in Stage B.

The effect of loads below the constant amplitude fatigue limit in cumulative damage tests on treated specimens remains as yet unresolved. If the damaging effect of low loads is principally due to relaxing residual stress, then it is to be expected that the sensitivity to low loads during Stage A in treated specimens will be lower than in the case of untreated specimens.

DISCUSSION OF THE SIGNIFICANCE OF THE UNIQUE STAGE A V. TOTAL LIFE PLOT

As a matter of convenience the plot of life in Stage A versus total life to failure will simply be referred to as the plot in the following discussion.

It has been argued that the reason for the relationship exhibited in the plot is the dependance of initiation micro-crack propagation and macro-crack propagation on the stress fields due to the notch and the cracked state of the specimen. If the same style of behaviour is evident in other specimen configurations and a relation between parameters of the plot and specimen geometry are established then extensions to cover such phenomena

as size effects are possible.

Crack growth, during the macro-crack propagation stage is dependant on crack length, accelerating rapidly with increasing crack length. Therefore for the purpose of this discussion the length of the macro-crack propagation phase at a given stress level in different sized specimens may be treated as a quasi-stationary quantity.

It has been argued that the sharply notched specimen which is capable of producing non-propagating cracks is one limiting case where the slope of the plot is close to 45° and most of the life is spent in Stage A. The other limiting case is the plain specimen where Stage B behaviour should be expected to predominate giving a minimal slope to the plot with probably a large intercept on the life in Stage A axis which represents purely an initiation phase. Thus for specimens of the same test section at constant amplitude it is expected that the slope of the plot should vary between 0° and 45° depending on the severity of the stress concentration.

It has been shown both in this and the previous chapter that the major part of the scatter in tests results occurs in the length of Stage A. The work of Puckridge suggests that this is further confined to the actual initiation of a micro-crack (a discontinuity less than 1 grain in length) rather than micro-crack propagation. This explains the apparent anomaly in results where a sharply notched specimen is claimed to be dominated by Stage A behaviour but exhibits a much smaller scatter in test results. The time taken to form a micro-crack of the order of 1 grain depth is very small in terms of the overall life and therefore variation in scatter is small but life in Stage A is prolonged by slow micro-crack propagation due to high stress gradients. As the stress concentration becomes less severe the balance between initiation and micro-crack propagation during Stage A alters with initiation becoming relatively longer leading to

increased scatter in test results.

There are two main considerations when extending specimen performance both to different sizes and cumulative damage work and they are as follows:-

1) Geometrically identical specimens will be subject to the same elastic stress fields, and theoretical stress concentration factors. Do differences in overall size affect significantly the parameters connected with the plot?

2) Although subject to the same pattern of stress field, is there a difference in the behavioural pattern of different sized specimens i.e. does the difference in the gross size of the stress fields and the gross stress gradient alter the sensitivity to low loads during Stage A or Stage B?

Alternative (1)

If macro-crack propagation is considered as a quasi-stationary property then when looking at the effects of overall size we are looking for significant variations in the length of Stage A. It seems logical to postulate that the two main factors influencing the length of Stage A are the value of the octahedral shear stress and the stress gradient. For similar loading conditions the elastic surface stress conditions should be identical. The gross stress gradient would be lower in the large specimen and therefore a decrease in the length of Stage A would be expected but the situation is complicated by the effect of the micro-crack in modifying the stress field due to the notch. In the large specimen the small crack of the same overall length will be a more severestress concentration which could well cancel out the detrimental effects of the reduced gross stress gradient due to the notch.

An important point arises when the method of loading occurs. Short cantilever bending specimens with high end loads may have significant shear

stresses due solely to the mode of loading when deeply notched specimens are used.

The actual length of crack required to produce the macro-crack propagation phase may also vary with specimen size. If this is the case then an investigation into the stress fields associated with small cracks in notched specimens is required to establish the critical stress conditions required to produce macro-crack propagation.

Alternative (2)

The many and complex factors possibly affecting the ratio between life in Stage A and Total life have been discussed briefly in the preceding sections. Although the slope of the plot may well remain almost unchanged when specimen sizes are scaled up a very likely occurrence is that the behavioural patterns in Stages A and B change. The less severe gross stress gradients associated with the larger specimen probably mean that much lower stress levels can contribute to the rate of accumulation of damage.

In the triangular modulation tests stress levels down to 0.57 of the fatigue limit stress were investigated and found to contribute to the rate of accumulation of damage. The cumulative damage test on specimen 2.4.9. described in Chapter 5 showed that large blocks of stress at approximately this level ($0.55 - 0.60\ \sigma_f$) not only stabilized crack growth at this level but reduced the damage rate at higher stress levels. This could be interpreted as approaching the limit for this specimen configuration when stress levels lower than this cease to be damaging but when applied in very large blocks may stabilize the crack propagation rates. It is probable that this limit is lower for larger but geometrically similar specimens.

There is also the case that both of the alternatives above combine, together with any correction for size in relating the plot via material properties to the S-N curve, to account for size effects in both constant

amplitude and cumulative damage test results.

The next stage of the testing program was clear the main points requiring investigation were:-

1) If the arguments presented to explain the existence of a unique life in Stage A v. life to failure plot are correct then this pattern of behaviour should exist in other specimen configurations.

2) Which of the alternatives discussed above may be the most significant contribution to size effects?

The Amsler pulsator was now available and so it was decided to conduct constant amplitude tests on axial and large plane bending specimens similar in geometric properties to the rotating bending specimens. Constant amplitude tests were also performed on the plane bending specimens in the electromagnetic rigs. These tests would establish whether a unique plot existed for a wide range of specimen sizes and to a limited extent specimen configuration, and also whether the slope of the plot varied for geometrically similar specimens but different overall sizes.

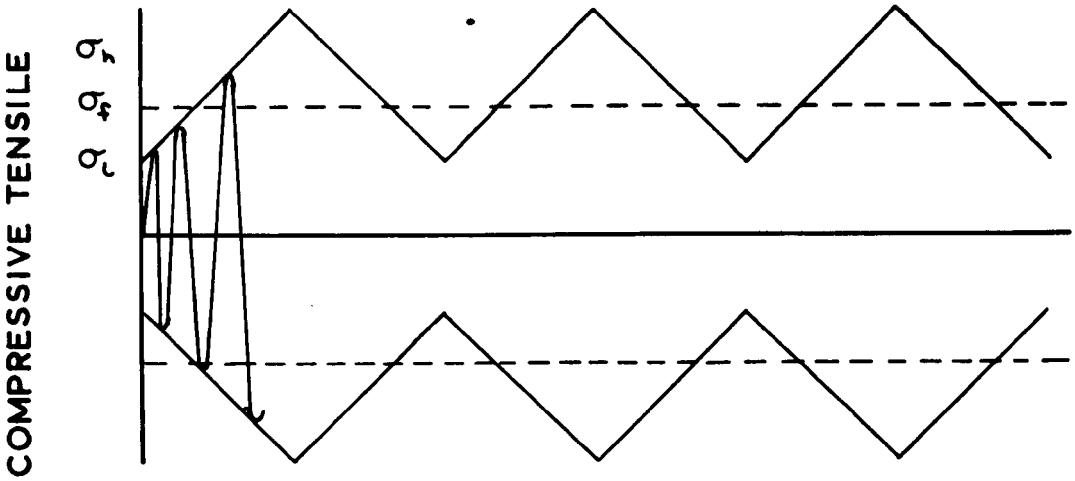

σ_h = HIGHEST STRESS LEVEL.
σ_l = LOWEST STRESS LEVEL.
σ_f = CONSTANT AMPLITUDE FATIGUE LIMIT.

TRIANGULAR MODULATION OF LOAD ENVELOPE ON ROTATING BENDING MACHINES.

FIG. 6.1.

S-N CURVE FOR SPECIMENS USED IN TEST PROGRAM 3.

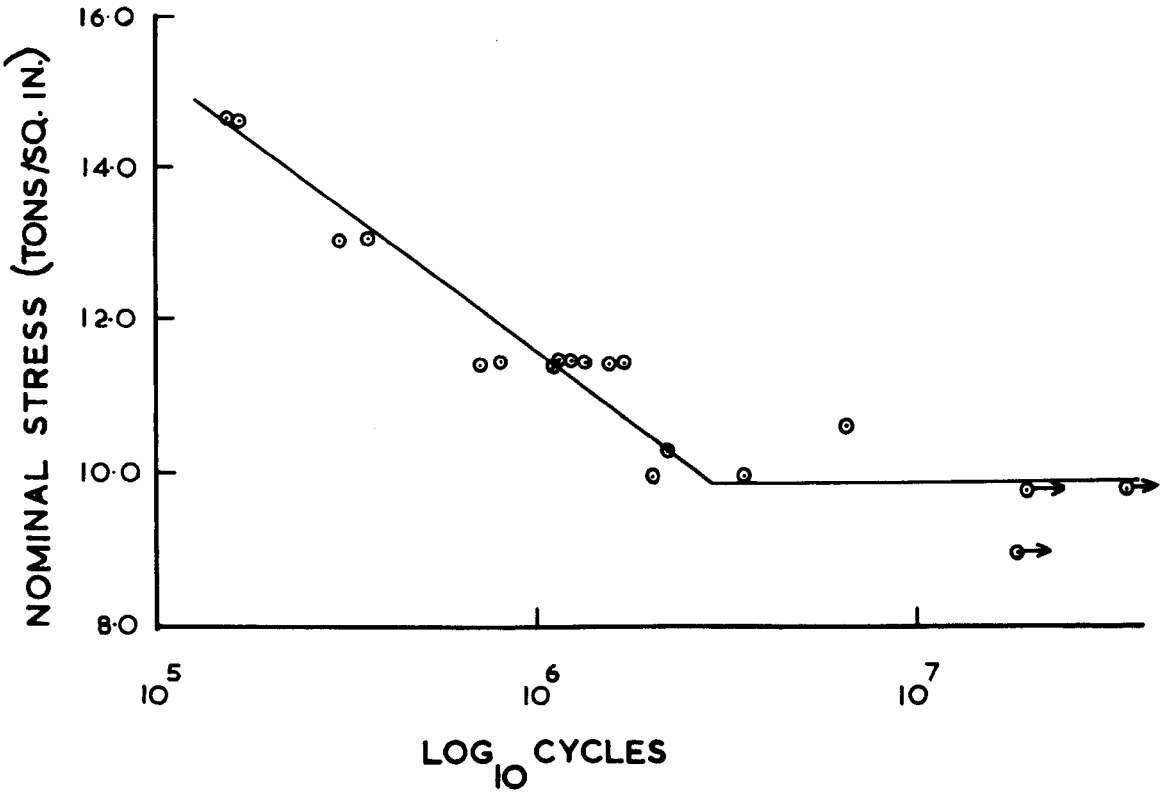

FIG. 6.2.

PLOT OF CUMULATIVE FORSTER READING V CYCLES, LOAD MODULATED BETWEEN 12·24 & 8·98 TONS/SQ.IN. NOMINAL

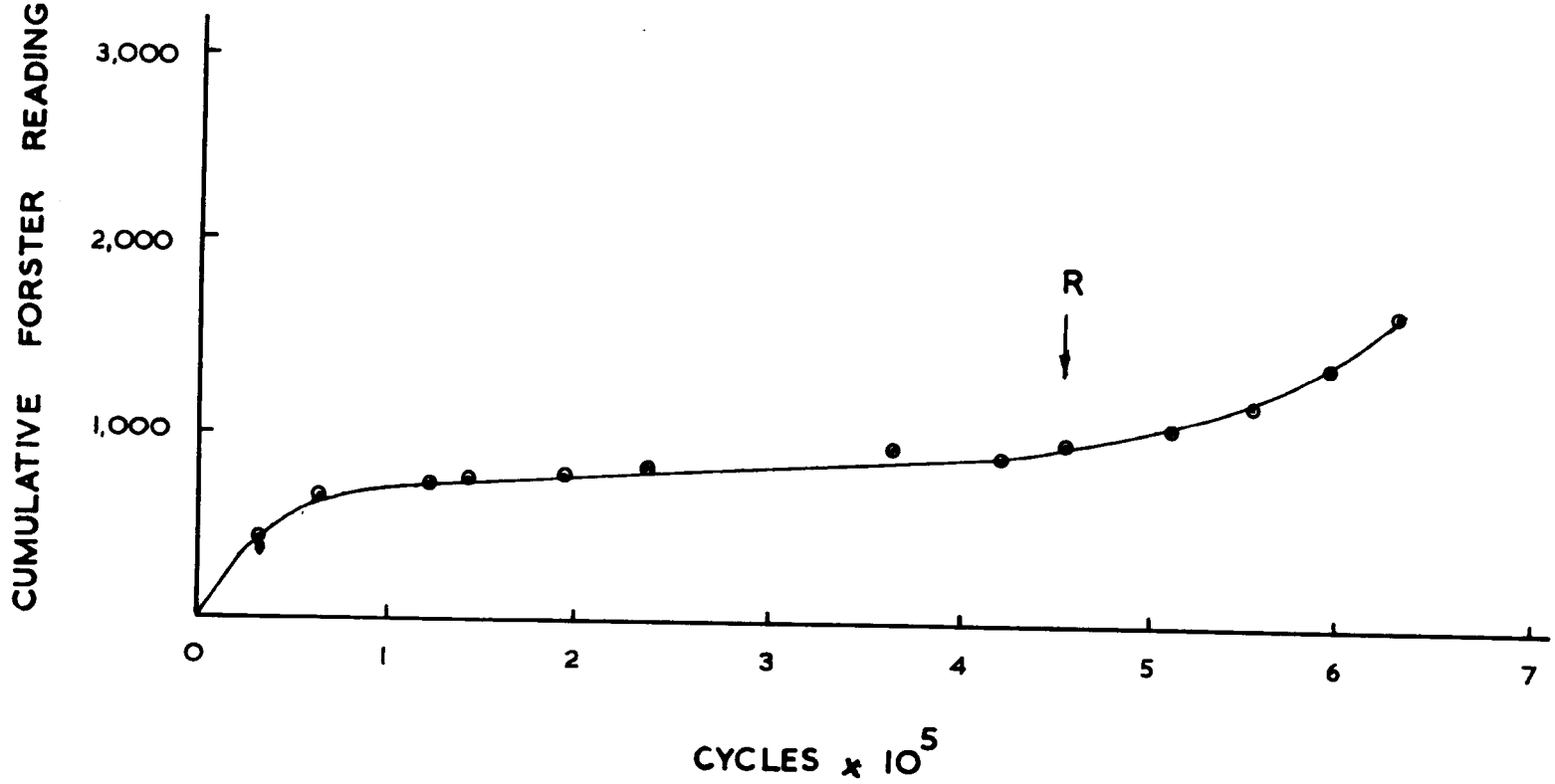

FIG. 6.3

PLOT OF CUMULATIVE FORSTER READING V CYCLES, LOAD MODULATED BETWEEN 12·24 & 9·79 TONS/SQ.IN. NOMINAL

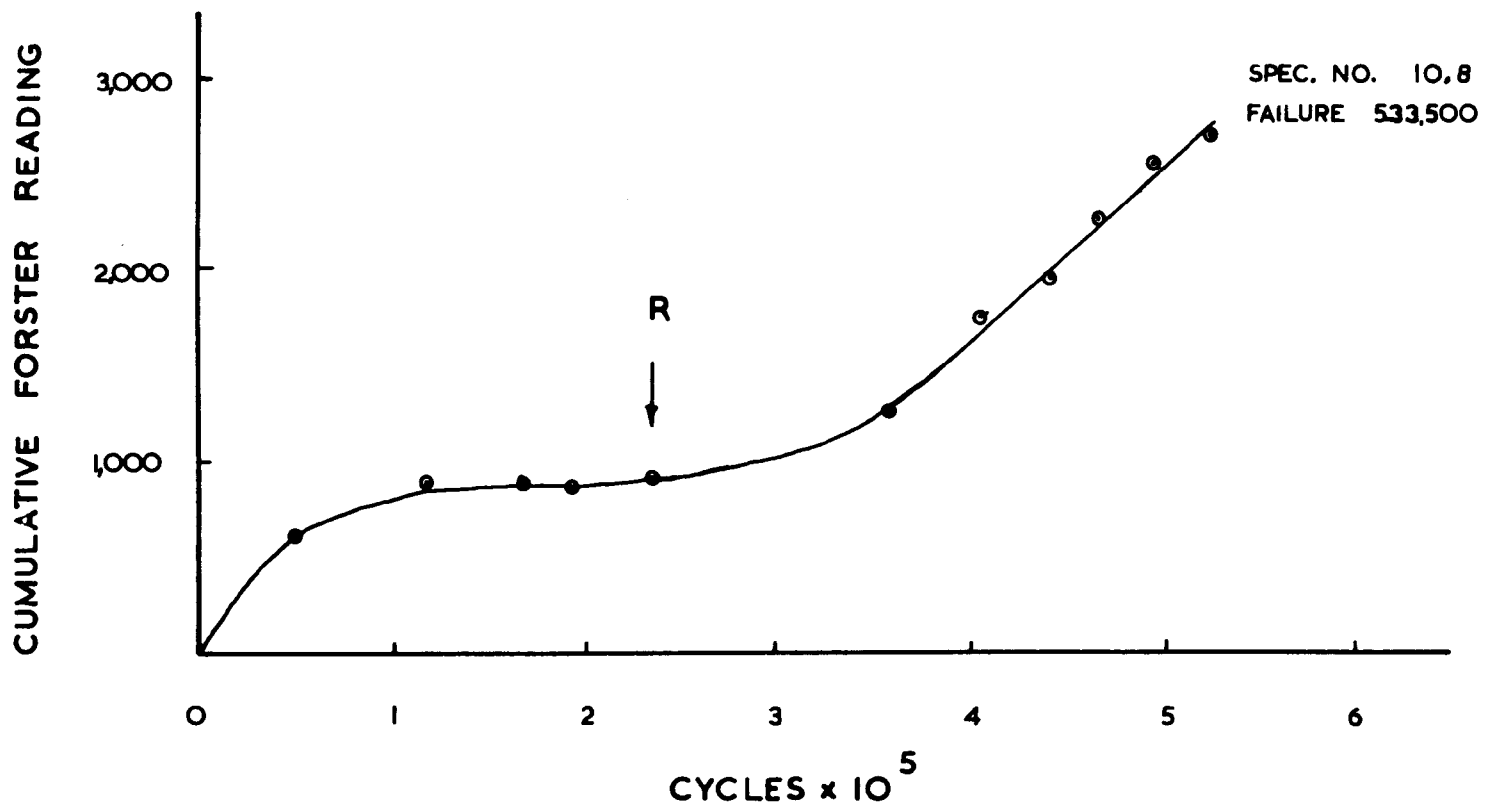

FIG. 9.4

TABLE 6-1

LOAD CONDITION	SPECIMEN No.	No. OF CYCLES IN A	No. OF CYCLES IN B	No. OF CYCLES TO FAILURE	MACHINE No.	No. OF BLOCKS	$\Sigma \frac{n}{N}$ FAILURE	$\Sigma \frac{n}{N}$ IN A	$\Sigma \frac{n}{N}$ IN B
12·24 ↓ 9·79	2 — 3	280,900	357,900	648,800	2	191	0·45	0·20	0·25
	23 — 5	362,300	379,800	742,100	2	218	0·51	0·25	0·26
	11 — 2	176,800	160,200	337,000	1	99	0·23	0·12	0·11
	2 — 4	292,800	274,500	567,300	1	167	0·39	0·20	0·19
	10 — 8	236,600	296,900	533,500	3	148	0·37	0·17	0·20
12·24 ↓ 8·98	15 — 4	323,200	282,500	605,700	1	132	0·32	0·17	0·15
	15 — 3	600,300	329,400	929,700	1	202	0·48	0·31	0·17
	6 — 5	445,700	363,100	808,800	2	176	0·42	0·23	0·19
	13 — 1	592,700	376,300	969,000	3	202	0·50	0·30	0·20
	14 — 7	455,400	334,500	789,000	3	165	0·41	0·24	0·17
12·24 ↓ 8·16	1 — 7	482,500	358,000	840,500	1	142	0·34	0·20	0·14
	17 — 5	503,400	353,300	856,700	2	153	0·36	0·21	0·15
	17 — 2	409,000	323,900	732,900	2	131	0·31	0·17	0·14
	9 — 7	576,600	332,300	908,900	3	151	0·38	0·24	0·14
	21 — 5	307,500	380,800	688,300	3	115	0·29	0·13	0·16
12·24 ↓ 7·75	9 — 1	292,100	294,900	587,700	2	89	0·22	0·11	0·11
	11 — 1	317,400	407,500	724,900	1	110	0·27	0·12	0·15
	12 — 3	286,500	422,600	709,100	1	107	0·27	0·11	0·16
	7 — 6	268,200	310,100	578,300	2	88	0·22	0·10	0·12
	19 — 2	276,900	461,200	738,100	3	108	0·28	0·11	0·17

TABLE 6–2

LOAD CONDITION	SPECIMEN No.	No. OF CYCLES IN A	No. OF CYCLES IN B	No. OF CYCLES TO FAILURE	MACHINE No.	No. OF BLOCKS	$\Sigma \frac{n}{N}$ FAILURE	$\Sigma \frac{n}{N}$ IN A	$\Sigma \frac{n}{N}$ IN B
12·24 ↓ 8·16	17–8	190,000	294,400	484,400	3	110	0·20	0·08	0·12
	23–3	—	—	924 300	3	210	0·38	—	—
	16–3	260,000	285,800	545,800	3	124	0·23	0·11	0·12
	23–2	—	—	902,800	3	205	0·37	—	—
	3–1	—	—	1,022,800	3	232	0·42	—	—
12·24 ↓ 7·34	13–4	316,400 *	350,000 *	666.400	3	128	0·23	0·11 *	0·12 *
	20 2	277 300 *	360 000 *	637 300	1	123	0·22	0·10 *	0·12 *
	21–1	473,800 *	360,000 *	833,800	1	160	0·28	0–16 *	0·12 *
	16–4	190,000	403,800	593,800	3	114	0·21	0·07	0·14
	19 4	671,000 *	360,000 *	1,031,000	3	198	0·35	0·23 *	0·12 *
12·24 ↓ 6·53	23–8	400,000	551,700	951,700	3	159	0·28	0·12	0·16
	22–1	560,000	370,000	930,000	3	155	0·28	0·17	0·11
	16–2	70,000	255,500	325,500	3	54	0·10	0·02	0·08
	11–6	270,000	426,100	696,100	3	116	0·21	0·08	0·13
	22–8	100,000	306,900	406,900	3	68	0·12	0·03	0·09
12·24 ↓ 5·71	10–6	480,000	348,100	828,100	1	122	0·22	0·13	0·09
	1–3	460,000	404,500	864,500	3	127	0·22	0·12	0·10
	20–4	410,000	309,000	719,000	3	106	0·19	0·11	0·08
	16–5	110,000	353,300	463,300	3	68	0·12	0·03	0·09
	12–4	701,900	354,700	1,056,600	1	155	0·27	0·18	0·09

* DEPENDANT ON OTHER EXPERIMENTAL DATA

FORSTER RESPONSE	CRACK DPTH INCHES
190·0	0·006
225·0	0·009
265·0	0·011
275·0	0·011
320·0	0·024
345·0	0·026
410·0	0·033
490·0	0·047

TABLE 6-3 FORSTER RESPONSE AND CRACK DEPTH MEASUREMENTS.

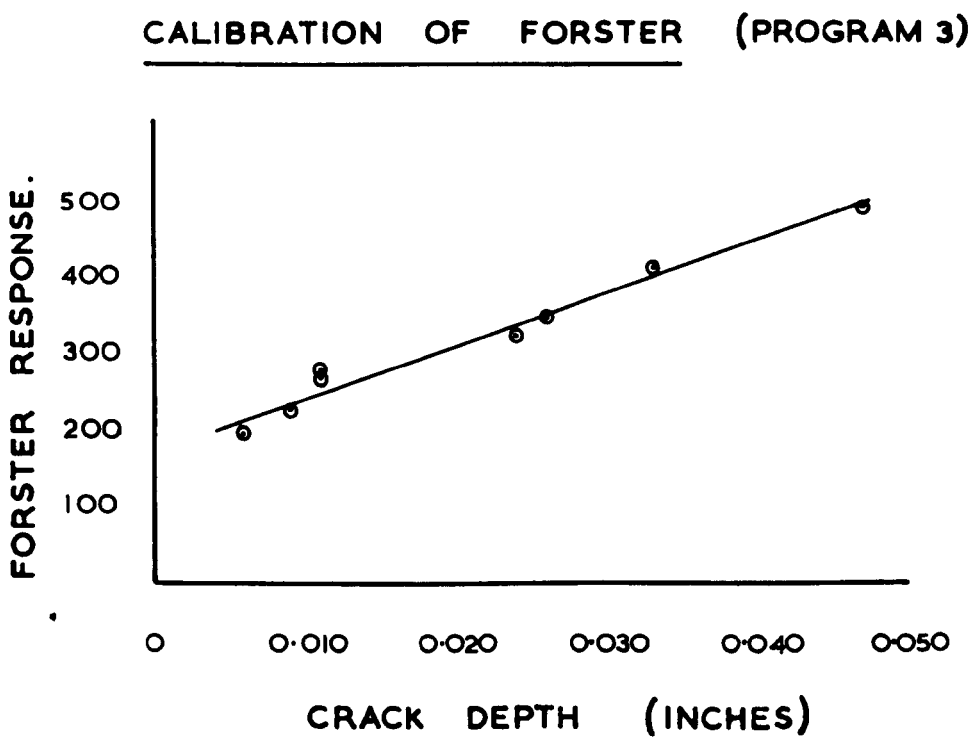

FIG. 6.5

TEST OF FIT OF MINER SUMMATION VALUES TO LOG NORMAL DISTRIBUTION.

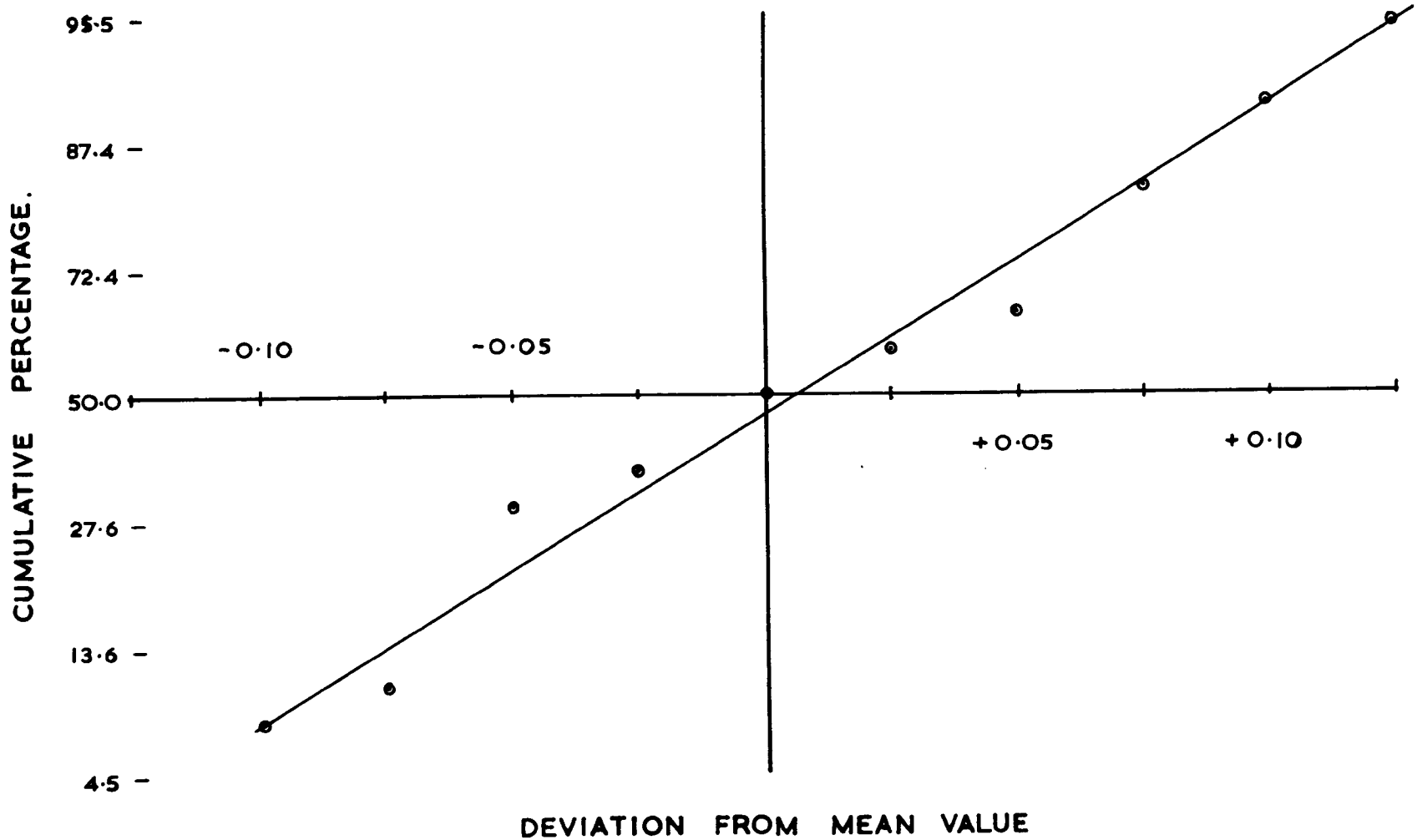

FIG. 6.6

LOAD CONDITION	MINER IN STAGE A	MINER IN STAGE B	MINER TO FAILURE
12·24 - 9·79	0·23	0·19	0·42
12·24 - 8·98	0·25	0 17	0·42
12·24 - 8·16	0·23	0·15	0·38
12·24 - 7·75	0·13 ⊙	0·16 ⊙	0·29
12·24 - 7·34	0·17 •	0·13 •	0·30
12·24 - 6·53	0·11 ⊙	0·13 ⊙	0·24 ⊙
12 24 - 5·71	0·15	0·10	0·25

• COMBINATION OF TEST DATA

⊙ RESULTS NOT STATISTICALLY VIABLE

TABLE 6-4

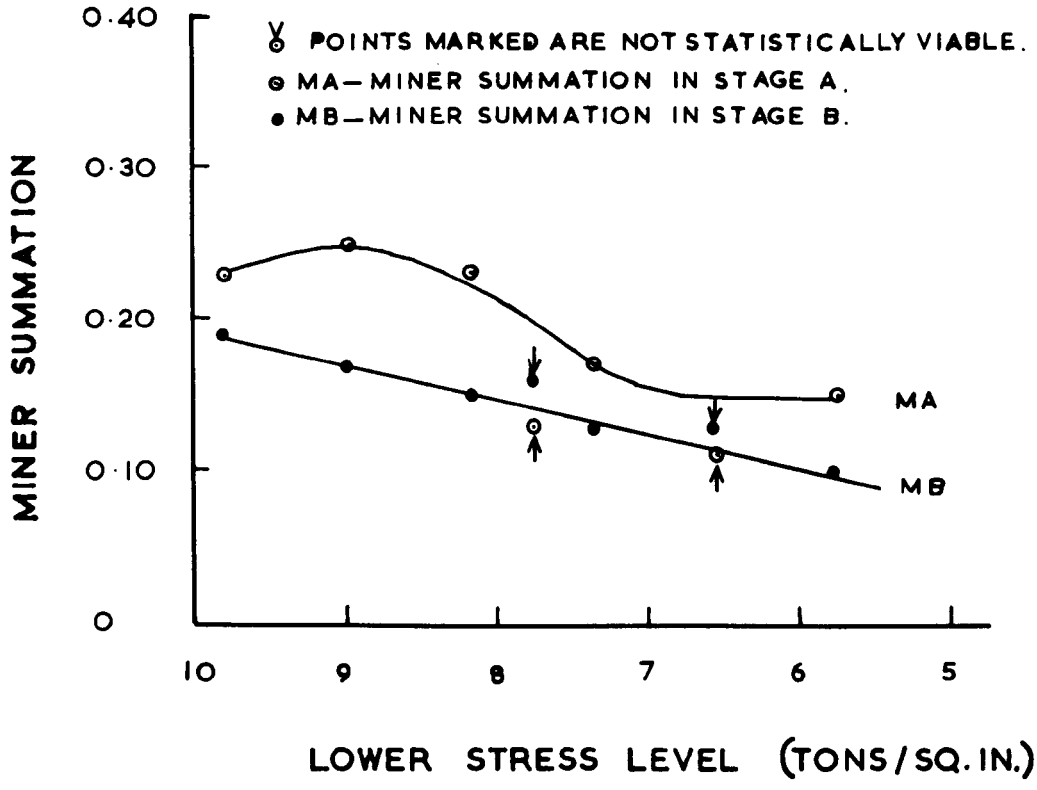

FIG. 6.7

PLOT OF MINER SUMMATION V LOWER STRESS LEVEL SHOWING BOTH LIFE TO FAILURE AND SECTIONS IN STAGEA AND STAGE B.

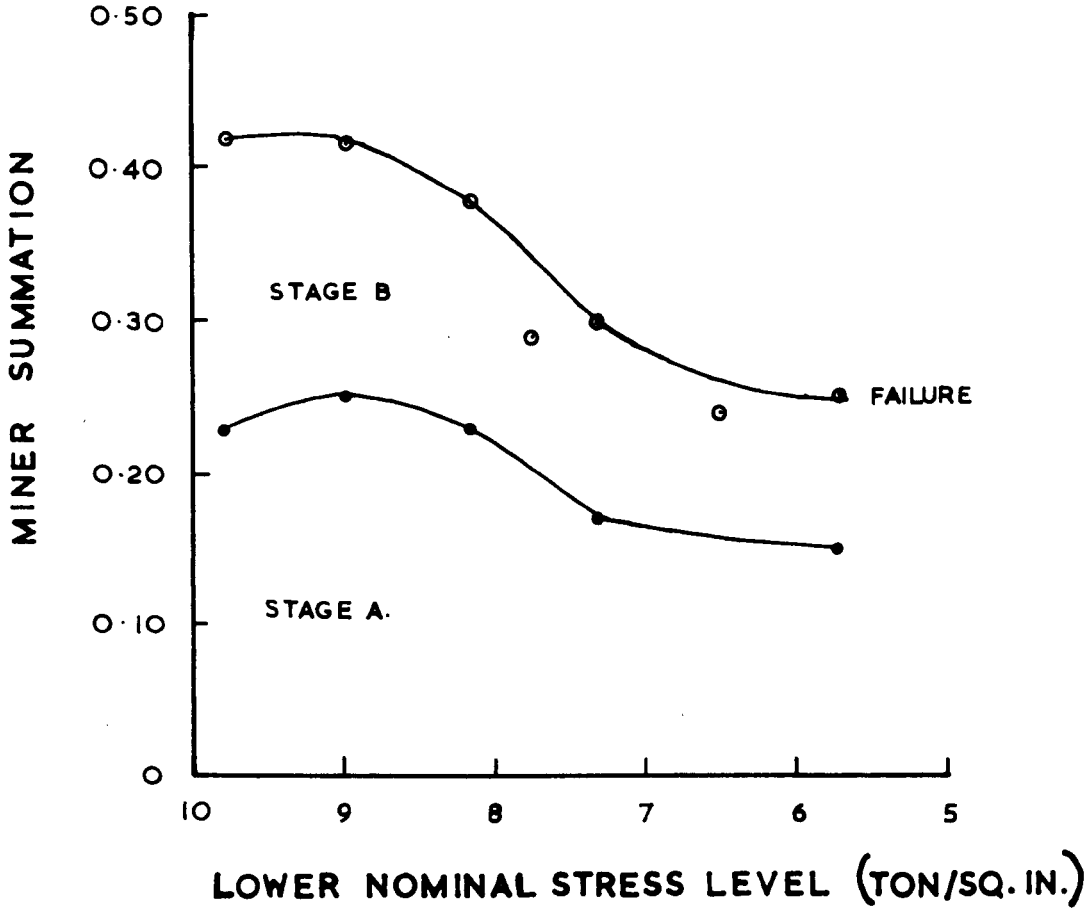

FIG. 6.8

LOADING CONDITION	PREDICTED LIFE IN STAGE A	PREDICTED LIFE IN STAGE B	PREDICTED LIFE TO FAILURE	ACTUAL LIFE TO FAILURE	RATIO OF PREDICTED / ACTUAL
12·24–9·79	333,000	343,000	676,000	565,700	1·19
12·24–8·98	333,000	343,000	676,000	820,400	0·83
12·24–8·16	333,000	343,000	676,000	805,400	0·84
12·24–7·75	333,000	343,000	676,000	667,400	1·01
12·24–7·34	333,000	343,000	676,000	752,400	0·90
12·24–6·53	358,000	343,000	701,000	662,000	1·07
12·24–5·71	409,000	343,000	752,000	786,200	0·96

TABLE 6–5 PREDICTED AND ACTUAL LIVES FOR TRIANGULAR MODULATION TESTS.

FIG. 6.9

PLOT OF LIFE IN STAGE A V LIFE TO FAILURE FOR CONSTANT AMPLITUDE TEST RESULTS.

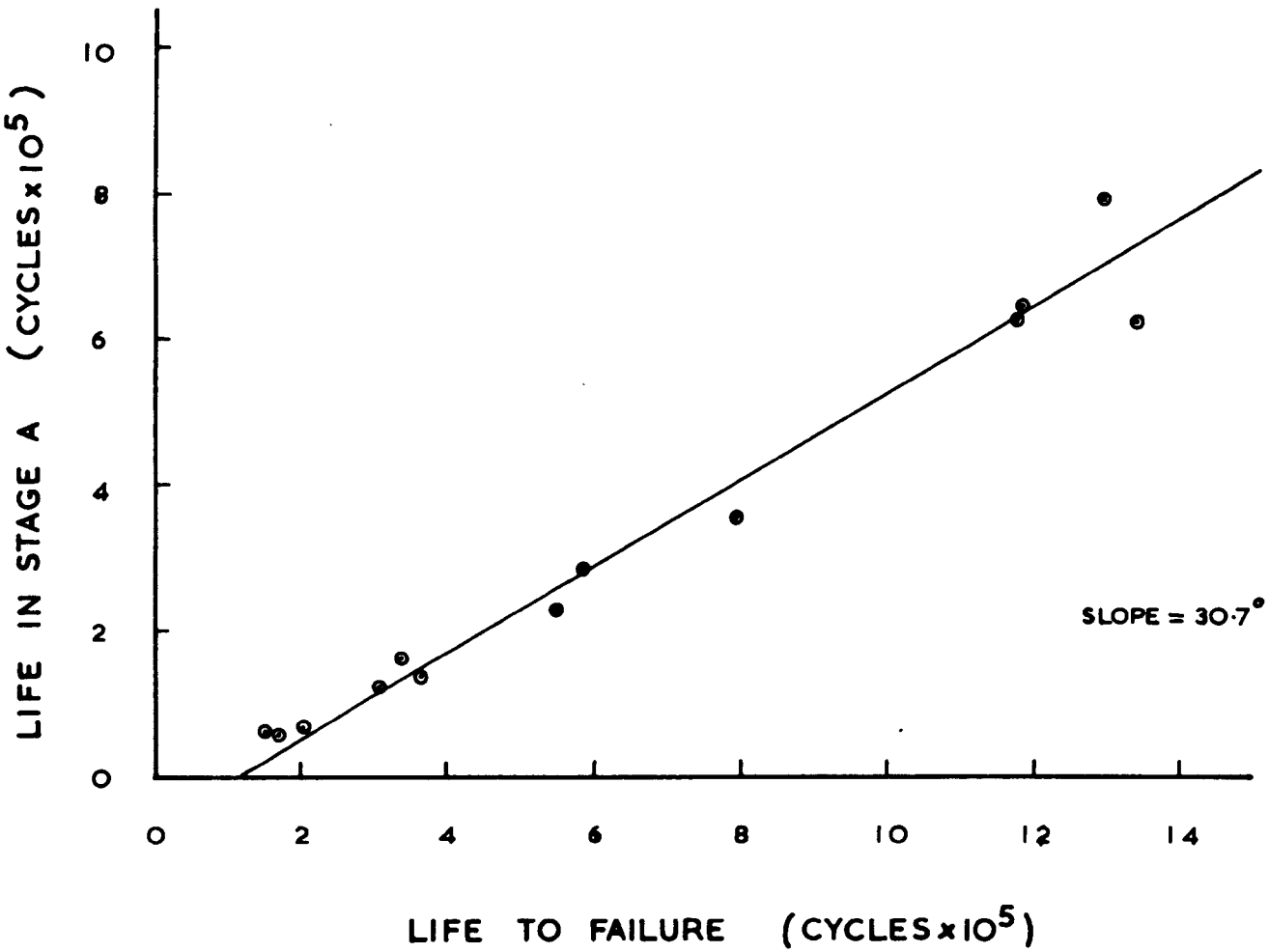

PLOT OF LIFE IN STAGE A V LIFE TO FAILURE FOR TWO DIFFERENT BATCHES OF MATERIAL BUT SIMILAR SPECIMEN GEOMETRY.

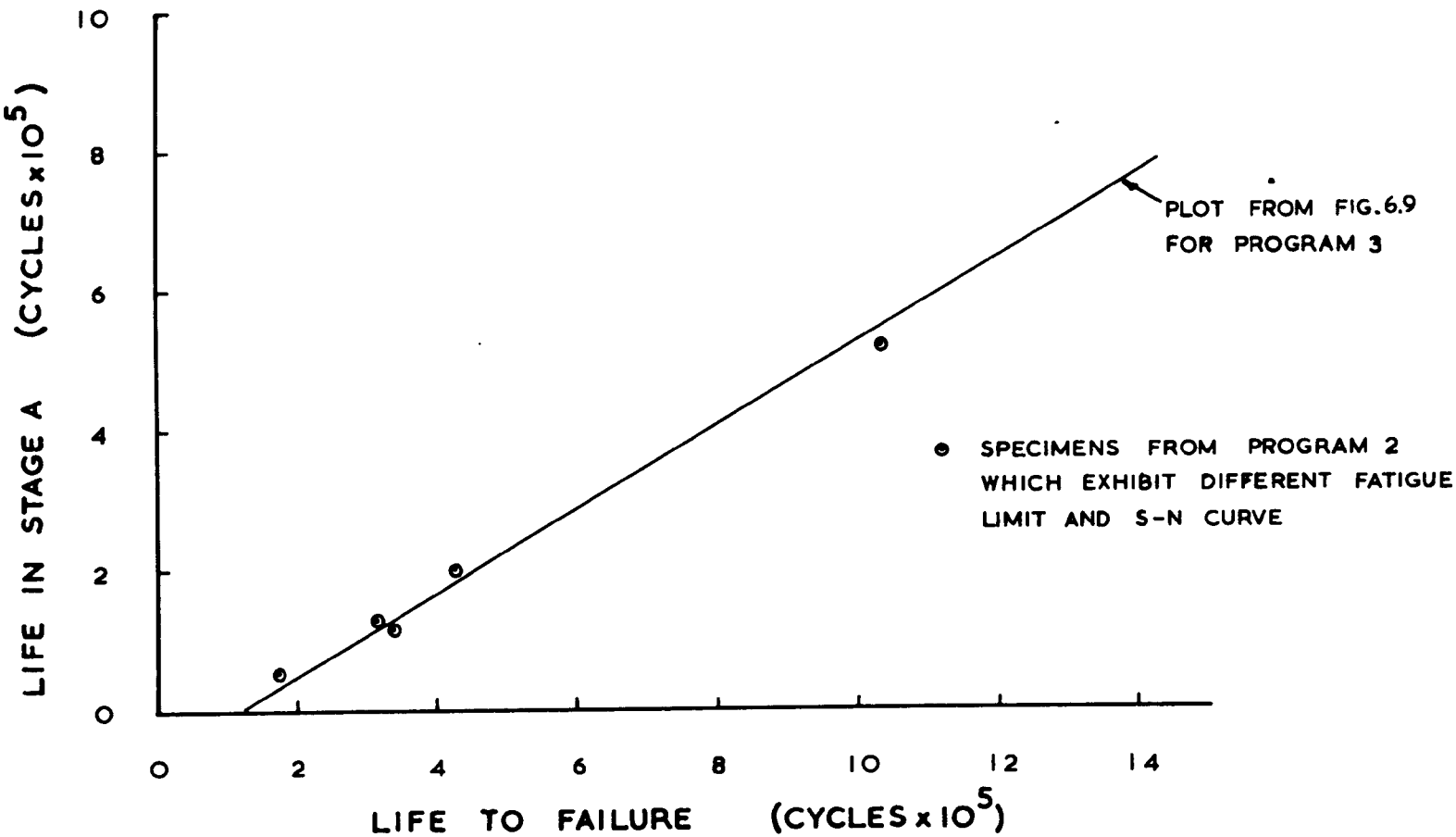

FIG. 6.10

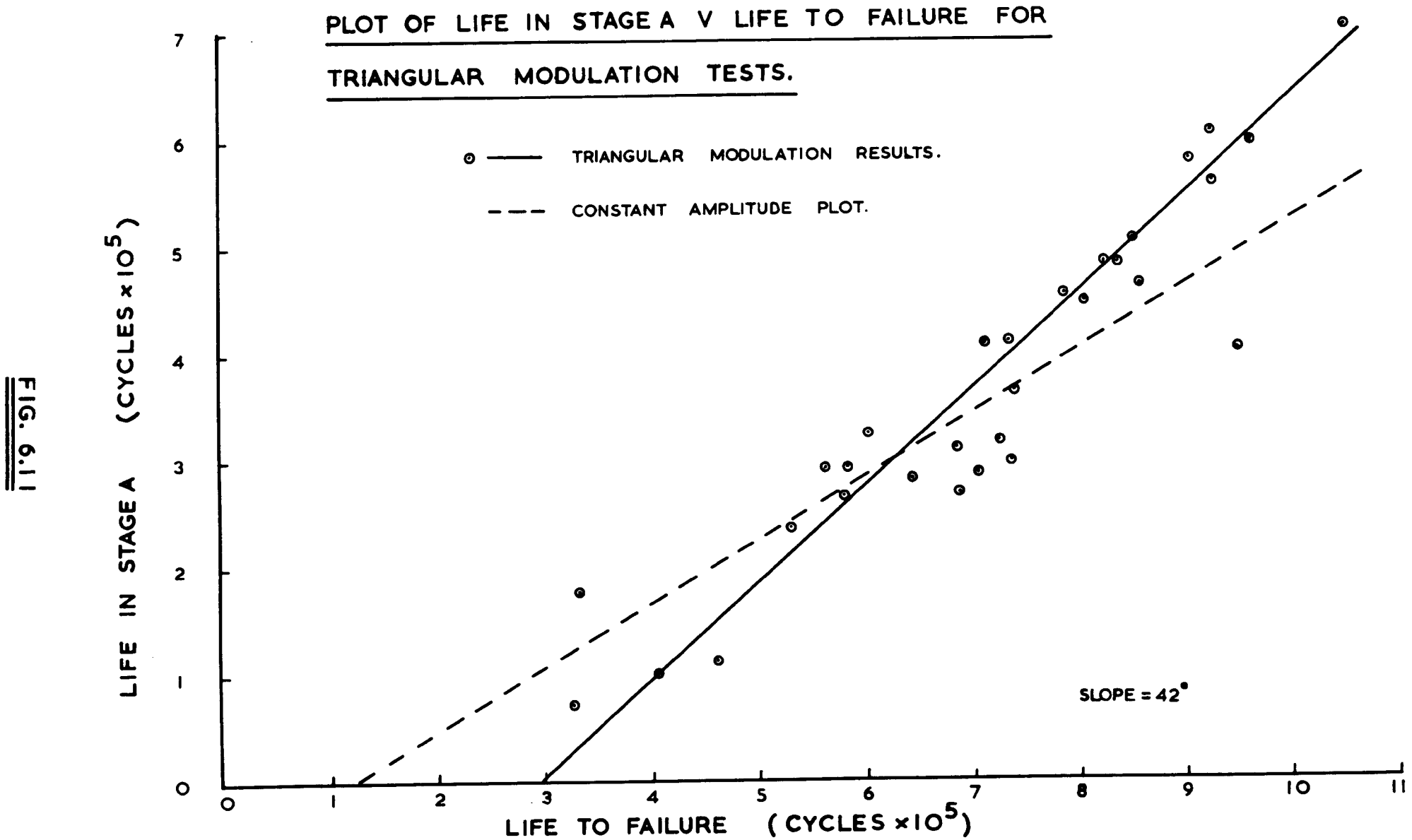
PLOT OF LIFE IN STAGE A V LIFE TO FAILURE FOR
TRIANGULAR MODULATION TESTS.
TRIANGULAR MODULATION RESULTS.
CONSTANT AMPLITUDE PLOT.
SLOPE = 42°
LIFE IN STAGE A (CYCLES × 10^5)
LIFE TO FAILURE (CYCLES × 10^5)
0
1
2
3
4
5
6
7
8
9
10
11

FIG. 6.11

PLOT OF CUMULATIVE FORSTER READING V CYCLES FOR STRESS RELIEVED SPECIMEN.

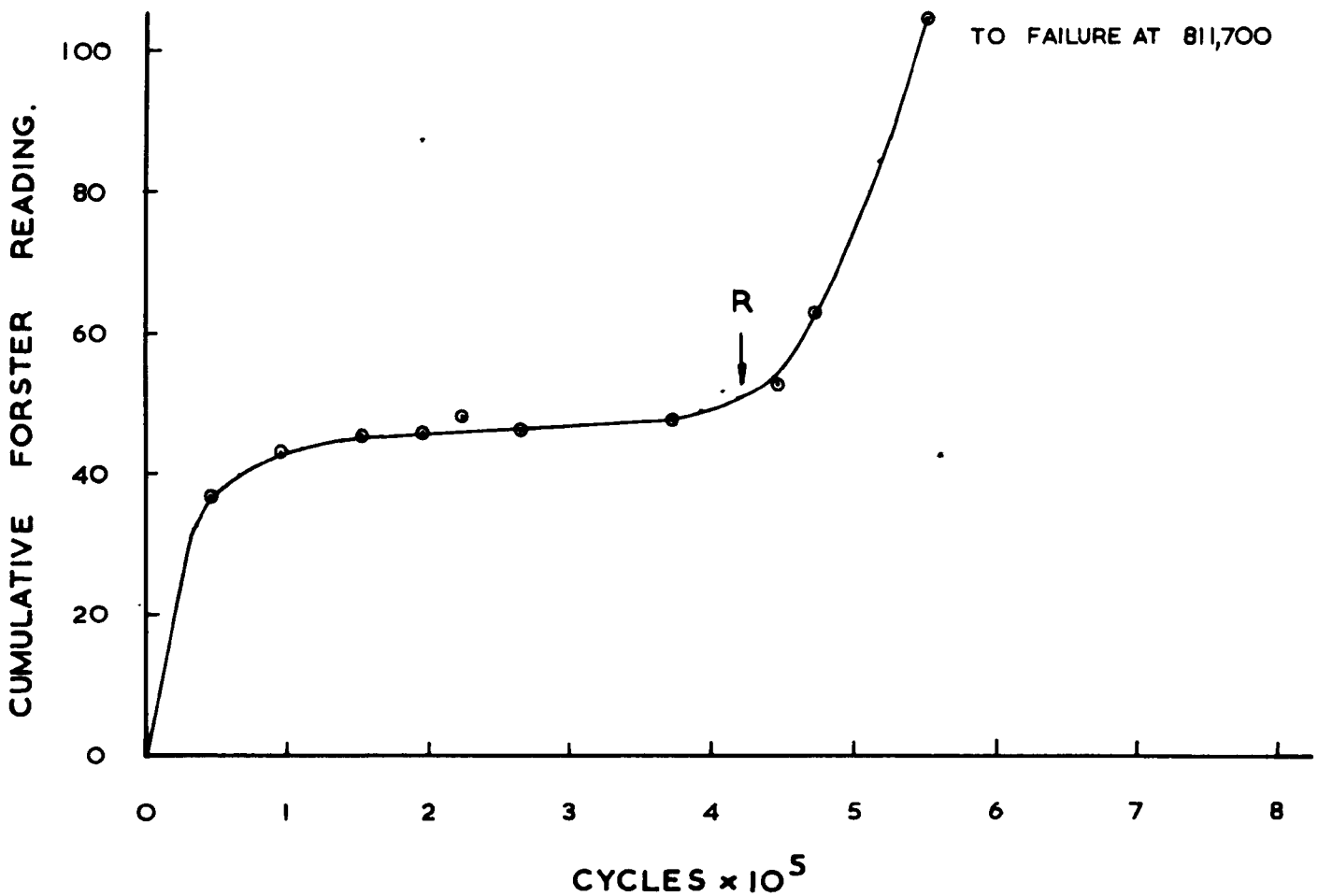

FIG. 6.12

	LIFE IN STAGE A	LIFE IN STAGE B	LIFE TO FAILURE
	120,000	272,100	392,100
	420,000	391,700	811,700
	200 000	281 800	481,800
SCATTER	300,000	119,600	

TABLE 6-6 TEST RESULTS FOR STRESS RELIEVED SPECIMENS AT 11·42 TONS/SQ. IN.

PLOT OF LIFE IN STAGE A V LIFE TO FAILURE FOR STRESS RELIEVED AND UNRELIEVED SPECIMENS AT CONSTANT AMPLITUDE.

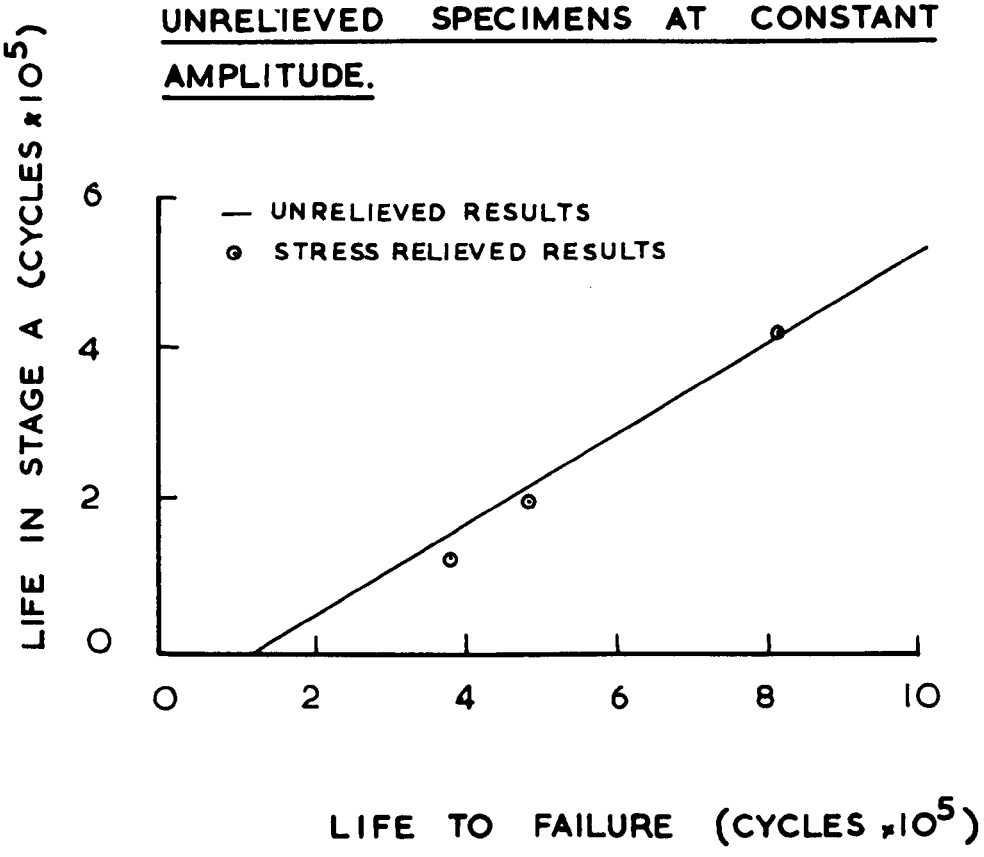

FIG. 6.13

CHAPTER 7

This chapter presents principally the results obtained on the Amsler Pulsator and deals with certain points raised by these results in correlation with the work presented in Chapter 6 and extends and compares the cumulative damage rate with other results in the literature. Also presented are the results of constant amplitude tests on the electromagnetic rigs.

The importance of a plot of life in Stage A versus cycles to failure for a particular section configuration and loading conditions has been established in the previous chapter. The objective of this set of experiments was to see whether this type of behaviour existed over a much greater range of specimen configurations and loading arrangements. The Amsler Pulsator is equipped to perform both axial and bending tests but, as the ram is single acting, tests have to be conducted with a pulsating load about a tensile mean load. This fact is of no particular importance in mild steel as both Frost (1962) and Lee (1968) have reported that mean load has no effect on crack propagation rates in this material.

The design of both the axial and bending specimens was dealt with in Chapter 3. Due to the inertia of the moving parts on the Amsler correction must be made to the applied loads to allow for the specimen stiffness and mass. It is important that the stiffness of the specimen be measured in the machine so that give in the loading devices is accounted for properly.

The manufacturers recommend that brown paper smeared with graphite is inserted between working surfaces to reduce wear due to fretting. In the case of the axial tests where this paper lies between the actual jaws

and the main body of the machine in the slides, great care must be taken to ensure that there is no relative movement between the jaws and the locating slides.

An axial specimen was run for several thousand cycles until the specimen was well bedded into the jaws. The stiffness was then measured and the loading correction factor calculated. Due to the high stiffness of the specimen and its short overall length the corrections proved negligible at the highest machine speed of 750 c.p.m.

There were no specific problems with bending attachments and after bedding in the specimen stiffness was measured and the load correction when calculated was 0.55% for a speed of 375 c.p.m. The higher speed could not be used as a certain amount of chatter set in on one of the valves with high quantity high speed delivery of oil.

The large bending specimens were cylindrical and no flats were machined at the loading points. This proved to be quite adequate as far as conditions under load were concerned but there was the possibility of the specimen rolling out of the machine if the machine came off load due to specimen failure or some other cause. If the trips are set close to the needles on the gauges the possibility of complete specimen fracture before the machine cuts out is extremely remote. Therefore two straps were placed at either end of the bending beam to catch and locate the specimen in the event of specimen or machine failure.

BENDING TEST RESULTS

The bending specimens were marked during machining to enable them to be set to the required accuracy in the longitudinal direction in the Amsler. The large size of the specimen meant that additional care had to be taken to ensure that Forster readings were taken in the most

fatigue prone region, this was due to the large size of the groove, it having to be scanned longitudinally as well as circumferentially with the Forster. A line was marked on the specimen surface parallel to the longitudinal axis. Then both sides of each notch were taped and two reference points marked on either side of the centre-line at approximately $\frac{3}{4}$ inch intervals. Forster readings were taken for each groove at these five points and the regions inbetween were scanned at intervals. The centres of the end load reaction plates on the Amsler were also marked. Thus when the specimen was loaded all the centre lines were aligned, this together with the control of longitudinal location ensured both that the specimen was set accurately in the Amsler and that the Forster readings were being taken in the correct place with minimum coverage required to be sure of picking up first cracking.

The main objective of this test program, as already stated, was to see if the same style of behaviour existed in large scale specimens. The same policy of steel direct from a commercial stockist was maintained and this meant that different bars had to be purchased to manufacture a total of 10 specimens due to their length. However it had already been established that variations in the material properties did not affect the plot of life Stage A v life to Failure and therefore this caused no great concern. The calibration for the Forster was of course not applicable to the large bending specimens. The usual procedure of running specimens and the sectioning and observing crack length was not viable for the following reasons:-

1) The relatively low speed of the machine necessitated rather a long testing period.

2) The cost of each specimen for steel alone was close to £10. If realistic machining and handling costs are allowed for small batch production, the cost of each specimen is approaching a total of £20. Any

sectioning mistake is therefore costly.

It was decided to waive the usual calibration curve on the above grounds. The Forster response is sensitive to the load actually on the specimen at the time of testing. The rotating bending specimens had been examined with no load but this was not practicable with the large bending specimens. The only methods available for taking all load off the specimen quickly would have necessitated re-setting the specimen in the machine each time that a reading was taken. As this operation could take up to twenty minutes it was convenient to keep the machine running on a small mean load with no alternating load. A constant machine load of 1 ton was therefore used for all measurements taken with the Forster on the large plane bending specimens. The tests were run with a mean surface stress at the root of the notch of 20 tons/sq.in. The first constant amplitude tests showed the same pattern of Forster response as on the rotating bending specimens. In order to get some idea of the crack lengths involved a specimen was run with block programming applied manually. The pattern of Forster readings was then compared with the program markings on the specimen, thus some information was gained on propagation at low stress levels as well as gaining an approximate idea of the crack length calibration of the Forster.

A photograph of the program markings concerned are shown in Fig. 7.1. and the plot of Cumulative Forster Readings v. Cycles for the fractured end of the specimen is shown in Fig. 7.2. Comparison of the markings with the Forster readings on this and one other specimen subjected to block programming showed that the crack length when the Forster indicated steady and continuous growth was less than 0·020 inches. A typical plot of Cumulative Forster Reading v. Cycles for a constant

amplitude test is shown in Fig. 7.3. The results of the constant amplitude tests are shown tabulated in terms of life in Stage A, Stage B and Total life in Table 7-1. This data is shown as a plot of life in Stage A v. Life to Failure in Fig. 7.4. and as can be seen the same unique curve is obtained even though the fatigue strength of the two batches of material was different.

The limitation of the Forster with depth was particularly obvious in these tests but it should be remembered that even at short lives with large specimens more than 50% of the life is covered by the Forster and in the case of long running specimens this rises to greater than 90%. In some cases the other groove on the specimen was sectioned and the cracks observed. This provided some classic examples of the difficulty of observing cracks through pearlite grains and also the action of pearlite grains as crack stoppers and dispersers.

The photograph in Fig. 7.5. shows the difficulty of tracing the crack path in a pearlite grain, if the crack were not clearly visible on either side of the grain its detection using standard observations is virtually impossible, interference or stereoscopic techniques would be required. Fig. 7.6. gives a classic example of the dispersive effect of the pearlite grain on crack development. On approaching the pearlite grain the crack front splits and attempts to move in both directions around the grain and also through it.

AXIAL TESTS.

The axial test specimens have been described previously in chapter 3. The mean stress on the surface of the groove was the same value as for the large plane bending specimens, i.e. 20 tons/sq.in.

The specimens, which had been stored heavily smeared in oil, were cleaned with carbon tetrachloride before testing. The surface on either side of the groove was taped and then 8 reference points were marked on the tape equally spaced around the circumference of the specimen. Forster readings were taken at these eight points and the intervening spaces were scanned at intervals.

The problem of load during reading with the Forster also occurred with the axial tests. Occasionally, when load was reduced to zero, the bottom set of grips drop away from the specimen, the ram pulses upwards and the machine cuts-out, the ram then drops right to the bottom micro-switch. This means that the whole setting up process has to be repeated. The problem was accentuated by the difficulties encountered as a result of the special fretting protection measures. Relative movement between the grips and the locating slides has already been mentioned, but the Amsler was particularly prone to developing this fault at loads under 2 tons. Once this developed the only way to overcome it was to shut down the machine, knock the grips off the specimen and remove them, then clean the slides and replace the carbon smeared papers. In order to avoid operator fatigue and obtain consistent testing a mean load of 2 tons was maintained during reading with the Forster.

Testing was confined to constant amplitude tests with a few simple block programming tests which were applied manually. In the program tests, the mean load was kept constant and the amplitude of the fluctuating load was varied. The technique of using a block program test to give approximate crack length calibration curves for the Forster was used again in this test program.

The same pattern of Forster response emerged again in these axial tests. A typical plot of Cumulative Forster Reading versus Cycles is

shown in Fig. 7.7. The results of the constant amplitude tests categorizing the length of Stage A and Stage B are shown in Table 7-2. These results are shown plotted as life in Stage A v. Total Life to Failure in Fig. 7.8.

PLANE BENDING TESTS ON SMALL SPECIMENS.

These tests were conducted on the specimens described in Chapter 3. in the electro-magnetic rigs. The small size of the specimens and the nature of the test limits the possibility of cracking starting to two small areas at the top and bottom of the groove. These areas were scanned with the Forster and the maximum response noted during testing. The results of constant amplitude test results are shown in Table 7-3 split into life in Stage A and Stage B and a typical plot of Forster Reading v. Cycles is shown in Fig. 7.9, exhibiting the same style of behaviour. The plot of life in Stage A v. Total Life to Failure is shown in Fig. 7.10. and again a straight line plot has been obtained. As yet a calibration curve for the Forster has not been obtained on this specimen configuration, but an intensive cumulative damage program is planned on the electro-magnetic rigs and an accurate calibration curve will be obtained by the sectioning methods described previously.

DISCUSSION AND ANALYSIS OF RESULTS

The same pattern of Forster response has been noted for all of the four specimen configurations investigated and the same style of unique curve for the plot of life in Stage A v. Total Life has been exhibited by each specimen. These results validate the argument that the relationship between the life in Stage A and Total Life is basically a relation between the stress fields due to the geometry of the specimen and those due to the cracked state of the specimen. The basic pattern

of behaviour has therefore been established in a wide variety of specimen geometries, ranging from 0.250 inches to 4.300 inches test sections and K_T values from 1.67 to 2.21.

The most interesting feature of the results is the value of the slope of the plot for the three specimens whose K_T values are close to 2.1. These values, together with K_T values, test section size and type of loading are shown below.

Specimen	Rotating Bending	Large Plane Bending	Axial
Test section size (ins)	0.531	4.300	1.000
K_T	2.00	2.21	2.17
Slope of plot	30.7°	35.2°	34.7°

The slopes are very constant for such a wide range of test section sizes and loading methods. It therefore seems likely that the slope of the plot is independant of overall specimen size and only dependant on the specimen geometry and loading conditions as expressed through the K_T value of the notch. There is probably therefore a relationship between the K_T value and the slope of the plot. Four points have already been established experimentally and a further limiting case can be established by argument.

It has already been argued that one of the limiting cases is the sharply notched specimen which produces non-propagating cracks but before utilizing this an expansion of the argument is necessary. The normal view of the behaviour of the sharply notched specimen is that it initiates a crack in the first few thousand cycles and therefore the rest of the life is spent in macro-crack propagation. This is a perfectly reasonable assumption but the observation of the behaviour of cracks in notched specimens together with the results already existing in the literature

leads to the definitions given earlier of Stage A and Stage B. The macro-crack propagation phase, or Stage B as termed, is bounded by more rigid confines, it is deemed to start when the crack growth becomes a steady and continuous process and the specimen cannot be regarded as in the macro-crack propagation phase unless the applied nominal stress is capable of propagating that crack to failure i.e.the stress field associated with the cracked state of the specimen is sufficient to ensure propagation. The sharply notched specimen which is being stressed below the constant amplitude fatigue limit contains a small crack which will not propagate to failure unless the stress level is raised and, in the normal view this would be deemed to be in a macro-crack propagation phase whereas here it has been defined as still in a micro-crack propagation phase, or in Stage A. Thus if we consider the sharply notched specimen close to the fatigue limit the macro-crack propagation phase Stage B is a quasi-stationary quantity and although damage will be initiated in a very short period the large variation in life occurs in propagating this initial damage through to the macro-crack propagation phase. Therefore variations in the life of sharply notched specimens due to change in stress level may be regarded as taking place for the major part in Stage A i.e. the slope of the life in Stage A v. Total Life plot for constant amplitude test results is approaching 45°.

If we accept the specimen that produces a non-propagating crack as being linked to a slope of 45° on the life in Stage A v. Total Life plot then the work of Frost (1961) provides the necessary data. He has established a critical K_T value of 3.8 to produce non-propagating cracks for a single notch depth. This limiting case together with the experimental points already established give 5 results covering the range of interest. Fig. 7.11. shows a log log plot of $1/K_T$ against sec θ . Although the log log plot reduces scatter the fit of the straight line to the results is quite

good with a slope of 4 for the plot. It is worthwhile to note and discuss a certain aspect of this plot before developing the relationship further. The straight line in Fig. 7.11. passes very close to the origin and this is the point $K_T = 1$ and a slope for the life in Stage A v. Life to Failure plot of 0 degrees. At first this seems to be ridiculous in normal terms for what this suggests is that the plain specimen is dominated by Stage B behaviour i.e. macro-crack propagation. A plain specimen certainly does not spend most of its life in a cracked state but the value of 0 degrees for the slope of the life in Stage A v. Total Life plot can be explained rationally by examining again the definition of Stage A and its implications.

Stage A includes both initiation and micro-crack propagation and, in the case of plain specimens, initiation of damage occupies a longer period than for notched specimens. However the absence of the stress gradients associated with a notch means that the micro-crack propagation phase is virtually non-existant i.e. the specimen passes straight from initiation of damage to the macro-crack propagation. The range of surface stress required to produce the same variation in life is much smaller in the case of plain specimens for example using the results of Marsh(144):-

	Surface Stress tons/sq.in.	Life x 10^6	Stress Range	Life Range
Plain	16.0	0.340	2.25	1.999
	14.0	2.339		
Notched	136	0.288	47.50	2.147
	88.5	2.435		

It can therefore be argued that for the plain specimen we are rapidly approaching the case where the initiation of damage is a quasi-stationary quantity and as the micro-crack propagation phase dominated by a specimen

geometry is absent the major variation in life is in the macro-crack propagation phase. If these arguments are correct then the life in Stage A v. Total Life plot for plain specimens in constant amplitude tests should be parallel to the Total Life axis i.e. a slope of zero but with an intercept on the life in Stage A axis which denotes purely an initiation phase.

At this point the first major step in expanding the cumulative damage rule has been achieved. An empirical relationship has been obtained which allows the split between Stage A and Stage B to be obtained for any specimen geometry subject to the limitations imposed on accuracy by lack of knowledge of the intercept. If these methods are to be extended to the life prediction of more complex structures than specimens then more information is required in certain areas.

The relationship of initiation and micro-crack propagation within the Stage A as defined is an important factor, it requires further investigation but this in itself would be a complete project. The question of predicting crack growth rates for large cracks in sheet specimens has been attacked successfully since 1960 by both "phenomenological" laws and more so by the continuum mechanics approach first developed in the field of fracture mechanics.

This gives hope that the methods will be developed to cover a greater range of materials and configurations in the macro-crack propagation phase. The observations made in this thesis have also confirmed that the macro-crack propagation phase is generally a steady growth rate period but also that in the terms of overall life of the notched specimen particularly in the long life region this phase of the specimen life is relatively short. The prediction of macro-crack growth rates is extremely important in engineering terms in order to be able to decide

on inspection periods and techniques but in terms of a simple cumulative damage rule covering the long life period its importance diminishes rapidly with the diminishing proportion of the life which it represents.

Notched specimens in general exhibit less scatter than plain specimens. It has been shown that most of the scatter occurs in Stage A and this reduces the field to either initiation or micro-crack propagation and as it has been argued that micro-crack propagation is virtually non-existant in plain specimens, it is likely that most scatter is accounted for in the initiation of damage. This means that for notched specimens a most critical portion of the life (micro-crack propagation) exhibits little scatter and therefore should be amenable to predictions most probably on a stress analysis basis. Small cracks in the presence of mild notch geometries which affect the stress fields in which the crack exists and propagates fall outside the present range of conditions investigated in crack propagation work. As it seems likely that the micro-crack propagation phase was dominated by critical stress field conditions a knowledge of these is desirable to give a basis for the extrapolation of specimen results to more complex structures. Stress Analysis programs were developed to deal with edge notches, edge cracks and edge notches with cracks formed at the root of the notch. Although the programs have been run, certain points which require investigation and clarification are more easily and quickly accomplished after the upgrading of the University computer, the critical factor being store size, therefore general results from the programs are not presented but a description of the programs and their formulation is given in Appendix II.

The plot of $\log_{10} {}^{1}/K_T$ versus $\log_{10} \sec\theta$ shown in Fig. 7.11. emphasized several important factors as discussed in the previous paragraphs, it also established that ${}^{1}/K_T \propto (\sec\theta)^4$. Fig. 7.12. shows a plot of ${}^{1}/K_T$ versus $(\sec\theta)^4$ for the results, and this plot results in the following equation relating the value of K_T to the cosine of the slope of the plot:-

$$ {}^{1}/K_T = -0.1255(\sec\theta)^4 + 0.7360 \qquad - (1). $$

The establishment of this type of relationship together with the relatively small degree of scatter exhibited at $K_T \simeq 2.1$ by widely varying specimen sizes has certain important implications in the formulation and application of cumulative damage rules. In Chapter 6 two main alternatives were put forward with respect to the plot of life in Stage A v. Total Life and cumulative damage behaviour and they were briefly as follows:-

(1) That the slope of the plot is sensitive to changes in overall specimen size.

(2) That the slope remains unchanged but that behavioural patterns during Stages A and B are different.

Of course there is the possibility of a combination of these two alternatives. The existance of the relationship given in equation 1 and the low degree of scatter exhibited around $K_T \simeq 2.11$ means that in practical terms we may ignore the first alternative and concentrate on the second. The question of intercept values also arises, but the small variation shown between Figs. 6.9., 7.4., 7.8. covering section sizes from 0.531 inches to 4.30 inches indicates that this may be neglected when considering size effects with only a very small error. Although it is now possible to concentrate on behavioural patterns as an explanation of size effects it must be remembered that the cumulative damage rule proposed is based on the S-N curve for the particular specimen under consideration and this

factor alone will account for some effects.

The behavioural patterns of specimens with the same test section size but different notch severity should be essentially the same and a relationship has been derived which allows the slope of the plot to be predicted over a wide range of K_T values. The intercept value of the plot of life in Stage A v. Total Life seems also to be a function of notch severity according to the plots available. Except in the cases of lives of 5×10^5 and less this could safely be neglected and this region of short lives is dealt with more capably by other methods, and so it is not necessary in terms of accuracy to be specific about the value of the intercept.

It is useful at this stage to summarize the progress made in the development of the cumulative damage rule, outline its areas of application and include certain limitations in its use within these broad areas.

(1) The rule proposed deals only with stress histories giving severe interaction effects and is based on consideration of the behaviour in two main stages of the life.

(2) The pattern of behaviour in Stages A and B has been established for a test section size of 0.531 inches with the further limitation that stresses down to $0.6\,\sigma_f$ only have been examined in Stage B. If reference is made to the cumulative damage investigations on Spec.No. 2.4.9. (Chapt.5) then there is strong evidence to suggest that any extended period of application of loads below this level leads to a stabilization of the crack front and possibly a higher level of resistance to propagation when higher stress levels are re-applied. Hardrath (1964) has observed a stabilization of crack growth upon reducing loads in a 7075-T6 aluminium alloy.

(3) An empirical relationship between the K_T value of a notch and the slope of the life in Stage A v. Total Life plot has been obtained which allows the rule to be extended over a complete range of K_T values.

(4) It has been established that size effects are not accounted for by variations in the slope of the plot but by the S-N curve and a variation in behavioural patterns not as yet established. It is expected therefore that the rule as proposed can be applied to a small range of section sizes about a mean of 0.53 inches.

The real test of any cumulative damage rule is the fit obtained on other test data published in the literature. The rest of this chapter is devoted to the extension of the cumulative damage rule proposed and its comparison with experimental results in the literature. To avoid laborious calculations being repeated the use of the cumulative damage rule to predict results in two cases, that of the triangular modulation tests described in Chapter 6 and narrow band random tests on sharply notched specimens, are given in full detail in Appendix III.

In order to extend the rule to cover different stress spectra it is necessary to rationalize results already existing in the literature. A feature of the rule is the concept of a top damaging stress level and in triangular modulation tests this is the top level present because of the frequency of its occurrence relative to the rest of the spectra. It is not rational for example to assume that in a Rayleigh distribution a 3.8xrms peak with a probability of occurrence of less than 0.1% is the top damaging level. Naumann (1962) has shown that infrequently occurring high stress peaks in blocks of 10 cycles or less are in fact beneficial. It is therefore suggested that when considering random or very well mixed block programming data the top damaging stress level should be considered as that level which is attained or exceeded by 0.5% of the stress peaks

or in the case of block programs the closest value to 0.5% but not less than 0.1%. This factor may well be amended in the light of further experimental data particularly for low r.m.s. values of the signal.

The first sets of data examined are those presented in Chapter 6. It is interesting to compute the predicted lives using the empirical relationship to derive the slope of the life in Stage A v. Life to failure plot and assuming that it passes through the origin. The detail calculations and application of the cumulative damage rule are shown in Appendix III. The results are presented in TableIII-1 and as can be seen the errors induced by the assumption that the life in Stage A v. life to failure plot passes through the origin are negligible (refer to Table 6-5 Chapter 6). The comparison of the proposed prediction to Miners Law is very favourable, the maximum unsafe error being 19% for the proposed method as compared to 417% from Miners Law.

The second set of test data examined is that of Fralich (1961) who subjected notched plate cantilever bending specimens of SAE 4130 normalized steel to a signal which proved to give a Gaussian response for stress levels on the specimen in a narrow frequency band around the resonant frequency of 123 c.p.s. i.e. a narrow band Rayleigh distribution. The specimens were $^{3}/_{16}$" thick edge notched specimens with a net test section width of $^{3}/_{8}$". The notch was a 60 degree included angle V slot with a root radius of 0.005 inches to a depth of $^{5}/_{16}$ inches. The K_T value of this notch is given as 7.25 in an axially loaded specimen and this puts the specimen into the sharply notched region where all the life can be assumed to be spent in Stage A behaviour. The value of the intercept may be neglected to obtain reasonably accurate life predicitions. This in fact means that we are only considering stresses down to $0.7\sigma_f$ as damaging during the macro-crack propagation phase but this assumption

should not introduce sufficiently large errors to distort the overall accuracy or lack of fit of the method. The detail calculations are shown in Appendix III for this particular case but Fig. 7.13 shows the actual experimental results and the predicted curve using the cumulative damage rule proposed. Fig. 7.14. shows the curve for the experimental results, the Palmgren-Miner prediction and the prediction of the proposed rule. It can be seen that the proposal is considerably more accurate and most important safer than the Palmgren-Miner prediction particularly in the long life regions.

Marsh has published several sets of results in the literature including a set of triangular modulation tests which cover a wider range of conditions than those investigated in Chapter 6.

Marsh (1964) used mild steel rotating bending specimens with a 0.4 inch net test section. The notch was a 55° included angle with root radius as sharp as possible. Marsh quotes the K_T values in excess of 13.6 for the notch used and all specimens were stress relieved immediately prior to testing. Constant amplitude tests were conducted showing a fatigue limit at approximately 6.1 tons/sq.in. nominal. In the triangular modulation tests the highest and lowest stress levels were denoted σ_h and σ_l respectively and Marsh investigated four different values of the stress ratio $\alpha = \frac{\sigma_l}{\sigma_h}$ with several values of σ_h at each value of α. The results of these tests in terms of endurance, endurance predicted by the method proposed and the ratio of predicted to actual lives are shown in Table 7-5.

An examination of the ratio of predicted to actual lives seems at first most disappointing however a closer study seems to prove the results a little more encouraging. The values of the former ratio are fairly constant for the values of $\alpha = 0.5$, 0.25 and 0.0 but the values at $\alpha = 0.77$ diverge by approximately 30% on mean based on the high values.

If the stress levels involved at $\alpha = 0.77$ are examined it can be seen that relative to the fatigue limit they are in the region, where the approximation of a straight line in the life in Stage A versus lower load level plot is the worst fit to data ref. Fig. 6.7. The mean values of the ratio pred/actual at the other conditions of α are 2.37, 2.58 and 2.35 and although these values are remarkably constant for a wide range of load conditions they appear unduly pessimistic. For the above conditions the predictions in terms of range are 20% better than the hypothetical S-N curve proposed by the Corten-Dolan-Marsh hypothesis. The major difference between the work of Marsh and that described earlier in Chapter 6 is that Marsh's specimens were stress relieved after the machining of the notch. The few results on stress relieved specimens have been presented and it was shown that they did not appear to deviate from the life in Stage A v. Total life plot for unrelieved specimens i.e. that there was merely an overall reduction in life and an explanation was put forward to cover this behaviour. It has also been postulated that the major effect of low stress levels is the relaxation of residual stresses and as the triangular modulation tests were performed on unrelieved specimens our cumulative damage rule will automatically have included the factor due to residual machining stresses. It is likely therefore that the pattern of behaviour will remain the same but with some factor accounting for the effect of the residual machining stresses on the total life. The ratio of unrelieved/relieved lives of the few specimens available is calculated to be 2.15. If the previous arguments are correct then this factor has been built into the cumulative damage rule proposed and should be taken out when dealing with stress relieved specimens as in the case of Marsh's results. The case for $\alpha = 0.77$ is that most of the predicted lives should be higher if behavioural

patterns had been simulated with no approximations but the final mean values of the ratio of predicted life to actual life taking into account correction for residual stresses are as follows:-

	$\alpha = 0.77$	$\alpha = 0.5$	$\alpha = 0.25$	$\alpha = 0$
Ratio $\frac{\text{Predicted}}{\text{Actual.}}$	0.79	1.10	1.20	1.09

The extrapolation of this theory can be further tested on the results of the plain specimens tested by Marsh (1964). The tests were performed on an exactly similar basis with a specimen diameter of 0.300 inch at the test section. The fatigue limit in this case was approximately 13.80 tons/sq.in. The plain specimen which may be considered as the other limiting case where the slope of the life in Stage A v. total life plot is almost zero. There will of course be an intercept on the life in Stage A axis which will be dependant on the initiation period. If we neglect this then we should again be able to predict the pattern of behaviour with some success in the long life region. An analysis of the results for stress ratios of $\alpha = 0.9$ and $\alpha = 0.77$ corrected for residual stress are presented in Table 7-6. Results from the lower values of α are not investigated because of the following reasons.

1) The lower stress levels start to go outside the range investigated.

2) The plain specimens and higher loads mean that the time taken to traverse from high to low becomes quite lengthy in some cases over 5,000 cycles. This means that long periods are spent with low loads reducing the overall severity of interaction effects.

The values of the Miner Summation are also presented in Table 7-6 and although in a few cases the predicted lives are optimistic the vast improvements in estimates of life, when most of the stress cycles are below the fatigue limit, as compared to those from Miners Law are obvious.

It was suggested that the cumulative damage rule proposed was limited to well mixed spectra which would produce severe interaction effects. A further set of data was available on rotating bending specimens and this again concerns the work of Marsh (1968). Marsh claims to have simulated both a Rayleigh distribution and a wide-band Gaussian stress distribution by seven stress level block programs in a rotating bending machine. Quite what degree of simulation of a wide band process is expected from a machine only capable of full stress reversals on each cycle is not discussed by Marsh, however the results provide useful well mixed block programming data.

SIMULATION OF RAYLEIGH STRESS DISTRIBUTION (MARSH)

The program used by Marsh to simulate the Rayleigh Stress Distribution was of the following composition:-

Peak s/σ_{RMS}	Total number of cycles.	Number of Sub-blocks.	Size of Blocks (cycles).
4.20	5	1	5
3.75	45	4½	10
3.10	300	3	100
2.40	1,350	13½	100
1.80	3,600	36	100
1.20	7,400	37	200
0.60	5,000	50	100
Total	17,700		

Note the longest sub-block length is 200 cycles.

In comparison to the total number of cycles in the block the top level of 4.2 x$_{RMS}$ is less than 0.03%.

Therefore in these tests the stress level 3.75σ will be considered as the top damaging level for all values of σ.

The specimens used are identical to those previously described being sharply notched mild steel rotating bending specimens.

Fig. 7.15 shows the actual test results curve with the predictions based on the rule proposed and corrected for residual stress effects. The Palmgren-Miner prediction as calculated by Marsh and also a prediction based on the Corten and Dolan hypothetical S-N curve modified by Marsh (stresses down to 0.8 σ_f considered as damaging) are included on the plot. The method proposed compares very favourably relatively both to the Palmgren-Miner prediction and the Corten and Dolan-Marsh prediction.

Marsh has no justification on the basis of the experimental results in including a fatigue limit on the plot and the modified portion of the curve in the region of lives of the order of 50×10^6 can be seen to be following very closely the predicted pattern.

It is interesting to note that the Corten and Dolan-Marsh prediction is based on the following factors, the original S-N curve, two level block programming tests to determine certain constants, and Marsh's previous testing experience on specimens of this nature in suggesting stresses down to 0.8 σ_f as damaging.

SIMULATION OF GAUSSIAN STRESS DISTRIBUTION (MARSH)

As stated previously this test program cannot be realisticly regarded as simulating a wide band Gaussian signal, it does however provide a useful set of data. The program used by Marsh to simulate the Gaussian distribution was of the following composition:-

s/σ	Total number of cycles.	Number of Sub-Blocks	Size of Blocks (cycles)
4.20	5	1	5
3.75	45	$4\frac{1}{2}$	10
3.10	550	$5\frac{1}{2}$	100

S/σ	Total number of cycles.	Number of Sub-Blocks.	Size of Blocks (cycles)
2.40	3,000	15	200
1.80	9,400	47	200
1.20	23,000	46	500
0.60	64,000	64	1,000
Total	100,000		

The level which is attained or exceeded closest to 0.5% is the 3.1σ level which together with the 3.75σ and 4.20σ levels represents 0.6% of the total cycles applied to the specimen. The level 3.1σ is therefore taken as the top damaging level for all r.m.s. stress levels investigated.

Fig. 7.16. shows the predicted values both as a curve and also as straight line S-N curves together with the experimental results, Palmgren-Miner prediction and the Corten and Dolan-Marsh prediction. Again the results compare very favourably.

Marsh (1967) has also published results on sharply notched axial specimens subjected to a narrow band Rayleigh distribution stress history with a tensile mean load. To try and extend the range of applicability of the cumulative damage rule a prediction was made for these results.

The notch form is the same as that previously described for the rotating bending specimens of Marsh with a net test section of 0.410 inches diameter. All life can therefore be assumed to be spent in Stage A and the top damaging level to be that exceeded by 0.5% of the signal which is the 3.25σ level. Fig. 7.17. shows the actual test results, the Palmgren-Miner predictions, the Corten-Dolan-Marsh prediction and that due to the cumulative damage rule proposed here. The fit to data is not as good as that obtained on block-loading and triangular

modulation data but none the less the prediction is more accurate and safer than either the Palmgren-Miner or Corten-Dolan-Marsh hypothesis in the long-life region. In the same paper Marsh has performed 25 step block loading tests which simulate a Rayleigh distribution truncated at a peak to r.m.s. ratio of 3.0. The 25 levels comprised a block of 200,000 cycles but each level occurred twice so that there are effectively 50 sub-blocks in the 200,000 cycles. Both ordered and random block tests were performed with no significant variation in the results. This means the blocks of low load below σ_f will be in sections of greater than 4,000 cycles.

It has been shown in Chapter 5 that block lengths of this order of magnitude when the stress levels are below the fatigue limit have no effect. Therefore it is expected that the multi-level block programming data will prove to be highly optimistic as a simulation of the random process and further that the construction of the simulation procedure, related to the knowledge of the behaviour of the specimen configuration, will produce a result which is in very close agreement with the Palmgren-Miner prediction deviating when the highest stress present approaches the fatigue limit i.e. in the very long life region where there are more than 10^7 cycles to failure. Fig. 7.18 shows the S-N curve, the Rayleigh distribution block tests and the Palmgren-Miner prediction. As stated the Palmgren-Miner hypothesis provides accurate predictions until approaching 10^7 cycles. Fig. 7.19 shows the actual Rayleigh distribution test results, the multi-level block simulation results and the prediction of the cumulative damage rule proposed. It is interesting that the prediction of the cumulative damage rule is more accurate and safer than test results from a program designed specifically to simulate a given stress spectra.

The two comparisons given above really vindicate the approach to cumulative damage proposed i.e. that any stress spectrum must be considered both in terms of its general mode of composition and the type of behaviour that this will produce in the particular specimen geometry.

The cumulative damage rule proposed has been applied to a fairly broad variety of cumulative fatigue damage data and has been demonstrated as an improvement on existing methods in the long life region. It has already been stated that this particular rule is probably restricted to certain types of stress history and therefore one is faced either with a small number of cumulative damage rules which each deal with a limited range of stress histories or the overall method has to be developed to cover a wider range. A more sophisticated solution is perhaps possible by consideration of the life in Stage A v. Total life plot under cumulative damage conditions. If the properties of this plot i.e. the slope and intercept could be related to a particular stress history and the material properties of the specimen then a more general rule would have been formulated. The block programming results from the first test program provide further information along which this theme can be developed.

The life with a crack greater than 0.005 inches in depth was estimated for a number of specimens on the basis of extrapolating crack propagation data. This crack length corresponds to the changeover from Stage A to Stage B and Fig. 7.20 shows this estimated data as a life in Stage A v. life to failure plot. Again the same straight line plot is obtained but the most interesting feature is the slope of plot which is in fact 42.3 degrees. This compares to a slope of 42.0 degrees for the triangular modulation tests. The similarity between the two slopes is easily explained when considering the significance of the slope of the

plot in cumulative damage observations. A slope close to 45 degrees is an expression of the fact that the macro-crack propagation phase has become a quasi-stationary quantity where all the stress levels present are sufficiently well mixed to produce a damage rate which is equivalent to all stress cycles being equally damaging. Only stresses down to $0.6\sigma_f$ have been examined and in the block programming tests all stress levels were above this value, and it has been shown in Chapter 5 Section iii that these stress levels in blocks of 10,000 cycles do produce relatively high damage rates. If lower stresses in relation to the fatigue limit proved to be non-damaging and these were present in the stress history then this would alter the slope as the length of the macro-crack propagation phase in terms of the total number of cycles would be extended. The intercept will obviously depend on the number of non-damaging cycles during Stage A, the life at the highest damaging stress level in the stress history and the behavioural patterns during Stage A. Further information is required on the response to loads below $0.6\sigma_f$ and also on a greater variety of stress spectra.

FIG. 7.1.

PLOT OF CUMULATIVE FORSTER READING V CYCLES FOR BLOCK LOADING BENDING SPECIMEN.

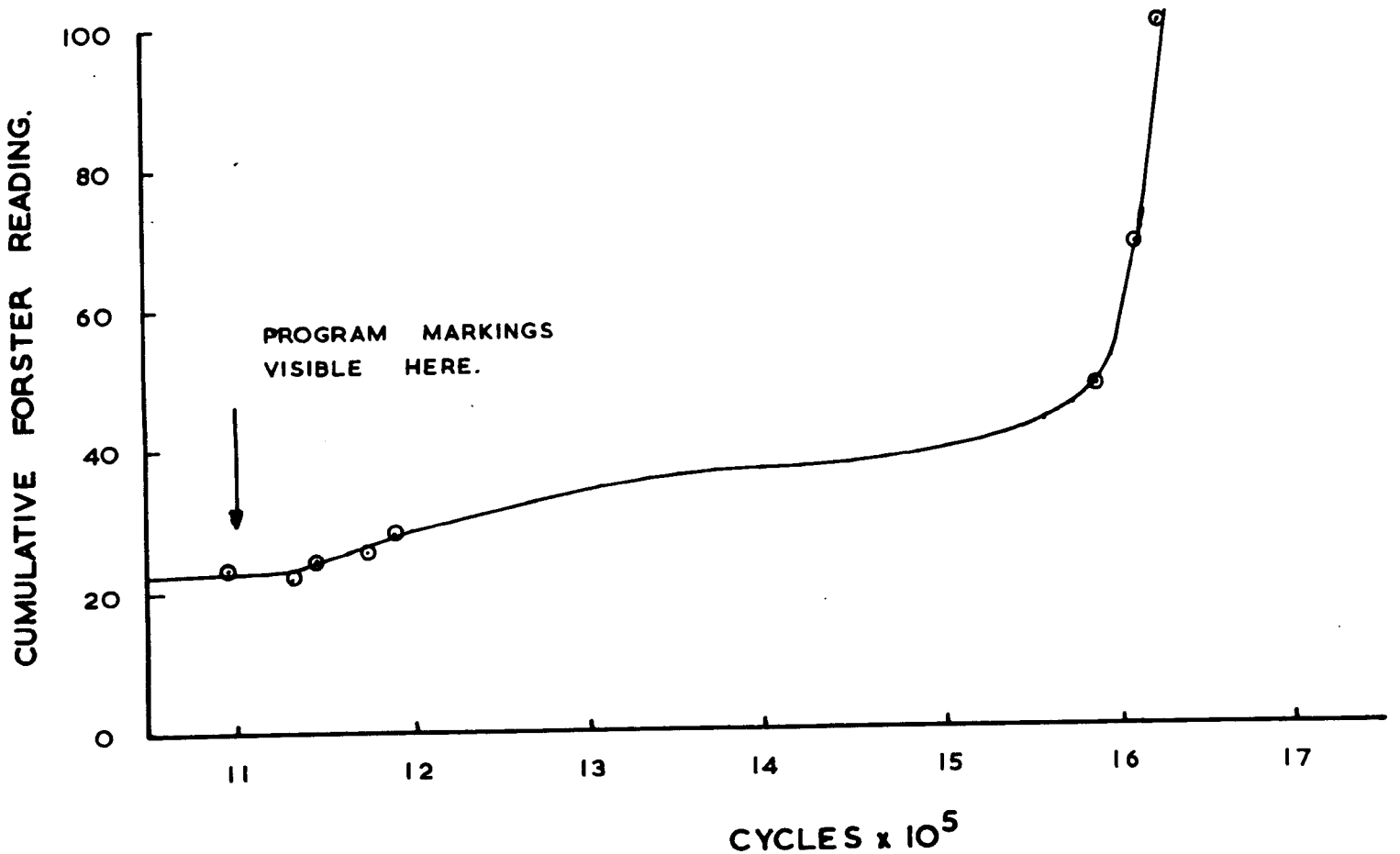

FIG. 7.2

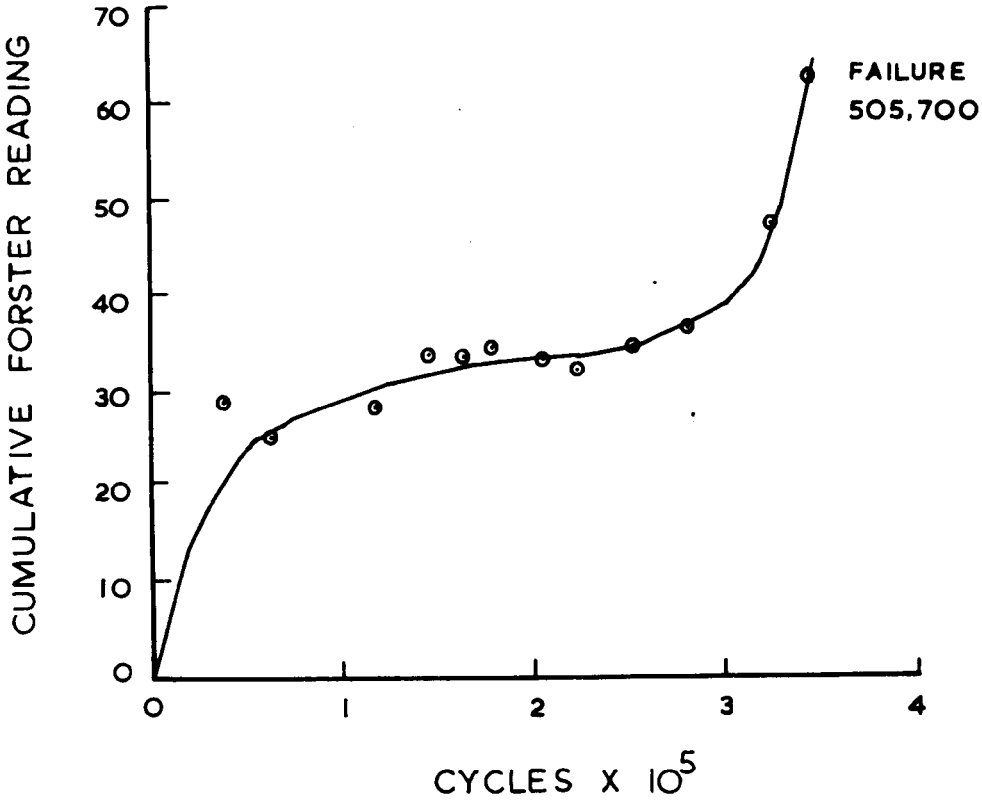

FIG. 7.3 PLOT OF CUMULATIVE FORSTER READING V CYCLES FOR LARGE BENDING SPECIMEN

LIFE IN STAGE A CYCLES	LIFE IN STAGE B CYCLES	TOTAL LIFE TO FAILURE
180,000	184,300	364,300
300,000	205,700	505,700
450,000	215,900	665,900
680,000	417,100	1,097,100
800,000	356,800	1,156,800

TABLE 7—1 LARGE BENDING DATA

PLOT OF LIFE IN STAGE A V LIFE TO FAILURE FOR LARGE BENDING SPECIMENS.

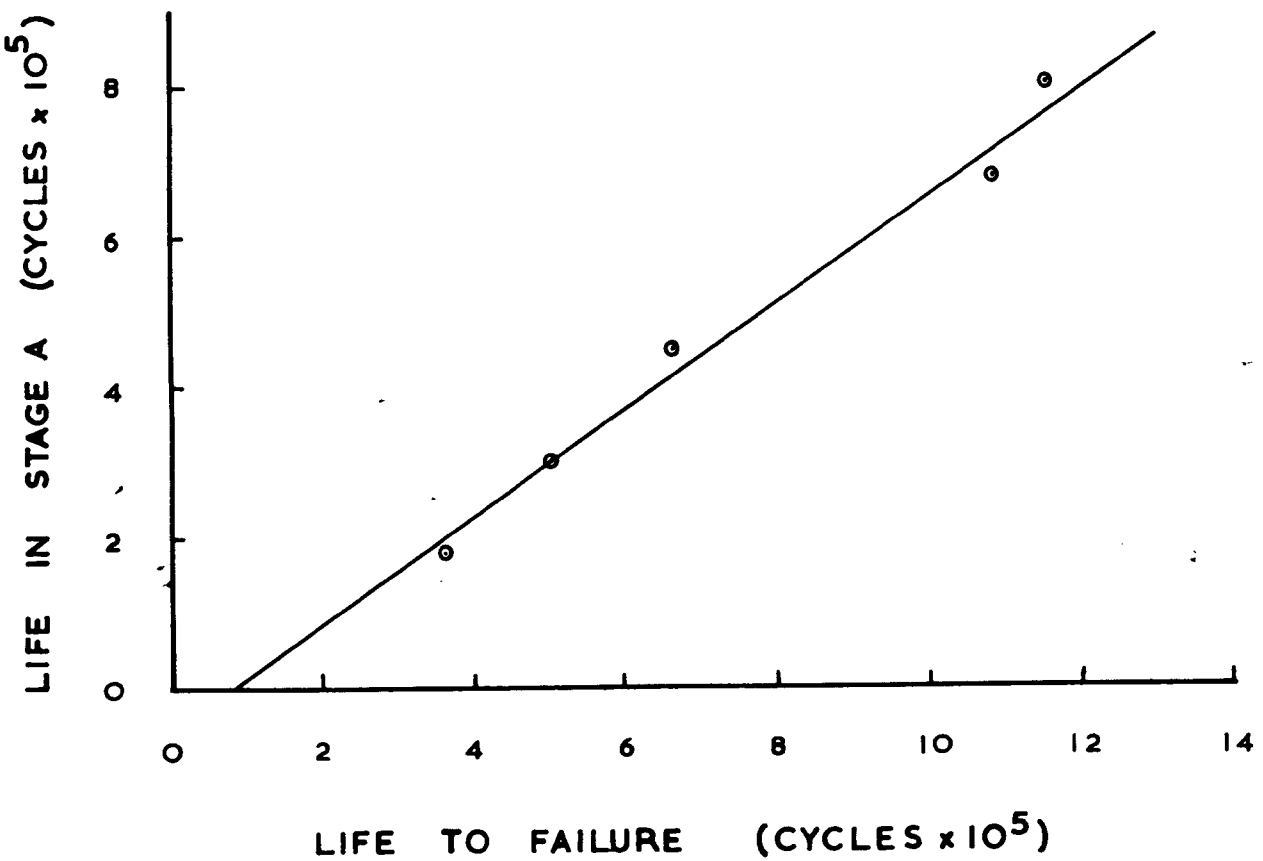

FIG. 7.4

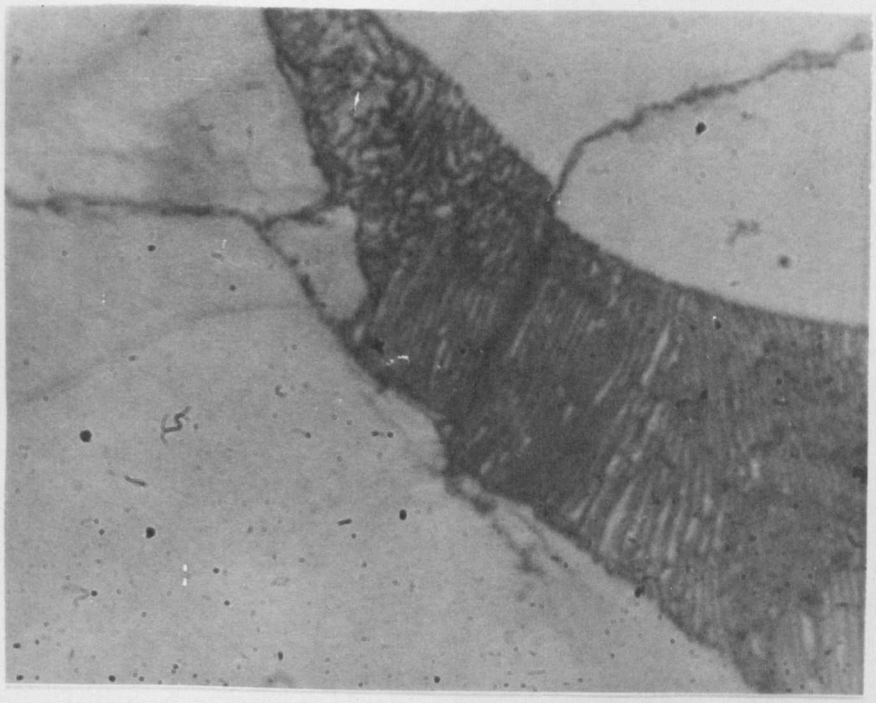

FIG. 7.5.

→ DIRECTION OF CRACK GROWTH

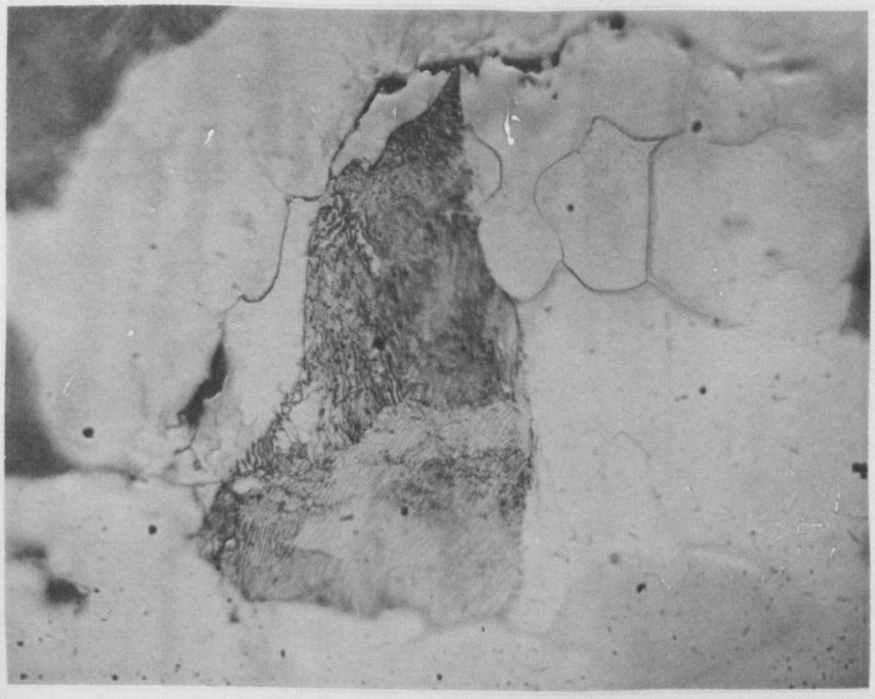

MAG. X 900

FIG. 7.6.

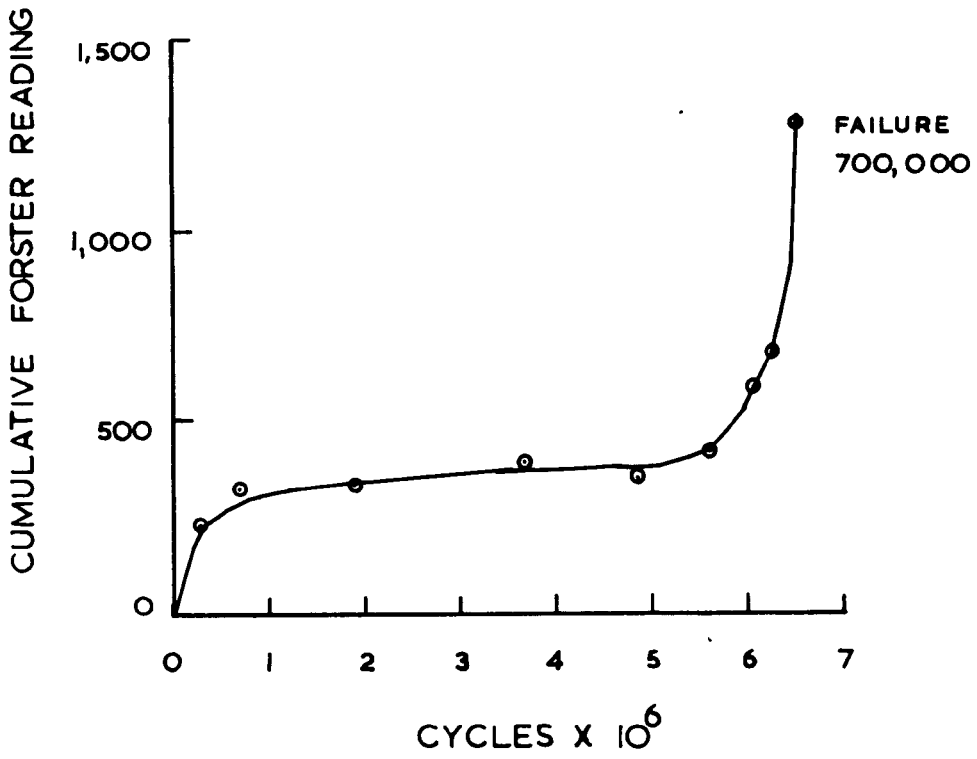

FIG. 7.7 PLOT OF CUMULATIVE FORSTER READINGS V CYCLES FOR AXIAL SPECIMEN

	LIFE IN STAGE A CYCLES	LIFE IN STAGE B CYCLES	LIFE TO FAILURE CYCLES
	600,000	381, 700	981, 700
	508,100	294,400	802, 500
	500,000	200,000	700,000
	360,000	322,000	682,000
	350,000	210,000	560,000
	130,000	180,000	310,000
VARIATION	470,000	201,700	671,700

TABLE 7-2 DATA FOR CONSTANT AMPLITUDE AXIAL TESTS

PLOT OF LIFE IN STAGE A V LIFE TO FAILURE FOR AXIAL SPECIMENS.

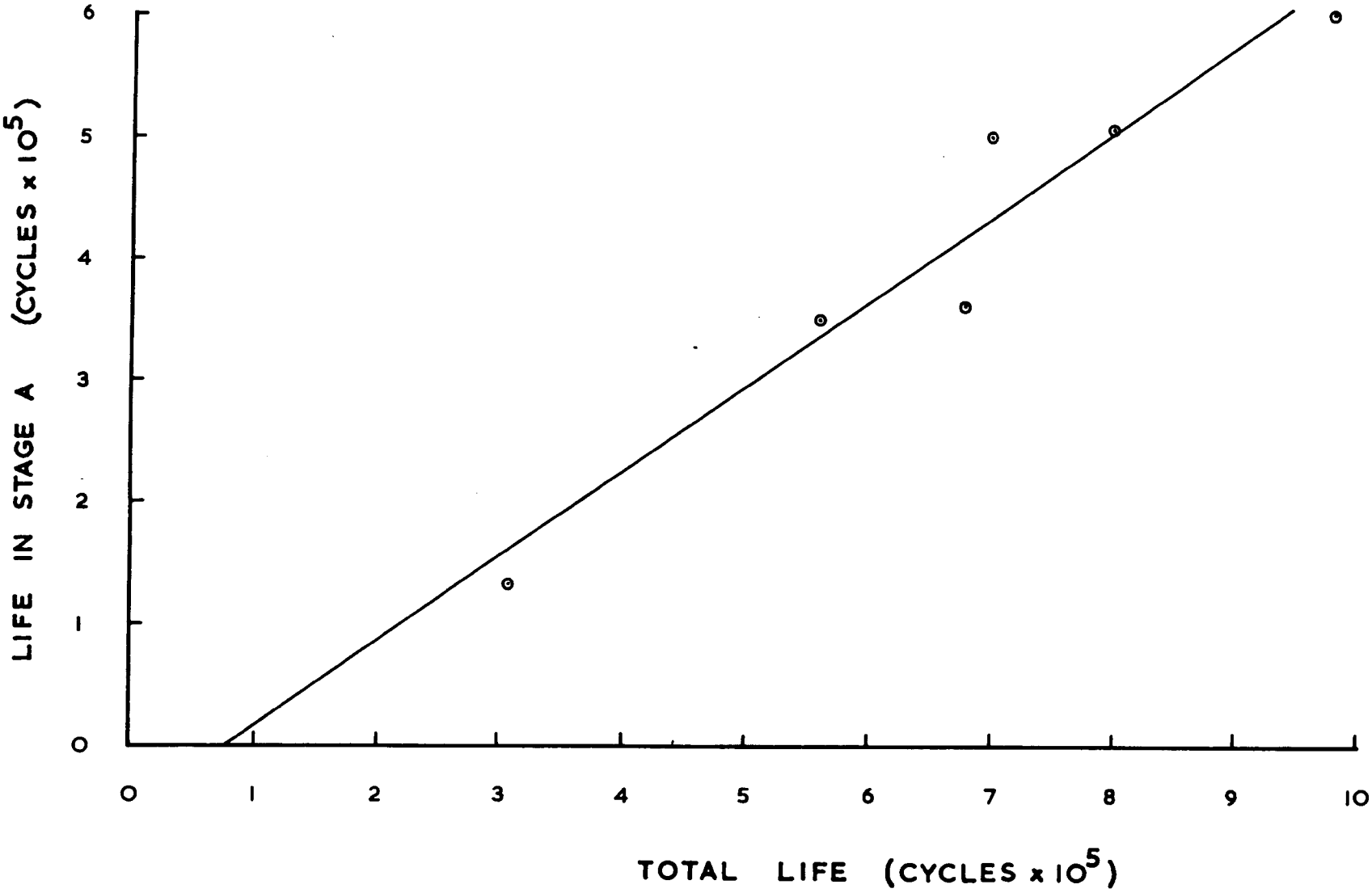

FIG. 7.8

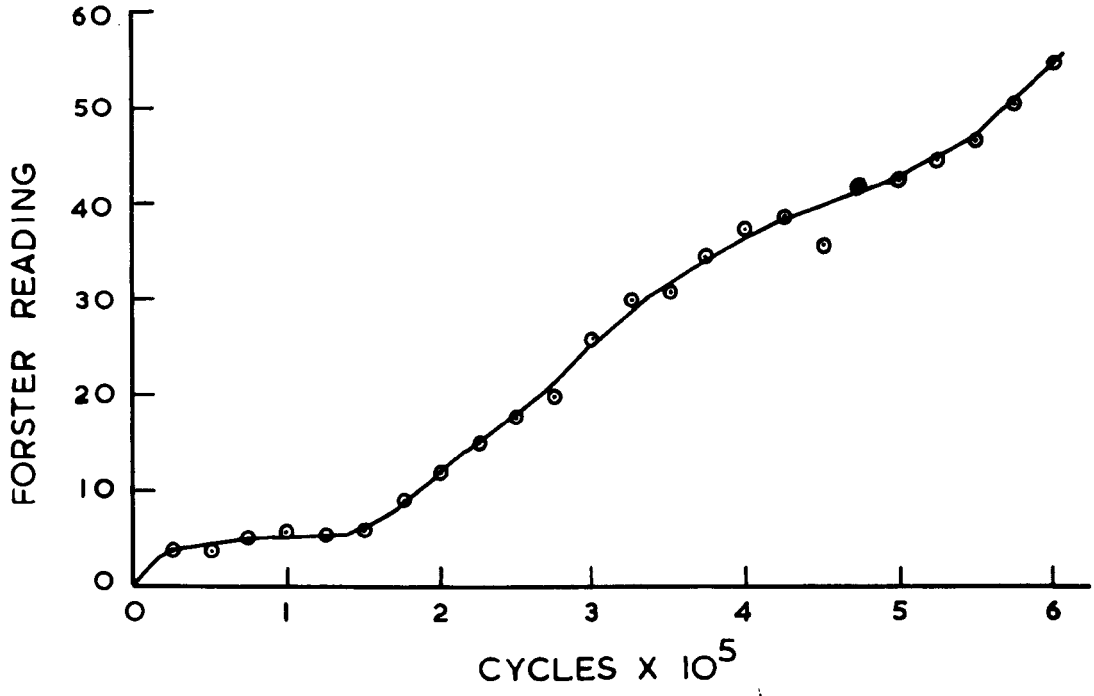

FIG 7.9. PLOT OF FORSTER READING V. CYCLES FOR SMALL PLANE BENDING SPECIMEN

LIFE IN STAGE A (MINUTES)	LIFE IN STAGE B (MINUTES)	LIFE TO FAILURE (MINUTES)
5	15	20
5	20	25
15	45	60
15	55	70
19	51	70
15	63	78
12	68	80
13	95	108
22	97	119
40	100	140
40	140	180
30	189	219
25	195	220
30	224	254
80	185	265
26	246	272
65	275	340

1 MINUTE = 2,700 CYCLES

TABLE 7-3 CONSTANT AMPLITUDE TEST DATA FOR SMALL PLANE BENDING SPECIMENS

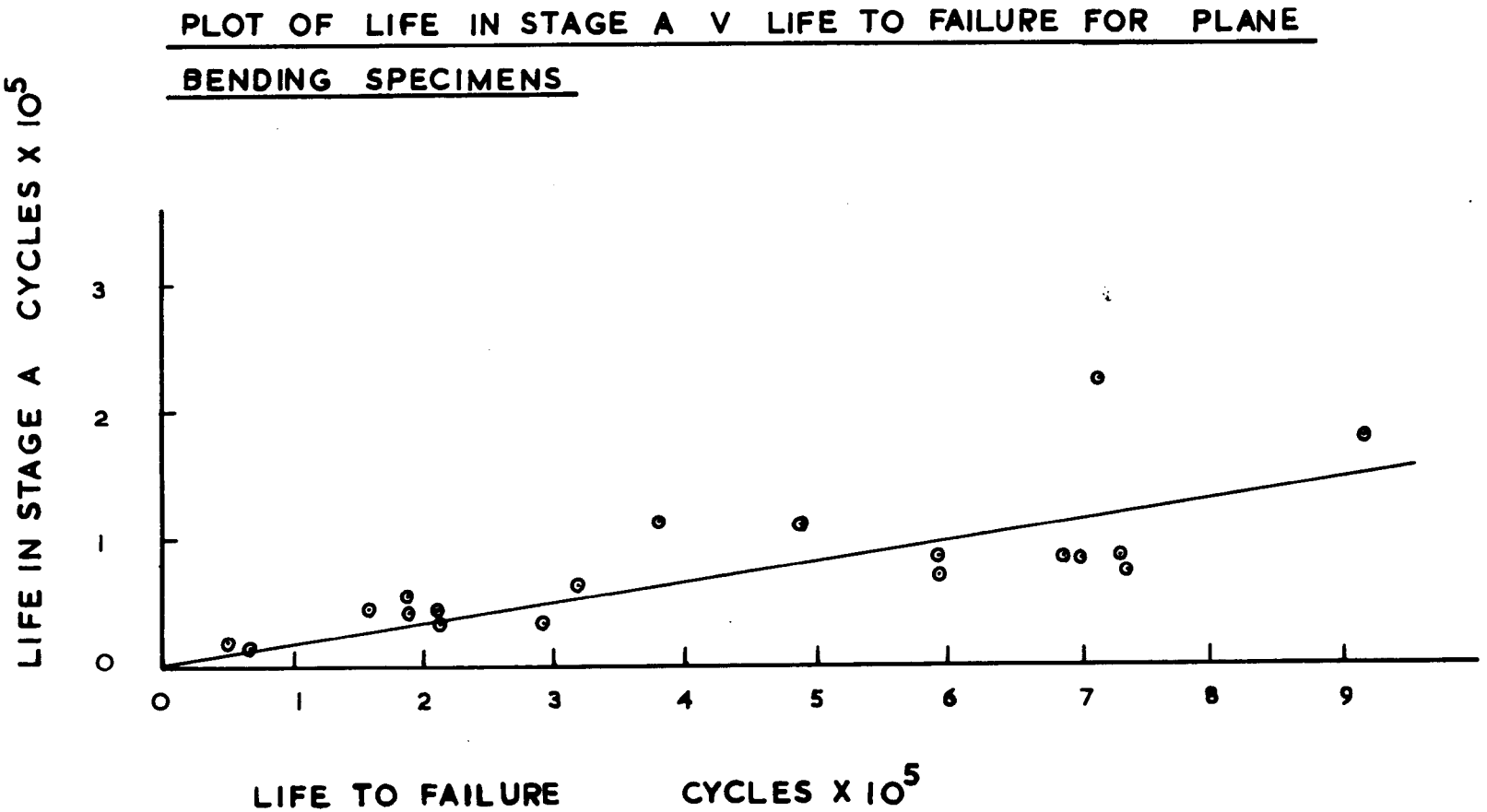
PLOT OF LIFE IN STAGE A V LIFE TO FAILURE FOR PLANE BENDING SPECIMENS
LIFE IN STAGE A CYCLES X 10^5
LIFE TO FAILURE CYCLES X 10^5
0
1
2
3
4
5
6
7
8
9

FIG. 7.10.

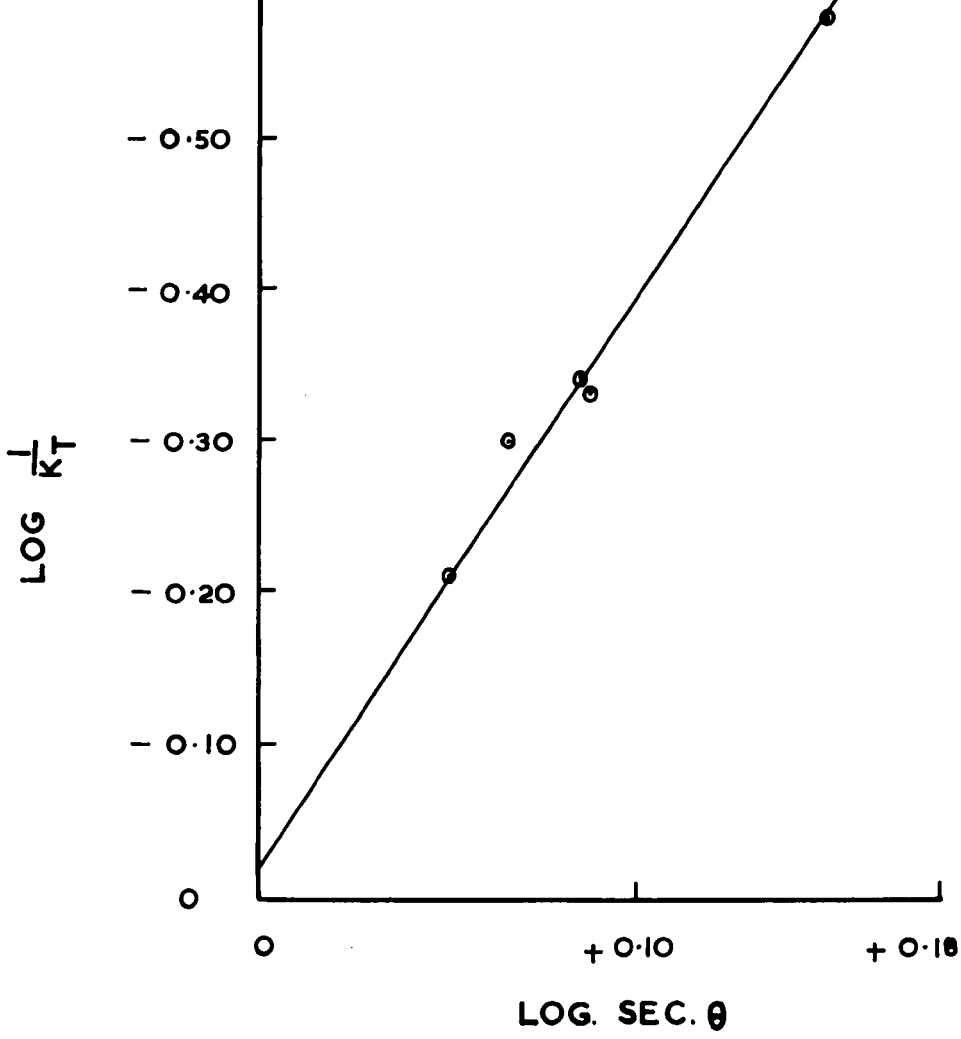

FIG. 7.11. PLOT OF LOG $\frac{1}{K_T}$ V LOG. SEC.θ FOR FIVE SPECIMEN CONFIGURATIONS.

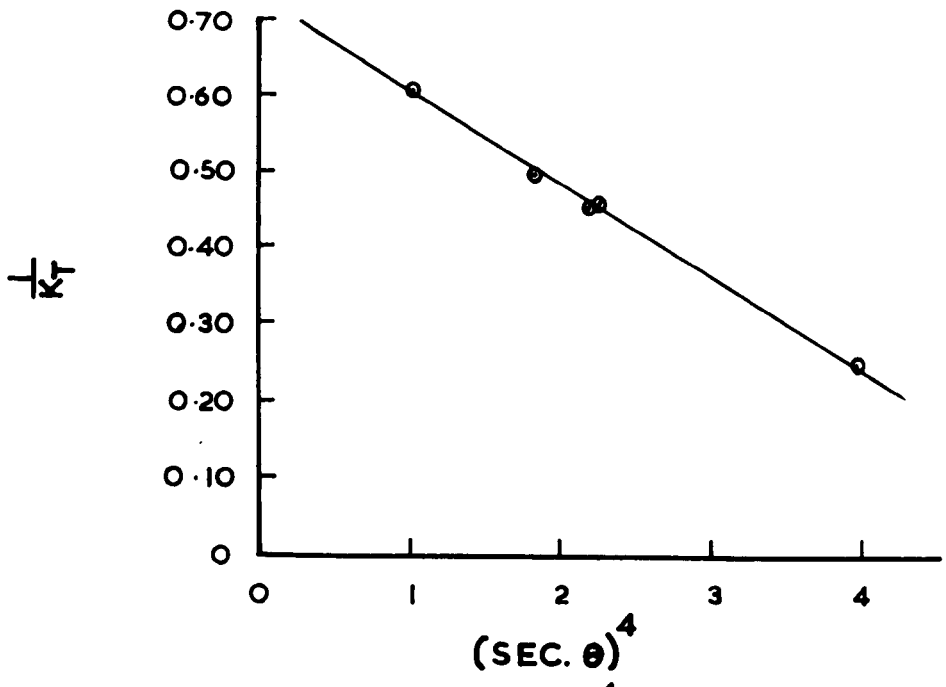

FIG. 7.12. PLOT OF $\frac{1}{K_T}$ V (SEC θ)^4

COMPARISON WITH THE TEST RESULTS OF FRALICH

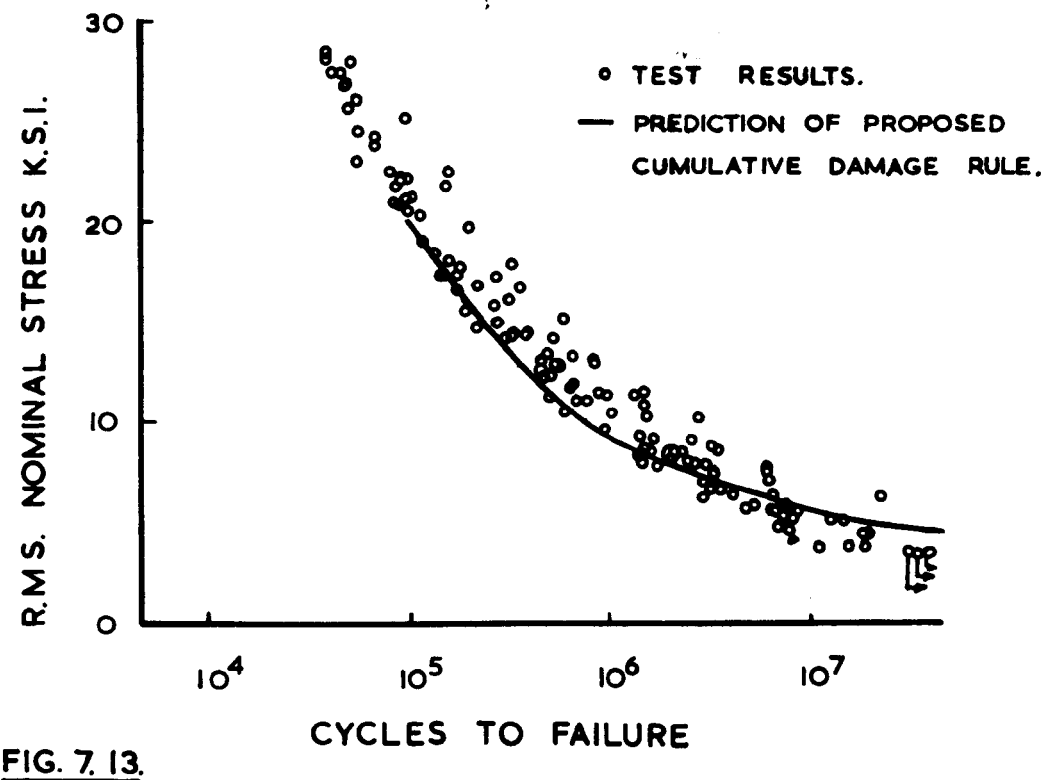

FIG. 7.13.

COMPARISON OF CUMULATIVE DAMAGE RULES TO FRALICHS TEST RESULTS

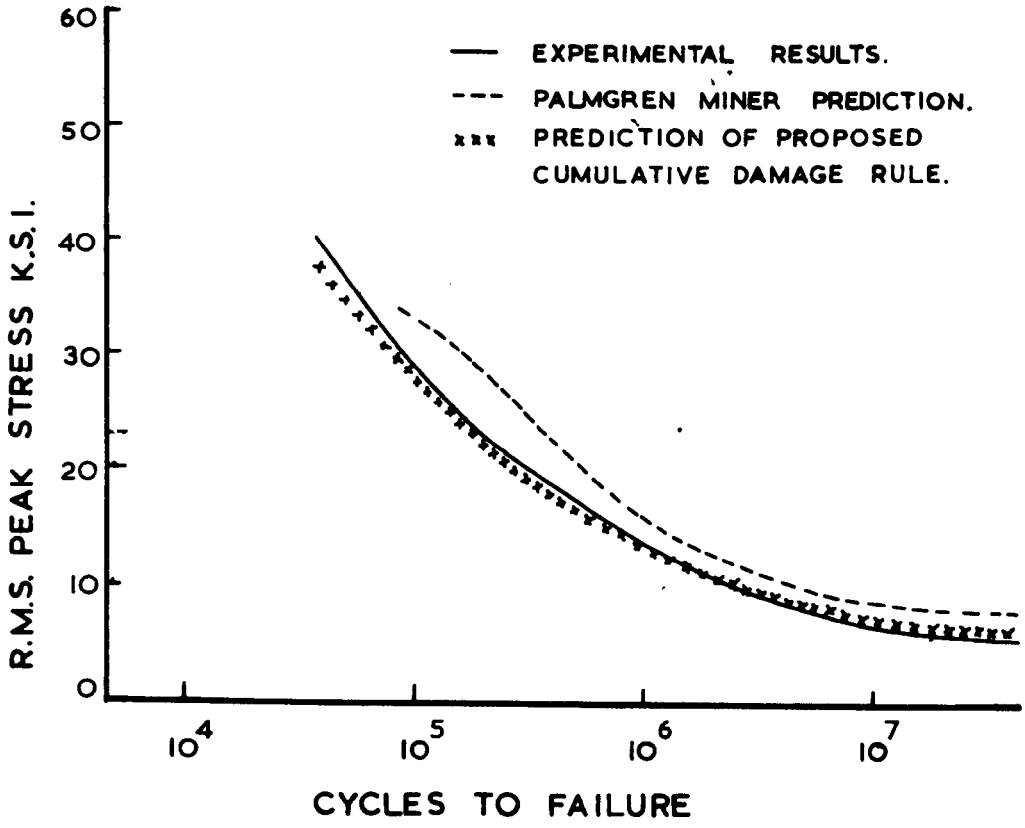

FIG. 7.14.

Stress Ratio $\sigma_h/\sigma_1 = 0.77$

σ_h Tons/ Sq. In.	σ_1 Tons/ Sq. In.	Miner Summ.	1 Endurance Cycles x 10^6	2 Predicted	Corrected predicted	Ratio 1/2
9.0	6.93	0.960	0.740	0.475	0.950	1.56
8.0	6.16	0.930	1.104	0.792	1.584	1.40
7.0	5.39	0.569	2.366	1.251	2.502	1.89
6.5	5.00	0.323	5.107	2.435	4.870	2.10
6.25	4.81	0.159	5.608	3.795	7.590	1.48
6.0	4.62	-	58.363U	U	U	

Stress Ratio $\sigma_h/\sigma_1 = 0.50$

σ_h Tons/ Sq.In.	σ_1 Tons/ Sq.In.	Miner Summ.	1 Endurance Cycles x 10^6	2 Predicted	Corrected Predicted	Ratio 1/2
10.0	5.0	0.804	0.710	0.288	0.576	2.46
9.0	4.5	0.765	1.165	0.475	0.950	2.46
8.0	4.0	0.653	1.660	0.840	1.680	1.98
7.0	3.5	0.453	4.154	1.600	3.200	2.60
6.5	3.25	0.283	8.460	3.55	7.100	2.38
6.25	3.125	0.141	10.881	6.01	12.020	1.81

TABLE 7-5

Stress Ratio $\sigma_h/\sigma_1 = 0.25$

σ_h Tons/ Sq. In.	σ_1 Tons/ Sq. In.	Miner Summ.	1 Endurance Cycles x 10^6	2 Predicted	Corrected Predicted	Ratio 1/2
11.0	2.75	0.780	0.589	0.231	0.462	2.55
10.0	2.50	0.744	1.057	0.374	0.748	2.83
9.0	2.25	0.761	1.578	0.678	1.356	2.33
8.0	2.00	0.633	3.240	1.274	2.548	2.54
8.0	2.00	0.633	3.200	1.274	2.548	2.51
7.0	1.75	0.448	6.027	2.410	4.820	2.50
7.0	1.75	0.448	6.215	2.410	4.820	2.58
6.5	1.625	0.259	9.845	5.330	10.660	1.85
6.5	1.625	0.259	19.069	5.330	10.660	3.58

Stress Ratio $\sigma_h/\sigma_1 = 0.0$

σ_h Tons/ Sq. In.	σ_1 Tons/ Sq. In.	Miner Summ.	1 Endurance Cycles x 10^6	2 Predicted	Corrected Predicted	Ratio 1/2
11.0		0.781	0.861	0.307	0.614	2.80
10.0		0.795	1.376	0.503	1.006	2.74
9.0		0.754	2.191	0.905	1.810	2.42
8.0		0.647	3.576	1.700	3.400	2.10
7.0		0.420	6.316	3.210	6.420	1.97
7.0		0.420	6.687	3.210	6.420	2.08
6.5		0.279	16.550	7.100	14.200	2.33
6.5		0.279	11.825	7.100	14.200	1.67
6.25		0.192	38.902	12.000	24.000	3.24
6.25		-	71.938U	12.000	24.000	-

TABLE 7-5

σ_h tons/sq.in.	σ_L tons/sq.in.	Endurance cycles x 10^6	Miner Summ.	Predicted Life x 10^6	Ratio Act/Pred.
19.0	17.1	0.076	1.037	0.090	0.84
18.0	16.2	0.132	0.973	0.166	0.80
17.0	15.3	0.201	0.774	0.282	0.71
16.0	14.4	0.370	0.734	0.564	0.66
15.33	13.8	0.954	1.058	0.980	0.97
14.75	13.27	2.076	0.979	1.824	1.14
14.25	12.83	1.827	0.220	3.82	0.48
14.25	12.83	2.389	0.288	3.82	0.63
13.95	12.56	5.327	0.078	7.10	0.75

Stress ratio $\alpha = 0.77$

σ_h tons/sq.in.	σ_L tons/sq.in.	Endurance cycles x 10^6	Miner Summ.	Predicted Life x 10^6	Ratio Act/Pred.
19.0	14.63	0.081	0.649	0.090	0.90
18.2	14.0	0.189	0.908	0.148	1.28
17.75	13.67	0.298	1.064	0.200	1.49
17.75	13.67	0.211	0.751	0.200	1.06
17.25	13.28	0.276	0.691	0.280	0.98
16.25	12.5	0.434	0.505	0.502	0.86
15.25	11.74	1.449	0.633	1.05	1.38
14.5	11.17	2.991	0.354	2.40	1.25
14.0	10.78	5.545	0.061	6.18	0.90
14.0	10.78	31.097U	-	6.18	

TABLE 7-6

COMPARISON OF CUMULATIVE DAMAGE RULES TO BLOCK PROGRAM TESTS SIMULATING A RAYLEIGH DISTRIBUTION.

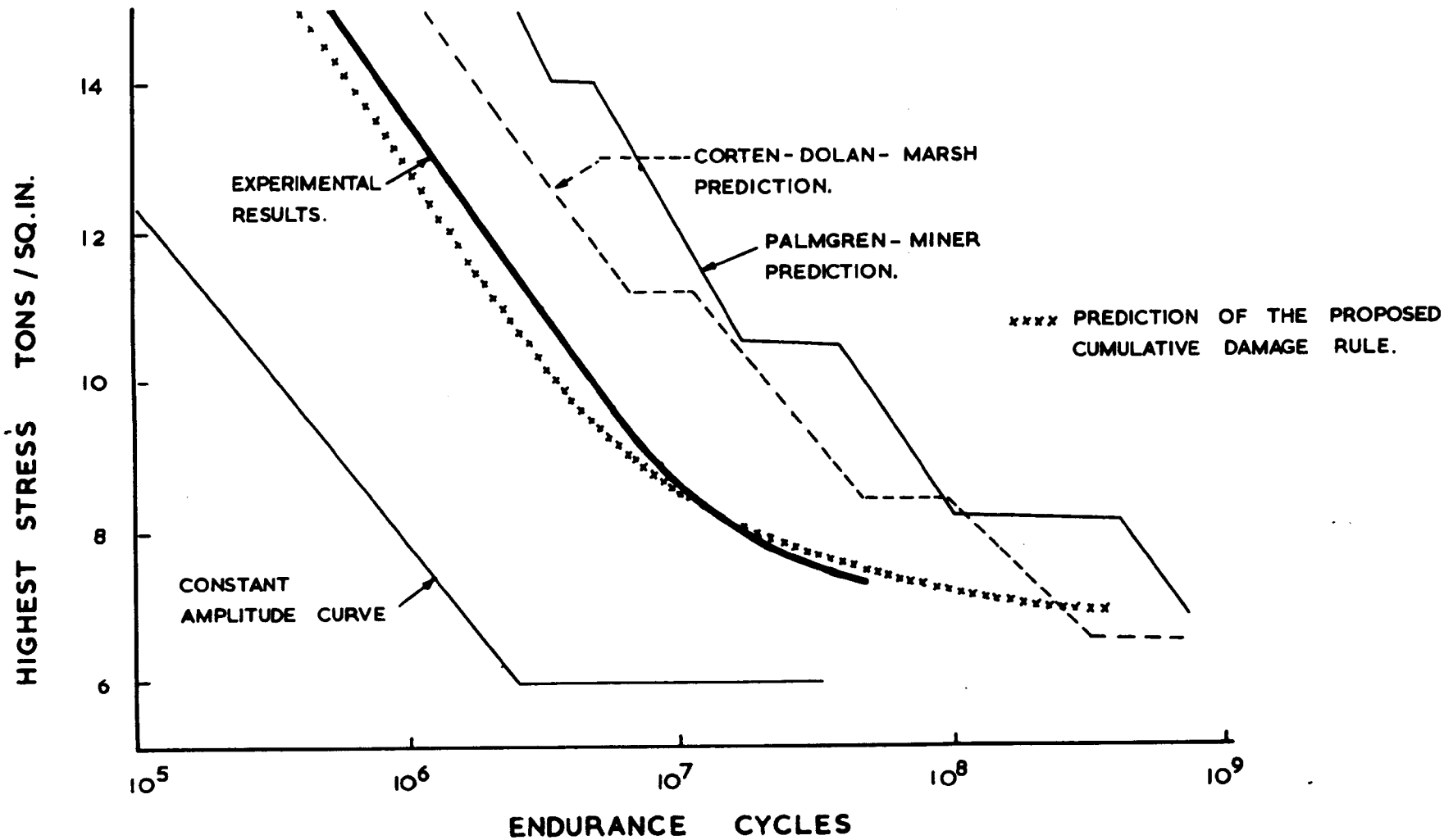

FIG. 7.15.

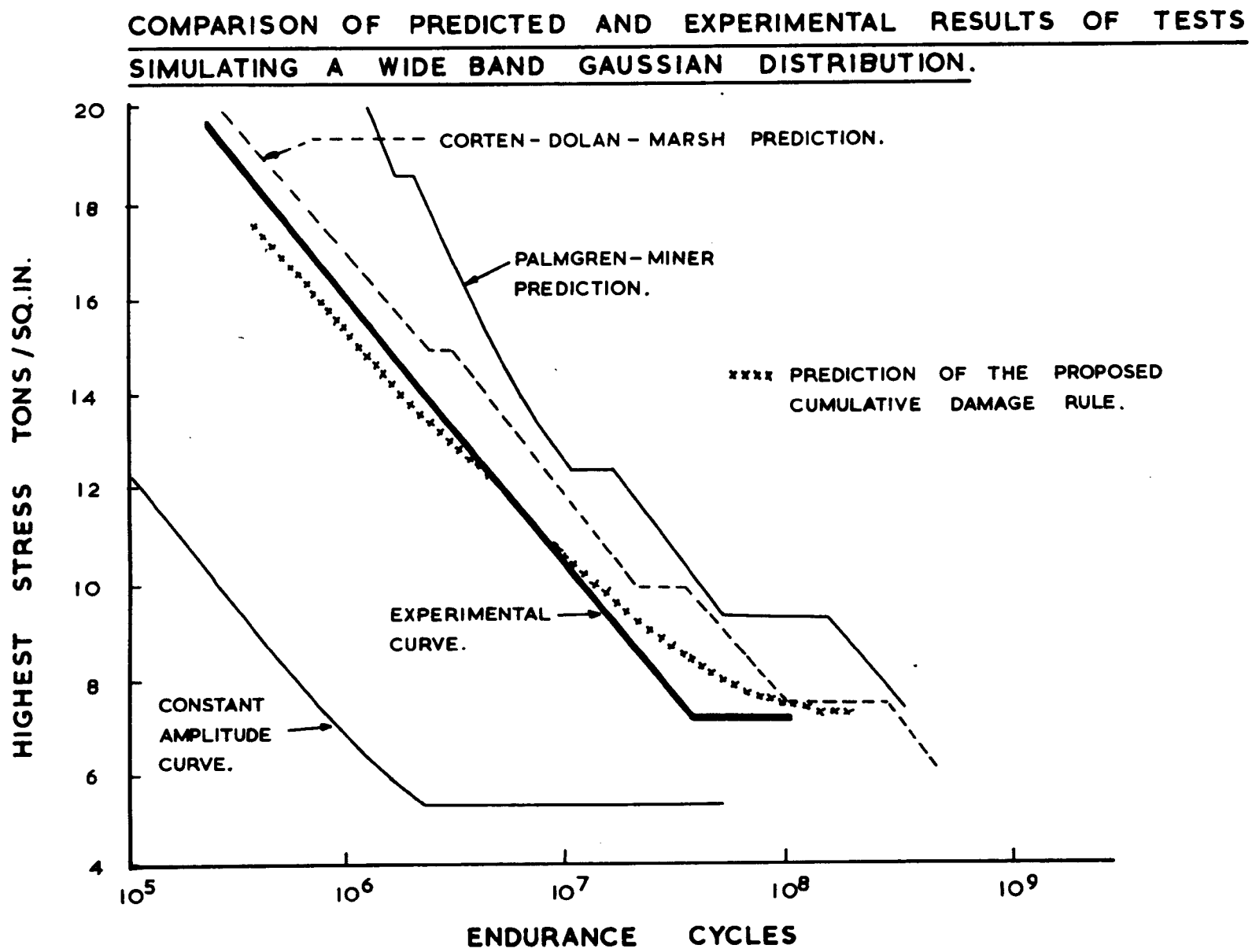
COMPARISON OF PREDICTED AND EXPERIMENTAL RESULTS OF TESTS SIMULATING A WIDE BAND GAUSSIAN DISTRIBUTION.
CORTEN - DOLAN - MARSH PREDICTION.
PALMGREN - MINER PREDICTION.
**** PREDICTION OF THE PROPOSED CUMULATIVE DAMAGE RULE.
EXPERIMENTAL CURVE.
CONSTANT AMPLITUDE CURVE.
HIGHEST STRESS TONS / SQ.IN.
20
18
16
14
12
10
8
6
4
10^5
10^6
10^7
10^8
10^9
ENDURANCE CYCLES

FIG. 7.16.

COMPARISON OF CUMULATIVE DAMAGE RULES TO THE RAYLEIGH DISTRIBUTION TEST DATA OF MARSH.

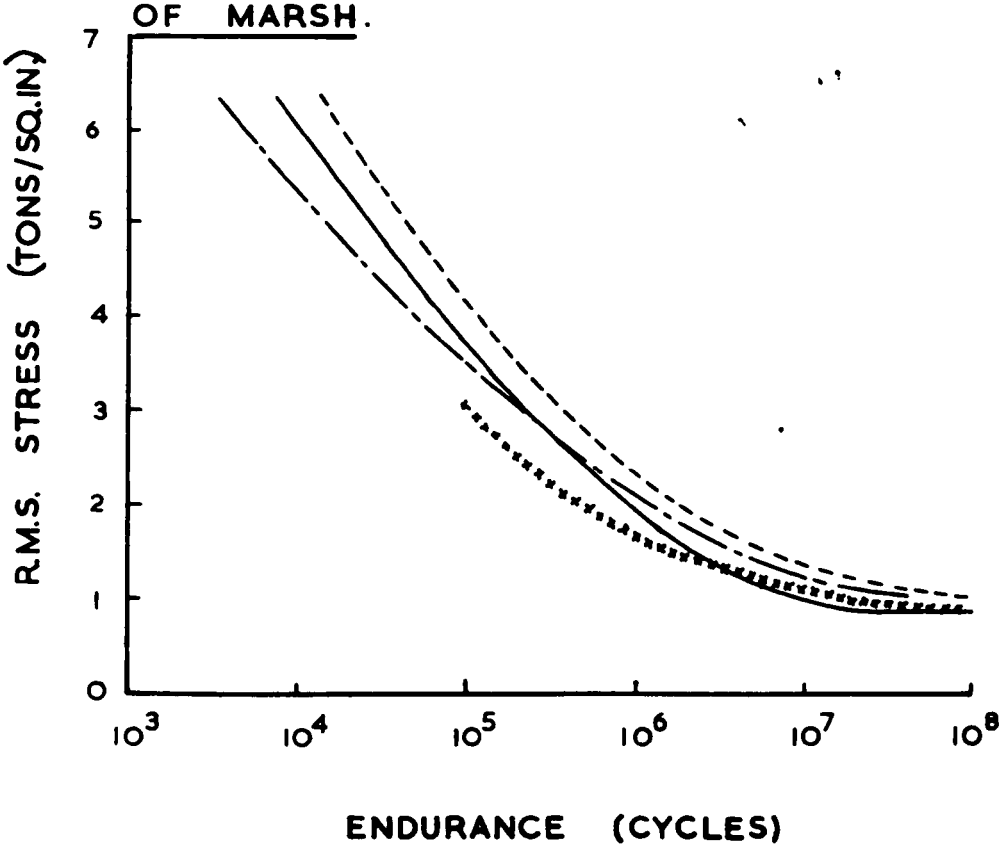

——— EXPERIMENTAL RESULTS.

- - - - - PALMGREN - MINER PREDICTION.

——·—— CORTEN - DOLAN - MARSH PREDICTION.

****** PREDICTION OF THE PROPOSED CUMULATIVE DAMAGE RULE.

FIG. 7.17.

COMPARISON OF BLOCK LOADING TESTS TO PALMGREN-MINER PREDICTION.

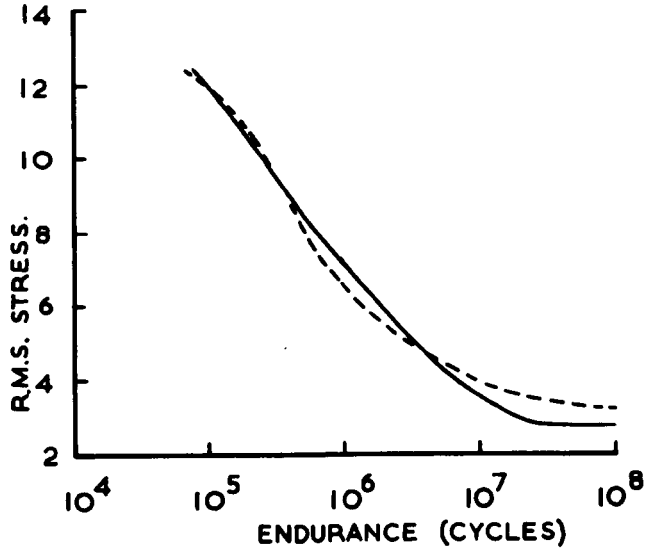

—— RAYLEIGH DISTRIBUTION BLOCK LOADING TESTS.

---- PALMGREN-MINER PREDICTION.

FIG. 7.18.

BLOCK AND RANDOM LOADING TESTS (MARSH)

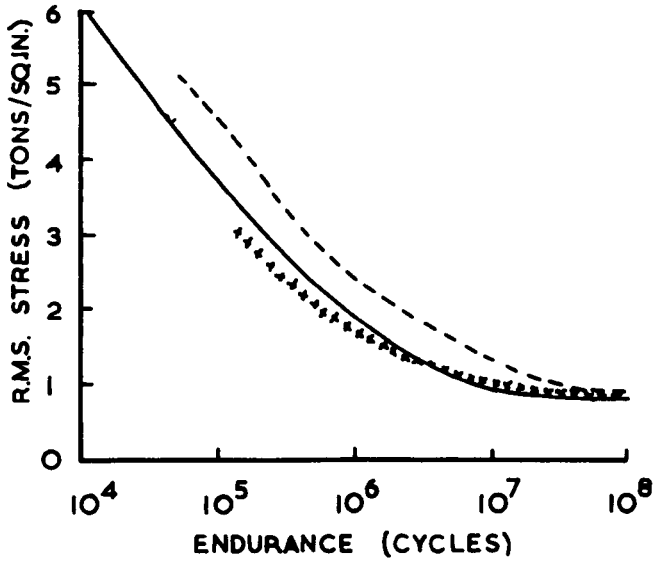

---- BLOCK LOADING TESTS.

—— RANDOM LOADING TESTS.

×××× PREDICTION OF PROPOSED CUMULATIVE DAMAGE RULE.

FIG. 7.19.

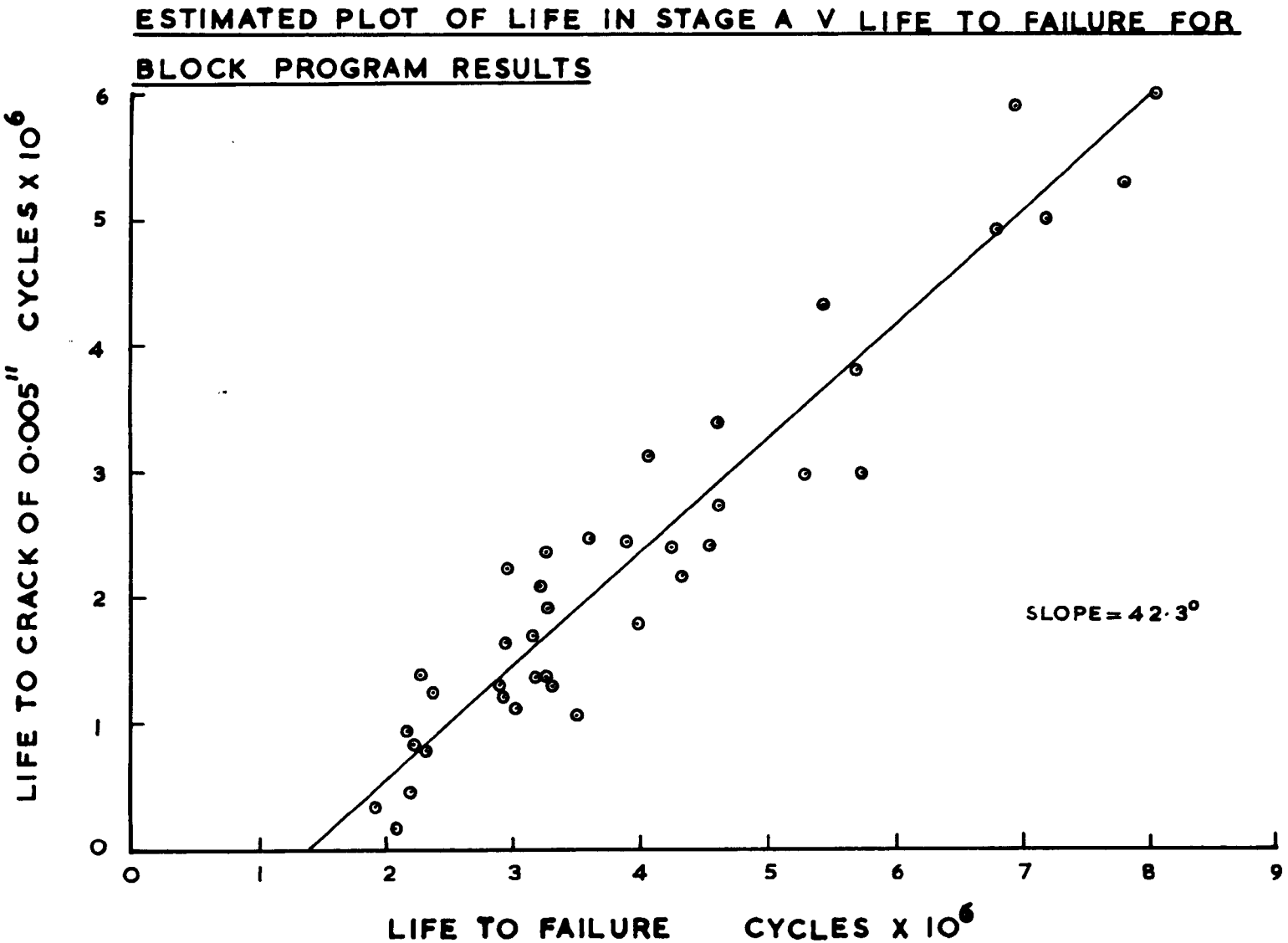
ESTIMATED PLOT OF LIFE IN STAGE A V LIFE TO FAILURE FOR BLOCK PROGRAM RESULTS
LIFE TO CRACK OF 0·005" CYCLES X 10⁶
LIFE TO FAILURE CYCLES X 10⁶
SLOPE = 42·3°
0
1
2
3
4
5
6
7
8
9

FIG. 7.20.

CHAPTER 8

The objective of the work was to try and improve cumulative fatigue damage life predictions in the region of lives greater than 5×10^5 cycles with large proportions of the stress cycles below the original constant amplitude fatigue limit. It has been stressed that inadequate provision is made in cumulative damage rules previously proposed for the damaging effect of stress levels below the original constant amplitude fatigue limit, and further it must be emphasized that past attempts to include the effects of low loads contain no indication of what the effect of low loads are in other specimen configurations. One is left to assume what modifications are required to fit other data. Miners Law of course makes no allowance for stresses below the fatigue limit or their interaction with stress above the fatigue limit, but the type of interaction theories proposed by Corten and Dolan and Freudenthal are particularly interesting when other research workers have attempted to use them as a life prediction technique.

The Corten and Dolan hypothesis involves using simple block programming data to predict the slope of the S-N curve, but the slope is used by Marsh as another convenient parameter to obtain fit to data i.e. the value given by the block programs is rejected if it does not fit the data very well. Marsh has also established that allowing for stresses down to $0.8\sigma_f$ as being damaging gives a better fit to his data and suggests that stress below this should be considered as non-damaging in mild steel specimens. The hypothesis presented here would predict that working on sharply notched specimens would lead to this conclusion. Even though Marsh has made this allowance the severity of the interaction effects has not been adequately allowed for as evidenced by the fit to data. The rule proposed provides a better basis on which to tackle life predictions

in the limited areas outlined.

The rule is based on splitting the life into two main stages, each state linked to a physical condition or its development. These two stages have been termed Stage A and Stage B and consist of initiation and micro-crack propagation in the first stage and macro-crack propagation in the second. It has been argued that Stage A is dominated by the elastic stress field due to the cracked state of the specimen, and further that as these stress fields and the fatigue behaviour associated with them are unique that a relationship should exist between the length of the two stages for a particular geometry. Such a relationship has been established for four different specimen configurations. The importance of this relationship hinges on the construction of the cumulative damage rule proposed.

It was postulated that cumulative fatigue damage behaviour would be different in Stage A and Stage B. This fact has been established in tests with triangular modulation of applied load and certain quantitative information which was statistically viable was obtained from these tests. It was found that the best fit to data was obtained by considering all stress cycles equally damaging in Stage A down to a stress level of $0.7 \times \sigma_f$ the constant amplitude fatigue limit, the same style of behaviour was evident in Stage B but with no non-damaging limit apparent down to the lowest level examined which was $0.57\ \sigma_f$. The cumulative damage behaviour was characterized by the constant amplitude behaviour at the highest damaging stress level occurring in the spectrum. The critical feature was the length of Stages A and B at this stress level but in a constant amplitude test. Once this number of damaging cycles have been accumulated then that particular stage is complete.

Thus the information required to manipulate the rule is simply a

constant-amplitude S-N curve and a knowledge of how the life is split between Stage A and Stage B. In order to eliminate lengthy testing with crack detection work an empirical relationship between the K_T value of the notch and the slope of the life in Stage A v. Total life to failure plot has been developed. The value of the intercept on this plot appears also to be closely connected with the K_T value of the notch but neglecting the intercept only incurs small penalties in life predictions greater than 5×10^5 cycles when the desirable accuracy of design rules is considered. This dependance of the slope of the life in Stage A v. Total life to failure plot on the K_T value of the notch means that specimens with different notch sharpness on the same nett test section are expected to behave in a different manner in cumulative damage. If we consider achieving the same total life then due to the difference of the ratio of Stage A/Stage B in constant amplitude tests the allowable surface stresses at the notch root may well be significantly different. The difference in behaviour of specimens with different notches is explained on two counts, firstly by the difference exhibited in the S-N curve and secondly by the different lengths spent in Stage A and Stage B at the same total lives. The more sharply notched specimens will always exhibit a lower sensitivity to loads below the constant amplitude fatigue limit, as they spend a higher proportion of their life in Stage A behaviour in the long life region.

The definition of the highest damaging stress level is critical when applying the rule to block programming tests or to complex stress spectra with isolated occurrences of highest stress levels. It is unrealistic in cumulative damage terms to assume that the highest stress level experienced is the top damaging level in the cumulative damage rule. As previously quoted small numbers of high stress levels have been shown to be beneficial and it was postulated that the top damaging stress level should be

considered as that level which is equalled or exceeded by 0.5% of the total number of stress cycles applied. This assumption gave very good fit to data on the two sets of complex block programming data examined. The rule was also compared to Marsh's data for sharply notched axial specimens subjected to a tensile mean load and a narrow band Rayleigh stress distribution. Although the predictions were not so good at the important low r.m.s. values as at higher r.m.s. values, they were still more accurate and safer than the Miner or Corten-Dolan-Marsh predictions. Furthermore the proposed prediction method was a great deal better than 25 level block program specifically designed to stimulate the distribution.

The fit to the results of Fralich on sharply notched bending specimens was very good but the predictions were again becoming optimistic at very low r.m.s. levels. It should be noted that the method depends critically on the value taken from the S-N curve for the life at the top damaging stress level. It is therefore recommended that for life predictions at low r.m.s. values, where the highest stress levels are only just above the fatigue limit, special care should be taken in determining the S-N curve close to the fatigue limit in order to ensure more accurate predictions. It should be noted that in all the cases examined, where a considerable proportion of the stress levels were below the constant amplitude fatigue limit, the method proposed was more accurate and safer than the Palmgren-Miner hypothesis. Further in the comparisons made on the test results of Marsh, the method was again safer and more accurate in the long life region than the Corten and Dolan hypothesis as amended by Marsh both in slope value for the S-N curve and in the lower damaging stress level.

The extension of the cumulative damage rule to cover the results of Marsh is based on 3 factors:-

(a) The slope of the life in Stage A v. life to failure plot.

(b) The treatment of the difference in curred by stress relieving.

(c) The behavioural patterns in Stages A and B.

The factors (a) and (b) have already been dealt with in previous chapters but further evidence is available to support the assumption that behavioural patterns in Stages A and B are the same for similar net test section sizes. It has been observed in Chapter 5 that the effect of blocks of load below the fatigue limit during Stage A is negligible i.e. the cycles must be well mixed before their damaging effect is significant. Evidence of this style of behaviour is shown in the results of Marsh's two level block programming tests in an Amsler vibrophore. Details of the tests are as follows:-

Sharply notched axial fatigue specimens subjected to a 6 tons/sq.in. tensile mean load and two level block program with 4,000 cycles at σ_h and 16,000 cycles at σ_l.

σ_h tons/sq.in.	σ_l tons/sq.in.	Endurance cycles x 10^6	Miner Endurance
5.0	3.0	0.913	1.32
5.0	2.6	1.146	1.32
5.0	2.2	1.038	1.32
5.0	1.8	1.188	1.32

The fatigue limit is 3.0 tons/sq.in. and as can be seen the variation in total life when the lower stress level goes below the fatigue limit is negligible and certainly would yield no information statistically and yet Marsh claims the above set of data as validating the hypothesis that stress levels below $0.8\sigma_f$ may be neglected for this material. Similar evidence was presented in Chapter 7 regarding more complex block prgramming results.

The cumulative damage rule proposed might be considered very similar to those of either Grover or Freudenthal and Heller in some respects but Grover presented no rational method of determining the two stages in life or the parameters associated with them, while Freudenthal and Heller having derived a particular relationship for plain specimens conclude that the patterns of behaviour are very different for other specimen configurations. The proposed method accepts and recognizes that cumulative damage behaviour patterns in varying specimen configurations are different. A method of dealing with this problem has been proposed and some of the basic data required has been obtained. Proposals have been made which cover the entire range of K_T values. The question of size effects has been looked at and some of the alternatives examined. It now seems likely that the causes of size effects may be reduced to either more severe interaction effects or different behavioural patterns in Stages A and B i.e. a sensitivity to much lower stress levels.

It is also most important that the properties of the stress spectrum to which the specimen is subjected are approached in a rational manner and, there seems no hope that merely specifying the overall content of the spectrum and not the general pattern in which it is applied is a satisfactory approach. It has been effectively demonstrated by the work presented and by consideration of the work of other authors that the manner in which the loads are applied is of extreme importance. Even more important is the hypothesis that the same pattern of loading will produce an overall response which is quite different for differing geometries. The problem will be accentuated with materials which are mean load sensitive but the recent advances in signals analysis give hope that parameters which have fatigue significance will become available in the future.

The universal elixir cumulative damage rule which was sought for a long time will probably never materialize, but it is possible by rationalising the great mass of detailed information which exists in the whole

spectrum of associated fields of activity to make progress in certain areas.

CONCLUSIONS

(1) The proposed cumulative damage rule gives more accurate and safer life predictions than some existing rules over a wide range of data. The applied stress spectra must be such as to produce severe interaction effects and so far the rule has been compared to complex block loading data (short block lengths essential), triangular modulation data and narrow band Rayleigh distribution test data. The fit over this range of stress spectra was encouraging. Block programs in which individual blocks of one stress level are very long, i.e. greater than 2,000 cycles cannot be dealt with by this rule. The rule is as yet confined to small test section sizes less than approximately 0.8 inches and greater than 0.20 inches.

(2) The geometry of a specimen will effectively dominate its response to any given stress spectra in cumulative fatigue damage behaviour.

(3) When assessing the performance of a particular specimen the stress spectra and geometry of the specimen cannot be regarded as separate entities, they must be considered in conjuntion with one another, the response being unique for that particular combination of stress spectra and geometry.

SUGGESTIONS FOR FURTHER RESEARCH

It is possible to suggest research projects or aspects worthy of investigation almost ad infinitum but the suggestions are limited to cover four main aspects which have not as yet yielded some sort of solution or which have arisen from this project. Needless to say the whole concept requires further and more detailed examination and comparison with other

results.

(1) The balance between initiation and micro-crack propagation during Stage A required detailed experimental study for varying notch geometries.

(2) The nature of size effects needs to be firmly established, certain possibilities have already been eliminated and a carefully planned experimental cumulative damage program is required to finalise a solution.

(3) A wide variety of stress spectra should be examined to establish the bounds of the method proposed and any necessary modifications to deal with more complex stress spectra.

(4) Stress field conditions should be rigorously investigated in notched details with small cracks with a view to extending the method to more complex structural components.

REFERENCES

1945

MINER, M. A. "Cumulative Damage in Fatigue" Journal of Applied Mechanics. Vol. 12. No. 1.

1956

CORTON, H. T. AND DOLAN, "Cumulative Fatigue Damage" International Conference on Fatigue of Metals.

FROST, N. E. AND PHILLIPS, C. E. "Studies in the Formation and Propagation of Cracks in Fatigue Specimens" International Conference on Fatigue of Metals. 1956.

1958

FROST, N. E. AND DUGDALE "The Propagation of Fatigue Cracks in Sheet Specimens" Journal of the Mech. and Phys. of Solids. 1958 Vol. 6.

1959

FREUDENTHAL, A. M. AND HELLER, R. H. "Stress Interaction in Fatigue and a Cumulative Damage Rule" Journal of Aerospace Science. Vol. 26 No. 7. July 1959

LIU, H. T. AND CORTEN, H.T. "Fatigue Damage During Complex Stress Histories" N. A. S. A. T. N. D-256 November 1959

1960

GROVER, H. J. "An Observation Concerning the Cycle Ratio in Cumulative Damage"
Symposium on Fatigue of Aircraft Structures.
A.S.T.M. S. T. P. No. 274.

LIU, H. T. AND CORTEN, H. T. "Fatigue Damage Under Varying Stress Amplitudes"
N. A. S. A. T. N. D-647 November 1960.

1961

FRALICH, R. W. "Experimental Investigation of Effects of Random Loading on the Fatigue Life of Notched Cantilever-Beam Specimens of S. A. E. 4130 Normalised Steel"
N. A. S. A. T. N. D-663

FROST, N. E. "Significance of Non-Propagating Cracks in the Interpretation of Notched Fatigue Data"
Journal of Mechanical Engineering Science. Vol.3. No.4

1962

FROST, N. E. "Effect of Mean Stress on Rate of Growth of Fatigue Cracks in Sheet Metals"
Journal of Mechanical Engineering Science. Vol.4. No.1.

NAUMANN, E. C. "Variable Amplitude Fatigue Tests With Particular Attention to the Effects of High and Low Loads"
N. A. S. A. D-1522

KAECHELE, L. "Review and Analysis of Cumulative Damage Theories" R. M. - 3650 - P. R.

PARIS, P. C. AND ERDOGAN, F. "A Critical Analysis of Crack Propagation Laws" Trans. A. S. M. E. December 1963

1964

HARDRATH, H. F. "Cumulative Damage" Sagmore Army Materials Research Conference.

MARSH, K. J. "Cumulative Fatigue Damage Under a Symmetrical - Sawtooth Loading Program" NEL Report No. 136.

PARIS, P. C. "The Fracture Mechanics Approach to Fatigue" Sagmore Army Materials Research Conference.

1965

MANSAN, S.S., NACHTIGALL, A. J., ENSIGN, G. R. AND FRECHE, J.C. "Further Investigation of a Relation for Cumulative Fatigue Damage in Bending" Trans. A. S. M. E. Journal of Engineering for Industry, February 1965

KANAMOTO MINORU AND KIOBUCHI KOJI "Estimation of Fatigue Lives Under Actual Loads by Hereditary Method" J. S. M. E. Vol. 8 No. 29.

1967

BROOK, R. H. W. AND PARRY, J. S. C. "An Aspect of Cumulative Damage in Fatigue" Report to Aeronautical Research Council. A. R. C. 28709 January 1967.

FORMAN, R. G., KEARNEY, V. E. AND ENGLE, R. M. "Numerical Analysis of Crack Propagation in Cyclic-Loaded Structures" Trans. A. S. M. E. Journal of Basic Engineering. September 1967.

MARSH, K. J. AND MACKINNON, J. A. "Random-Loading and Block-Loading Fatigue Tests on Sharply Notched Mild Steel Specimens" Journal of Mechanical Engineering Science. Vol.10 No.1.

1968

LEE, B. S. "Fatigue Crack Propagation in Mild Steel" Ph. D. Thesis. October 1968. University of Nottingham

MARSH, K. J. "Further Varying Amplitude Fatigue Tests on Sharply Notched Mild Steel Specimens" N. E. L. Report. No. 373.

A

FREUDENTHAL, A. M. AND HELLER, R. A. "Accumulation of Fatigue Damage" Dept. of Civil Engineering and Eng. Mechanics. Columbia University, New York.

This appendix is a more detailed account of the work performed by Puckridge together with an appraisal of the cracked stated of the specimen during what were originally termed stages 1 and 1A.

Temperature effects have been discussed in Chapter 5 and this program of work was closely allied to these effects. The objective was to investigate the possibility that the sharp initial rise in Forster response was indicative of fast initial cracking of < 0.005 inches, the long stationary or slowly rising portion of the Forster response denoting a pause in crack growth. Also a general picture of the cracked state of the specimen during this period of life was required.

The great problem with rotating bending specimens is that when observations of crack depth are required the specimen must be sectioned with the consequent loss of important information. This is particularly awkward in this case because it is never possible to determine relatively which point in its life the specimen has obtained. The only approach is to section a number of specimens which have shown varying lengths of quasi-stationary behaviour and attempt to rationalise this information into an overall pattern of behaviour. Puckridge was also hampered by the necessity of using specimens from the third batch which had a high carbon content (0.33%). The high pearlite content of this steel made detection and observation of small cracks extremely difficult using standard optical techniques. It also proved extremely difficult to eliminate rounding of the edge of the notch profile during polishing operations, the eventual technique developed to eliminate most of the rounding was described in Chapter 5.

In these test the Forster was being used at the limits of its sensitivity, the manufacturers claim a capacity for detection of flaws of 0.002 inches depth and greater. Subsequent tests in the department by Mr. Chatterjee, using rigorous temperature correction techniques, have shown

that at maximum sensitivity reliable detection of cracks of 0.001 inches depth can be achieved. As stated previously what was required from this work was qualitative information on the cracked state of the specimen not an account calibration of the Forster in this region.

Some ambiguity existed about differentiating between grain boundaries and cracking in several of the specimens examined but the general conclusions are based solely on those results whose evidence of cracking was firmly established. Puckridges photographs are of poor quality and therefore they are not reproduced here. There was no evidence to suggest that the rapid initial rise in Forster response was connected with actual cracking, the overall pattern of the results was that this phase of the life (Stages A and 1A) represented an initiation and micro-crack propagation period with most of the period spent in attaining a discontinuity of 1 grain length. These conclusions are supported by the results of first tests performed on the Forster for calibration purposes, the very low readings were generally in Stage A and in several cases cracks of up to 0.006 inches were detected. The photographs shown in Fig. 5.24 and 5.25 support these arguments and confirm that the Forster sensitivity cannot be questioned. In particular Fig. 5.24 shows the mass of small defects to which a definite Forster response was noted.

Puckridge concluded that cracks of up to 0.010 inches were present at the end of Stage A i.e. when the steady and continuous crack growth became evident. Finally a very strong argument can be presented on the basis of the test performed on Spec. No. 2.4.25 (ref. Fig. 5.23). This specimen was stopped within 10,000 cycles of exhibiting the start of steady propagation, if up until this point no cracking is present than a crack of 0.008 inches has developed in 10,000 cycles or less, which would give a further life to failure of approximately 180,000 cycles, assuming a linear

and constant rate of propagation, as compared to an experimental value of 180,000, table 5-2. The crack propagation has been shown to be logarithmic and this presents strong evidence for the existance or developement of cracking in a prior period.

APPENDIX II

The objectives of the stress analysis was to gain information on the elastic stress fields during Stage A of the fatigue life i.e. when no crack was present and when small cracks were growing away from the root of the notch. This information could then be used both to attempt to correlate the behaviour of different specimen geometries and if such a correlation proved feasible to extend the results to more complex geometries which are more typical of service components.

The particular solutions considered initially were for edge notched plates, edge cracked plates, and edge notched plates with cracks growing away from the root of the notch. The cracks were simulated by very flat ellipses and specimen conditions approximated by plane strain assumptions on the plate section solution.

The elastic stress fields in any given member can be described by use of the Airey stress function ϕ . It was shown by Airey that a function can be selected such that the biharmonic equation $\nabla^4 \phi = 0$ is the solution for the elastic stress field in the plane stress condition when the stresses are given by the following equations:-

$$\sigma_{xx} = \frac{\partial^2 \phi}{\partial y^2} \qquad \sigma_{yy} = \frac{\partial^2 \phi}{\partial x^2} \qquad \tau_{xy} = -\frac{2\partial^2 \phi}{\partial x \partial y}$$

The use of this type of solution has been limited in the past by the necessity to satisfy complex boundary conditions. The advent of computers and the use of relaxation techniques has opened up a much wider range of possible solutions.

The programs written are based on the central finite difference solution to the biharmonic equation. The equations required and extrapolation and interpolation techniques based on Taylors series are all treated in many standard texts. The treatment of boundary conditions is also standard and it is not proposed to discuss these points in detail here.

As the objective of the programs was to deal with as many different geometries as possible they are written in a general form and a brief description of overall program construction is given. The programs were split into main sections as follows:-

(1) Setting up data.

(2) Calculation of all points concerned with boundary conditions around the complex geometry, their location, intercept values, boundary values and type of extrapolation involved.

(3) Calculation of boundary interpolation and extrapolation constants for all the points in (2).

(4) Calculation of the ϕ values at all points in (2) and setting them, relaxation of the mesh and maintenance of all points concerned with boundary conditions at the correct value during the relaxation process.

(5) Calculation of stresses and print out.

(6) Reduction in mesh size, i.e. calculating and setting up the basic data required for all the above processes from (2) onwards to be repeated at increased accuracy.

Whole sub-blocks can be replaced so that for example the change from axial to bending can be made by changing the card deck (1). Similarly different geometries can be investigated by changing card deck (2) or changing up to 12 cards within the deck.

Geometry properties can be specified in the data input, depth of notch, radius, type of ellipse and depth of crack.

All the progams have been run and proved within limited accuracy limits but the general nature of the programs make large demands on the store capacity and therefore for final testing and actual information runs either a larger store capacity is required or data has to be written up on magnetic tape and then subsequently pulled down and re-calculated. The run times would increase by several factors and as the upgrading of the University computer was imminent the programs await the use of the faster and larger computer.

Specimen results from the edge crack program with axial loading are presented in Fig.II.1. As can be seen the ears of high stress are predicted and although the concentration of the stress at the crack tip is not very high it has been shown on other runs that increased accuracy i.e. small mesh size only significantly modifies the values within 2 mesh points of the tip and not the surrounding gross field. The qualitative results of the program has so far been satisfactory and reliable quantitative information should be available in the near future.

```
STRESS FIELDS AROUND CRACKS;
"BEGIN"
        "INTEGER" K,N,DEPTH,X,Y,RED,REP,AR,SIDE,TOP;
        "READ" K,N,DEPTH,RED;
        "BEGIN"
        "REAL" RADIUS,RATIO,NO,MESH;
        "ARRAY" Z,P,Q,R,DEL,SIGMA[1:K,1:N];
        "READ" RADIUS,RATIO;
        "PRINT"'K=',SAMELINE,K,''S2'',N=',N,''S2',
        'DEPTH=',DEPTH,''S2'','RED=',RED,''S2','RADIUS=',
        RADIUS,''S2','RATIO=',RATIO,''L5'';
        "BEGIN"
        "REAL" DIV;
        "ARRAY" A[1:N],B[1:N];
        DIV:=1/(N-4);
        A[N]:=2*DIV;
        A[N-1]:=DIV;
        A[N-2]:=0;
        "FOR" Y:=N-3 "STEP" -1 "UNTIL" 1 "DO"
        "BEGIN"
        A[Y]:=A[Y+1]+DIV;
        "END";
        "FOR" Y:=1 "STEP" 1 "UNTIL" N "DO"
        "BEGIN"
        B[Y]:=A[Y]↑2/2;
        "FOR" X:=1 "STEP" 1 "UNTIL" K "DO"
        "BEGIN"
        Z[X,Y]:=B[Y];
        "END";
        "END";
        "END";
        "FOR" X:=1 "STEP" 1 "UNTIL" K "DO"
        "BEGIN"
        "FOR" Y:=1 "STEP" 1 "UNTIL" N "DO"
        "BEGIN"
        P[X,Y]:=0;
        Q[X,Y]:=0;
        R[X,Y]:=0;
        DEL[X,Y]:=0;
```

```
        SIGMA[X,Y]:=0;
        "END";
        "END";
        NO:=0.5;
        "FOR" REP:=1 "STEP" 1 "UNTIL" RED "DO"
        "BEGIN"
        Y:=2;
        NO:=NO*2;
        MESH:=1/NO;
        AR:=DEPTH/MESH;
        "BEGIN"
        "INTEGER" IT;
        "INTEGER" "ARRAY" UP,TEST[1:50],OUT[1:50];
        "ARRAY" CON[1:50,1:8],L,BOUND[1:50];
        "FOR" X:=1 "STEP" 1 "UNTIL" 50 "DO"
        "BEGIN"
        TEST[X]:=100;
        "END";
        "BEGIN"
        "REAL" B,C,D,E,F,G,P,Q,R,S,VERT,WOC;
        "INTEGER" NUM;
        NUM:=2;
        IT:=1;
        B:=RATIO*RADIUS;
        C:=RATIO*B;
        D:=C-DEPTH;
        OUT[2]:=0;
REPEL:  D:=D+MESH;
        E:=SQRT(B↑2*(1-D↑2/C↑2));
        Y:=Y+1;
        "IF" E<(IT-1)*MESH "THEN" "GOTO" ALTERN "ELSE"
        "IF" E<MESH "THEN"
        "BEGIN"
        L[Y]:=MESH-E;
        OUT[Y]:=4;
        "END"
        "ELSE" "IF" E<2*MESH "THEN"
        "BEGIN"
        L[Y]:=2*MESH-E;
```

```
        OUT[Y]:=5;
        "END"
        "ELSE" "IF" E<3*MESH "THEN"
        "BEGIN"
        L[Y]:=3*MESH-E;
        OUT[Y]:=6;
        "END"
        "ELSE" "IF" E<4*MESH "THEN"
        "BEGIN"
        L[Y]:=4*MESH-E;
        OUT[Y]:=7;
        "END"
        "ELSE" "IF" E<5*MESH "THEN"
        "BEGIN"
        L[Y]:=5*MESH-E;
        OUT[Y]:=8;
        "END"
        "ELSE" "IF" E<6*MESH "THEN"
        "BEGIN"
        L[Y]:=6*MESH-E;
        OUT[Y]:=9;
        "END";
        IT:=ENTIER(E/MESH);
        "IF" OUT[Y]>OUT[Y-1] "THEN" SIDE:=OUT[Y];
        TOP:=Y;
        NUM:=NUM+1;
        TEST[Y]:=2;
        BOUND[Y]:=0.5-(Y-2)/((N-4)*NO);
        "PRINT"'Y=`,SAMELINE,Y,''S2``,'TEST[Y]=`,
        TEST[Y],''S2``,'OUT[Y]=`,OUT[Y],''S2``,'L[Y]=`,
        L[Y],''S2``,'BOUND[Y]=`,BOUND[Y],''L3``;
        "IF" Y<(DEPTH/MESH+1.90) "THEN" "GOTO" REPE1
        "ELSE" "GOTO" CALC;
ALTERN: Y:=Y-1;
        E:=(IT+1)*MESH;
REPE2:  Y:=Y+1;
        TEST[Y]:=0;
        E:=E-MESH;
        OUT[Y]:=E/MESH+3;
```

```
        VERT:=SQRT(C↑2*(1-E↑2/B↑2));
        WOC:=VERT-C+DEPTH;
        "IF" (WOC+(Y-2)*MESH)>-MESH "THEN"
        "BEGIN"
        UP[Y]:=Y;
        L[Y]:=(Y-2)*MESH-WOC;
        "END"
        "ELSE" "IF"(WOC+(Y-3)*MESH)>-MESH "THEN"
        "BEGIN"
        UP[Y]:=Y-1;
        L[Y]:=(Y-3)*MESH-WOC;
        "END"
        "ELSE" "IF"(WOC+(Y-4)*MESH)>-MESH "THEN"
        "BEGIN"
        UP[Y]:=Y-2;
        L[Y]:=(Y-4)*MESH-WOC;
        "END"
        "ELSE" "IF"(WOC+(Y-5)*MESH)>-MESH "THEN"
        "BEGIN"
        UP[Y]:=Y-3;
        L[Y]:=(Y-5)*MESH-WOC;
        "END"
        "ELSE" "IF"(WOC+(Y-6)*MESH)>-MESH "THEN"
        "BEGIN"
        UP[Y]:=Y-4;
        L[Y]:=(Y-6)*MESH-WOC;
        "END";
        BOUND[Y]:=0.5-(WOC-2)/((N-4)*NO);
        NUM:=NUM+1;
        "PRINT"' Y=`,SAMELINE,Y,''S2``,'TEST[Y]=`,
        TEST[Y],''S2``,'OUT[Y]=`,OUT[Y],''S2``,'L[Y]=`,L[Y],
        ''S2``,'BOUND[Y]=`,BOUND[Y],''S2``,'UP[Y]=`,
        UP[Y],''L3``;
        TOP:=UP[Y];
        "IF" E>(+0.005) "THEN" "GOTO" REPE2 "ELSE"
        "GOTO" CALC;
CALC:   "FOR" X:=3 "STEP" 1 "UNTIL" NUM "DO"
        "BEGIN"
        L[X]:=L[X]/MESH;
        B:=(2+L[X])/(1+L[X])↑2;
```

```
        C:=(1+L[X])/(2+L[X])↑2;
        D:=(3+2*L[X])/((1+L[X])*(2+L[X]));
        E:=1/(1+L[X])↑2;
        F:=1/(2+L[X])↑2;
        G:=1/((1+L[X])*(2+L[X]));
        P:=(1-L[X])↑2;
        Q:=(1-L[X])↑3;
        R:=L[X]↑2;
        S:=L[X]↑3;
        CON[X,1]:=1+P*(C-B)+Q*(F-E);
        CON[X,2]:=P*B+Q*E;
        CON[X,3]:=P*C+Q*F;
        CON[X,4]:=(1-L[X])+P*D+Q*G;
        CON[X,5]:=1+R*(C-B)-S*(F-E);
        CON[X,6]:=R*B-S*E;
        CON[X,7]:=R*C-S*F;
        CON[X,8]:=L[X]-R*D+S*G;
        "END";
        "END";
        "BEGIN"
        "INTEGER" M,A,B,C,D,E,F,G,H,I,J,SUM,BEG,MIS;
        "ARRAY" SET[1:20,1:50];
        MIS:=DEPTH/MESH+2;
        "FOR" X:=1 "STEP" 1 "UNTIL" 20 "DO"
        "BEGIN"
        "FOR" Y:=1 "STEP" 1 "UNTIL" 50 "DO"
        "BEGIN"
        SET[X,Y]:=-1;
        "END";
        "END";
        "FOR" M:=1 "STEP" 1 "UNTIL" 100 "DO"
        "BEGIN"
        "FOR" Y:=3 "STEP" 1 "UNTIL" 50 "DO"
        "BEGIN"
        SUM:=2;
        "IF" TEST[Y]>10 "THEN" "GOTO" RELAX "ELSE"
        "IF" TEST[Y]<1 "THEN" "GOTO" START1 "ELSE"
        "GOTO" START2;
START1: Z[OUT[Y],UP[Y]]:=CON[Y,5]*BOUND[Y]+CON[Y,6]*
```

```
        Z[OUT[Y],(UP[Y]+1)]-CON[Y,7]*Z[OUT[Y],(UP[Y]+
        2)]-CON[Y,8]*MESH;
        Z[OUT[Y],(UP[Y]-1)]:=CON[Y,1]*BOUND[Y]+CON[Y,2]
        *Z[OUT[Y],(UP[Y]+1)]-CON[Y,3]*Z[OUT[Y],(UP[Y]+
        2)]+CON[Y,4]*MESH;
        SET[OUT[Y],UP[Y]]:=Z[OUT[Y],UP[Y]];
        SET[OUT[Y],(UP[Y]-1)]:=Z[OUT[Y],(UP[Y]-1)];
        "GOTO" COUNT;
START2: "IF" (L[Y]-MESH)<0.0001 "THEN" "GOTO" START3
        "ELSE" "GOTO" START4;
START3: SET[(OUT[Y]-1),Y]:=BOUND[Y];
        "GOTO" COUNT;
START4: Z[OUT[Y],Y]:=CON[Y,5]*BOUND[Y]+CON[Y,6]*Z[(
        OUT[Y]+1),Y]-CON[Y,7]*Z[(OUT[Y]+2),Y];
        Z[(OUT[Y]-1),Y]:=CON[Y,1]*BOUND[Y]+CON[Y,2]*
        Z[(OUT[Y]+1),Y]-CON[Y,3]*Z[(OUT[Y]+2),Y];
        SET[OUT[Y],Y]:=Z[OUT[Y],Y];
        SET[(OUT[Y]-1),Y]:=Z[(OUT[Y]-1),Y];
COUNT:  SUM:=SUM+1;
        "END";
RELAX:  "FOR" F:=1 "STEP" 1 "UNTIL" (N-4) "DO"
        "BEGIN"
        G:=F+1;
        H:=G+1;
        I:=H+1;
        J:=I+1;
        "FOR" A:=1 "STEP" 1 "UNTIL" (K-4) "DO"
        "BEGIN"
        B:=A+1;
        C:=B+1;
        D:=C+1;
        E:=D+1;
        Z[C,H]:=(8*(Z[D,H]+Z[C,G]+Z[C,I]+Z[B,H])-
        2*(Z[D,G]+Z[D,I]+Z[B,G]+Z[B,I])-Z[E,H]-Z[C,F]-
        Z[C,J]-Z[A,H])/20;
        "IF" H>TOP "THEN" "GOTO" RELEASE
        "ELSE" "IF" C>SIDE "THEN" "GOTO" RELEASE
        "ELSE" "GOTO" JACK;
JACK:   "FOR" X:=1 "STEP" 1 "UNTIL" SIDE "DO"
```

```
          "BEGIN"
          "FOR" Y:=1 "STEP" 1 "UNTIL" TOP "DO"
          "BEGIN"
          "IF" SET[X,Y]>0 "THEN" Z[X,Y]:=SET[X,Y]
          "ELSE" Z[X,Y]:=Z[X,Y];
          "END";
          "END";
          Z[2,MIS]:=Z[3,MIS];
          Z[4,MIS]:=Z[3,MIS];
          BEG:=ENTIER(DEPTH/MESH)+1;
          Z[3,BEG]:=-1.5*Z[3,(BEG+1)]+3.0*Z[3,(BEG+2)]-
          0.5*Z[3,(BEG+3)]+3.0*MESH/(N-4);
RELEASE:"END";
          "END";
          "FOR" X:=3 "STEP" 1 "UNTIL" K "DO"
          "BEGIN"
          Z[X,1]:=-1.5*Z[X,2]+3.0*Z[X,3]-0.5*Z[X,4]+3.0*
          MESH/(N-4);
          "END";
          "FOR" Y:=1 "STEP" 1 "UNTIL" N "DO"
          "BEGIN"
          Z[1,Y]:=Z[5,Y];
          Z[2,Y]:=Z[4,Y];
          "END";
          "IF" M>125 "THEN" "PRINT" SAMELINE,M,''S3``,
          Z[3,3],''S3``,Z[3,4];
          "IF" REP<1.5 "THEN" "GOTO" EQUALS "ELSE"
          "GOTO" NOTEQ;
EQUALS:   "FOR" X:=1 "STEP" 1 "UNTIL" K "DO"
          "BEGIN"
          Z[X,N]:=Z[X,N-4];
          Z[X,N-1]:=Z[X,N-3];
          "END";
NOTEQ:    "END";
          "FOR" F:=0 "STEP" 1 "UNTIL" (N-3) "DO"
          "BEGIN"
          G:=F+1;
          H:=G+1;
          I:=H+1;
```

```
J:=I+1;
"FOR" A:=1 "STEP" 1 "UNTIL" (K-3) "DO"
"BEGIN"
B:=A+1;
C:=B+1;
D:=C+1;
E:=D+1;
P[C,H]:=(Z[C,G]-2*Z[C,H]+Z[C,I])*((N-4)↑2/
MESH↑2);
Q[C,H]:=(Z[D,H]-2*Z[C,H]+Z[B,H])*((N-4)↑2/
MESH↑2);
R[C,H]:=-((Z[D,G]-Z[B,G]+Z[B,I]-Z[D,I])/4.0)*
((N-4)↑2/MESH);
DEL[C,H]:=0.3*(P[C,H]+Q[C,H]);
SIGMA[C,H]:=SQRT(((P[C,H]-Q[C,H])↑2+(Q[C,H]-
DEL[C,H])↑2+(DEL[C,H]-P[C,H])↑2/2+3*R[C,H]↑2));
"END";
"END";
"FOR" X:=3 "STEP" 1 "UNTIL" K "DO"
"BEGIN"
"FOR" Y:=1 "STEP" 1 "UNTIL" N "DO"
"BEGIN"
"PRINT" SAMELINE,ALIGNED(2,5),Z[X,Y],``S2``,P[X,Y],
``S2``,Q[X,Y],``S2``,R[X,Y],``S2``,DEL[X,Y],``S2``,
SIGMA[X,Y],``L1``;
"END";
"PRINT"``L3``;
"END";
"PRINT"``L10``;
F:=K+3;
"BEGIN"
"ARRAY" W[1:F,1:N];
B:=1;
"FOR" Y:=2 "STEP" 2 "UNTIL" N "DO"
"BEGIN"
B:=B+1;
A:=1;
"FOR" X:=1 "STEP" 2 "UNTIL" (K-1) "DO"
```

```
"BEGIN"
A:=A+1;
W[X,Y]:=Z[A,B];
"END";
"END";
E:=1;
"FOR" Y:=2 "STEP" 2 "UNTIL" N "DO"
"BEGIN"
E:=E+1;
A:=0;
"FOR" X:=2 "STEP" 2 "UNTIL" K "DO"
"BEGIN"
A:=A+1;
B:=A+1;
C:=B+1;
D:=C+1;
W[X,Y]:=0.5625*(Z[B,E]+Z[C,E])-0.0625*(Z[A,E]+
Z[D,E]);
"END";
"END";
E:=1;
"FOR" X:=1 "STEP" 2 "UNTIL" (K+3) "DO"
"BEGIN"
E:=E+1;
A:=0;
"FOR" Y:=3 "STEP" 2 "UNTIL" (N-1) "DO"
"BEGIN"
A:=A+1;
B:=A+1;
C:=B+1;
D:=C+1;
W[X,Y]:=0.5625*(Z[E,B]+Z[E,C])-0.0625*(Z[E,A]+
Z[E,D]);
"END";
"END";
E:=1;
"FOR" Y:=3 "STEP" 2 "UNTIL" (N-1) "DO"
"BEGIN"
E:=E+2;
```

```
        A:=-1;
        "FOR" X:=4 "STEP" 2 "UNTIL" K "DO"
        "BEGIN"
        A:=A+2;
        B:=A+2;
        C:=B+2;
        D:=C+2;
        W[X,Y]:=0.5625*(W[B,E]+W[C,E])-0.0625*(W[D,E]+
        W[A,E]);
        "END";
        "END";
        "FOR" Y:=1 "STEP" 1 "UNTIL" N "DO"
        "BEGIN"
        W[2,Y]:=W[4,Y];
        "END";
        "FOR" X:=1 "STEP" 1 "UNTIL" K "DO"
        "BEGIN"
        W[X,2]:=0.5;
        W[X,1]:=-1.5*W[X,2]+3.0*W[X,3]-0.5*W[X,4]+3.0*
        MESH/(2*(N-4));
        "END";
        "FOR" Y:=1 "STEP" 1 "UNTIL" N "DO"
        "BEGIN"
        "FOR" X:=1 "STEP" 1 "UNTIL" K "DO"
        "BEGIN"
        Z[X,Y]:=W[X,Y];
        "END";
        "END";
        "END";
        "END";
        "END";
        "END";
        "END";
"END";
```

FIG. II.1.

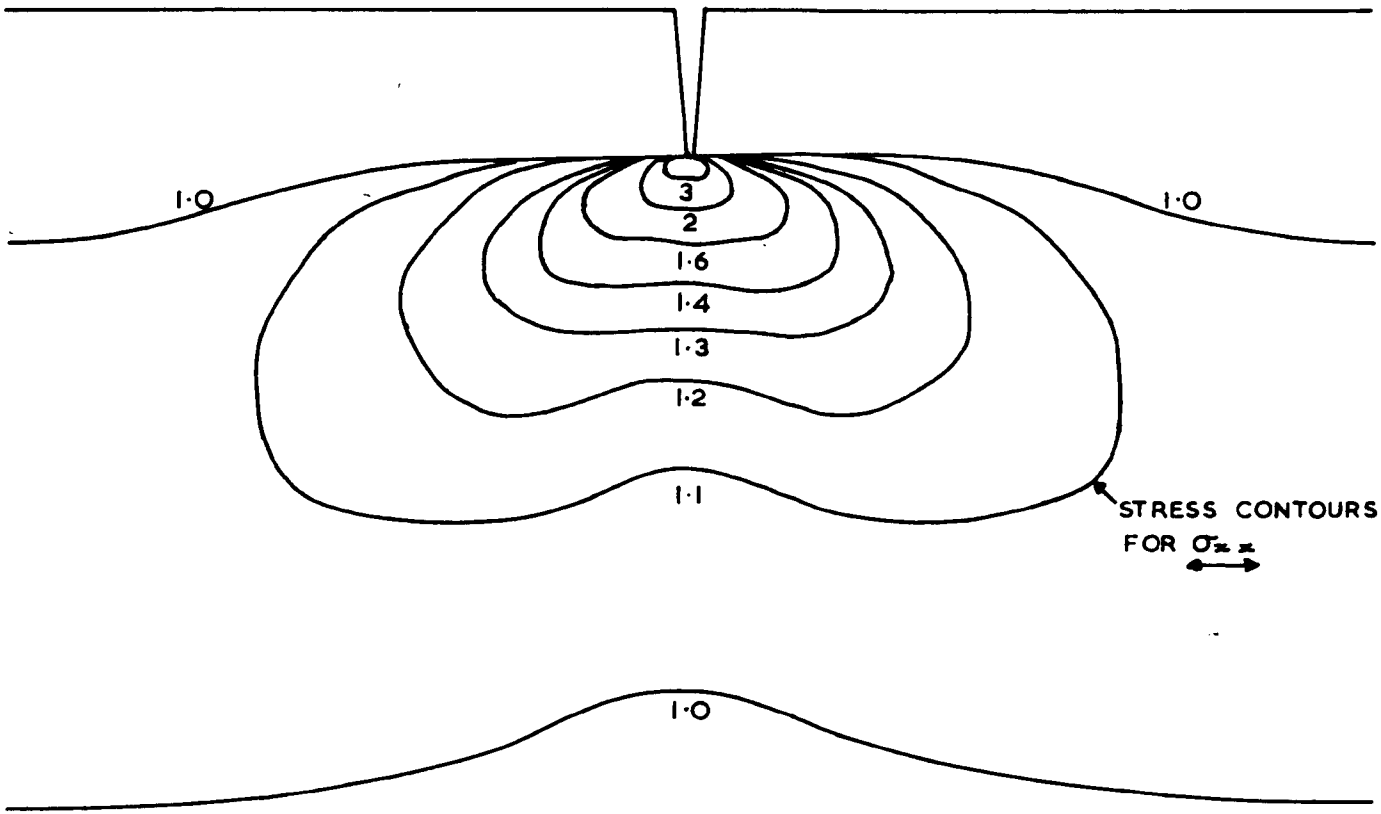

LOADING CONDITIONS – UNIAXIAL TENSION

CRACK DEPTH 1 UNIT.

PLATE WIDTH 32 UNITS.

APPENDIX III

USE OF THE PROPOSED CUMULATIVE DAMAGE RULE TO MAKE LIFE PREDICTIONS

In this appendix the calculations required to make life predictions in two cases given:-

(a) When the life is split between both Stage A and Stage B.

(b) When it may be assumed that all the life is spent in Stage A.

Case (a) Triangular Modulation tests described in Chapter 6

(1) Establish the slope of the life in Stage A v. life to failure plot.

(2) Establish non-damaging stress levels in Stage A and Stage B.

(3) At each test condition establish the value of the top damaging stress level in the spectrum.

(4) Determine the constant amplitude life at each of the stress levels mentioned in (3) and divide these values into life in Stage A and Stage B using the slope obtained and assuming the life in Stage A v. Life to failure plot passes through zero.

(5) Using the values of non-damaging stress levels already established derive the proportion of damaging cycles in the spectrum for both Stage A and Stage B.

(6) The proportions established in (5) can now be used to predict the total number of cycles in Stage A and Stage B and these can then be summed to obtain the predicted life to failure.

Calculations

(1) We know

$$\frac{1}{K_T} = -0.1255(\sec\theta)^4 + 0.7360 \text{ from Chapter 7}$$

K_T value of notch = 2.0

$$-0.1255\ (\sec\theta)^4 = \frac{1}{2.0} - 0.7360$$

$$(\sec\theta)^4 = \frac{+0.2360}{0.1255}$$

$$\theta = 31^\circ\ 22'$$

(2) Non-damaging stress levels

From S-N curve σ_f = 9.7 tons/sq.in.

Non damaging level Stage A = 0.7 x 9.7

= 6.79 tons/sq.in.

Non damaging level Stage B → stress levels established as damaging down to the lowest stress level used in these tests. Therefore all stresses are considered as damaging in Stage B for these tests.

(3) For triangular modulation tests with a large proportion of high stress levels the top stress level occurring is considered as the top damaging level, and this is 12.24 tons/sq.in.

The calculation for the test condition 12.24 — 5.71 tons/sq.in. is performed in detail below and calculations for all conditions are shown tabulated in Table III/1.

(4) Constant amplitude life at 12.24 tons/sq.ins is 676,000 cycles from S-N curve given in Fig. 6-2.

Life in Stage A = Life to failure x tan θ.

Stage A = 676,000 x tan $33^\circ\ 22'$

= 412,000 cycles

$\therefore$ Stage B = 264,000 cycles.

(5) Stress range 12.24 - 5.71 tons/sq.in. = 6.53 tons/sq.in.

Non damaging level in Stage A (2) = 6.79 tons/sq.in.

Proportion of non-damaging cycles = $\frac{6.79 - 5.71}{6.53} = \frac{1.08}{6.53}$ as all levels have equal probability of occurrence in a triangular modulation test.

Proportion of damaging cycles in Stage B is 100%

(6) There are 412,000 damaging cycles in Stage A re.(4) and the proportion of non-damaging cycles is $\frac{1.08}{6.53}$ ref.(5).

Predicted life in Stage A = $412,000 \times \frac{6.53}{5.45}$

= 493,000 cycles.

Predicted life in Stage B = $264,000 \times 1.0$

= 264,000 cycles.

Predicted life to failure = 757,000 cycles.

Actual mean life to failure at this condition was 786,200 cycles.

As stated the normal tabulated form of calculation is shown in Table III/1 together with the ratio of predicted/actual lives. The ratio of actual/predicted life varies from 0.84 to 1.21 for the range of conditions investigated. These figures give a maximum error on the unsafe side of 19% as compared to 417% in the case of the Palmgren-Miner predictions.

Case (b) Calculation of predicted lives for sharply notched cantilever specimens subject to narrow band random Rayleigh distribution Stress spectra.

Further details of the actual tests are given in the main text of Chapter 7. The K_T value of the notch is 7.6 in an axially loaded condition and this value puts the specimen above the critical level of 3.8 i.e. we may assume that all the life if spent in Stage A or alternatively that the slope of the life in Stage A v. life to failure plot is 45 degrees.

Again one r.m.s. value of the signal will be considered in detail and the other values are shown tabulated in Table III/2.

Calculations for a r.m.s. nominal stress of 10 K.s.i. following the same steps as in Case (a).

(1) Slope of Life in Stage A v. Life to Failure Plot = 45° as $K_T > 3.8$.

(2) R.M.S. value of constant amplitude fatigue limit = 12.3 K.s.i.

Non damaging stress level in Stage A = 0.7 x 12.3 x 1.414

= 12.2 K.s.i. p.p.

(3) Top damaging stress level is that level exceeded by 0.5% of total number of cycles. This is the 3.25σ level for a Rayleigh distribution.

Top damaging stress level = 3.25 x 10

= 32.5 K.s.i.

R.M.S. value of top damaging level = 23 K.s.i.

(4) Constant amplitude life at 23 K.s.i. r.m.s. = 369,000 cycles

Life in Stage A = 369,000 cycles

Life in Stage B = 0.

(5) Non damaging peak stress = 12.2 K.s.i. in Stage A.

Peak/r.m.s. ratio = $12.2/10$ = 1.22.

For Rayleigh distribution

Peaks exceeding 1.22 peak/r.m.s. ratio = 48%.

Non damaging cycles = 52% in Stage A

(6) Predicted life in Stage A = $\frac{369,000}{0.48}$

= 768,000 cycles

Predicted life in Stage B = 0.

Predicted Total life to failure = 768,000 cycles.

Actual mean life to failure 1,000,000 cycles.

Miner Prediction 1,500,000 cycles.

The other values of r.m.s. level are shown in the normal tabulated form in Table II/2. Plots of the predictions which compare to the experimental results and the Palmgren-Miner hypothesis are shown in Chapter 7.

CALCULATION OF PREDICTED LIVES ON TRIANGULAR MODULATION TESTS USING THE PROPOSED CUMULATIVE DAMAGE RULE

Loading Condition tons/sq.in.	Top Damaging Stress Level tons/sq.in.	Constant Amplitude Life at T.D.S.L. cycles	Life in Stage A Constant Amplitude	Life in Stage B Constant Amplitude	Proportion Damaging in Stage A	Proportion Damaging in Stage B	Predicted Life in Stage A	Predicted Life in Stage B	Predicted Life to Failure	Actual Life to Failure	Ratio Act/Pre Lives	Miner Summ.
12.24-9.79	12.24	676,000	412,000	264,000	100%	100%	412,000	264,000	676,000	565,700	0.84	0.42
12.24-8.98	12.24	676,000	412,000	264,000	100%	100%	412,000	264,000	676,000	820,400	1.21	0.42
12.24-8.16	12.24	676,000	412,000	264,000	100%	100%	412,000	264,000	676,000	805,400	1.19	0.38
12.24-7.75	12.24	676,000	412,000	264,000	100%	100%	412,000	264,000	676,000	667,400	0.99	0.29
12.24-7.34	12.24	676,000	412,000	264,000	100%	100%	412,000	264,000	676,000	752,400	1.11	0.30
12.24-6.53	12.24	676,000	412,000	264,000	95.4%	100%	432,000	264,000	696,000	662,000	0.95	0.24
12.24-5.71	12.24	676,000	412,000	264,000	83.5%	100%	493,000	264,000	757,000	786,200	1.03	0.25

TABLE III/1.

CALCULATION OF PREDICTED LIVES FOR NARROW BAND RANDOM RAYLEIGH DISTRIBUTION ON SHARPLY NOTCHED SPECIMENS (FRALICH).

R.M.S. Stress Level K.S.I.	Top Damaging Stress Level K.S.I.	Constant Amplitude Life at K.S.I.	Life in Stage A Constant Amplitude	Peak/R.M.S. Ratio of Non=Damaging Level	%age of Non-Damaging Stress Peaks	Predicted Life to Failure
20	46	78,600	78,600	0.61	18.5	96,500
15	34.5	171,000	171,000	0.815	28.5	240,000
10	23	369,000	369,000	1.22	52.0	768,000
7	16.1	1,000,000	1,000,000	1.74	78.5	4,450,000
6	13.8	2,000,000	2,000,000	2.04	86.0	14,200,000
5	11.5			-	-	

TABLE III/2.

ACKNOWLEDGMENT

The author is indebted to:-

F. Sherratt, B. Sc. Ph. D., project supervisor,

The school of Engineering Science for the provision of facilities,

The British Railways Board for their support during the past year,

The staff of the University Workshop,

The laboratory technicians and in particular Mr. J. Hawkins for their assistance and interest,

Miss J. A. Green and Mrs. G. Gammage for their assistance in the preparation of this thesis.